CONDENSATION OF STEAM ON SHORT TUBES IN HORIZONTAL ROWS PLACED IN A VERTICAL GRID

A THESIS
submitted in fulfilment of the
requirements for the award of the degree
of
DOCTOR OF PHILOSOPHY
in
CHEMICAL ENGINEERING

By

BIKASH MOHANTY

DEPARTMENT OF CHEMICAL ENGINEERING
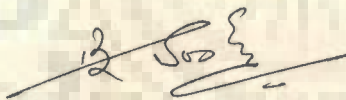UNIVERSITY OF ROORKEE
ROORKEE-247 667 (INDIA)

December, 1987

CANDIDATE'S DECLARATION

I hereby certify that the work which is being presented in the thesis entitled **CONDENSATION OF STEAM ON SHORT TUBES IN HORIZONTAL ROWS PLACED IN A VERTICAL GRID** in fulfilment of the requirement for the award of the Degree of Doctor of Philosophy, submitted in the Department of Chemical Engineering of the University is an authentic record of my own work carried out during a period from January 1980 to December 1987 under the supervision of Prof. B.S.Varshney and Dr.S.C.Gupta.

The matter embodied in this thesis has not been submitted by me for the award of any other degree.
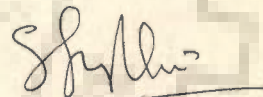
Bikash Mohanty
(Bikash Mohanty)

This is to certify that the above statement made by the candidate is correct to the best of our knowledge.

Date: 22-12-87

(B.S.Varshney)
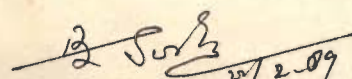Professor
Deptt. Of Chem. Engg.
Univesity of Roorkee
Roorkee-247 667 India
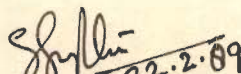
(S.C.Gupta)
Reader
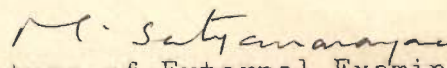Deptt. of Chem. Engg.
University of Roorkee
Roorkee-247 667 India

The candidate has passed the Viva-Voce examination held on.. 22-2-1989....at. U.O.R. ROORKEE........ The thesis is recommended for the award of Ph.D. Degree.

(B.S. Varshney) 22/2-09   (S.C. Gupta) 22.2.09   M. Satyanarayan (Signature of External Examiners)
22/2/1989

ABSTRACT

The present investigation has been carried out to study experimentally the condensation of low pressure steam on four horizontal short tubes(L/d = 13.6), placed in a vertical grid. The tubes were housed in a rectangular vessel of 300 mm length, 310 mm breadth, and 750 mm height. Each tube of the condenser was 341 mm long with an inside diameter of 25 mm and outside of 28.8 mm. The tubes were held in perfect horizontal position by means of specially fabricated check-nuts. The clearance between two nearest tubes was 97 mm. In order to measure the temperature of outer surface of each tube, twelve copper-constantan thermocouples were embedded at four locations at distances of 21, 121, 221, and 321 mm, respectively measured from the leading edge of the tube. Every location had three thermocouples, one placed at each of the top-, the side-, and the bottom-regions of the tube. The thermo-e.m.f. signals from all the tube wall thermocouples on analysis showed periodic variation with time. Due to the large amplitude of variation a hardware-based signal integrating system comprising of Keithley programmable DMM with GPIB interface and Z-80 micro-processor was adopted to find out time-averaged value of the fluctuating signals. This scheme was thought adequate in view of its being fast in processing large number of data points.

A specially designed and developed home-made mechanical hand was employed to measure the temperature of steam bulk around the tubes in a vertical plane by means of thermocouples. It had two arms each containing a copper-constantan thermocouple. It was

possible to control the vertical and horizontal positions of the thermocouples in a vertical plane, containing tubes, from outside the test condenser with a minimum accuracy of 1.0 mm.

The steam used in this investigation was raised in an oil fired boiler. To ensure that the steam entering the condenser was dry and saturated, extra precaution was exercised by employing an upright U-loop having a vertical drain pipe with steam trap at its free end in the pipe line connecting the boiler to the test condenser. In fact this helped in removing the condensate coming along with steam from the boiler before entering the test condenser. The temperature of steam was monitored by copper-constantan thermocouples attached to mechanical hand. An air vent with continuous steam purging was used to keep the test condenser free from noncondensables. To check the absence of noncondensables, the temperature of the steam was measured. When the temperatures maintained by the thermocouples placed near the top and bottom tubes were found equal to saturation temperature corresponding to the pressure of steam, it was taken that the steam was free from noncondensables. To maintain a quiescent environment of steam around the tubes of the condenser the incoming steam through a steam nozzle placed off-line to the vertical grid of tubes was allowed to impinge on a cup and then passed through a perforated plate. The above arrangement reduced the velocity of steam to a practical possible minimum value.

The cooling water was pumped into the tubes through rotameters. The provision of inverted U-bend at the exit of each

tube ensured that the tubes were always full with cooling water, which was very necessary.

The temperature distribution of cooling water was determined theoretically for the estimation of heat flux distribution along different segments of each tube. This was done by iterating the heat rate equation with heat balance equation and finally matching the calculated exit temperature of cooling water with experimentally determined value. For this purpose each tube was considered to be made of four isothermal segments of 71, 100, 100, and 70 mm length, respectively.

Experiments were conducted for steam pressures ranging from 146.75 to 269.38 kPa and cooling water flow rate from 11.6 to 17.1 lpm.

The present investigation has shown the expected behaviour that the temperature of the wall of the tubes varies circumferentially. It is also observed that due to the continuously decreasing values of cooling water-side heat transfer coefficient, unlike that of long tube (L/d > 50) having high flow rate of cooling water, the value of the average circumferential wall temperature continuously increases throughout the length of the tubes irrespective of the row in which the tube lies. Thus the surfaces of the tubes become nonisothermal when condensation occurs on short tube condensers. It is established that for a given tube-row the average circumferential wall temperature of the tube is found to possess a specific functional relationship with the cooling water flow rate, it's inlet temperature, steam pressure, and distance from

the leading edge of the tube.

For the calculation of condensing heat transfer coefficient from an available correlation for the first row tube, a relationship for the weighted wall temperature for short tube, in terms of operating parameters is also obtained. These experimentally determined weighted wall temperatures of the first row tube of the bundle show a good agreement with the model of Bromley within a maximum deviation of +35%. The experimental data for the condensation of quiescent steam on first row tube of the bundle are correlated best by the Mikheyev correlation within a maximum deviation of -18.0 % to 10 %, followed by the correlation due to Henderson and Marchello within a maximum deviation of -26 % to 6%. For the determination of weighted condensing heat transfer coefficient for short tubes in second-, third-, and fourth- rows, based on the present experimental data, an empirical correlation is recommended within a maximum deviation of ±10%, which establishes that heat transfer coefficient of a tube in rows other than the first row possesses a functional relationship with the heat transfer coefficient of first row tube and the row number in which the tube lies.

It is also found that the predictions from Kern's correlation and the experimental values of weighted condensing heat transfer coefficient of second-, third-, and fourth-row tubes agree excellently within a negligible deviation. The finding of the present investigation is that Jakob's correlation for heat transfer coefficient for tubes in different rows of the

tube bundle is a conservative one is in conformity with the observation reported by Marto.

ACKNOWLEDGEMENTS

C O N T E N T S

LIST OF FIGURES   page no.

LIST OF TABLES page no.

NOMENCLATURES

C_f	Fanning friction factor
C_p	specific heat of liquid, J/kg °C
g	acceleration due to gravity, m/s^2
d	diameter of tube, m
h_s	top/side/bottom condensing heat transfer coefficient of a segment, W/m^2°C
$\bar{h}_s$	average condensing heat transfer coefficient of a segment, W/m^2°C
$\bar{h}_{s,wt}$	weighted average of hs value for the entire length of tube W/m^2°C
$\bar{\bar{h}}_n$	mean heat transfer coefficient of n tubes, W/m^2°C
$\bar{h}_{n,wt}$	weighted average heat transfer coefficient of nth tube W/m^2°C
h	local condensing heat transfer coefficient along the circumference of the tube, W/m^2°C
$\bar{h}$	mean condensing heat transfer coefficient , W/m^2°C
$\bar{h}_N$	mean condensing heat transfer coefficient as predicted from Nusselt's equation, Eq.2.2 , W/m^2°C
$\bar{h}_{N1}$	mean condensing heat transfer coefficient of top-row tube in a vertical grid of horizontal tubes as predicted by Nusselt's equation, Eq.2.2 , W/m^2°C
h_i	water side heat transfer coefficient of a segment, W/m^2°C
h_{ia}	average hi from leading edge upto the segment mentioned, W/m^2°C
k	thermal conductivity, W/m°C
k_t	thermal conductivity of tube wall , W/m °C

$L_{c,s}$	length of tube from the leading edge upto the endof the segment, s
L	length of tube , m
L_e	thermal entry length , m
L_e/d	dimensionless thermalentry length
n	number of horizontal tubes in a vertical grid
P	pressure of steam , kPa
Q	heat picked up by cooling water, W
R_x	thermal resistance of cooling water plus tube plus scale defined in equation, Eq.2.13
r	radius of tube, m
S	factor in Eq. 2.44
R	$\overline{h}_{exptl,wt}$ / $\overline{h}_{predt,wt}$
t	temperature , °C
Δt	temperature drop(t_s-t_b) across the condensate film, °C
$t_{w\alpha}$	outer wall temperature at a perticular angle α measured from the top of the tube, °C
Δt_t	total temperature drop between vapour and cooling water, in Eq.2.11 and 2.15 , °C
Δt_{avg}	average temperature drop across condensate film in Eqs.2.11 and 2.16, °C
$\Delta t_{x\,av}$	average temperature drop across cooling water plus tube plus scale in Eq.2.15, °C
Δt_x	temperature drop across cooling fluid plus tube plus scale, °C
t_s	temperature of saturated vapour , °C
U	overall heat transfer coefficient, $W/m^2 °C$

w	cooling water flow rate, lpm
x	length of tube from leading edge ,m
*	multiplication sign

Greek letters

α	angle measured from top of the tube , °C
β	dimensionless number defined in Eq.2.12
β	multiplication constant in Eq.2.24
μ	viscosity, Ns/m^2
Γ	mass flow rate of condensate per unit length of tube in Eq. 2.31
σ	surface tension, N/m
λ	latent heat of vaporization, kJ/kg
lpm	liters per minute
ρ	density, kg/m^3
Δ	difference
ξ	acceleration effect parameter , $k\Delta t/\lambda$,dimensionless

Superscripts

$-$	mean
$=$	mean of mean condensing heat transfer coefficients, W/m^2 °C
$'$	iterated/modified

Subscripts

m	mean
w	wall
l	liquid
s	saturation /segment

I,II,III, IV	segment no.
v	vapour
avg	average
i	inside
o	outside
t	tube wall
x	cross section/water film plus tube plus scale in Eqs.2.15 and 2.17
f	film
n	number of tubes
wt	weighted
exptl	experimental
predt	predicted

Dimensionless numbers

Re	Reynold's number [$2\Gamma/\mu$]
Ga	Galileo number [$do^3 g \rho^2/\mu^2$]
Pr	Prandtl number [$\mu Cp/\kappa$]
H	phase change number [$Cp(ts-tw)/\lambda$]
Nu	Nusselt number [hdo/k]
K	Kutateladze number [$\lambda/Cp\Delta t$]
Noh	Ohnesorge Number [$\mu/(\rho\sigma d)^{0.5}$]

INTRODUCTION

The subject of condensation of vapours over horizontal tubes is extremely important, since it has a wide range of applications in chemical- ,petrochemical-,refineries-,refrigeration-, power plant-and many other allied industries. Because of this,the condensers are manufactured worth several crores of rupees annually. This signifies the need of reliable and economical design of condensers. One of the important requirements for the design of condensers is the knowledge of accurate values of heat transfer coefficient during condensation of vapours as a function of geometric-and operating-parameters, and physico-thermal properties of condensing vapours.

Nusselt was the first to undertake the study of condensation of pure vapours on vertical plates to obtain condensing heat transfer coefficient. Based on theoretical model ,he derived an equation relating condensing heat transfer coefficient to characteristic length , physico- thermal properties of condensate at the film temperature, and the difference between saturation temperature of vapour and wall temperature of the plate. He also succeeded in recommending an equation for condensation of pure vapours on a single horizontal tube. Later on, the experimental data for the condensation of pure vapours of differing physico-thermal properties were carried out by other investigators.

As regards the correlations for the condensation of vapours on horizontal tubes, some of the investigators have

recommended that the Nusselt equation could correlate their data only when its constant was modified to some suitable values; whereas in other investigations it has been suggested that the Nusselt equation was capable of correlating their data if the physico- thermal properties of the condensate appearing in it were evaluated at the film temperature rather than at the saturation temperature of the condensing vapour. Yet another group of investigators has attempted to make the Nusselt equation more rigorous by incorporating the effects of those factors which were neglected by Nusselt in an attempt to simplify his model, though these factors influence the condensation process. The merit of these correlations lies in the fact that they account for one or more factors like latent heat transfer accompanied by sensible heat transfer from the condensate[17,18], acceleration in the condensate film[14], nonlinear temperature distribution in the condensate film (17,18) ,drag at the vapour-liquid interface (59,60,61,62)and others.

Attempt has also been made to modify the Nusselt equation by taking into account the droplet detachment which occurs in the bottom region of a horizontal tube [11]. Some of the correlations have also been recommended by extending the theory of similarity to condensing heat transfer process[23].

An examination of the available literature reveals that inspite of many research investigations there is no single correlation available which is able to correlate all or most of the experimental data of various investigators for the vapours of differing physico- thermal properties.

It is important to note that these correlations facili-tate the calculation of condensing heat transfer coefficient from the knowledge of characteristic length of the tube, the physico-thermal properties of condensate at the film temperature, and the difference between saturation temperature and that of the tube surface , or alternatively , condensate flow rate per unit length of the tube.

Therefore, the calculation of condensing heat transfer coefficient of a vapour at a given pressure is possible provided the distribution of tube wall temperature, in addition to other parameters, is known. As a matter of fact ,in industrial conden-sers the temperature distribution of tube wall is not a predeter-mined value ; instead it attains a continuously varying value from the inlet to outlet of the tube ,dictated by the flow rate of cooling water inside the tube , its inlet temperature , pressure of condensing vapour and the ratio of length to diameter (L/D) of the tube. For tubes having L/D ratio less than 50 (known as short tubes) the value of heat transfer coefficient of flowing water keeps on decreasing continuously along the tube-length, unlike in tubes having L/D > 50 where the heat transfer coefficient decreases initially and then becomes constant. However, the temperature of water increases progressively due to heat pick-up as it flows down the tube length. These adverse thermal characteristics of flowing water are likely to provide an appreciable compound thermal insulation effect to the condensa-tion of vapour over the length of short tubes. As the magnitude of this adverse effect increases from inlet to outlet of the tube

3

,it impedes the condensation rate progressively along the tube-length. A review of literature shows that most of the experimental data on condensation of vapours pertain to long tubes. Therefore, it seems necessary to carry out investigation in which condensation of vapour is carried out on short tubes for the generation of new data for design engineers and for the furtherance of knowledge in the area of condensation.

For specific reasons , the horizontal industrial surface condensers consisting of tube-bundles inside a shell employ water as a coolant flowing inside the tubes whereas vapours condense over the tubes. Tubes for these condensers are arranged on a specific pitch in vertical rows. When condensation of vapours occur on the tubes, they get enveloped with condensate layer. With the passage of time the thickness of condensate layer on the tubes keeps on increasing and attains a value beyond which the condensate no more remains adhering on them, but drops off the bottom-region of the tubes(11).

Like many industrially important organic vapours , the condensation of steam over horizontal tubes is important. Depending upon the application of steam, its condensing pressure varies from low to high values. The condensation of steam at high pressures has been extensively studied. But the studies related to condensation of steam under low pressure are scarce. Therefore,there is a need to study the various thermal charac- teristics associated with the condensation of steam at compara- tively low pressures.

In this process the condensate from the tubes lying

4

in the top-most row of the bundle, hitherto called first row , flows down on the tubes in the second row and thus thickness of the condensate layer on them becomes greater than that on tubes in the first row. Consequently, the thermal resistance to condensation of vapours on tubes in second row also increases correspondingly. Thus , the tubes in the second row become less efficient thermally vis-a-vis those in the first row. For the same reason, the condensate layer thickness on tubes in the third row becomes still greater. As a result they become still less effective in causing condensation. This behaviour continues for rows in the downward direction. To appreciate this thermal deterioration of the tubes , it is necessary to measure the wall temperature of the tubes in different rows at different points on them both circumferentially as well as longitudinally. As a first step, an experimental investigation can be programmed for a limited number of rows with a single tube in each row. This , in fact , would provide a facility to study thermal behaviour of the tubes for their entire surface exhaustively and thus would lead to an in-depth knowledge of the condensation of vapours on tubes in different vertical rows for future research related to industrial horizontal surface condensers.

It will not be out of place to point out that most of the research outputs for the design of condensers remain in the files of R & D organizations, where such investigations have been carried out. Unfortunately, the published work is not adequate enough to help the design engineers to carry out economic design of condensers for various industrial applica-

tions. As a result this calls for concentrated research efforts to optimise the various parameters in the design of condensers.

Keeping the above considerations in view ,the present investigation for the condensation of steam on four short tubes in horizontal rows placed in a vertical grid was planned with the following major objectives:

1. To conduct experimental data for the condensation of steam, at low pressures ,on horizontal short tubes including measurement of circumferential and longitudinal wall temperatures of the condenser tubes in different rows with different flow rates of cooling water.

2. To determine the thermal response of short tubes, one in each of the four vertical rows, to changes in pressure of the condensing steam, and the flow rate of cooling water with the specific aim to obtain a procedure for the calculation of wall temperature of tubes lying in different rows of horizontal surface condensers.

   Also to scrutinize the available model for the prediction of wall temperature of the tubes of the condensers with the help of present experimental data.

3. To scrutinize the applicability of available correlations for condensing heat transfer coefficient for single tube and horizontal tube bundle with the help of the data obtained in the present investigation.

6

LITERATURE REVIEW

Because of ever-increasing industrial applications of condensation heat transfer, a concentrated research effort has been made to investigate the different aspects involved in it. The studies have been carried out to determine the parametric effects of physico-thermal properties of condensing fluids, the system pressure , the presence of noncondensables , the orientation of a tube (horizontal, vertical or inclined) over which condensation occurs ,the condensation over a bundle of tubes, etc. Accordingly literature related to a variety of aspects is available.

2. PRESENT INVESTIGATION

The present investigation deals with condensation of pure vapours of steam on four short horizontal tubes placed one over the other in vertical rows. Therefore, in the following sections attempt has been made to compile the literature related to condensation of pure vapours on a single horizontal tube, condensation on horizontal tubes spaced in vertical rows,and heat transfer in the thermal entrance region of a tube.

2.1.0 CONDENSATION ON A SINGLE HORIZONTAL TUBE

In 1916 , Nusselt(1) conducted his pioneering research on film condensation of pure vapours on surfaces. In his efforts he idealized the problem by assuming a pure quiescent vapour around the surface, uniform surface temperature, linear

temperature distribution in condensate film, laminar flow of condensate film due to gravity , absence of vapour shear effects, condensate-vapour interface at saturation temperature and no acceleration in the condensing film. His analysis resulted in the following forms of Nusselt equation for local heat transfer coefficient, h and average heat transfer coefficient, $\bar{h}$:

$$h = 0.693(k^3 \rho^2 g \sin\alpha / \Gamma\mu)^{1/3} \qquad (2.1)$$

$$\bar{h}_N = 0.725(k^3 \lambda \rho^2 g / (d_o \mu \Delta t))^{1/4} \qquad (2.2)$$

$$\bar{h}_N \left[\frac{\mu^2}{k^2 \rho^2 g} \right] = 1.2 \, Re^{1/3} = 1.51(4\Gamma/\mu)^{-1/3} \qquad (2.3)$$

$$\frac{\bar{h}_N}{k}(\mu/\rho)^{2/3} \frac{1}{g^{1/3}} = 0.955(\Gamma/\mu)^{-1/3} \qquad (2.4)$$

$$Nu = \frac{\bar{h}_N d_o}{k} = 0.725(Ga * Pr / H)^{1/4} \qquad (2.5)$$

Nusselt's constant , 0.725 in Eq.2.2 ,depends on the value of the integral $4/3 \int_o^\pi \sin^{1/3}\alpha \, d\alpha$ .According to him ,the value of the integral comes out to be 3.428. Later on ,the same integral was reevaluated more precisely by McAdams(2) using the value of gamma function as given by Pierce(3)and reported to be 3.4495. Using the above corrected value, the constant of Eq.2.2 comes out to be 0.728.Therefore,the modified Nusselt equation takes the form:

$$\bar{h}_N = 0.728 \left[\frac{k^3 \rho_1 (\rho_1 - \rho_v) g \lambda}{d_o \mu \Delta t} \right]^{1/4} \qquad (2.6)$$

Parr (4), in his analysis, assumed the local rate of

8

condensation to be uniform along tube perimeter, instead of assuming temperature drop across the condensate film to be constant. Thus based on his assumptions,Parr derived a constant of 0.75 compared to the value of 0.725 as obtained by Nusselt,Eq.2.2.

2.1.1 PREDICTED ERROR LIMITS FOR NUSSELT EQUATION

McAdams (2) undertook a comprehensive study to compare the experimental data of several authors (5-9) for steam and eighteen organic vapours condensing outside horizontal tube with Eq.2.2. He found that the experimental values of heat transfer coefficient ranged from 36% lower to 70% higher(10) than those predicted by Eq.2.2. Later on, Henderson and Marchello (11) also compared the experimental data of sixteen authors with Eq.2.2 and reported a deviation of -30% to +140%.

Chen (12) observed that the heat transfer coefficient often varied between 80 to 170 percent of Nusselt's predicted value.

2.1.2 NUSSELT TYPE EQUATIONS

Othmer and Berman (13) planned a comprehensive experimental study on eighteen alcohols, esters, ketones and water for the estimation of heat transfer coefficient during condensation on a horizontal tube. Based on their own experimental data they have recommended the following correlation for average heat transfer coefficient within ± 5% accuracy at a positive pressure of 5 to 10 mm of mercury :

$$\frac{\bar{h}}{k}\left[\frac{\mu}{\rho}\right]^{2/3}\frac{1}{g^{1/3}} = 1.62(\Gamma/\mu)^{-1/2} \tag{2.7}$$

It is important to note that the correlation, Eq. 2.7 differs from equation due to Nusselt, Eq. 2.4 with regard to the constant and the exponent of (Γ/μ) .The constant in Eq. 2.7 is 1.62 compared to a value of 0.955 in Eq. 2.4 while the exponents of the quantity (Γ/μ) are -1/2 and -1/3, respectively. They have further argued that the deviation from the theoretical exponent of -1/3 may be due to the effect of the condensate collecting on the lower portion of the condensing surface in a heavier layer than what can be accounted for by the equilibrium between opposing forces of viscosity and gravity acting on the fluid film.

2.1.3 VARIABLE WALL TEMPERATURE AND ACCELERATION IN CONDENSATE FILM

Peck and Reddie (14) have conducted studies based on analytical approach to calculate the average heat transfer coefficient. Their analysis accounts for a variable temperature drop across the condensing film around the tube and also an acceleration in the film . In other words ,they have attempted to make Nusselt's analysis more rigorous. They have recommended the following equation, wherein the variation in temperature drop across the condensing film around the tube has been incorporated:

$$\bar{h} = 0.725 \frac{\left[t_s - (a_o - a_2/7) \right]^{3/4}}{(t_s - a_o)} \sqrt[4]{\frac{k^3 p^2 g \lambda}{\mu d_o}} \qquad (2.8)$$

It may be noted that, for a symmetrical temperature distribution when $a_2 \longrightarrow 0$,the Eq.2.8 reduces to the Nusselt equation, Eq. 2.2.

They also carried out a comprehensive study on the effect of acceleration in condensate film on average heat transfer coefficient. Accordingly ,they have proposed the following equation:

$$\frac{\bar{h}}{h_N} = K \left[\frac{k \Delta t}{\mu \lambda} \right]^m + M \qquad (2.9)$$

where K and m are variable parameters and M a numerical constant. They have not discussed the possible improvement in Nusselt theory due to the inclusion of acceleration effects in the condensate film.

Later on, they undertook a more comprehensive work to scrutinize their own data and those of 17 other investigators (5-9,15,16)for water and 16 organic vapours over a period of 26 years. As a result of this work they succeeded in obtaining the following empirical equation within -40% to +10% deviation :

$$\bar{h} = \bar{h}_N [\ 0.0206(\lambda\ \mu/k \Delta t)^{1/2} +0.79\ ] \qquad (2.10)$$

Bromley et al (17) undertook a serious investigation, both experimental and theoretical ,to determine the extent of effect on heat transfer coefficient due to the variation of temperature of condensing film around the tube . In fact ,this investigation was an attempt to modify the Nusselt equation, which made use of the fact that condensing film temperature around the tube was constant.

They have recommended correlations for calculating the temperature drop across the condensate film, Δt, for the following

11

cases:

(a) Tube of infinite thermal conductivity ($\alpha \rightarrow \infty$)

$$\Delta tt / \Delta t_{avg} = 1 + 0.8057 \, \beta^{3/4} (\Delta tt / \Delta t_{avg})^{1/4} \qquad (2.11)$$

where :

$$\beta = \left[\frac{R_x^4 k^3 p(p-pv)g \, \lambda}{3 r_o \mu \Delta tt} \right]^{1/3} \qquad (2.12)$$

$$R_x = \frac{r_o}{h_i \, r_i} + \frac{(r_o - r_i) r_o}{k_t \, r_m} + \text{scale resistances} \qquad (2.13)$$

$$\alpha = \frac{k_t (r_o - r_i)}{r_m} \left[\frac{1}{h_i \, r_i} + \frac{(r_o - r_i)}{2 k_t \, r_m} \right] \qquad (2.14)$$

The dimensionless number α is a measure of the tendency of the tube to conduct heat circumferentially rather than radially.

(b) Tube of zero circumferential thermal conductivity($\alpha \rightarrow 0$)

$$\frac{\Delta t}{\Delta tt} = \frac{1}{\beta \left[\dfrac{\sin\alpha}{\alpha} \right]^{1/3} \left[\dfrac{\Delta tt}{t_{x,av \, 0-\alpha}} \right]^{1/3} + 1} \qquad (2.15)$$

where :

$$t_{avg} = \frac{1}{\pi} \int_0^\pi \Delta t \, d\alpha \qquad (2.16)$$

$$t_{x,av \, 0-\alpha} = \frac{1}{\alpha} \int_0^\alpha \Delta t_x \, d\alpha \qquad (2.17)$$

Finally, they have concluded that the effect of the variation in the temperature in the condensing film on heat transfer coefficient is not appreciable and thus Nusselt Eq. 2.2 does not require any modification due to this effect alone.

12

2.1.4 EFFECT OF SENSIBLE HEAT TRANSFER

It may be noted that at moderate pressure the latent heat of vaporization of liquids is large. Thus ,for condensing vapours under moderate pressure, the possible contribution of the sensible heat of the condensing film to the latent heat will be small. However, at high pressure and larger temperature difference between the saturated vapour and the tube temperature, the contribution of sensible heat term becomes appreciable in comparison to the latent heat of vaporization, since the value of the latter quantity decreases with pressure.

Bromley (17) has attempted to study this important aspect pertaining to the relative contributions of sensible heat and latent heat of vaporization during condensation.As a matter of fact,the contribution due to sensible heat to the total heat transfer to the coolant becomes more and more significant when condensation of vapour passes from low pressure to high pressure. He finally recommended the following equation for the average heat transfer coefficient which accounts for condensate cooling and heat capacity effect :

$$\bar{h} = 0.728\left[\frac{k^3\rho(\rho-\rho_v)g\lambda(1+0.4(\Delta tCp/\lambda)^2}{do\mu\Delta t}\right]^{1/4} \qquad (2.18)$$

The above equation is basically a modified Nusselt equation incorporating the effect of sensible heat transfer from the condensate film. It is precisely valid for $Cp\Delta t/\lambda$ values upto 3.0.

13

Bromley has further observed that the effect of the quantity $Cp \Delta t/\lambda$ on heat transfer coefficient tends to be negligible when the value of $Cp \Delta t/\lambda$ does not exceed 0.5. It will be important to note that the heat transfer coefficient predicted by Nusselt equation correlates most of the data of earlier investigators as referred in(14) , the deviation being -40% to +10%. For all fluids the values of $Cp \Delta t/\lambda$ are within 0.5. To this deviation Bromley has agreed that either the data are not entirely reliable or there is some other predominating effect which tends to give increased heat transfer coefficient.

2.1.5 EFFECT OF CROSS FLOW IN THE CONDENSATE FILM

Bromley (17) has performed an analysis to find out average heat transfer coefficient by including nonlinear temperature distribution in condensate film but omitted the effect of cross flow within the film.

Rohsenow (18) has attempted to find out the correct nonlinear temperature distribution across the film of a vertical plate by including cross flow in condensate film. In his investigation ,he made all the assumptions as made by Nusselt,except the nonlinear temperature distribution in condensate film. The temperature distribution in the condensate could not remain linear since condensate at the saturation temperature was continuously getting into the condensate film.

For the vertical plates the equation arrived at by him is as follows :

14

$$\bar{h} = 0.943 \left[\frac{k^3 \rho (\rho - \rho_v) g\lambda (1+0.68(\Delta t C_p /\lambda))}{\mu \Delta t \, L} \right]^{1/4} \qquad (2.19)$$

He has observed that similar analysis for laminar film condensation on inclined plates and on the outside of horizontal tubes results in an identical type of correction factor as given below:

$$(1+0.68(C_p \Delta t /\lambda))^{0.25}$$

The Nusselt equation, Eq.2.2 takes the following form when the correction factor is included :

$$\bar{h} = 0.725 \left[\frac{k^3 \, \rho^2 g\lambda (1+0.68(\Delta t C_p /\lambda))}{d_o \mu \Delta t} \right]^{1/4} \qquad (2.20)$$

The effect of the refinement in the Nusselt analysis becomes more prominent at higher values of liquid subcooling, or more precisely, at higher values of $C_p \Delta t /\lambda$.

White (19) has conducted experiments for the condensation of R-12 over a horizontal tube. He, based on his own experimental data, has observed that the Nusselt equation overpredicts heat transfer coefficient by 13%. He has recommended the following form of Nusselt's equation :

$$\bar{h} = 0.633 \left[\frac{k^3 \, \rho^2 g\lambda}{d_o \mu \Delta t} \right]^{1/4} \qquad (2.21)$$

2.1.6 REFERENCE TEMPERATURE FOR EVALUATING THE PHYSICO-THERMAL PROPERTIES OF CONDENSATE LAYER

Many investigators (20-22) have attempted to evaluate

15

Nusselt's equation by altering reference temperature at which the physical properties of condensate film should be evaluated.

Drew (20) has recommended following expression to find reference temperature for viscosity of the condensate :

$$t_f = t_w + 0.25(t_s - t_w) \qquad (2.22)$$

Minkowycz and Sparrow (21) have defined the reference temperature for condensing steam as follows :

$$t_f = t_w + 0.31(t_s - t_w) \qquad (2.23)$$

According to Poots and Miles (22), the reference temperature can be calculated as :

$$t_f = t_w + \bar{\beta}(t_s - t_w) \qquad (2.24)$$

where the values of multiplier β depend on the value of parameter $(t_s - t_w)$ and are given in Table 2.1

Table 2.1 Values of $\bar{\beta}$ in Eq. 2.24

$\bar{\beta}$	0.33	0.32	0.30	0.26
$(t_s - t_w)$	100	70	40	10

Chen (34) has used boundary layer concept for laminar film condensation for single horizontal tube as well as a vertical bank of horizontal tubes. For the single tube he has included inertial effect and has considered the vapour to be stationary outside the vapour boundary layer. He has obtained the velocity and temperature profiles for $\rho_v \mu_v / \rho_l \mu_l \ll 1$ and has pointed out the existence of similarity near the top stagnation point and approximately for the most part of the tube. He has arrived at the following expression :

16

$$\frac{\overline{h}_n}{\overline{h}_{N1}} \, n^{1/4} = \left[1+0.2 \, H(n-1)\right] \left[\frac{1+0.68H+0.02 \, \xi H}{1+0.95\xi -0.15\xi H}\right]^{1/4} \qquad (2.25)$$

where;

$$H = \frac{Cp \triangle t}{\lambda} \qquad \text{(Heat capacity parameter)}$$

$$\xi = \frac{k \triangle t}{\lambda} \qquad \text{(Acceleration effect parameter)}$$

The range of applicability of Eq.2.25 is :

$0.05 \geq Pr \geq 1$;

$H < 2$; $\xi < 20$ for single tube,

$\xi < 0.01$ and $H(n-1) < 2.0$ for multiple tube.

2.1.7 EFFECT OF SURFACE TENSION AND TUBE DIAMETER

Henderson and Marchello (11) have studied condensation on the outside of horizontal cylinder for tubes of differing diameters. They have found that the data have not been adequately correlated by Nusselt's equation. They have argued that the deviation is due to the fact that the condensate layer thickness at the bottom falls in the form of drops along the bottom of the tube and depends upon surface tension. The force necessary to support the weight of the drop in fact is equal to the surface tension force times the circumference. Thus ,the surface tension and diameter should be considered as parameters affecting the condensation phenomenon around the tube. They have been unable to go further deep into the mechanism and behaviour of condensing film at the bottom. In the absence of a rigorous analysis they

17

have opted to include a dimensionless group ($\mu/(pd\sigma)^{1/2}$)
known as Ohnesorge Number (N_{Oh}) for correlating the Nusselt
equation as follows :

$$\frac{h}{h_N} = 0.057 \; N_{Oh}^{-0.373} \qquad\qquad (2.26)$$

Mikheyev (23) has studied the condensing heat
transfer by means of the theory of similarity and has recommended
the following correlation for computing condensing heat transfer
coefficient :

$$Nu = 0.42 \; K_0^{0.28} \; (Pr_s/Pr_w)^{0.25} \qquad\qquad (2.27)$$

where ; $K_0 = G_0 * Pr * K$

This analysis is based on a number of assumptions, such
as, the film flow is laminar, the inertial forces appearing in
the film are negligible compared to viscosity and weight, the
transport of heat by convection in the film is small compared to
conduction of heat across the film , there is no friction between
the condensate and vapour, the temperature at the outer surface
of the film is equal to vapour saturation temperature ,and the
physical properties of the condensate do not depend on the
temperature. Eq.2.26 has been tested against the experimental
data of condensation of steam and vapours of ethyl alcohol,
acetone, benzene, ammonia and air on horizontal and vertical
tubes and has been found to be in excellent agreement with
experimental values.

2.2 CONDENSATION ON HORIZONTAL TUBES SPACED IN VERTICAL ROWS

The condensation of vapours on a single horizontal tube
is of much academic interest. Accordingly, a large number of

investigations related to condensation on horizontal tube are available in literature. The condensation of vapours in a condenser differs widely from the condensation on a single tube, since the former represents a bundle of tubes placed on a pitch inside a shell. The heat transfer coefficient due to condensation on a tube in a bundle depends on the row on which the tube in question is placed. This happens so due to the reason that the condensate from the tube in top row of a tube bundle falls on the tube in the row below it or may follow a sideway path in the form of discrete droplets causing splashing and turbulence in the condensate film around. The magnitude of this phenomenon will increase for tubes placed in further down rows. Keeping this in view ,it can be concluded that the value of the heat transfer coefficient for condensation of vapours on a single tube cannot be considered as a representative value for the design of a condenser having a bundle of tubes.

Jakob (24) has attempted to extend the Nusselt's analysis for film condensation on a single tube to a vertical in-line row of horizontal tubes. He has assumed that the condensate from a given tube drains as a continuous sheet directly on to the top of the tube below it in a smooth laminar film. He has also assumed that the temperature difference (ts-tw) remains the same for all the tubes, in all the rows. Based on these assumptions, Jakob has recommended the following equation :

$$\frac{\bar{h}_n}{\bar{h}_{N1}} = n^{3/4} - (n-1)^{3/4} \qquad (2.28)$$

where h_n is the heat transfer coefficient for n^{th} tube and

19

h_{N1} is the heat transfer coefficient of the top tube as obtained from Nusselt equation, Eq. 2.2.

Berman (25) has tested Jakob's equation, Eq.2.28 over a range of experimental data. He has found that most of the data lie above the theoretical curve based on Jakob's equation. This discrepancy can be attributed to the following reasons :

(a) the actual condensate flow pattern is much different from laminar sheet wise flow as considered by Jakob.

(b) some of the tubes encounter high vapour velocities which tend to increase the coefficient as a result of vapour shear effects.

Kern (26) has realized that the condensate falls down as discrete droplets or jets of liquid instead of a continuous sheet, depending upon its surface tension . In fact, drops cause ripples in the condensate film and lessen the inundation effect. He, therefore, has proposed a less conservative relationship as follows :

$$\frac{\overline{h_n}}{\overline{h_{N1}}} = n^{-1/6} \qquad (2.29)$$

or

$$\frac{\overline{h_n}}{\overline{h_{N1}}} = n^{5/6} - (n-1)^{5/6} \qquad (2.30)$$

Grant (27) and Grant & Osment (28), based on experimental data , have proposed the following empirical equation which is in close agreement with Kern :

20

$$\frac{\overline{h_n}}{\overline{h_{N1}}} = (\Gamma_n / \gamma_n)^{-0.233} \qquad\qquad (2.31)$$

where Γ_n is the rate of condensate drainage from the nth tube and γ_n is the rate of condensate generated on the nth tube.

Short and Brown (29) have experimented on the condensation of Freon-11 on bundle of horizontal tubes arrayed in vertical rows for different condensate rates under stagnant vapour. They have put forward following equations :

$$\frac{\overline{\overline{h_n}}}{\overline{h_{N1}}} = 1.24 \ n^{-1/4} \qquad\qquad (2.32)$$

or

$$\frac{\overline{h_n}}{\overline{h_{N1}}} = (\Gamma_n / \gamma_n)^{-0.25} \qquad\qquad (2.33)$$

Butterworth (30) has shown that the empirical equations of both Grant and Osment (28) and Kern (26) are in close agreement with that proposed by Short and Brown (29).

Nobbs (31) has used an active tube in a dummy tube bundle. He has simulated additional condensate flow from above by using three porous tubes supplied with water. He has obtained a widely scattered data and has concluded that the value of h_n depends on steam to cooling water temperature difference and steam velocity. At a low steam velocity (5.4 m/s) the h_n / h_{N1} passes through a minimum.

Withers and Young (32) have carried out a

21

comprehensive experimental study for condensation of steam on vertical rows of horizontal corrugated and plain cupronickel and copper tubes arrayed in a scattered mode. The tube diameters for the above experiment were 25 mm (1") and 16 mm (5/8"). They have recommended following correlations for hn :

$$\overline{h}_n = 0.725 C_n \left[\frac{k^3 \, \rho^2 g \lambda}{n d_o \mu \, \Delta t} \right]^{1/4} \quad (2.34)$$

where C_n is a correction factor applicable to Nusselt's multi-tube expression. The values of C_n are as follows :

for 25 mm bare cupronickel tube $C_n = 1.07(n)^{0.170}$ (2.35)

for 16 mm bare copper tube $C_n = 1.20(n)^{0.0557}$ (2.36)

Young et al (33) have conducted experiments for condensation of saturated Freon-12 on five 19 mm O.D. ,102.5 cm. long copper tubes arranged horizontally one over other. The temperature range of condensing Fr-12 vapours was 29.4°C to 51.6°C and the inlet water flow rate ranged from 2.2 kg/min to 3.2 kg/min. They have attempted to correlate the total weight of condensate flowing over each tube with Reynold's Number ($4\Gamma/\mu$) to predict the condensing heat transfer coefficient but have not been successful . It has been pointed out that the Nusselt's equation underpredicts the data, except for the first tube. They have recommended following equations for the calculation of condensing heat transfer coefficient for tube number one to five:

$$\overline{h}_1 = 0.655(NC)^{1/4} \quad (2.37)$$

$$\overline{h}_2 = 0.576(NC)^{1/4} \quad (2.38)$$

$$\overline{h}_3 = 0.551(NC)^{1/4} \quad (2.39)$$

22

$$h_4 = 0.498(NC)^{1/4} \qquad\qquad (2.40)$$

$$h_5 = 0.464(NC)^{1/4} \qquad\qquad (2.41)$$

Where $NC = \dfrac{k^3 \, p^2 g\lambda}{do\mu\Delta t}$

Chen (34) has developed a modified Nusselt's equation considering the additional effect of the momentum gain of the falling condensate and the condensation of vapour on the sub-cooled condensate sheet between tubes. He arrived at an approximate expression that is valid for most ordinary applications :

$$\frac{\overline{h_n}}{h_{N1}} = n^{-1/4} \, [1+0.2 \, H(n-1)] \qquad\qquad (2.42)$$

provided that $H(n-1) < 2.0$.

Eissenberg (35) has experimentally investigated the effects of condensate inundation by using a test bundle containing 163 tubes in a tightly spaced (s/d =1.33), staggered arrangement. Based on his observation , he has postulated that the condensate does not always drain onto tubes aligned vertically but, instead can be diverted sideways, due to local vapour flow conditions,to follow a staggered path. Assuming a gravity- dominated situation, he has conceptualized that in this side drainage condensate strokes the lower tubes on their side rather than on their top, and the inundation influences the condensate flow only on the bottom portion of the tubes, which carry away less heat than the top. For this situation, he has derived an expression that predicts a minimum effect of inundation :

$$\frac{\overline{h_n}}{\overline{h_{N1}}} = 0.60 + 0.42 \, n^{-1/4} \qquad\qquad (2.43)$$

Experimental measurements have been made in studying the effect of condensate inundation (28,29,31,35,38-42). Marto(36)has shown that ,in general, the data are very scattered. For a system of four tubes in a row h_n/h_1 varies from 0.50 to 0.95. Out of the different expressions discussed ,Jakob (24) predicts the most conservative effect whereas the side drainage model of Eissenberg (35) is the least conservative. The available data (36) show considerable scatter around each of these theoretical expressions. Recently Berman (25) has conducted a compilation of film condensation data on bundles of horizontal tubes and has concluded that the wide variation in experimental data for tube bundle inundation is due to many variables, such as, bundle geometry (in-line or staggered) , tube spacing, type of condensing fluid, operating pressure , heat flux , local vapour velocity and, of course, the difficulties in attempting to measure directly or indirectly the local condensing coefficient.

2.3 HEAT TRANSFER IN THE THERMAL ENTRANCE REGION OF A TUBE

The effect of different entrance conditions on turbulent forced convection heat transfer has been studied experimentally as well as theoretically for a variety of entrance shapes. Experimental results are available for a range of Reynold and Prandtl numbers for varied entrance conditions.

In general ,there exist three types of entrance condi-

24

tions. In the first, the velocity distribution at the entrance to the heat transfer tube is fully developed. The second condition is represented by uniform velocity distribution at the entrance. In the third condition , the entrance shape causes extra turbulence as the fluid enters the heat transfer tube. The heat transfer inside the tube for present work falls in the first category. A detailed literature review on this aspect is included in the following Sections.

2.3.1 FULLY DEVELOPED FLOW AT THE TUBE ENTRANCE

This condition occurs when the heat transfer tube is preceded by a calming section of sufficient length. Most of the available data for the above case are given in the form of local heat transfer coefficient vs tube length curves. The general shape of these curves shows that local heat transfer coefficient, h_x , decreases with tube length asymptotically. The asymptotic value h_∞ is equal to the average heat transfer coefficient to be expected from a tube of infinite length. To obtain the average heat transfer coefficient for any tube length, h_l ,the graphical integration of h_x vs length curve is done upto that length(44).

Boelter et al(45) have suggested an equation of the form:

$$\frac{h_l}{h_\infty} = 1 + S \frac{d}{x} \tag{2.44}$$

to show functional relationship of h_l with X. The advantage of this type of equation is that it is valid for the whole range of tube length. At x/d =0, h_l = ∞ and, at x/d = ∞, h_l =h_∞. They have further suggested that S may be considered approximately constant

25

for x/d > 5. However, Kays and Perkins(46) suggested that it is true when x/d > 20. Since then lot of investigations have been carried out for different fluids to cover a wide range of Reynold and Prandtl numbers. M.Al-Arabi (44) has analysed the data of seven investigators generated for air,water, and oil for Reynolds number ranging from 5,000 to 100,000 and Prandtl number 0.7 to 75. He has proposed the following equation for the estimation of S :

$$\frac{S \, Pr^{1/6}}{(x/d)^{0.1}} = 0.68 + \frac{3000}{Re^{0.81}} \qquad (2.45)$$

The equation is valid for air, water and oil systems for values of x/d > 3, values of Reynold number from 5,000 to 100,000 and values of Prandtl number from 0.7 to 75. The maximum deviation from the experimental data ,as reported by the author, is 30% . According to the author, the 30% deviation in S values will correspond to around 12% deviation in h_1/h_∞ values and hence it does not pose much problem in the use of Eq.2.45.

For small tubes, 16 > L/d >5.2 Hausen (47) has proposed the following equation for the estimation of inside heat transfer coefficient :

$$Nu = 0.116[Re^{2/3} - 125]Pr^{1/3} [1+0.333(d/x)^{2/3}][\mu_b/\mu_w]^{0.14} \qquad (2.46)$$

The physical property values for above equation are calculated at bulk temperature , t_b . Experiments by Hartnett(49)and analysis by Deissler(50) have indicated that for Prandtl number of the order of 1 or more, the heat transfer

coefficient drops faster with increasing length, x than that indicated by the equation.

Hartnett (49) has conducted experimental investigation to study the dependence of the thermal entrance length for two different fluids , water and oil in a 16.5 mm I.D. ,19 mm O.D. 304 stainless steel tube of 122 mm length.The tube was heated by resistance heating .The range of Reynolds number covered in this experiment was 10^4 to 10^6 .The author has compared his results with constant wall temperature analysis of Latzko(51) and the boundary layer analysis of Deissler(50) and has reported good agreement for constant heat rate case.He has further concluded that for flow in circular tube with a constant heat input per unit length ,the thermal entrance length for the case of established flow at the position where heating begins is 10 to 15 diameter and is independent of Prandtl number (when Pr > 1).

He has put forward the following correlation for $(Le/d)_{5\%}$.- the position on the heat transfer coefficient versus length curve at which the local heat transfer coefficient deviates 5% from the ultimate value :

$$\left[\frac{le}{d}\right]_{5\%} = 112 \left[\frac{\mu Cp}{k}\right] \left[\frac{dv\rho}{\mu}\right] \left[\frac{Cf}{2}\right]^{1/2}$$ (2.47)

Eq.2.47 is valid where variations of physical properties of the fluid along the length are negligible.

Allen et al(52) have conducted experiments to study the variation of friction and local heat transfer coefficient for

27

the case in which hydrodynamically developed turbulent flow of water enters an uniformly heated circular tube .For their work they have selected a 19 mm I.D.,20.6 mm O.D. ,560 mm long stainless steel tube heated electrically by resistance heating.They have concluded that the trends of the measured heat transfer coefficient in the thermal entrance region agreed with those of Hartnett(49) within 1 to 2% for nominal test condition of Re=50,000 and Pr=7 ,and moderate heating at a bulk temperature rise of 1.66°C per 30 diameter.

Mikheyev(23) in the course of analysis and subsequent generalization of test data for turbulent flow (Re > 10,000 and L/d > 50) for smooth straight tubes extended following equation :

$$Nu = 0.021 Re_f^{0.8} Pr_f^{0.43} (Pr_f/Pr_w)^{0.25} \qquad (2.48)$$

The reference temperature for Eq.2.48 is the mean temperature of the fluid t_f while the reference diameter is the equivalent diameter, d_{eq}, which is equal to the quadrupled cross-section area of the conduit divided by the wetted perimeter :Eq.2.48 is valid for a range of 10^4 < Re < 5×10^6 and 0.6 < Pr < 2500. For a case where L/d < 50 ,Mikheyev has suggested that the heat transfer coefficient calculated from Eq.2.48 should be multiplied by a correction factor ϵ_l from Table.2.2 .

Table 2.2 Values of ϵ_1 for Eq.2.48

L/d Ref	1	2	5	10	15	20	30	40	50
10000	1.65	1.50	1.34	1.23	1.17	1.13	1.07	1.03	1
20000	1.51	1.40	1.27	1.18	1.13	1.10	1.05	1.02	1
50000	1.34	1.27	1.18	1.13	1.10	1.08	1.04	1.02	1
100000	1.28	1.22	1.15	1.10	1.08	1.06	1.03	1.02	1
1000000	1.14	1.11	1.08	1.05	1.04	1.03	1.02	1.01	1
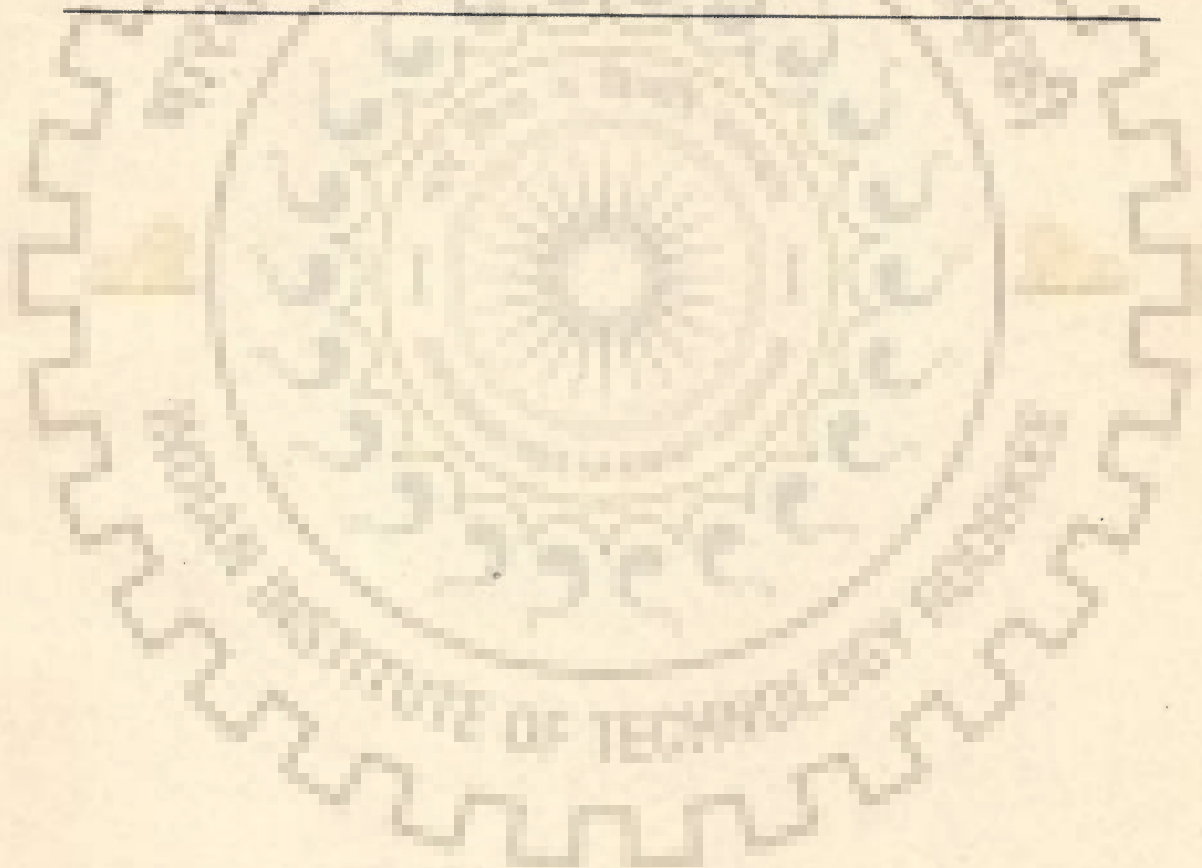
EXPERIMENTAL SETUP

Figure 3.1 shows the schematic diagram of the experimental facility for obtaining experimental data for the condensation of steam on short tubes in horizontal rows placed in a vertical grid. The photographic view of the same is in Figure 3.2

3.1 DESIGN CONSIDERATIONS

The main aim of the present investigation was to obtain thermal response of short tubes of a condenser in horizontal rows in a vertical grid at distances along the tubes from their leading edges to the changes in cooling water flow rate ,and condensing steam pressure. For accurate and reliable data , it was important that the tubes were in horizontal position, the measurement of wall temperatures of the tubes, temperature of steam bulk was accurate, and the steam entering the test condenser was dry, saturated and free from air/noncondensables. Therefore, a provision of suitable air vent to purge continuously the air/noncondensables was also necessary.

To meet the above requirements , the following design considerations were taken into account :

3.1.1 LAYOUT OF TUBES

For the sake of fabricational and experimental convenience ,it was considered desirable to limit to four rows' condenser with one tube in each row in a vertical grid. The tubes employed were 341 mm long and 25 mm inside diameter, having l/d ratio of 13.64.

WATER V1

STEAM FROM BOILER

U-LOOP

1. WATER TANK
2. TEST CONDENSER
3. PERFORATED PLATE WITH CUP
4. VAPOR GENERATOR
5. CONDENSATE VESSEL
6. VESSEL
7. ROTAMETER
8. WATER PUMP
9. CONDENSATE PUMP
10. HEATER
11. MECHANICAL HAND
12. CONDENSER TUBE (I, II, III, IV)
13. CONDENSATE TRAY
14. STRAINER
15. VENT
16. PRESSURE REGULATOR
17. OVER FLOW PIPE
18. FLANGE COVER
19. CONDENSATE ROTAMETER
20. WATER HEADER

PRESSURE GAUGE

RELIEF VALVE

GLOBE VALVE

GATE VALVE

NON RETURN VALVE

INSULATION

TO DRAIN

TO DRAIN

FIG.3.1. SCHEMATIC DIAGRAM OF THE EXPERIMENTAL SET-UP

31

FIG. 3.2. PHOTOGRAPHIC VIEW OF EXPERIMENTAL SET-UP

One of the important conditions for accurate data was to hold the tubes in horizontal position. As a matter of fact, any deviation from this makes the condensate slide also along the length of the tubes . But for accurate data the condensate should only slide circumferentially. To safe-guard against this possible error of the condensate sliding along the tubes, special home-made check-nuts were used to hold the tubes in horizontal position. With the provision of these check-nuts the pitch between the tubes could not be less than 5d ,which is about three times greater than the usual pitch of 1.6d. It is important to mention that the pitch between the tubes is not going to affect the value of condensing heat transfer coefficient. This, in fact ,is in accordance with the findings of Chen(34). Thus the data conducted on tubes lying on a pitch of 5d will also be applicable to the condenser with its tube layout on a pitch of 1.6d.

Calming section of 70d upstream and 20d downstream of each of the condenser tubes ensured the fully developed hydro-dynamic flow condition of the cooling water in each tube.

The measurement of temperature of cooling water at the inlets and outlets of the test condenser's tubes was another important consideration. As the inlet cooling water temperature was the same for all the tubes , its measurement at the inlet of first row tube was considered sufficient. For the temperatures of the cooling water at the outlets of the tubes, thermocouples were employed. Copper- constantan thermocouples measured these temp-eratures. A thermocouple, installed before the upstream-calming section of the first row tube, measured the temperature of

cooling water entering the tubes. For the outlet temperature of the cooling water , each tube had its own thermocouple installed after its downstream-calming section . This was necessary, otherwise the installation of thermocouples just at the inlet and the outlet of a given condenser-tube would have caused a change in the flow pattern of the cooling water flowing in it and thereby its heat transfer coefficient. Further, to eliminate any possibility of change in temperature of cooling water while flowing through the calming sections of the tubes due to exchange of heat with the atmosphere,the calming sections were thermally insulated. Thus, the respective readings of the thermocouples were taken as the temperatures of cooling water at the inlet and outlet of a given condenser tube.

It was equally important to ensure that condenser tubes were full of cooling water for all values of flow rates. This was achieved by installing an inverted U-bend to the exit of each tube.

3.1.2 MEASUREMENT OF THE WALL TEMPERATURES OF THE CONDENSER TUBES

To obtain the thermal response of each condenser tube, it was necessary to mount thermocouples over the entire surface of each tube at as many places as possible both along its length and circumference. In view of the small diameter of the tubes (O.D. 28.8 mm) , and practical difficulties of embedding thermocouples in the wall of the tubes, it was possible to embed only three thermocouples 90º apart along the circumference of each tube.

Due to variation in temperature and heat transfer

34

coefficient of the cooling water flowing inside the tubes of the test condenser , the wall temperature of each tube varies continuously along the length . It is a fact that it is not practically possible to obtain experimental values of wall temperature at too many places so as to represent a continuous distribution of it along the tube. This, indeed , is in view of the fact that the installation of too many thermocouples on the outer surface of the tube will alter the flow pattern of the condensate along the tube and thereby the wall temperature distribution. This demands that the number of thermocouples should be the minimum so as not to affect the pattern of flow of the condensate appreciably and at the same time the temperature distribution along the length of the tube based on the readings of these thermocouples should not deviate much from the actual distribution. As a matter of fact , for such situations it is adequately enough if the tube is considered to be consisting of several small segments in series and in every segment the wall temperature is assumed to be constant but of different magnitude to that in neighbouring segments. To measure the temperatures of these segments, thermocouples are installed at around mid-points of the segments. Thus the reading of each thermocouple is taken, without any appreciable error , as temperature of the entire length of the isothermal segment. Keeping in view the fact that the tubes of the test condenser were of short length , it was considered sufficient to divide each tube in four segments for the purpose of measurement of its wall temperatures.

The fact that the heat transfer coefficient of the

cooling water decreases at a maximum rate in the leading edge region of a tube suggests that the segment containing the leading edge should be smaller than the other segments. With these considerations in view the segments were 71 mm, 100 mm, 100 mm, and 70 mm long as shown in Figure 3.4 (a).

The thermocouples were of copper-constantan of 32 gauge having bead diameter of about 0.5 mm. They had insulating coating, followed by sleeves. At each predetermined position , a hole of 0.25 mm depth was drilled on the wall thickness of the tube by using a 1 mm drill bit. The hole was filled up with solder after filling it first with special flux. The thermocouple bead was finally coated with solder and was inserted into the hole in the wall of the tube by the help of a hot soldering iron. When the bead dipped half into the molten solder in the hole the extra solder present in the hole oozed out by the side of the bead. Then the protruded portion of the bead was levelled with the solder so as to give a curvature similar to that of the tube. After this, the solder around the bead was carefully grounded using emery paper. In fact, the installation of the thermocouples and the measurement of the temperature by them were carried out as detailed in (53,54,55). While grinding, a care was exercised to ensure that the surface did not have any crest or trough left on it. This was considered very important otherwise the thickness of the condensate at the crest would have been different than on the smooth surface of the tube, and thus the temperature maintained would have been more than the actual value. If the surface had a trough ,then the condensate collected there would have

36

remained without being rolled down the circumference of tube .
Thus the thermocouple readings would have been lower than the
actual value.

The condensate, if allowed to come in contact with the
thermocouple wire, would impair its insulation and cause erratic
functioning of the thermocouples. To circumvent over this diffic-
ulty, the thermocouple wires were covered with the teflon sleeves.

A proper colour coding was adopted for different
thermocouples for the identification of thermocouple wires.

3.1.3 TEMPERATURE OF STEAM BULK

The measurement of steam bulk temperature was another
important consideration. Due to distinct difference in the densi-
ties of steam and air, a stratification between them is inevi-
table. This amounts to a temperature variation in the steam bulk
from bottom to top of the test condenser. When the steam is free
from air , its temperature shall be uniform throughout and equal
to saturation temperature corresponding to the steam pressure.
Therefore, in order to be sure that the steam is not contaminated
with the air, it was felt necessary to install two copper-
constantan thermocouples to measure the temperature in the
vicinity of the top - and the bottom-tubes and compare their
readings.

3.1.4 DRY, SATURATED AND QUIESCENT STEAM

The present investigation was to conduct experiments
for the condensation of dry , saturated and quiescent steam on
tubes . Any deviation from this evidently would lead to error in
the experimental data. Therefore, a provision of an upright U-

37

loop having a vertical drain pipe with steam trap at its free end in the pipeline connecting the boiler to test condenser was necessary in order to remove the condensate from the steam coming from the boiler before entering the test condenser. As a matter of fact , the condensate flowing with the steam while passing through the U-loop will obviously fall into the vertical downtake pipeline and finally emerge out to atmosphere via steam trap. Also there was a need to thermally insulate the steam carrying pipeline adequately in order to eliminate the condensation of steam in it due to the dissipation of heat to atmosphere. In this way the steam to the test condenser was made dry and saturated. The steam pressure was maintained by means of steam pressure regulator manufactured by M/s. Spirax Marshall, Poona (India). To maintain a quiescent environment of steam around the tube bundle it is imperative that the steam should impinge on a suitable baffle before it comes in contact with tube bundle, thereby reducing its velocity to a practical possible minimum value. For this purpose the steam inlet nozzle of the condenser should be off-line to the vertical grid of the condenser tubes.

3.1.5 PURGING OF AIR/NONCONDENSABLES FROM THE TEST CONDENSER

The presence of small percentage of air/noncondensables in condensing steam reduces the condensing heat transfer coefficient drastically. For instance, a concentration of just 2.0 % in the condensing steam lowers the heat transfer coefficient to 30%. Therefore, it was of utmost importance that the condensing steam was free from air/noncondensables. This was achieved by providing

a vent. To check that the condensing steam was free from air/non-condensables,the temperature of the steam was measured. When the reading of thermocouple was found equal to saturation temperature corresponding to the pressure of steam , it was taken that the steam was free from air/noncondensables.

3.1.6 INSTRUMENTATION

The measurement of the wall temperature of the condenser tubes was the most ticklish.

Calibrated copper -constantan thermocouples were employed to measure wall temperature of the tubes at various points. The temperatures of outer surface of the tubes were likely to undergo considerable fluctuations. This was so due to the periodic enveloping of the tube surfaces with condensate layer followed by detachment at the bottom-regions of the tubes. The above behaviour of condensate flow produces periodic wall temperature fluctuation and ,in turn,makes the measurement of it difficult. The above problem was tackled through quasi-steady state concept. Plotting of wall temperature profiles showed that it was periodic in nature and repeated itself after a certain interval of time. It was also found that a wave with a small amplitude rode this periodic wave . To find the time averaged value of the temperature signals, a hard-ware integration scheme seemed to be reasonably suitable in view of its being fast in processing large number of data points accurately.

3.2 EXPERIMENTAL FACILITY

Figure 3.1 shows the schematic diagram of the experimental facility. It mainly consisted of test condenser[2], vapour

generator[4], condensate vessel[5],overhead cooling water tank[1], steam pressure regulator[16],cooling water pump[8], condensate pump[9] and instrumentation for temperature and liquid flow measurements.

3.2.1 TEST CONDENSER

Figure 3.3 exhibits the details of the test condenser employed in the present investigation. It was a rectangular hollow vessel[1] made of 304 stainless steel having 750 mm height, 300 mm length and 310 mm breadth. It had a flange [15] on the left hand side of the condenser. A perforated plate with cup [6,7] served as a baffle to the entering steam to the condenser. As a matter of fact, the perforated plate had many holes such that the sum of the flow areas of the holes was several times greater than that of the steam-carrying pipe to the condenser. The cup was oriented inline with the steam inlet nozzle of the test condenser so that the entering steam after undergoing an impact with it and thus losing its velocity, rebounded up to the top wall of the condenser vessel . Then the steam flew through the holes of the perforated plate . During the above process the velocity of the steam was practically reduced to a very low value; thus an almost quiescent steam atmosphere around the tubes of the condenser was achieved.

The test condenser had four 304 stainless steel tubes of 28.8 mm O.D. , 25 mm I.D. and 341 mm length placed hori-zontally in a vertical grid. The distance between two tubes was 97 mm. The top tube was placed 130 mm below the perforated plate.

Eight home-made check -nuts with matching rings and
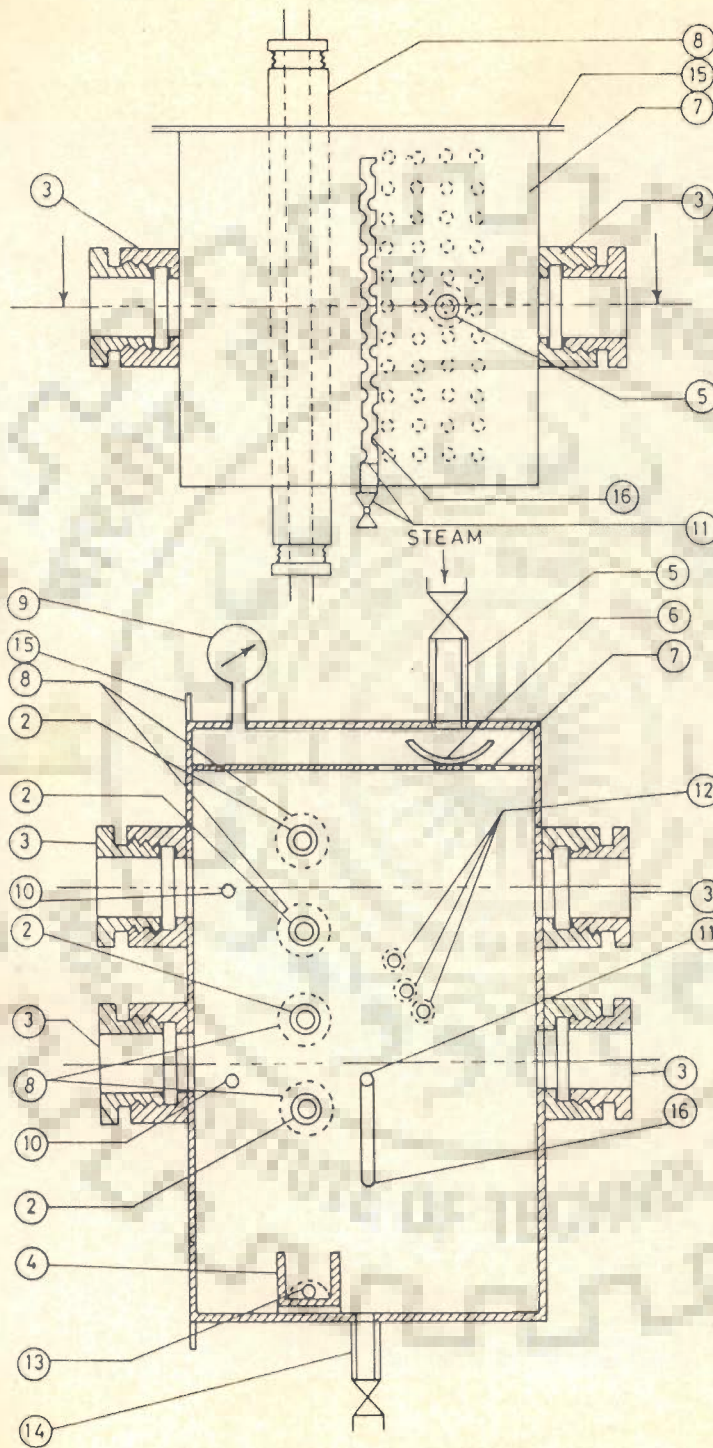
1. Shell of test condenser
2. Tubes
3. View ports
4. Condensate tray
5. Steam inlet
6. Cup
7. Perforated plate
8. Check-nut
9. Pressure gauge
10. Thermocouple adapter
11. Vent
12. Adapter for mechanical hand
13. Condensate drain for (4)
14. Drain
15. Flange
16. Z-Shape pipe

FIG. 3.3. DETAILS OF TEST CONDENSER

gasket kept the four condenser tubes in perfect horizontal position in a vertical grid without any leak of steam. Figure 3.5 (a) shows the details of this arrangement. A special fabricational technique with stress relieving made it possible to keep the check-nuts in perfect alignment even after welding. With the help of different matching ring pairs,the check-nuts could accommodate any tube diameter equal to or smaller than 40 mm.

Figure 3.4(a) shows the lengths of isothermal segments in which each tube was considered to be divided. The length of I,II,III and IV segments were 71 mm,100 mm,100 mm and 70 mm respectively.

For the measurement of outer surface temperature of the tubes, forty eight 32 gauge copper-constantan thermocouples in all were embedded on the condenser tubes at various points, as shown in Figure 3.4(b). As a matter of fact there were twelve thermocouples on each tube at four cross sections marked by x [=1,2,3,4]. Each cross section was provided with three thermocouples, placed at top-,side- and bottom - regions of the tube, as shown by the dots[.] on the tube.

Thermocouples marked 1,2 and 3 measured the wall temperature of the segment I of the first row tube at the top-,side-, and bottom-regions, respectively at x = 1. Number and position of these thermocouples and also of other wall thermocouples for all the four isothermal segments of each tube are shown in Figure 3.4 (b) and Table 3.1.
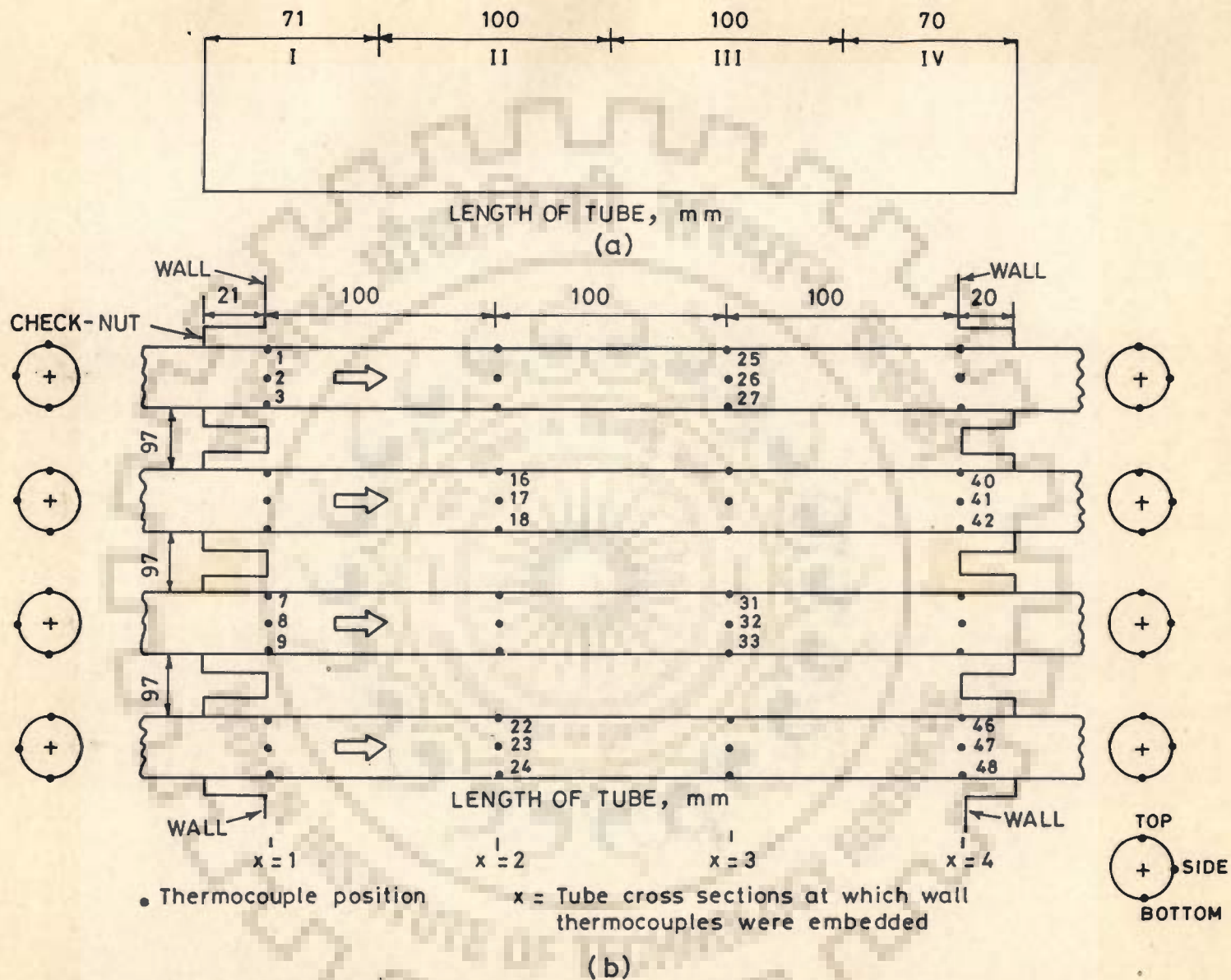
FIG. 3.4. (a) ISOTHERMAL SEGMENTS

(b) WALL THERMOCOUPLE NUMBERS AND THEIR LOCATIONS ON THE TUBES OF THE TEST CONDENSER

Table 3.1 Number of thermocouples on tubes of the bundle

segments	position	tube row			
		first	second	third	fourth
		thermocouple No.			
I	T	1	13	25	37
	S	2	14	26	38
	B	3	15	27	39
II	T	4	16	28	40
	S	5	17	29	41
	B	6	18	30	42
III	T	7	19	31	43
	S	8	20	32	44
	B	9	21	33	45
IV	T	10	22	34	46
	S	11	23	35	47
	B	12	24	36	48

T = top ; S = side ; B = bottom

The arrangement for taking out thermocouple leads from the test condenser is shown in Figure 3.5(b) . The surface thermocouples were divided into four bunches. Each bunch containing twelve thermocouples was passed through a 12 mm stainless steel tube sealed with araldite and m-seal at its both ends. Compression type fittings were used to hold the stainless steel tubes with the test condenser without any leakage to atmosphere . A similar arrangement was used for the mechanical hand, as detailed in Figure 3.5(c). The speciality of these fittings was to give a perfect leak proofing by applying a small torque on the nut[4].

Figure 3.6 gives the details of mechanical hand . It had two projected arms [1] soldered to the main scale [9]. The free ends of the arms had leaf springs [8]. The free end of each

(a)

12

45

40

25

75

21

(b)

(c)
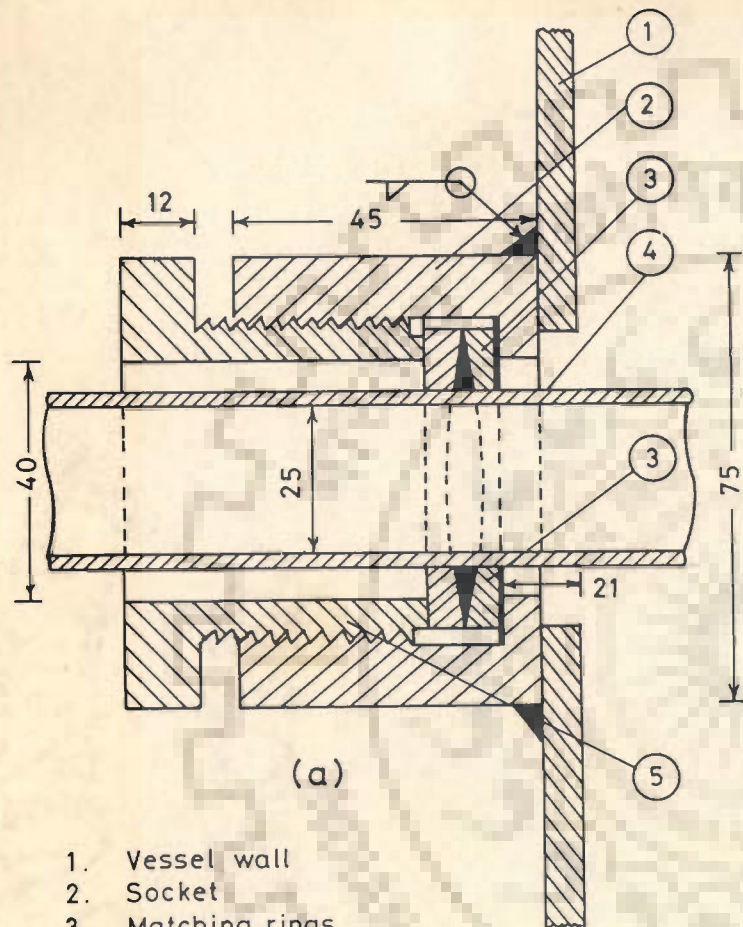
1. Vessel wall
2. Socket
3. Matching rings
4. Condenser tube
5. Check-nut
▪ Gasket

All dimensions in mm

1. Vessel wall 2. Socket
3. Teflon ferul 4. Check-nut
5. Driving rod

1. Socket 2. Teflon ferul
3. Thermocouple wires
4. S.S. Tube 5. Check-nut
6. Araldite 7. M-Seal
8. Vessel wall
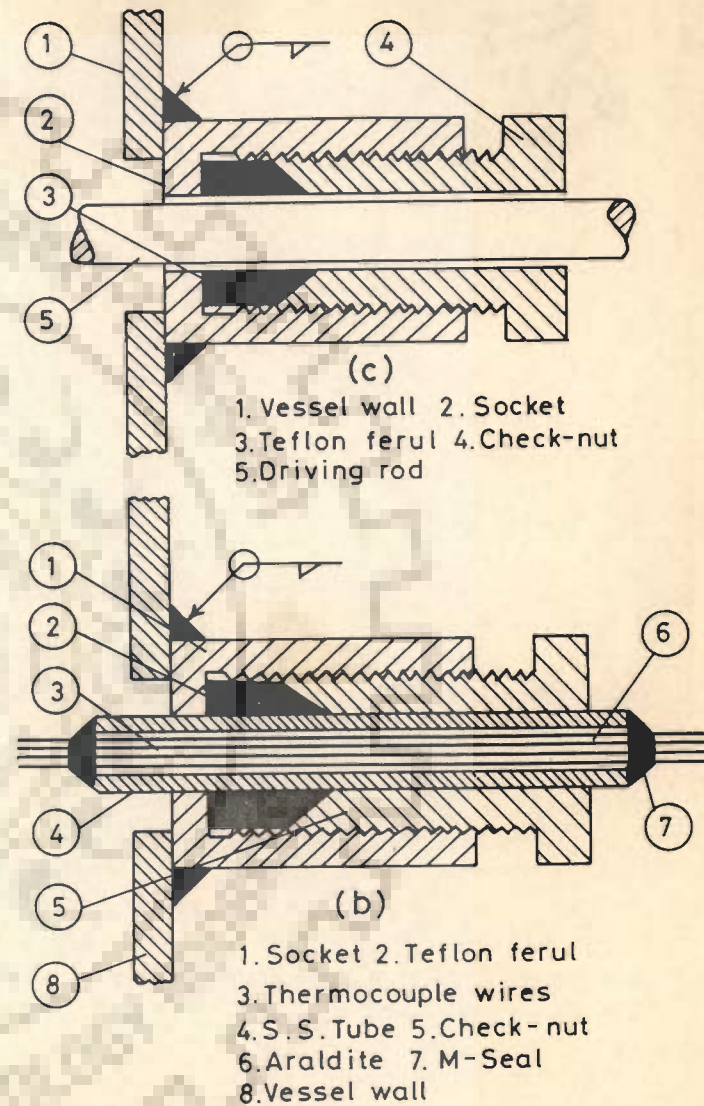
FIG.3.5. (a) CHECK-NUT TO HOLD CONDENSER TUBE
(b) COMPRESSION FITTING FOR DRIVING ROD
(c) COMPRESSION FITTING FOR TUBE CARRYING
THERMOCOUPLE BUNCH

TOP THERMOCOUPLE

20

10

25

19
18
17
16
15
14
13
12
11
10
9
8
7

1. Projected arm
2. Rack
3. Body
4. Graduated rods
5. Pinion
6. Vernier
7. Driving rod for body and scale
8 Leaf spring
9 Main scale
10 Thermocouple (⊷)

360

49

2
1
0
1
2

10

100

ALL DIMENSIONS IN m.m.

8
9
10
11
12
13
14
15
16
17
18
19

BOTTOM THERMOCOUPLE

10
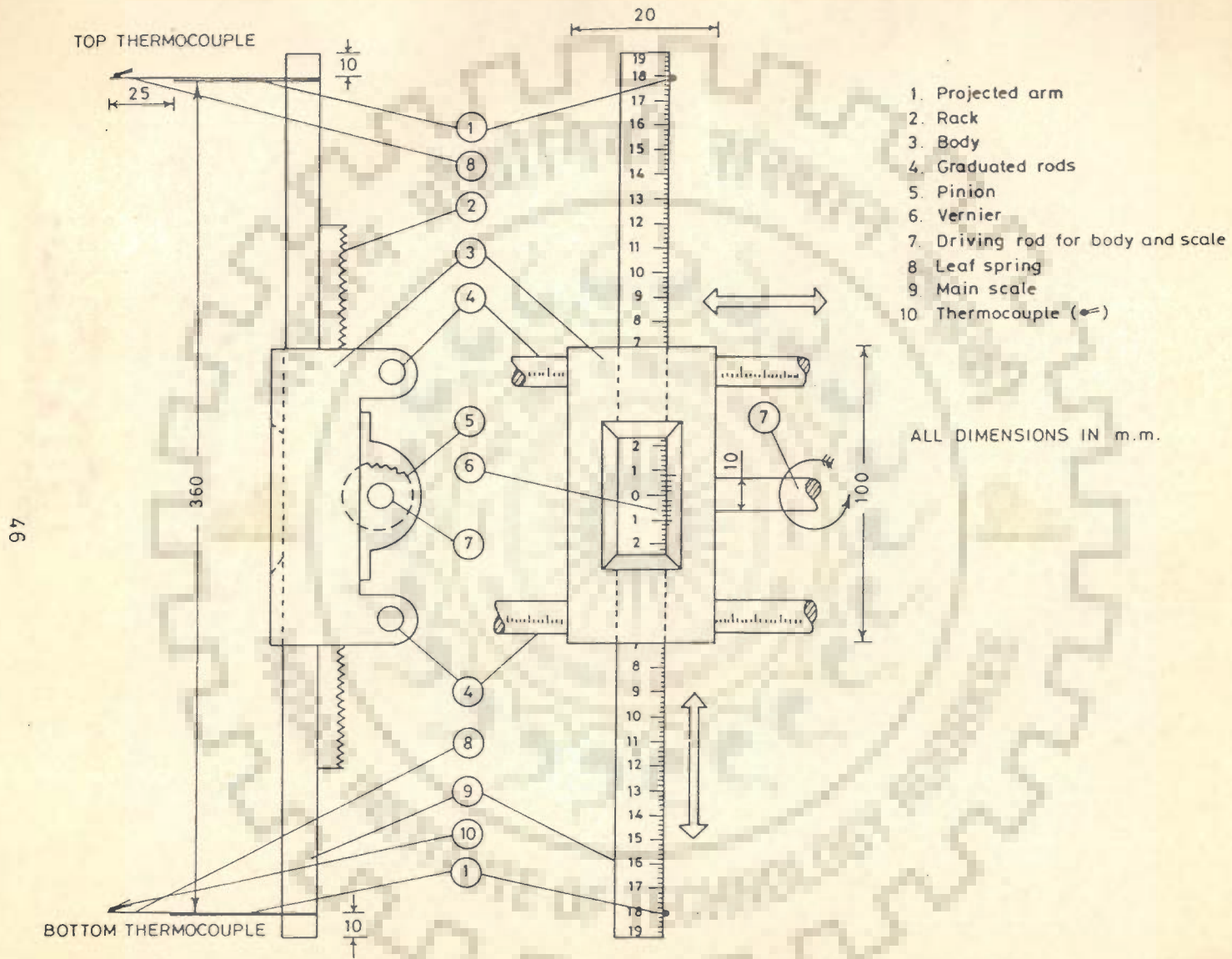
' FIG.3.6. DETAILS OF MECHANICAL HAND

leaf had a 32 gauge copper -constantan thermocouple[10]. These thermocouples were used to measure steam bulk temperature around the tubes of the test condenser. A rack [2] and pinion [5] arrangement was attached to the body [3] of the mechanical hand. The rack, in turn, was screwed to the main scale[10] . Thus the scale could move up and down as rack did. The vertical motion of the rack was achieved by rotating the driving rod [7]. With the help of main scale [9] and the vernier scale [6], attached to the body[3], the vertical position of each thermocouple in the vapour space could be determined within an accuracy of 0.1 mm. The thermocouples were moved horizontally by sliding the body [3] horizontally. A linear push / pull of driving rod [7] from outside the test condenser made the body slide in the horizontal direction on the graduated rods. The horizontal position of the thermocouples could be determined from the readings of the graduated rods [4].

Condensate tray[4] as shown in Figure 3.3 collected the condensate from the tubes. It was 100 mm wide,300 mm long and 100 mm deep. The tray was placed on the bottom surface of the test condenser vessel with an inclination of 20° with the hori-zontal plane. The tray was pitched so that the condensate could drain completely through the drain pipe[1] of Figure 3.3.

The vent [11]in Figure 3.3 was one of the most vital parts of the test condenser. This helped in driving off air/non-condensables from the system. For the present experimental faci-lity it was found that during start-up air/noncondensables accu-mulated in the vicinity of the fourth row tube . The vent, which

was placed at the mid-height of the test condensers was found to be less effective in removing noncondensables from the test condenser. To get rid of this problem a copper pipe[1], as shown in Figure 3.3, was attached to the condenser side end of the vent. The pipe was bent to form a Z- shape [16] with top horizontal arm and bottom horizontal arm 20 mm and 280 mm long, respectively with a vertical middle arm. The longer arm of the tube was made perforated and kept 50 mm below the fourth row tube. The Z-shaped pipe is detailed in Figure 3.3.

View ports [3] diametrically opposite on each side of the test condenser, as shown in Figure 3.3, allowed visual inspection of condensation phenomenon on all the four tubes.

The test condenser was thermally insulated to avoid condensation of steam due to heat dissipation from steam to atmosphere.

3.2.2 VAPOUR GENERATOR

A vapour generator was designed for producing organic vapours for studying their condensation on the tubes of the test condenser. The vapour generator had four immersion type electric heaters of 3 kW each, with a total capacity of 12 kW. It had a vertical slit to measure the liquid level accurately. The vapour generator was fitted with a demister made of 200 and 400 stainless steel wire mesh to remove entrained liquid particles from vapour and thus to supply a dry and saturated vapour. Safety valve, pressure gauge and temperature probes were mounted on the top lid of the vapour generator.

3.2.3 CONDENSATE VESSEL

It was a cylindrical vessel made of 304 stainless steel having diameter 250 mm and height 450 mm. This unit was to store steam condensate flowing from the condensate tray and then drained via valve V16, as shown in Figure 3.1. The condensate vessel was connected to the condensate pump to transfer organic condensate to the vapour generator. The vessel was properly insulated to ensure that the condensate did not dissipate heat to the atmosphere.

3.2.4 OVER-HEAD COOLING WATER TANK

It was a mild steel rectangular tank of 900 mm length, 450 mm breadth and 450 mm height painted with lead oxide to avoid rusting. The tank was connected with a 75mm overflow pipe[17], as shown in Figure 3.1, projected inside the tank to a height of 380 mm from its bottom so as to provide a constant water head in the tank. A 50 mm diameter pipeline connected it to the centrifugal pump[8].

3.2.5 COOLING WATER DISTRIBUTION SYSTEM

The water header [20] in the discharge line of the centrifugal pump [8] distributed cooling water to each of the tubes of the test condenser via respective rotameters [7].

A provision of inverted U-bend in the down stream end of the each tube helped in ensuring that each tube was always full of water for all cooling water flow rates.

3.2.6 INSTRUMENTATION

The main parameters requiring accurate measurement were wall temperatures of the condenser tubes, bulk temperature of

steam in the condenser vessel, inlet and outlet temperatures of cooling water , temperature and flow rate of the condensate from the condensate tray , and flow rate of cooling water in the condenser tubes. Figure 3.7 shows the detailed position of transducers and instruments employed in the present experimental set-up.

Accurate measurement of wall temperatures of the tube was important in view of the fact discussed in Section 3.1.6, that the wall temperatures were likely to undergo periodic fluctuations due to periodic variation in condensate layer thickness on the tubes. To understand the nature of signals and their amplitude of fluctuations , and the time periods of the periodic thermo-e.m.f. , the signals from all the thermocouples were first amplified 100 times with the help of a Kiethley 172 model DMM and then fed to a Digiscribe Series 5000 plotter. The chart speed was 12.5 cm/min and the plotter amplification was 1 volt full scale . Figures 3.8 (a),(b),&(c) show the nature of the fluctuations of the thermocouple signals for top-,side-, and bottom-regions of the first row tube respectively at a particular section.

From these plots it is clear that the fluctuations were of such a magnitude that it was necessary to find out the time-averaged value of thermocouple signals. For this purpose a suitable time period of integration was required which should be greater than the largest of all the time periods . An analysis of the plotted thermocouple signals showed that the maximum time period of the periodic wave was 6 seconds. Hence a time window

The diagram labels and legend are as follows:

1. DMM with GPIB interface
2. Z-80 Microprocessor
3. Cassette recorder
4. Pressure regulator
5. Rotameter
6. Pump
7. Condensate tray
8. Pressure gauge
9. Test condenser
10. Condensate tank
11. Level indicator
12. Selector switch
13. Strainer
14. Globe valve

• Wall thermocouple

ℓ Liquid thermocouple

✛ Travelling thermocouple (attached to mechanical hand)

TOP / SIDE / BOTTOM — Wall thermocouple positions on a tube

STEAM FROM BOILER

1750   500

KEITHLEY 192 DMM

GPIB

Z-80 μp

CASSETTE RECORDER

24 18 6 12 (×3)

All dimensions in mm

FIG. 3.7. DETAILS OF THE POSITIONS OF TRANSDUCERS AND INSTRUMENTS

51

(a) deviation ± 2.3%

(b) deviation ± 4.5%

(c) deviation ± 6.0%
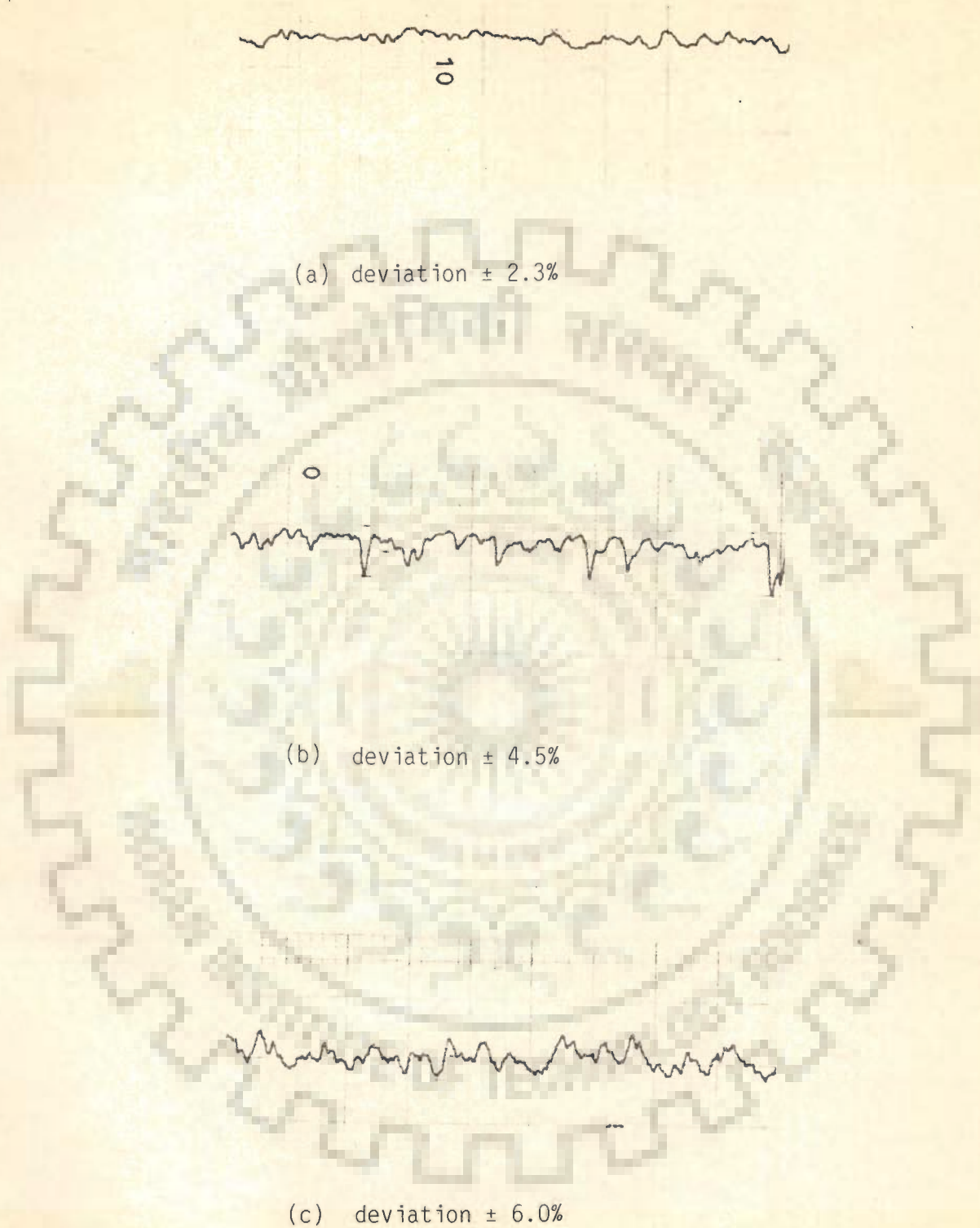
Fig.3.8 plot of transient thermo-e.m.f. for first row
tube at x=2,(a) top-region, (b) side-region,
and (c) bottom-region.

of 20 seconds for integration was considered adequate enough.

Integration of signals of a thermocouple were done in two steps. In the first step the signals were integrated for a period of 20 ms by using Keithley 192 model programmable DMM with IEEE-488 (GPIB) interface. The digital equivalents of the integrated signals were termed as data. These data were then sent to a Z-80 microprocessor once in a 125 ms interval for further integration for a period of 20 seconds. The necessary hard-ware and soft-ware for the interfacing of 192 model DMM and Z-80 microprocessor were developed in the Heat Transfer Research Laboratory, Chemical Engineering Department ,University of Roorkee , Roorkee(India). The listing of the soft-ware is given in Appendix D. Figure 3.9 shows the details of the hard-ware used for interfacing GPIB interface with Z-80 PIO. A provision for changing the integration period to 5,10 or 20 seconds through a selector switch B was there in the hard-ware. For the above scheme the DMM was used as a talker and Z-80 microprocessor as listener. The push-to-on switch A was used to initialize the timer of the Z-80 microprocessor. Once initialized, the timer started counting time and , depending upon the value of integration time period selected by selector switch B, it caused interrupt. At the same time,on the other hand, Z-80 microprocessor started scanning the intermittent data stream sent by the DMM. The DAV, NRFD and NDRC hand shaking signals were used for reading individual bits of the data. After one complete data (18 bytes) Z-80 microprocessor stripped off unnecessary information and the ASCII value was converted into binary integer value. Then

53
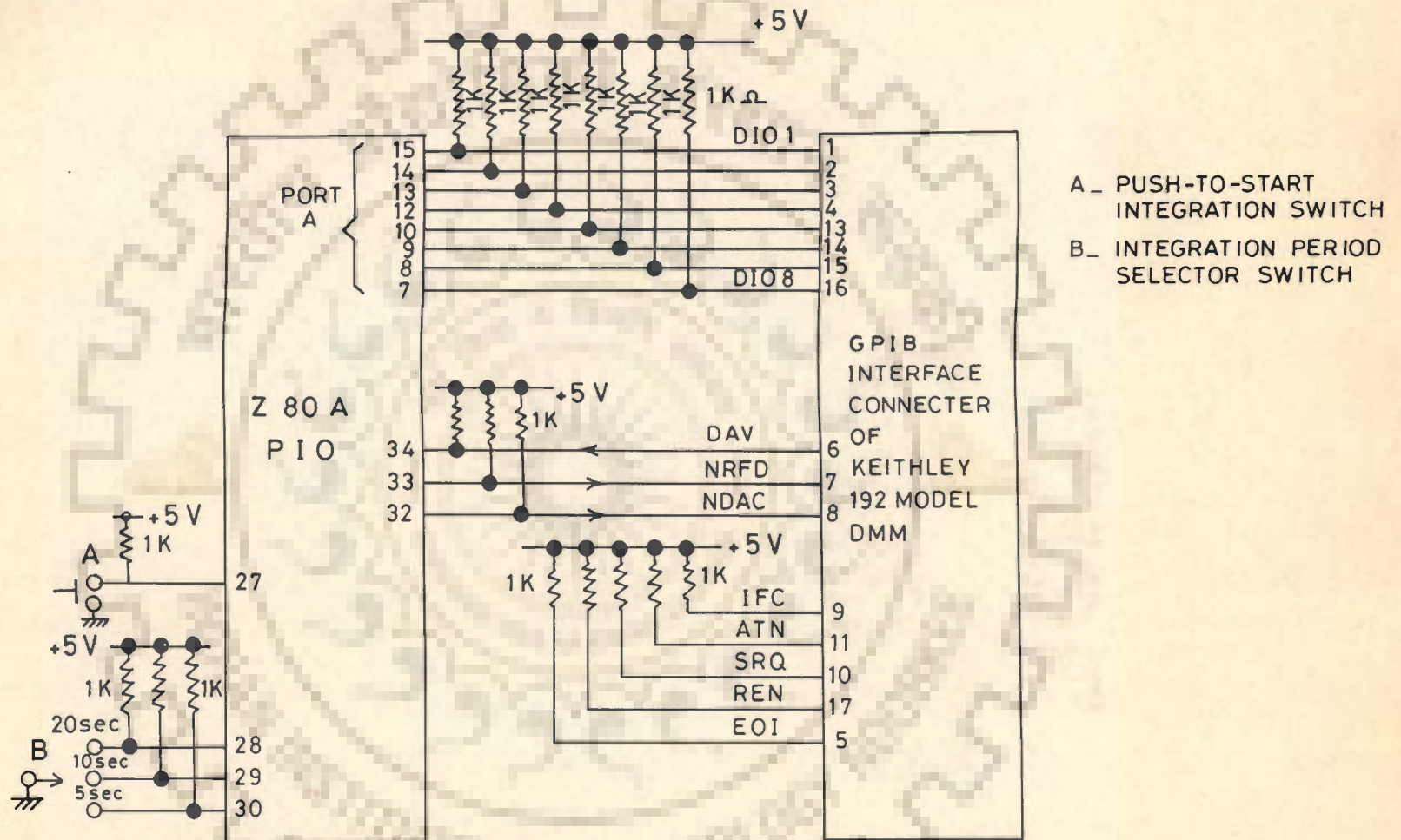
FIG.3.9. DETAILS OF HARD WARE USED FOR INTERFACING KEITHLEY 192 MODEL
DMM WITH GPIB INTERFACE WITH Z-80 MICROPROCESSOR

every subsequent data sent by the 192 model DMM was added to the previous one and a count of readings was updated. When the timer interrupted the CPU after a set interval of time , the total sum of the data values, along with the total number of data, were stored in a file with a predetermined file name. When the integration of a particular thermocouple's signals was over, the programme waited and the microprocessor blinked a green LED. The next push of the switch A restarted the programme for the integration of the next thermocouple's signals and so on. After the integration for all the 48 thermocouples' signals ,the integrated values were automatically stored in a file with a predetermined file name and were sent to a cassette recorder for storage.

The digital multimeters manufactured by Keithley Instruments ,Ohio ,U.S.A. were used . The 192 model programmable DMM was a 6 1/2 digit DMM with 1 microvolt least count in 200 mV range. The 177 model DMM had a least count of 1 microvolt in 20 mV range.

Top-and the bottom-thermocouples of the mechanical hand (Figure 3.6) measured the bulk temperature of steam in the test condenser , whereas the seathed calibrated thermocouples manufactured by M/s Thermo Electrics Ltd, Netherlands measured the cooling water inlet and outlet temperatures . The thermocouples of the same type were also used to measure the condensate temperature.

The calibrated rotameters with a least count of 0.1 lpm measured the cooling water flow rates. A home-made calibrated rotameter with 0.01 lpm least count measured condensate flow rate.

EXPERIMENTAL PROCEDURE

For conducting the experimental data for the condensation of steam on the tubes of the condenser the following procedure was followed :

The experimental facility was assembled as shown in Figure 3.1. The test condenser and condensate vessels were tested against the pressure integrity for twenty four hours after creating a pressure of five atmosphere and also against a vacuum of 600 mm of Hg. for the same duration of time.

The respective steam and water circuits were also tested against the leakage pneumatically and hydraulically.

All the thermocouples were calibrated before installation and were found to be accurate.After installation they were tested for their continuity. Their resistances were also measured with the help of 192 model DMM and compared amongst themselves to check for their satisfactory installation. They were also calibrated for a second time after embedding them in the walls of the tubes as follows: Cooling water at a given temperature was passed through the condenser tubes. After some time it was observed that the outlet temperature of the cooling water became equal to its inlet temperature. Then the readings of the wall thermocouples were noted . The off-sets of each thermocouple with respect to temperature of cooling water flowing through the tubes was calculated. Similar readings of the off-sets were obtained for different temperatures of the cooling water. It was found

that for different temperatures of the cooling water the off-sets for a given thermocouple was almost a constant value. While calculating the wall temperatures of the tubes, these values were considered along with the readings of the thermocouples. The pressure gauge was calibrated by dead weight pressure gauge tester . The rotameters were calibrated by collecting water for a given interval of time and accordingly the graduations on the scale were corrected.

First of all, the overhead water tank [1] was filled with the cooling water upto a given level by opening valve V1 in the water mains . In fact ,the overflow pipe line [17] regulated the water level in the tank and thus maintained a constant head on the suction side of the pump [8] . After this the water pump was switched on to push cooling water to water header [20] , from where water passed through rotameters [7] to the test condenser tubes I , II ,III & IV when valves V3,V4,V5 and V6 were opened. The water emerging out of the tubes was taken to vessel [6] and from there drained through valve V18. The flow rate of cooling water through all the four tubes of the test condenser was maintained the same by means of valves V3,V4,V5 and V6 and the by- pass valve V7.

An oil-fired boiler using demineralized water as boiler feed generated the steam. Before routing the steam to the test condenser , it was kept on passing through the downtake pipeline and draining via valve V19 till there was no scale coming out with the steam. After this valve V19 was closed and V20 opened. Thus any condensate formed in the steam pipeline during its flow

through U-loop fell into the downtake pipeline and flew to the drain via steam trap [14]. This way the steam was made dry and saturated . Now steam was sent to the test condenser by opening valve V9 and V10 after adjusting pressure regulator [16] at a given value of pressure. Before steam entered the condenser, air (non-condensables) was present there. For conducting data for condensation it was absolutely necessary that the steam should be free from air/non-condensables. To achieve this , valves, V11, V12 and V21 were kept open for some time. As the steam entered the test condenser , it displaced air to the atmosphere via air-vents [15]. During this process the readings of the thermocouples attached to mechanical hand (Figure 3.6) were intermittently recorded . The process continued till the readings of these thermocouples were the same and equal to the saturation temperature corresponding to the steam pressure in the test condenser . As a matter of fact , these thermocouples were installed to monitor the bulk temperature of steam. When bulk temperature was found equal to the saturation temperature of the steam , it indeed represented a steam with no air /noncondensables.

Now the valve V12 was closed and V13 opened to allow the condensate to flow from the tray to the condensate vessel [5] and finally to the drain via valve V16 . After this the experimental runs were conducted for a given value of cooling water flow rate in each tube and pressure of steam in the condenser vessel. Temperatures of cooling water at the inlet of first row tube and exit of each tube, bulk temperature of steam,

temperature of condensate and wall temperatures at various points on each tube were measured. The locations of all the cooling water, steam bulk-,condensate- and tube surface-thermo-couples are shown in Figure 3.7 . After some time, the steady state was attained and then readings of all the thermocouples , rotameters, and pressure gauge were recorded. This was repeated thrice at intervals of 30 minutes each to check the steady state and thereby the reliability and reproducibility of the data recorded were ensured.

Similar experiments were conducted for other values of cooling water flow rate keeping steam pressure constant. Similarly, experiments were conducted for different steam pressures. Table 4.1 lists the range of these parameters.

Table 4.1 Range of operating parameters

Steam pressure,kPa	Cooling water flow rate, lpm
269.38	11.6,13.8,15.8,17.1
244.85	11.6,13.8,15.8,17.1
195.80	11.6,13.8,15.8,17.1
146.75	11.6,13.8,15.8,17.1

RESULTS AND DISCUSSION

The present Chapter discusses the salient results obtained from the analysis of data of the present investigation and others, along with their interpretations. The experimental data are listed in Appendix A for the range of operating parameters given in Table 4.1.

5.1 CONSTRAINTS OF DATA ANALYSIS

One of the main objectives of the present investigation is to determine experimentally the distributions of local and average heat transfer coefficients for the condensation of steam on four short tubes in horizontal rows , placed in a vertical grid. This requires knowledge of wall temperature distribution along the circumference of each segment of the tubes(Figure 3.4(b)) and also the corresponding values of the heat flux.

Thermocouples for the measurement of wall temperatures of the condenser tubes along their circumferences have been embedded , as described in Section 3.2.1 , to a depth of 0.25 mm from their outer surface. This penetration depth is much smaller compared to the tube wall thickness of 1.5 mm. In fact , the temperature drop across a thickness of 0.25 mm is negligibly small. In view of this, the temperatures monitored by the thermocouples have been considered to be the outer surface temperature of the tubes at the respective thermocouple positions.

The appropriate method generally employed for calculating heat flux distribution is to consider the condenser tubes consisting of several isothermal segments as depicted in Figure 3.4(a). The heat flux for each isothermal segment is calculated indirectly by determining the change in enthalpy of the cooling water across it. This requires the knowledge of variation in temperature of cooling water along the tube.

In the present investigation, experimental facility allows the measurement of the temperature of water at inlet and outlet of the tubes only. The temperature of water at other distances from the leading edge of a tube, required for heat flux calculation, have been obtained by iterating the heat rate equation with heat balance equation and finally matching the calculated exit temperature of water with the experimentally determined value, as detailed in Appendix B.

The circumferential condensing heat transfer coefficient at the top-, side-, and bottom-regions on the tubes are calculated from the knowledge of the heat flux and the temperature drop across the condensate film at these places. Subsequently, employing the One Third Simpson rule, these values are used for calculating average heat transfer coefficient for various segments of each tube. The weighted average heat transfer coefficient for the entire tube is then calculated by summing-up the products of the average heat transfer coefficients of various segments and their lengths followed by dividing the value thus obtained by the length of the tube.

5.2 CONDENSATION OF VAPOURS

The condensation of saturated steam on the tubes lying in the first row of a horizontal tube bundle is different from that on tubes in other rows. As a matter of fact , the thickness of condensate on first row tubes is independent of the presence of the tubes in the other rows whereas the vice-versa is not true. For example , the thickness of condensate on second row-tubes is owing to two counts - condensation of vapours on them and also joining of condensate from first row tubes. Thus the thickness of condensate on second row tubes is greater than that on the first row tubes. Likewise , it increases further with the tube rows in a vertical downward direction. In this respect the condensation on tubes in the first row of a tube bundle is essentially the same as on a single tube. The condensation of vapours on a single horizontal tube has been widely studied. However, the condensation on tube bundles has not received the same amount of attention. In view of this ,the analysis of the data of the present investigation has been carried out in two separate sections dealing with condensation of steam on first row-tube on one hand ,and condensation on the tube-bundle on the other.

5.3 CONDENSATION OF QUIESCENT STEAM ON FIRST ROW TUBE

During the process of condensation of steam on a horizontal tube , the condensate flows from top-region to side- and then to bottom-region of it. Consequently, the circumferential thickness of condensate_layer at a given cross section of a tube becomes uneven being maximum at the bottom -

62

region, minimum at the top-region and in-between at the side-region of the tube. To appreciate the magnitude of thermal resistance offered by the condensate layer qualitatively for the condensing heat transfer , it is imperative to determine the variation in circumferential wall temperature of the tube as a function of operating and geometric parameters; namely, cooling water flow rate, steam pressure and distance of the cross section under consideration from the leading edge of the tube.

5.3.1 EFFECT OF COOLING WATER FLOW RATES ON CIRCUMFERENTIAL WALL TEMPERATURE OF FIRST ROW TUBE AT A GIVEN PRESSURE

Figures 5.1 and 5.2 have been drawn to represent the typical effect of cooling water flow rates on circumferential wall temperature of first row tube for the cross section(x=2) at a distance of 121 mm from the leading edge of it for steam pressures of 146.75 kPa and 269.38 kPa, respectively. The cooling water flow rate varies from 11.6 lpm to 17.1 lpm. An examination of these plots reveals the following characteristic features:

1. At fixed steam pressure and cooling water flow rate, the circumferential wall temperature at any cross section of the tube decreases from top-, to side- , to bottom- region of the tube.

2. The trend in change of temperatures at the top-, the side-, and the bottom- region of the tube is same for all water flow rates. However, the respective temperature values decrease with increase in water flow rates.

The above typical behaviour is attributed to the fact

63
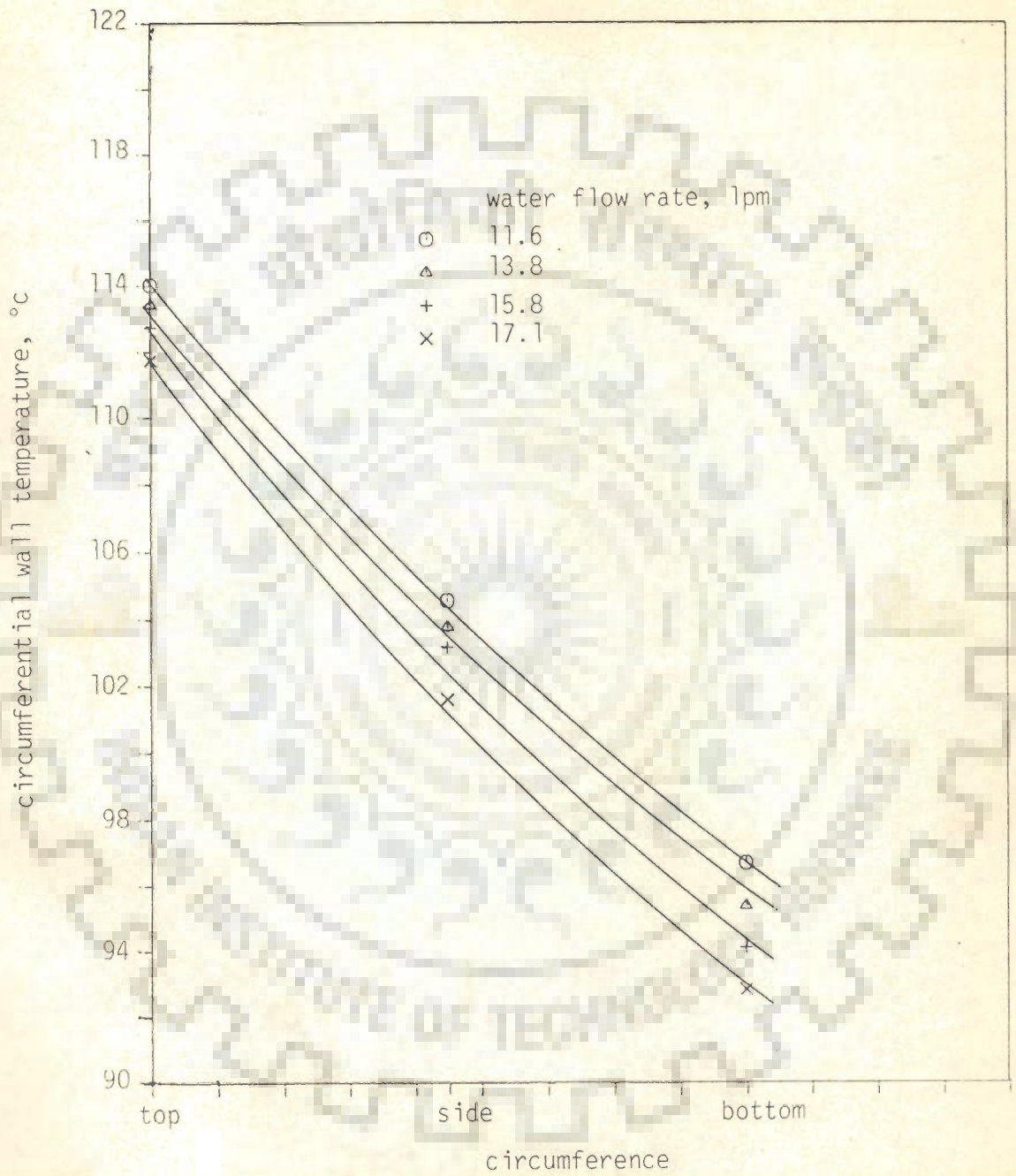
Fig.5.1 variation of wall temperature of first row tube
along the circumference (Ps = 269.38 kPa and x=2)

64
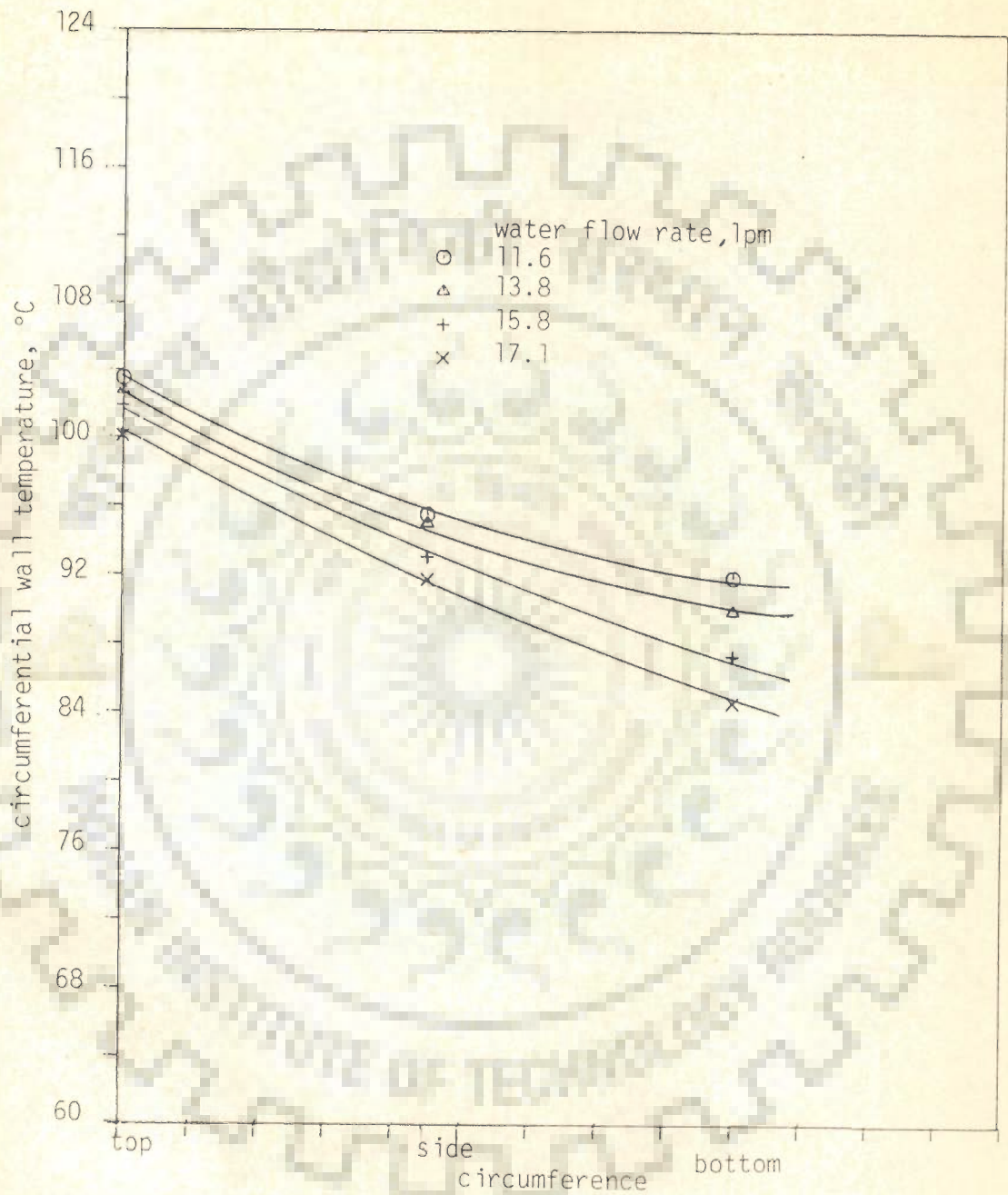
Fig 5.2   variation of wall temperature of first row tube along its circumference(Ps = 147.38 kPa and x=2)

that the thermal resistance to heat flow across the condensate layer increases from top- to side- to bottom- region due to increased layer thickness. Consequently wall temperature at the top-region attains a value followed by side-, and bottom-regions in decreasing order.

The decrease in circumferential wall temperature for a given steam pressure and cross section of tube with the rise in cooling water flow rate is attributed to the following facts : An increase in cooling water flow rate raises water- side heat transfer coefficient, which, in turn ,enhances the steam condensation on the tube. This increases the thickness of condensate layer on the tube, thereby an increase in thermal resistance to condensing heat transfer. As a consequence of it , the circumferential wall temperatures decrease with the increase in cooling water flow rate.

5.3.2 EFFECT OF STEAM PRESSURE ON CIRCUMFERENTIAL WALL TEMPERATURE OF FIRST ROW TUBE AT A GIVEN COOLING WATER FLOW RATE

Figures 5.3 and 5.4 show the typical effect of pressure on circumferential wall temperature of first row tube for a cross section at (x = 2) , 121 mm away from tube inlet, when cooling water flow rates are 11.6 lpm and 17.1 lpm, respectively. From these plots the following characteristic features are noted :

1. For a given cooling water flow rate , steam pressure, and cross section of the tube the circumferential wall temperature at the top-region of the tube is greater than that at the
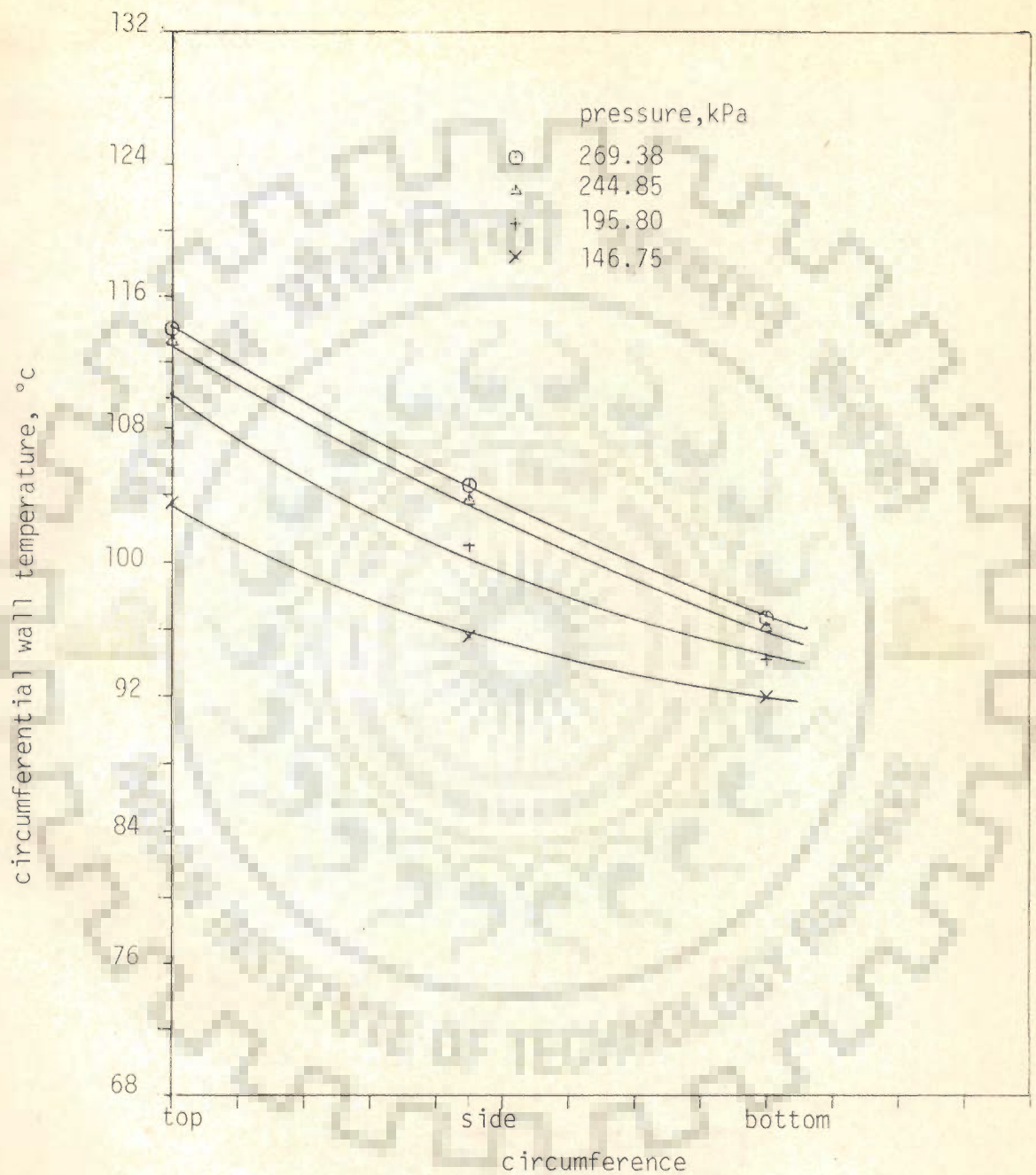
Fig.5.3   variation of wall temperature of first row tube along its circumference for various steam pressures (w = 11.6 lpm and x=2)
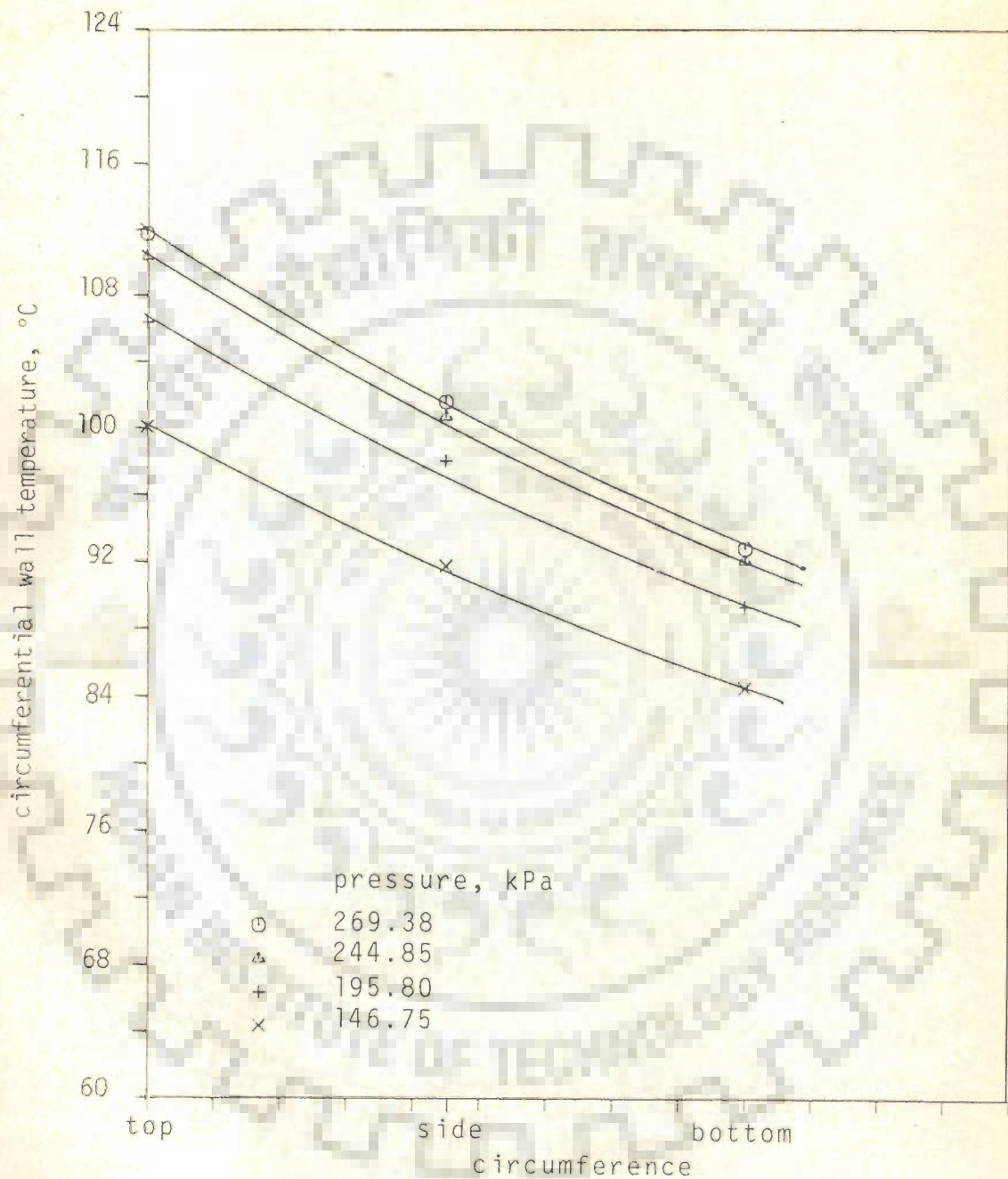
Fig. 5.4 variation of wall temperature of first
row tube along its circumference for
various steam pressure (w=17.1 lpm and
x = 2)

side-region and still greater than that at the bottom-region of the tube.

2. With the rise in steam pressure, for a given cooling water flow rate, the circumferential wall temperatures increase consistently.

As regards this typical trend of circumferential wall temperature distribution, the possible reasons have been discussed in Section 5.3.1. The above mentioned effect of steam pressure on the values of circumferential wall temperature can be argued as follows: When pressure of condensing steam increases, there is a corresponding increase in its saturation temperature. This, in turn, results in increasing the overall temperature difference between condensing steam and cooling water, thereby the rate of heat flow from condensing steam to cooling water also increases. This is possible only when temperature difference on water side, $(t_w - t_b)$ also increases, since water-side heat transfer coefficient remains almost constant. Further, the values of average bulk temperature of cooling water, t_b, in view of the high flow rates of cooling water in short condensing tube, do not change appreciably. This fact has been experimentally established in the present investigation. Hence any increase in the values of $(t_w - t_b)$ is possible only if the wall temperature of tube, t_w also correspondingly assumes greater value.

5.3.3 VARIATION OF CIRCUMFERENTIAL WALL TEMPERATURE ALONG THE LENGTH OF FIRST ROW TUBE

As shown in Figure 3.4(b), the present investigation provides information of circumferential wall temperature distri-

bution at four different cross sections ,21 mm ,121 mm , 212 mm and 321 mm away from the leading edge of the tube. Figures 5.5 and 5.6 have been drawn to represent the top-, the side-, and the bottom -region temperatures at these cross sections for respective steam pressures of 269.38 kPa and 195.80 kPa with corresponding cooling water flow rates of 11.6 lpm and 17.1 lpm. On inspection of these plots, the following observations are made :

1. A decreasing trend of circumferential wall temperature distribution from top-to side -to bottom-regions of the tube is observed at all cross sections investigated.

2. For a given flow rate of cooling water, and steam pressure,the circumferential wall temperatures at all cross sections of the tube increase steadily along the length of the tube.

This characteristic behaviour can be explained in view of the fact that the value of the water-side heat transfer coefficient decreases, while the bulk temperature of water increases along the length of the tube. Section 5.3.1 details this aspect of this observation. Due to this, the ability of cooling water to absorb heat from condensing steam worsens progressively along the tube and accordingly the rate of condensation decreases. Consequently the thickness of condensate layer also decreases. Thus the value of thermal resistance due to the condensate layer becomes less and less along the tube length which obviously makes the wall temperature rise progressively.
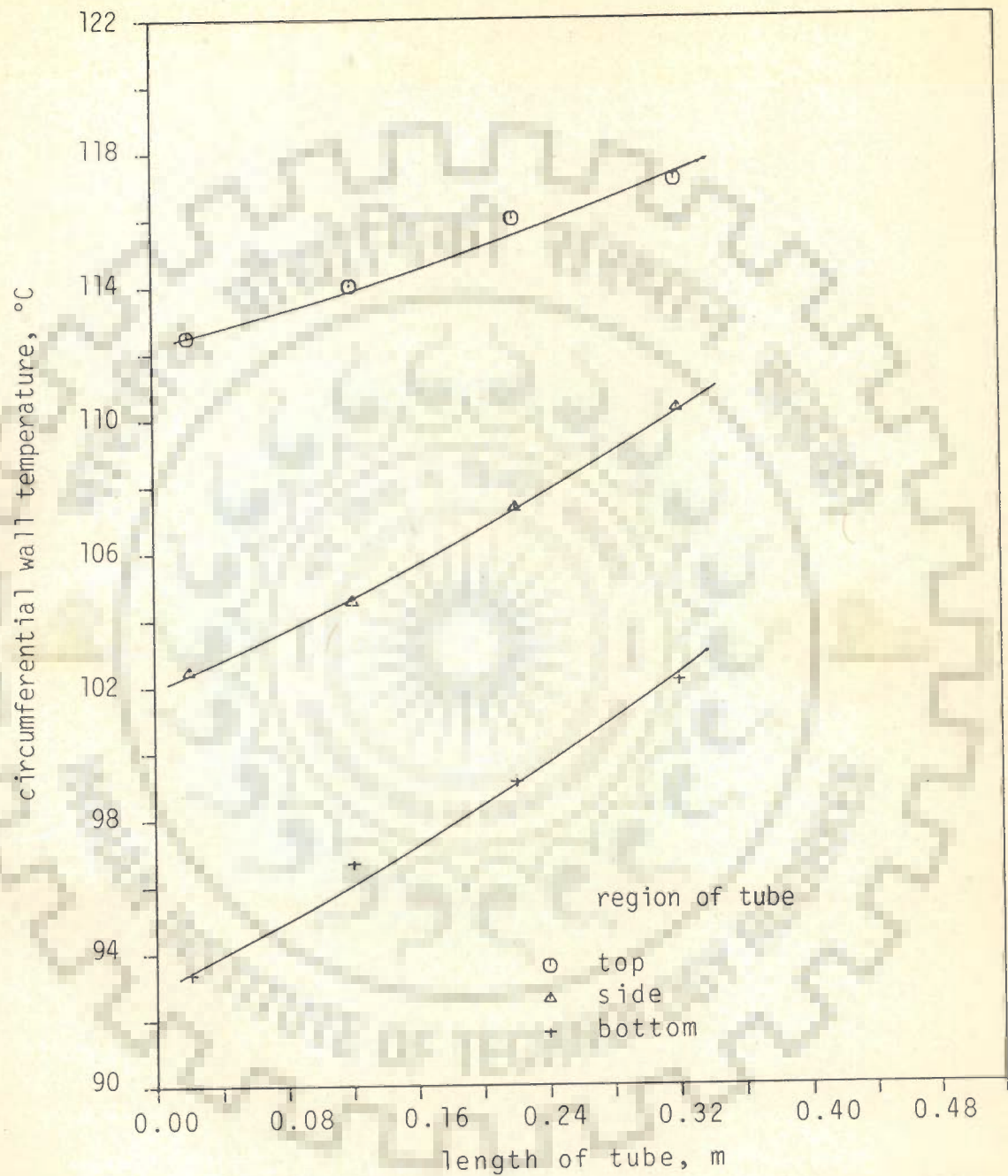
Fig.5.5   variation of top-,side-,and bottom-wall
temperature along the length of first row tube
(Ps=269.38 kPa,w=11.6 lpm)
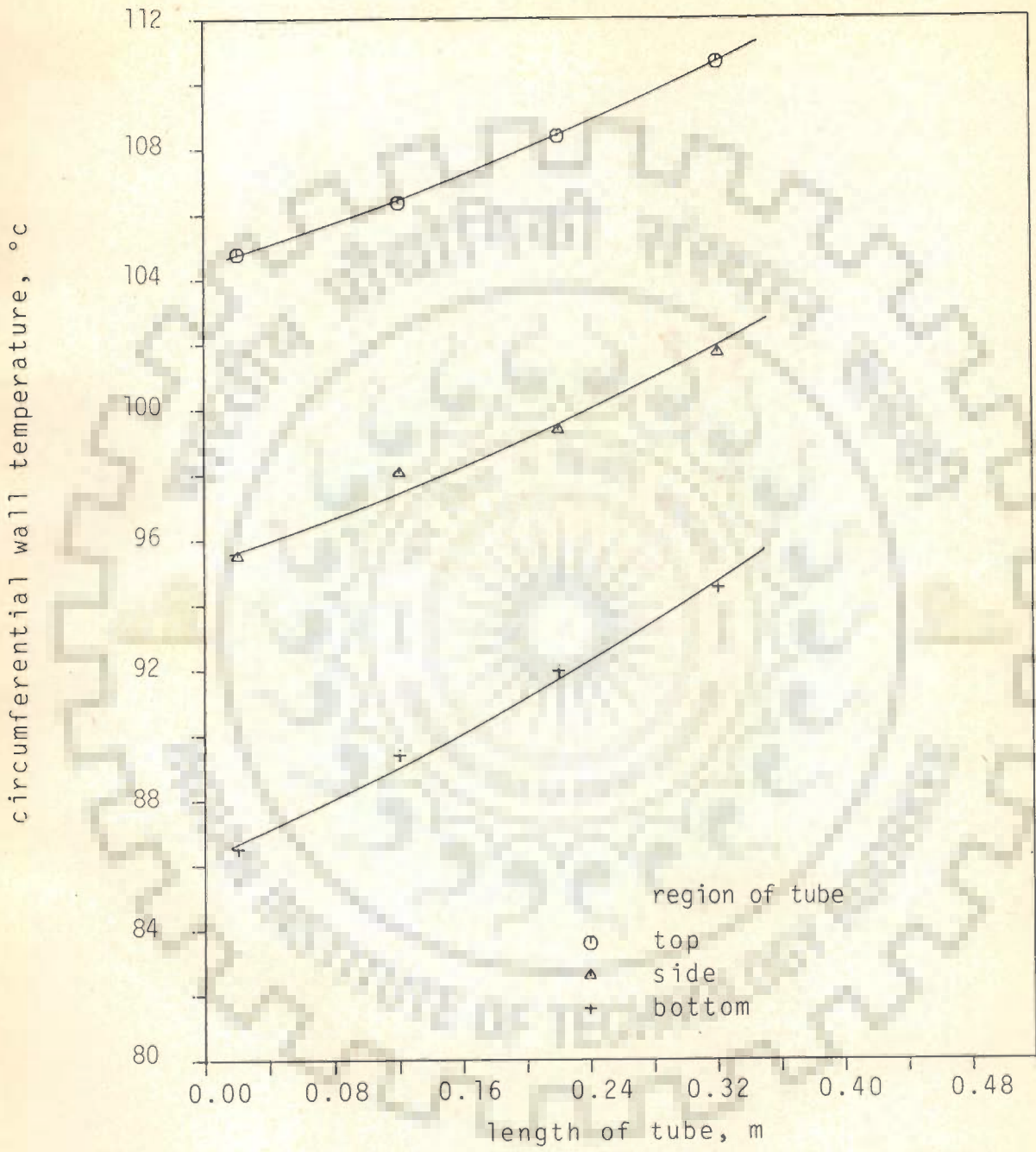
Fig.5.6 variation of top-,side-,and bottom-wall
temperature along the length of first row
tube (Ps=195.80 kPa,w=17.1 lpm)

72

5.3.4 EFFECT OF COOLANT FLOW RATE ON AVERAGE CIRCUMFERENTIAL WALL TEMPERATURE ALONG THE LENGTH OF FIRST ROW TUBE

A knowledge of the dependence of average value of circumferential wall temperature at various cross sections of the tube on cooling water flow rate is important to design engineers. The average values of circumferential wall temperatures have been determined as given in Appendix B.

Figure 5.7 represents a typical variation of average values of circumferential wall temperature along the length of the tube under a pressure of 244.85 kPa for various flow rates of cooling water. A scrutiny of this plot reveals the following characteristic features:

1. For a given flow rate of cooling water, the average wall temperature increases along the length of the tube. This observation is in conformity with the results discussed in Section 5.3.3.

2. For all cross sections of the tube, the average wall temperature depends on the cooling water flow rates: the higher the water flow rate, the lower is the average wall temperature.

This is primarily due to the increase in heat transfer coefficient of cooling water side with the rise in its flow rate. It, as a matter of fact, causes the condensation rate of steam to increase. In other words, thermal resistance across the condensate layer increases and thereby the average wall temperature falls with the increase in water flow rate.
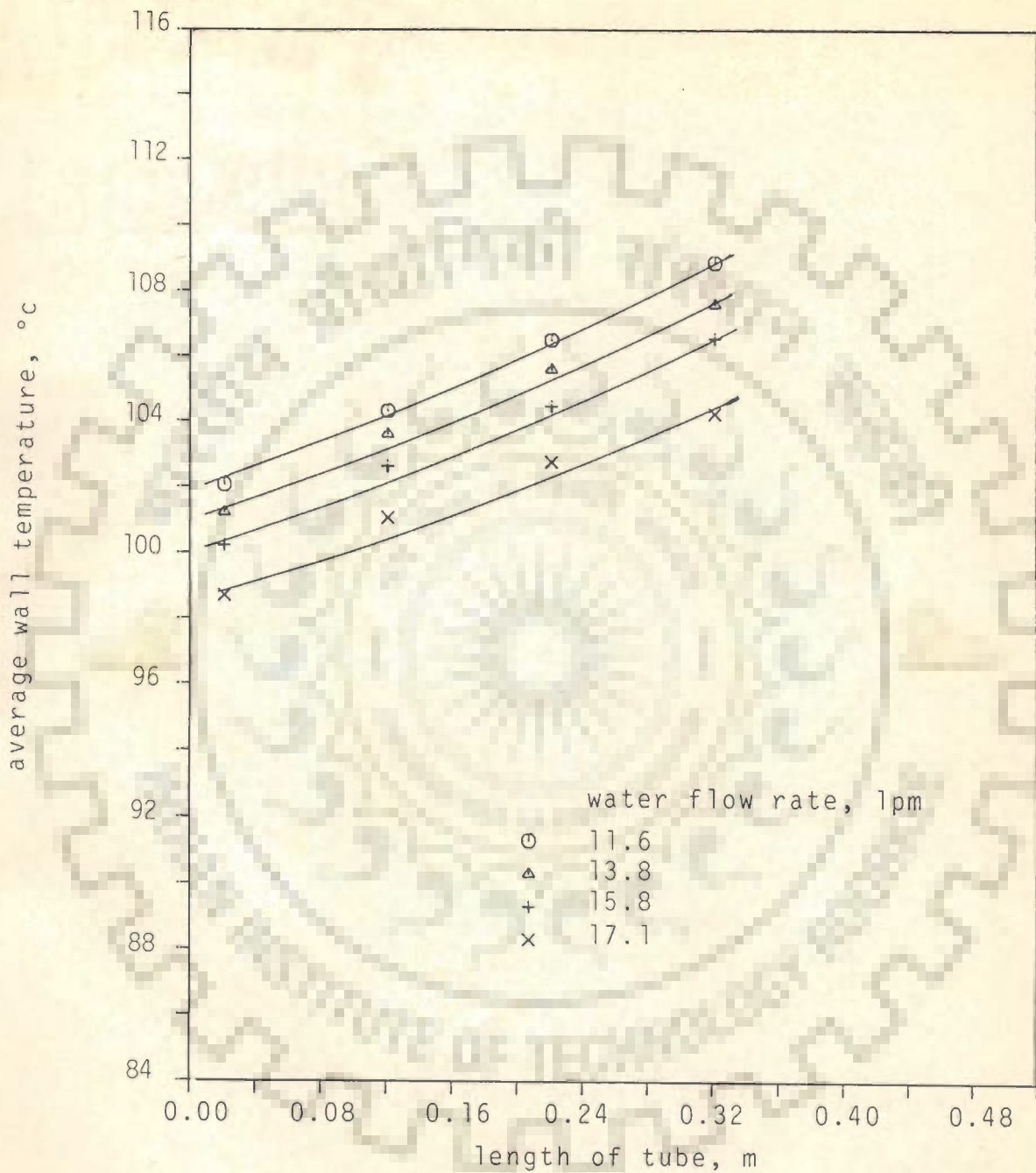
Fig.5.7   variation of average wall temperature
          along the length of first row tube
          for various cooling water flow rates
          (Ps=244.85 kPa)

74

5.3.5 EFFECT OF STEAM PRESSURE ON AVERAGE CIRCUMFERENTIAL WALL TEMPERATURE OF FIRST ROW TUBE

Figure 5.8 depicts the typical effect of steam pressure on average wall temperature of the tube when cooling water flow rate is maintained at 11.6 lpm :

1. For a given pressure, the average wall temperature of the tube increases along its length. In other words, the surface of tube becomes nonisothermal. This is explainable in view of decreasing value of water- side heat transfer coefficient and increase in the bulk temperature of water along the length of the tube. This causes a rise in the average wall temperature, as explained in Section 5.3.3.

2. For all cross sections of the tube, the average wall temperature increases with the rise in steam pressure. The possible reason for this behaviour is clearly explained in Section 5.3.2.

5.3.6 VARIATION OF COOLING WATER TEMPERATURE ALONG THE LENGTH OF FIRST ROW TUBE

For the condensation of steam on horizontal tube , it is important to know the variation in temperature of cooling water along its length. This information , in fact, helps in the determination of heat flux across various segments of the tube. Figure 5.9 represents a typical variation of cooling water temperature along the length of the first row tube ,when conden-sing steam pressure is maintained at 147.38 kPa . The cooling
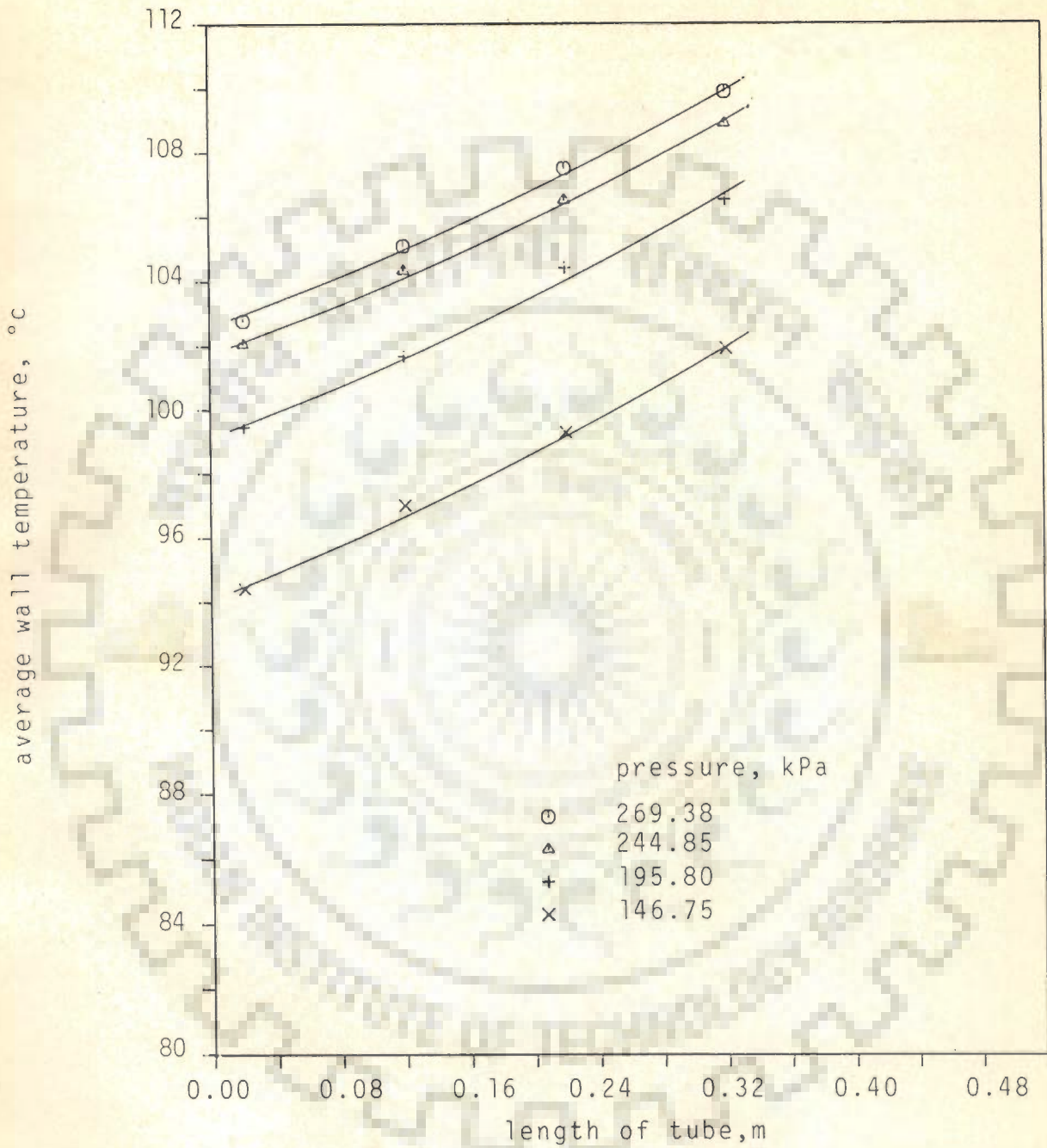
Fig.5.8 variation of average wall temperature
along the length of first row tube
for various steam pressures(w=11.6 lpm)

76
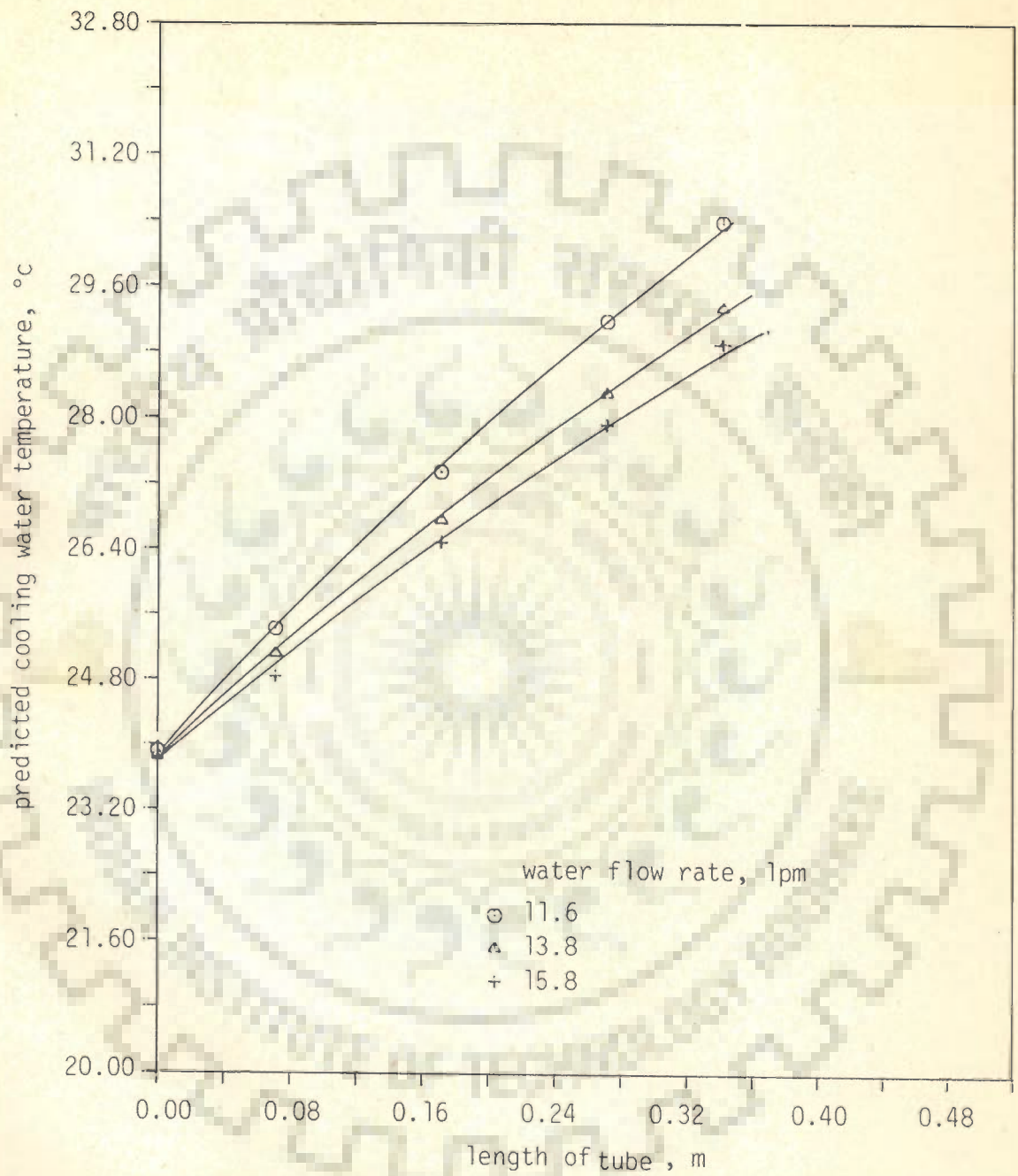
Fig.5.9 variation of predicted cooling water temperature along the length of first row tube for various cooling water flow rates (Ps = 147.38 kPa)

water temperature for all the flow rates of water increases linearly along tube length.The lines representing the temperature along the tube keep on shifting to left as the flow rate of cooling water is decreased. This , in fact, is an expected behaviour.

5.3.7 COMPARISON BETWEEN EXPERIMENTALLY- AND THEORETICALLY- DETERMINED COOLING WATER EXIT TEMPERATURE

Following the procedure, as detailed in Appendix B, the values of theoretically-determined cooling water exit temperature for different values of steam pressures and water flow rates have been calculated. The experimental set-up has the provision to measure these temperatures experimentally with the help of a copper-constantan thermocouple installed at the exit of the tube.

To compare these values , Figure 5.10 has been drawn between theoretically calculated and experimentally determined exit temperature of the cooling water. As is clearly seen from this plot, the two values agree well with each other, within 10%. In other words, it can be concluded that techniques used for the measurement of wall temperature ,cooling water inlet and exit temperatures and water flow rates are reasonably reliable , since cooling water exit temperatures , based on these values , compare well with the experimental values.

5.3.8 GENERALIZED CORRELATION FOR CIRCUMFERENTIAL WALL TEMPERATURE OF FIRST ROW TUBE

A nonlinear optimization method along with regression technique is employed to process the experimental data of
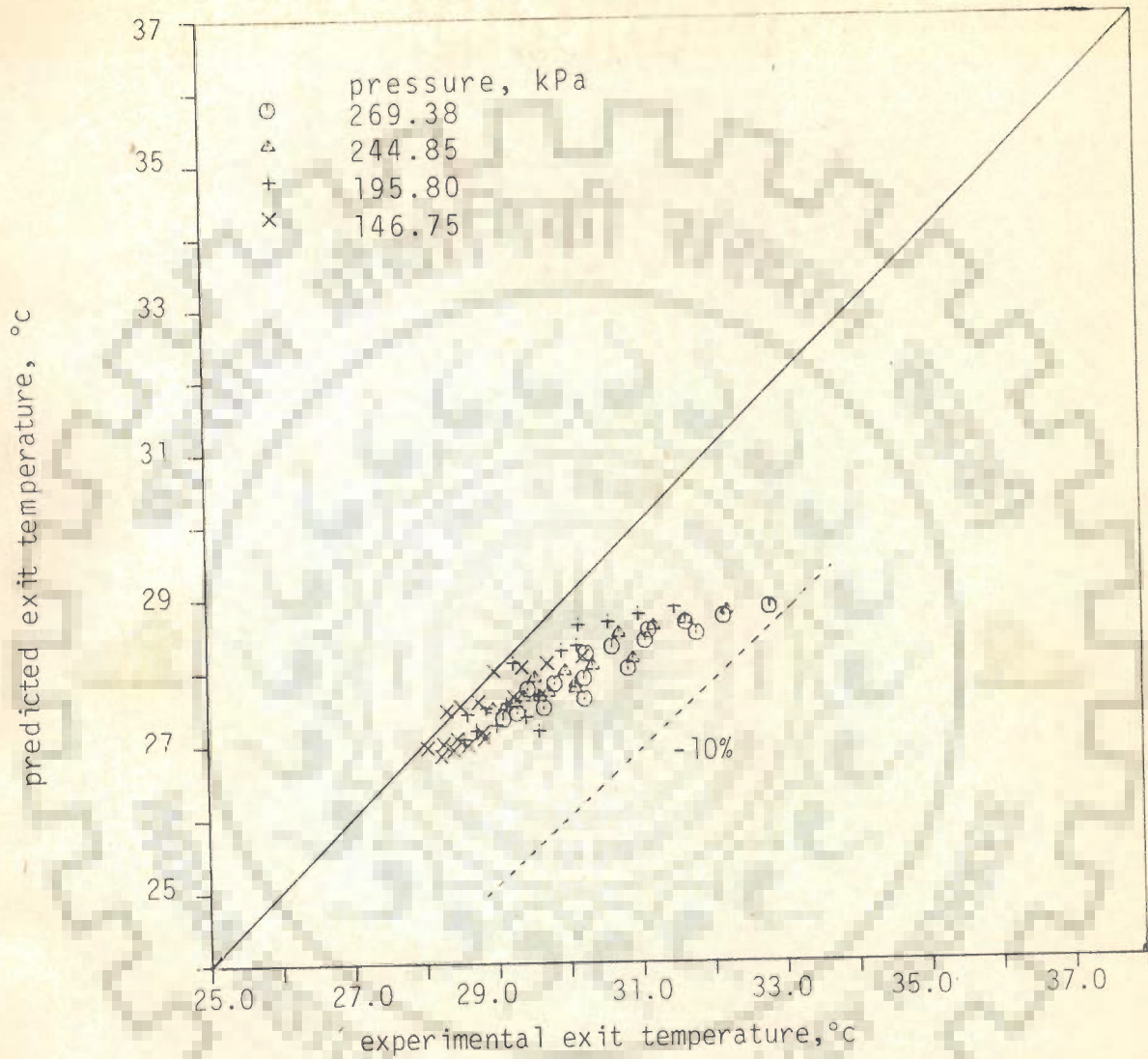
Fig.5.10 comparison between experimental and predicted cooling water exit temperatures.

Appendix A. Based on this method the following correlations are obtained to relate $t_{w,top}$, $t_{w,side}$, and $t_{w,bottom}$ with cooling water flow rate w, inlet temperature of cooling water t_i, pressure P and distance L , from the leading edge of the tube:

a. For top-region

$$t_{w,top} = 30.456 - 0.50452*w + 2.6995*t_i + 0.08577*P + 19.432*L \quad ...(5.1)$$

b. For side-region

$$t_{w,side} = 52.38 - 0.7241*w + 1.6326*t_i + 0.07538*P + 21.3662*L \quad ...(5.2)$$

c. For bottom-region

$$t_{w,bottom} = 76.77 - 0.9309*w + 0.6162*t_i + 0.05150*P + 26.2375*L \quad ...(5.3)$$

The values of wall temperatures predicted by Eqs. 5.1, 5.2 and 5.3 are plotted against the experimentally-determined values in Figures 5.11, 5.12 and 5.13, respectively. From these plots it is clearly seen that the two values match excellently within a maximum deviation of $\pm$ 2% only.

5.3.9 GENERALIZED CORRELATION FOR AVERAGE CIRCUMFERENTIAL WALL TEMPERATURE ALONG THE LENGTH OF FIRST ROW TUBE

It would be of practical importance if a correlation describing distribution of average wall temperature , $\bar{t}_w$ over the tube length is obtained . Using the technique of Section 5.3.9 , the following correlation has been obtained.

$$\bar{t}_w = 61.626 - 0.7286*w + 1.30300*t_i + 0.07164*P + 21.7857*L \quad ...(5.4)$$

The average values of wall temperatures predicted by Equation 5.4 are plotted against the experimental values in
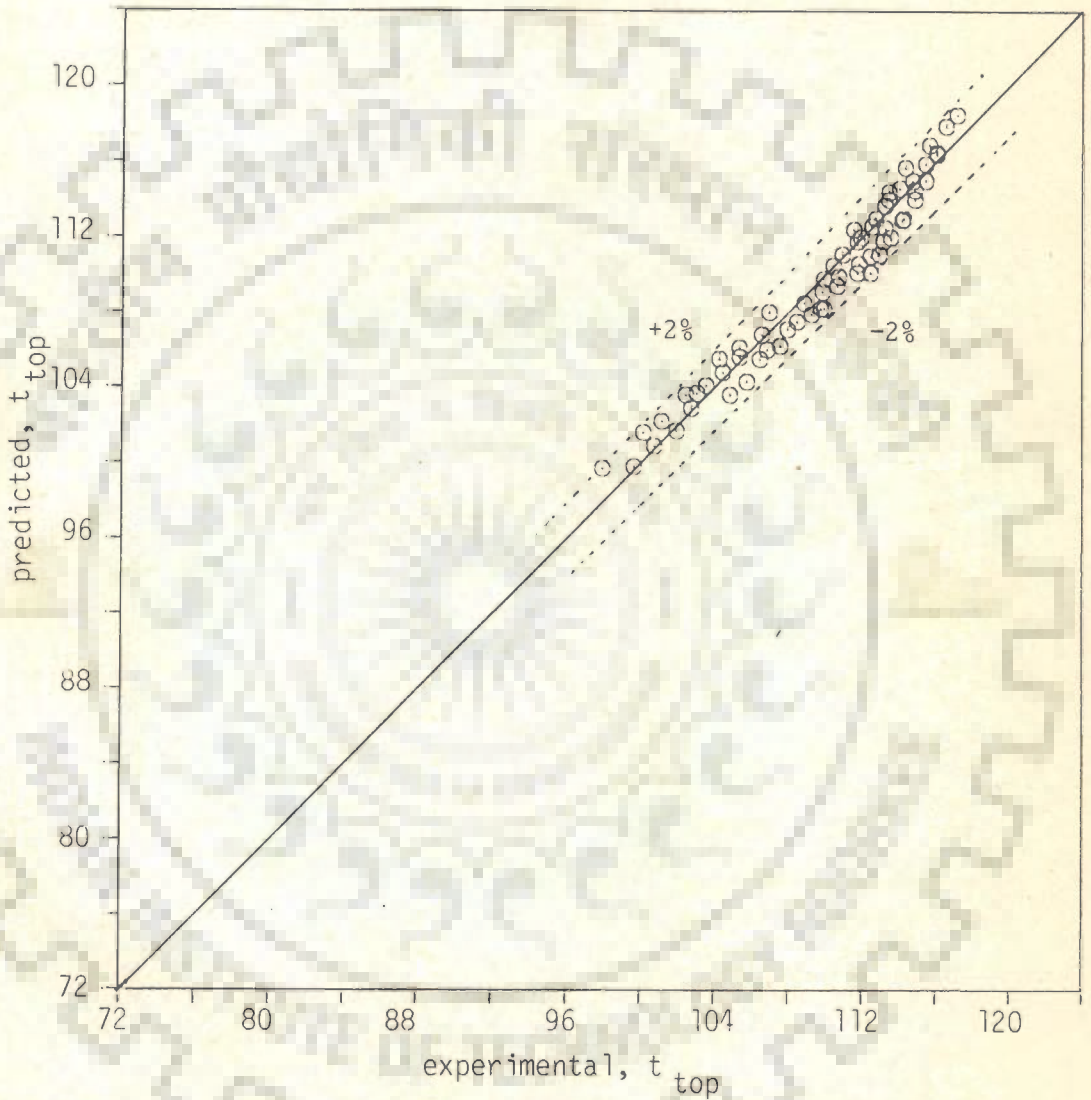
Fig. 5.11   comparison between experimental and predicted wall
temperature for top-region of first row tube from
present model, Eq. (5.1)
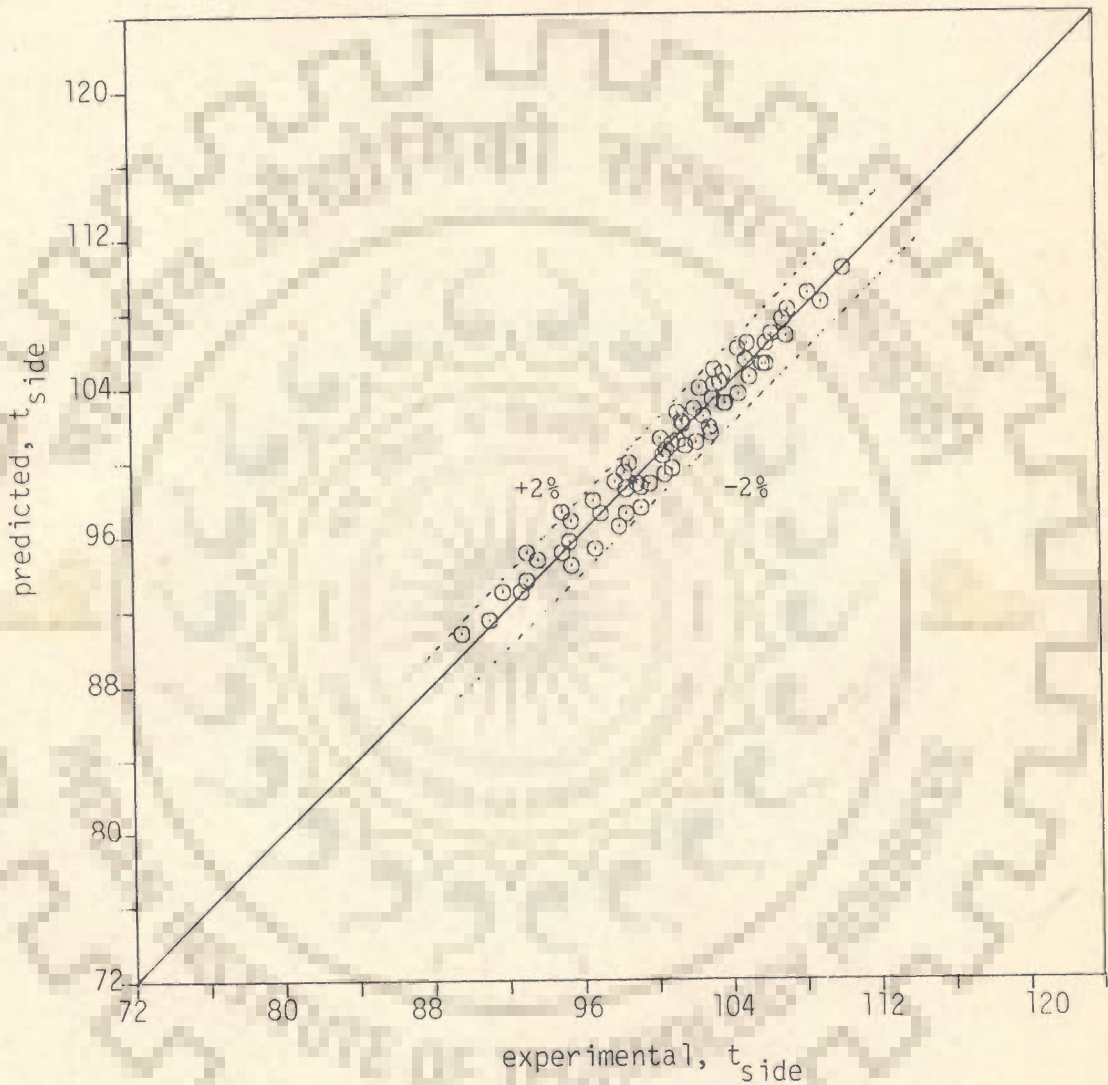
Fig. 5.12 comparison between experimental and predicted wall
temperature for side-region of first row tube
from present model, Eq. (5.2)

82
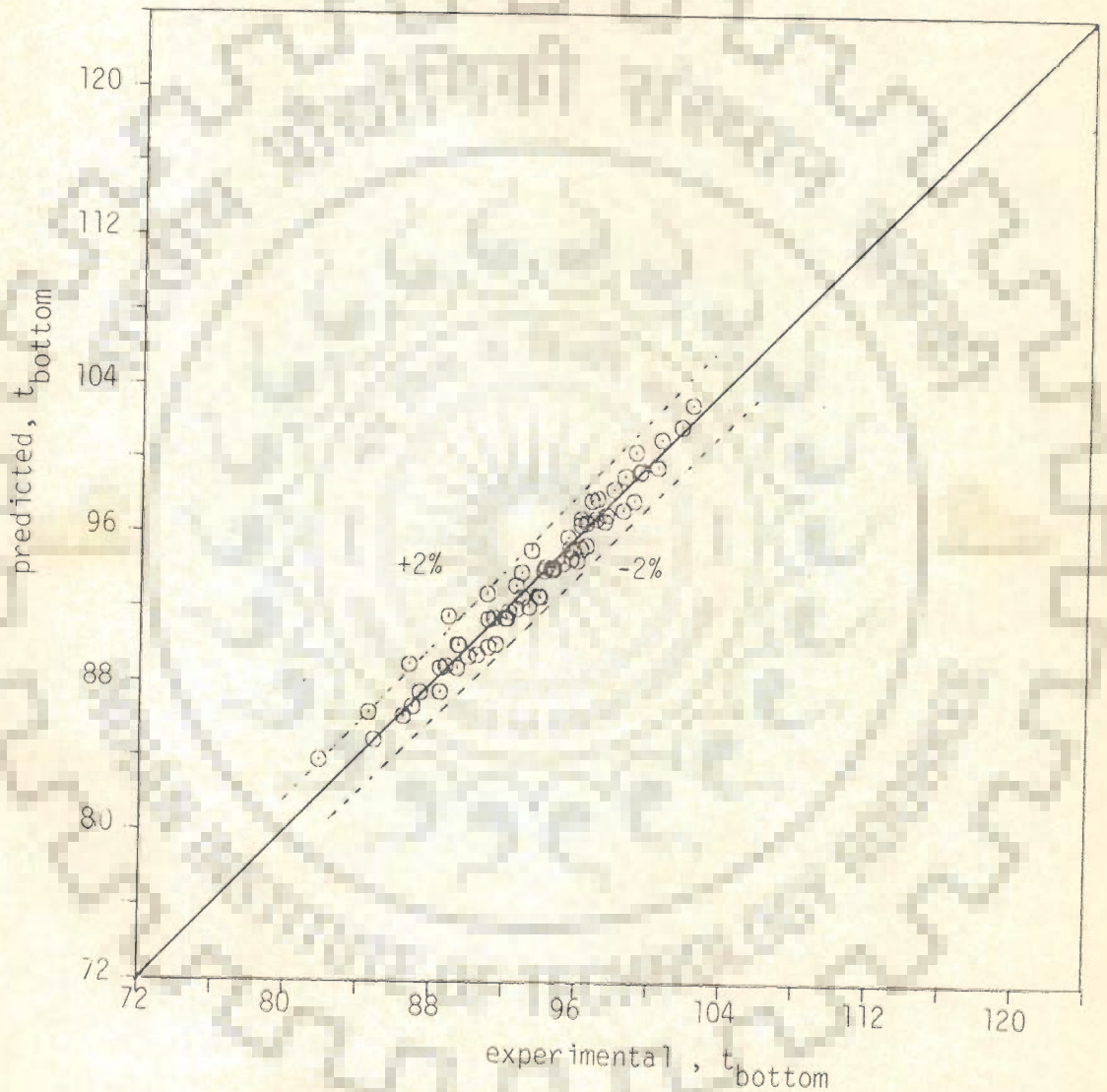
Fig. 5.13 comparison between experimental and predicted wall
temperature for bottom-region of first row tube
from present model , Eq. (5.3)

Figure 5.14. The match among them is once again excellent, with the maximum deviation being only $\pm$ 2% .

5.3.10 GENERALIZED CORRELATION FOR WEIGHTED WALL TEMPERATURE OF FIRST ROW TUBE

A design engineer would also like to have a correlation capable of predicting weighted wall temperature, $\bar{t}_{wt}$ as a function of cooling water flow rate, inlet temperature of cooling water and steam pressure. This, in fact, provides simplification in the design calculations. With this in view a correlation based on the present data is obtained as follows :

$$\bar{t}_{wt} = 57.489 - 0.7183*w + 1.6306*ti + 0.07096*P$$

$$...(5.5)$$

Figure 5.15 is a plot between the predicted values of weighted wall temperature of the first row tube from Eq.5.5 and the experimental values. Here again the match is within a maximum error of $\pm$ 2 % .

5.3.11 WEIGHTED WALL TEMPERATURE OF FIRST ROW TUBE

Bromley (17) , based on experimental data of investigators (57,58), including his own , has succeeded in correlating the average wall temperatures of the condenser tubes with a dimensionless parameter β, a function of steam temperature, cooling water flow rate and its inlet and outlet temperatures , tube diameter and thermal conductivity of the tube. Due to this reason , it is considered desirable to compare the experimental data of the present investigation with Bromley's model (Eqs. 2.15 through 2.17) in Chapter 2.

Figure 5.16 shows a plot between $\Delta t_{avg}/\Delta t$ and β. It is found that the present experimental data are correlated by

84
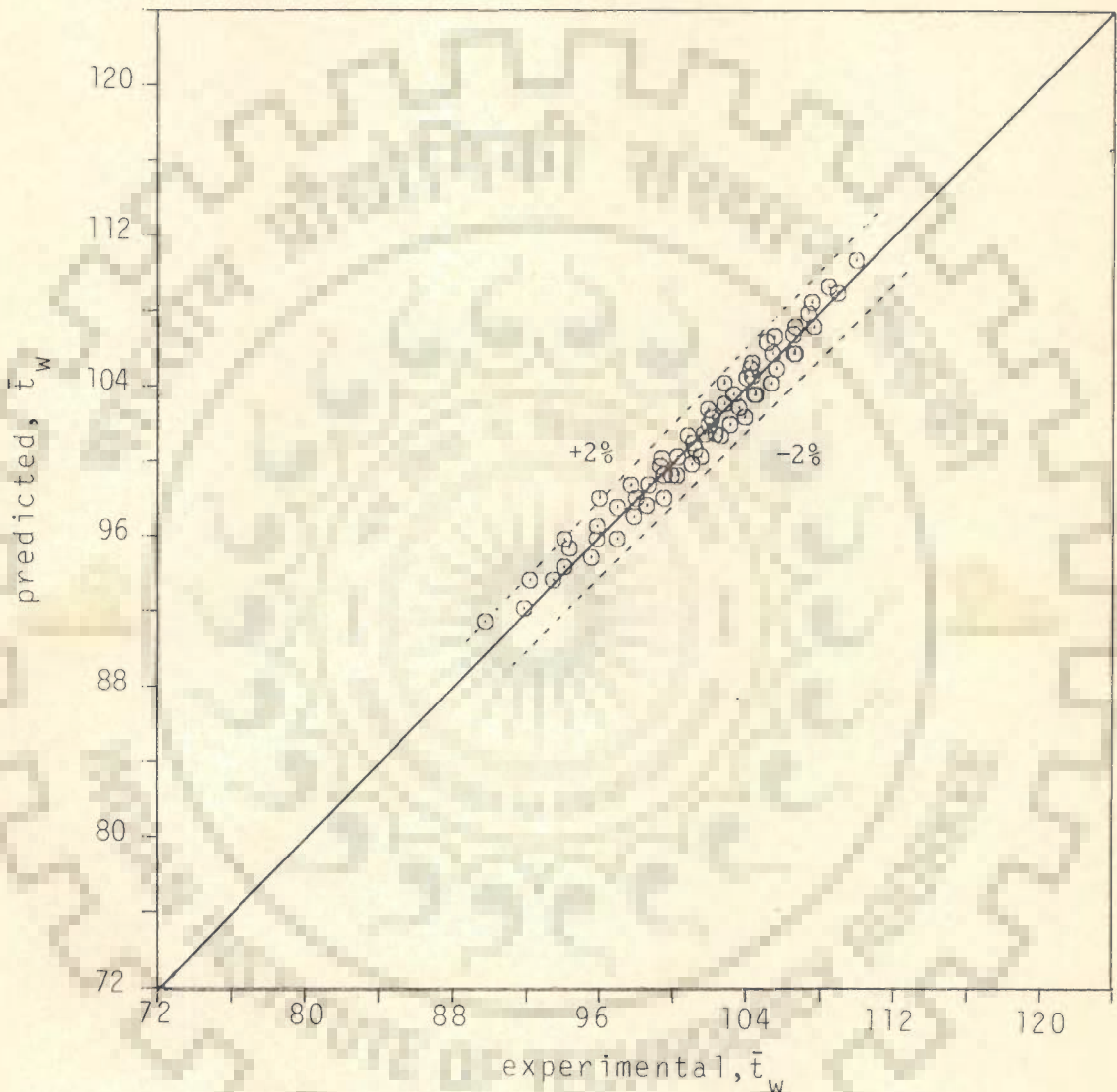
Fig. 5.14 comparison between experimental and predicted average wall temperature ($\bar{t}_w$) of first row tube from present model, Eq. (5.4)
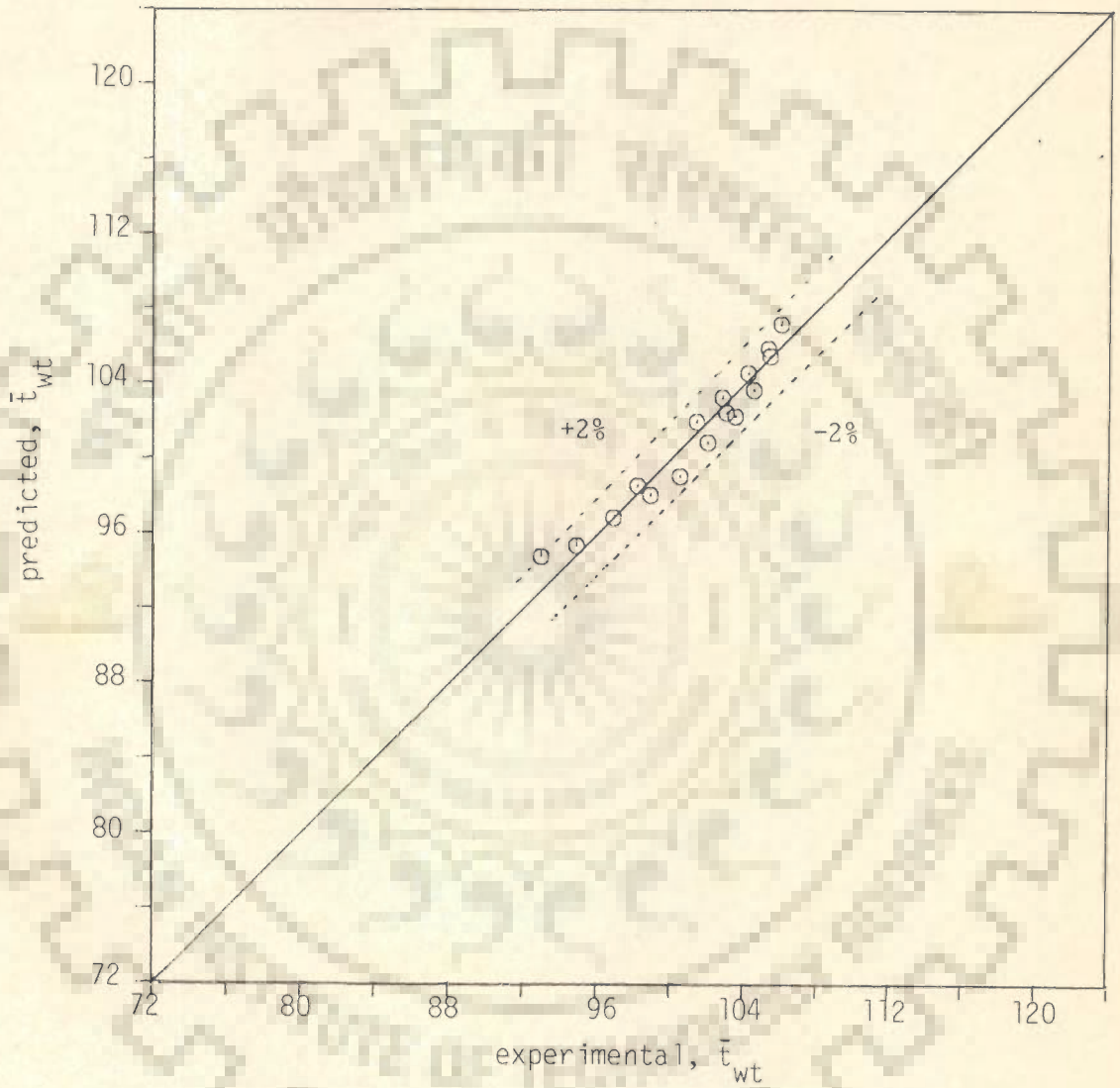
Fig. 5.15 comparison between experimental and predicted weighted wall temperature ($\bar{t}wt$) of first row tube from present model, Eq. (5.5)
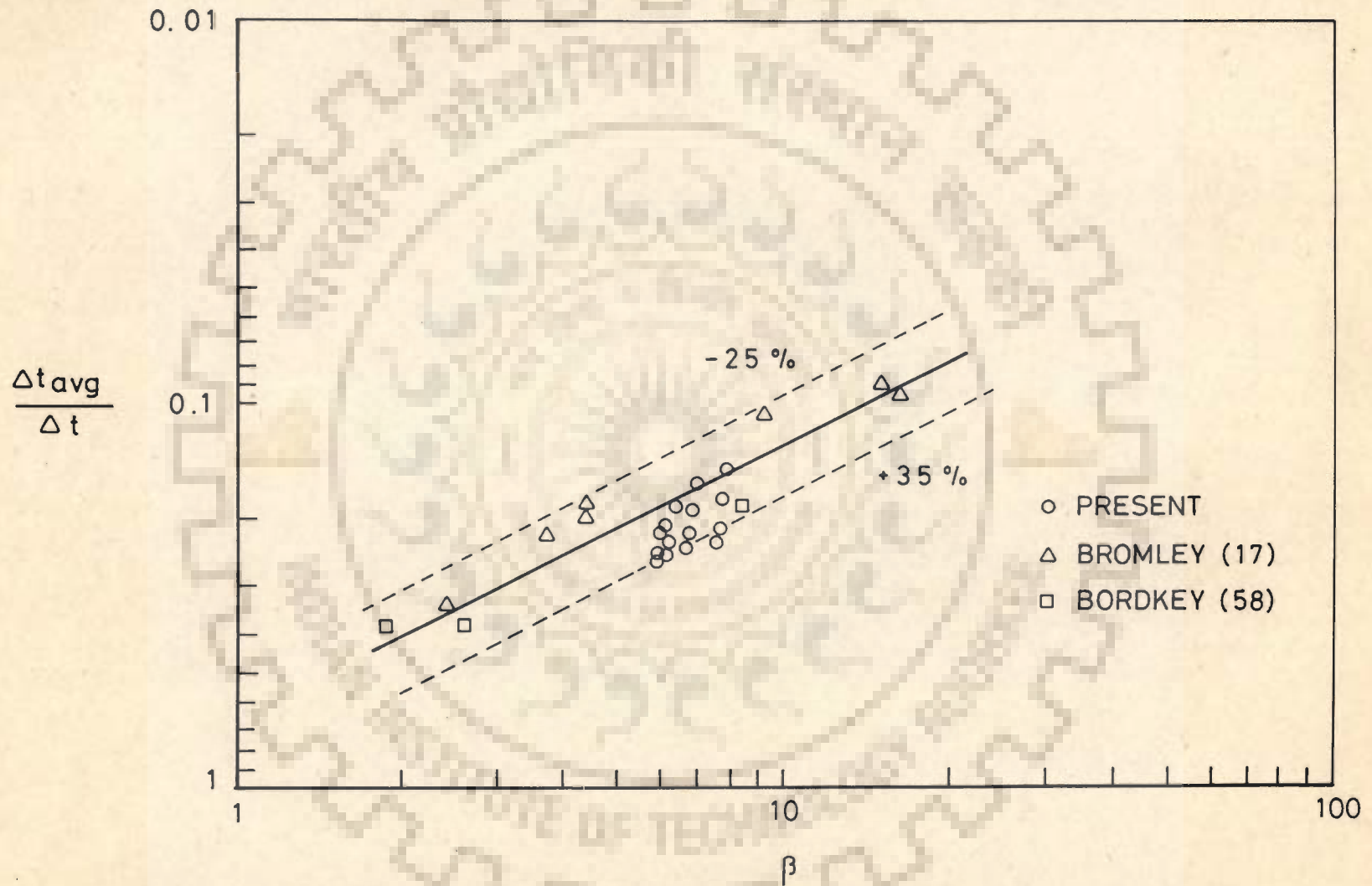
Fig.5.16. Comparison of experimental data for the condensation of steam investigation and those of earlier investigators with Bromley's model Eqs. (2.15 – 2.17)

Bromley's model within a maximum error of +27 to -25%. It is also interesting to note that even Bromley's (17) and Brodkey's(58) data have shown a scatter of ± 35 % from the above model. This, of course, seems to be within practical limits of error.

HEAT TRANSFER TO COOLING WATER

In the present investigation for the condensation of steam on a short horizontal stainless steel tube, water at room temperature has been chosen as the cooling medium. For the calculation of heat transfer coefficient for such tube the specific correlations, described in Section 2.3, are used and, of course, they are not applicable for long tubes.

5.3.12 VARIATION OF COOLING WATER SIDE HEAT TRANSFER COEFFICIENT FOR FIRST ROW TUBE

In the present investigation the operating parameters include cooling water flow rates varying from 11.6 lpm to 17.1 lpm and steam pressure from 146.75 kPa to 269.38 kPa, respectively.

Figure 5.17 represents a typical variation of cooling water side heat transfer coefficient for various values of water flow rate at a given steam pressure of 269.38 kPa. Values of heat transfer coefficient have been calculated using Mikheyev's correlation Eq.2.48. From the plot it is clearly seen that the heat transfer coefficient decreases continuously from inlet to exit of the tube. This variation in the value of heat transfer coefficient is an expected behaviour in view of the short length of the tube used. This is not so for the long tubes where the heat transfer coefficient attains a value asymptotically and thereafter remains constant along the length of the tube. With
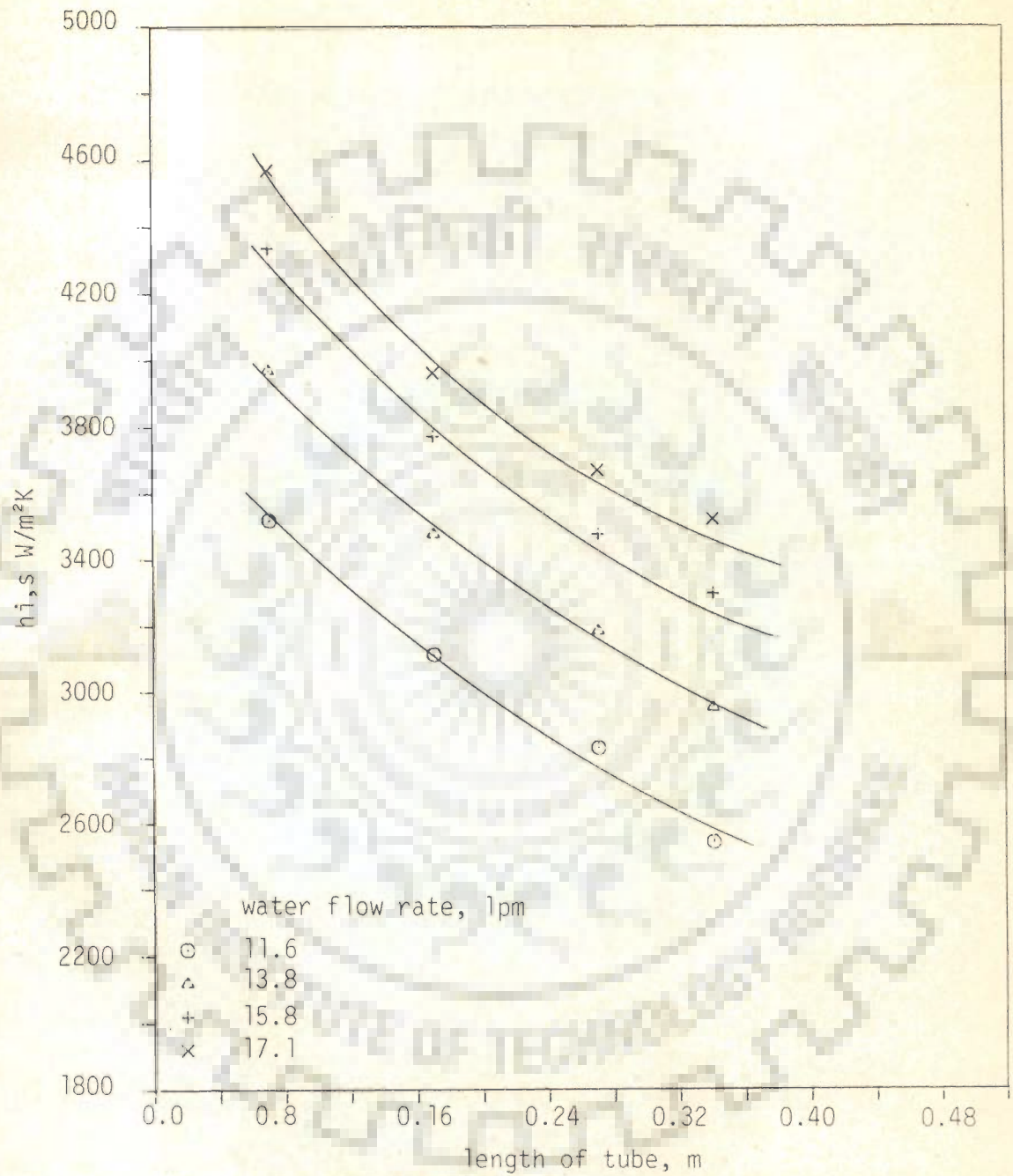
Fig.5.17 variation of cooling water side heat transfer coeff-
icient along the length of first row tube for various
cooling water flow rates (Ps=146.75 kPa)

89

the increase in cooling water flow rate, the heat transfer coefficient increases. This is evidently so due to increased turbulence of cooling water.

HEAT TRANSFER COEFFICIENT

For the design of a condenser with vapour condensing on its bundle of tubes , it is important to know the variation of condensing heat transfer coefficient both along the circumference and the length of the tube considering the effects of cooling water flow rates and steam pressure. This information is immensely helpful for the accurate calculation of heat transfer area needed for a given duty of condenser which ,in turn, eliminates the possibility of over-design or under-design of the condenser. The former results in the wastage of money specially when the material employed for the tube bundle is costly whereas the latter would lead to non-operability of the condenser.

In the following sections, an attempt has been made to describe the manner in which condensing heat transfer coefficient of steam on the top row tube changes when cooling water flow rate and steam pressure are altered. The calculation procedure for heat transfer coefficient is given in Appendix B .

5.3.13 EFFECT OF COOLING WATER FLOW RATE ON CIRCUMFERENTIAL CONDENSING HEAT TRANSFER COEFFICIENT FOR FIRST ROW TUBE

Figures 5.18 and 5.19 represent the effect of cooling water flow rate on circumferential heat transfer coefficient when condensing steam pressures are 146.75 kPa and 269.38 kPa, respectively. These plots reveal the following typical trends :

1.For a given steam pressure and segment of the
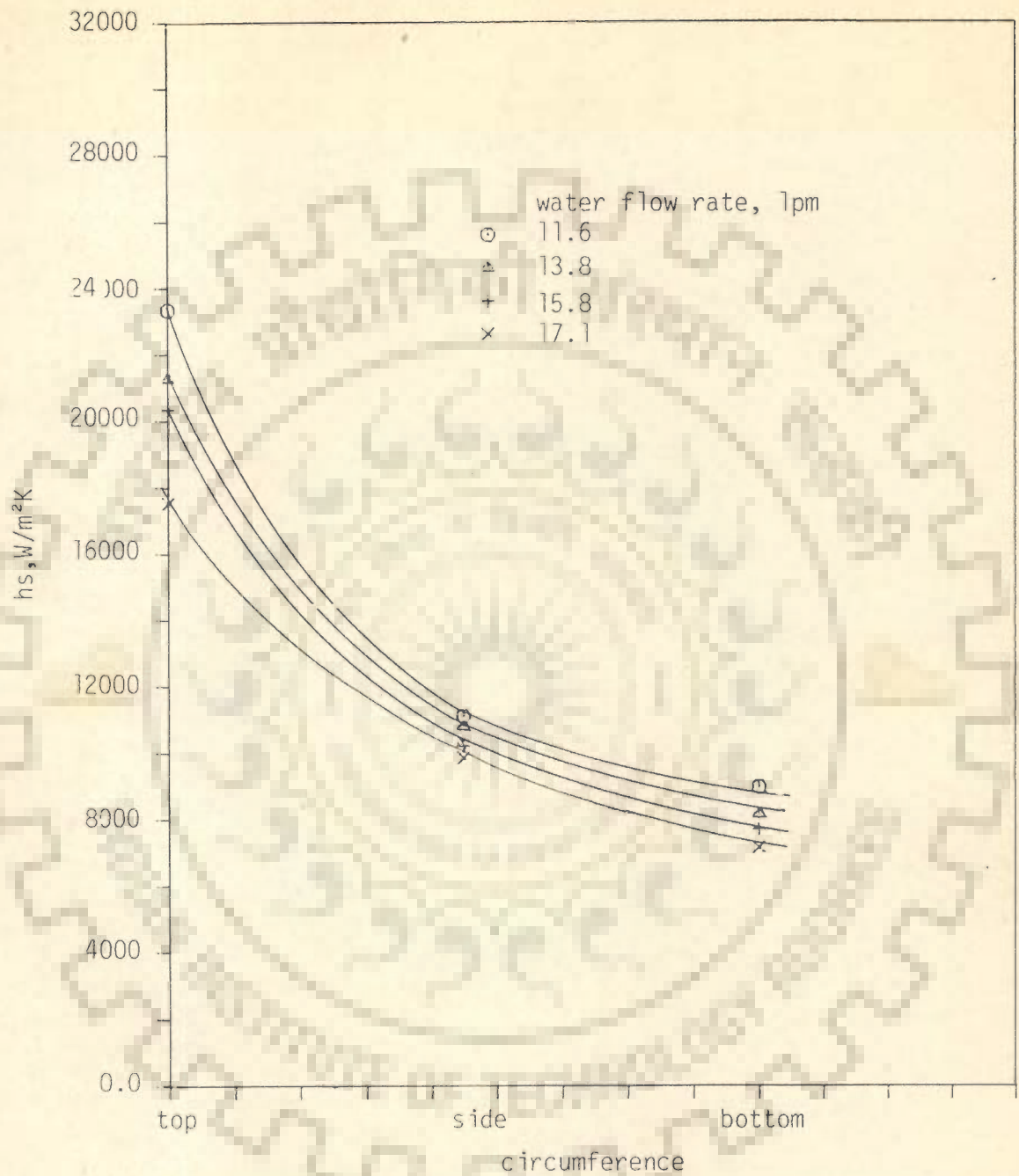
Fig.5.18 variation of condensing heat transfer coefficient
along the circumference of the first row tube for
various cooling water flow rates (Ps=146.75,kPa x=2)

91
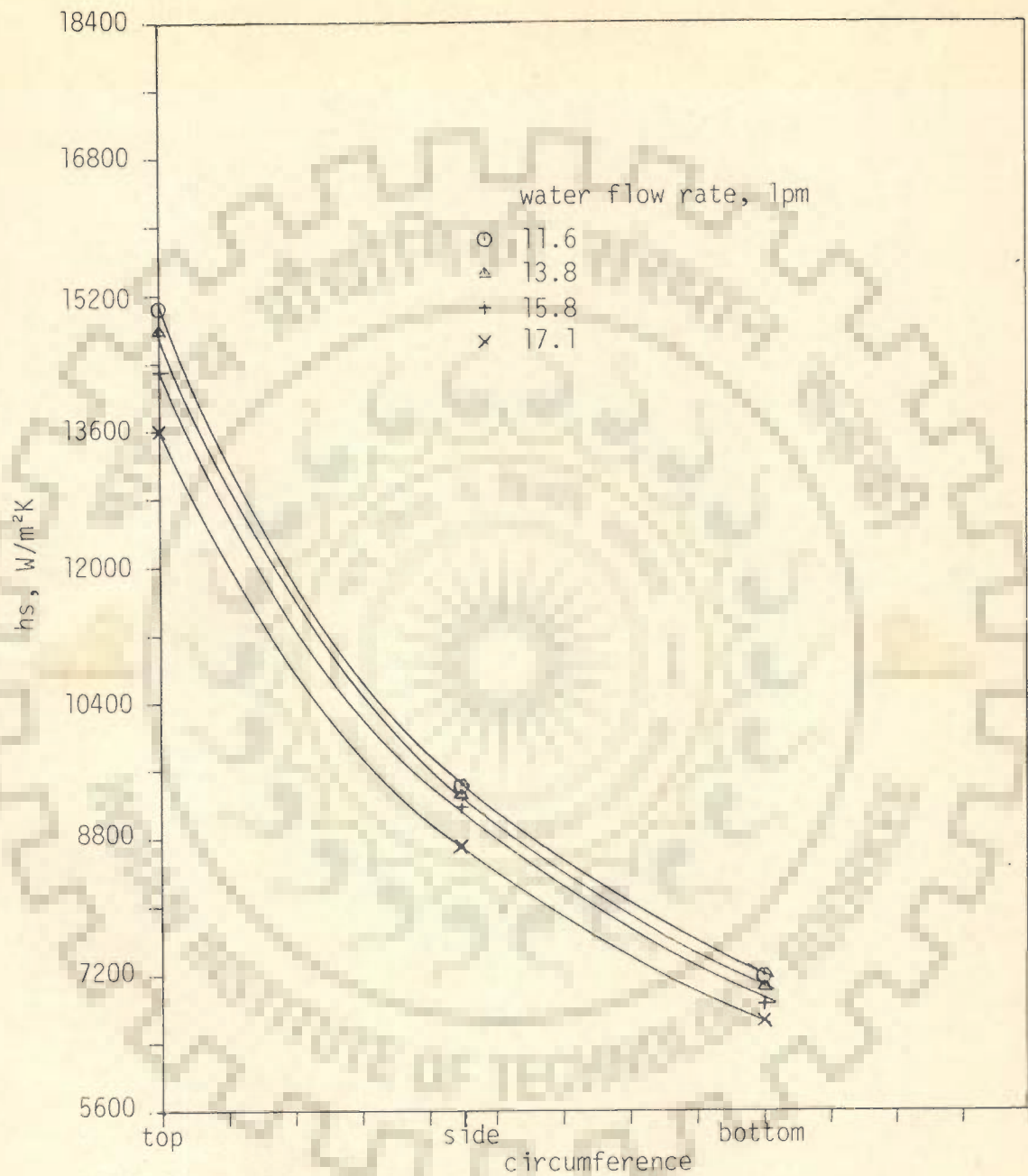
Fig.5.19 variation of condensing heat transfer coefficient
along the circumference of the first row tube
for various cooling water flow rates (Ps=269.38kPa
and x =2)

92

tube, heat transfer coefficient during steam condensation varies circumferentially. Its value changes from top- to side- to bottom-regions in decreasing order.

This observation is quite understandable in view of the fact that thickness of condensate layer increases progressively along the circumference of the tube from top to bottom region.

2. With increase in cooling water flow rate, the decrease in value of circumferential heat transfer coefficient is quite appreciable at the top-region of the tube. However the magnitude of decrease in its value reduces significantly at the side-and the bottom-regions.

The above fact can be explained as follows : The condensation rate is largely dependent on cooling water flow rate , if its inlet temperature is kept constant. The increase in cooling water flow rate results in enhancement of water side-heat transfer coefficient. This , in fact, increases the rate of condensation , especially when water side heat transfer coefficient is much smaller than that of steam-side. Due to this the condensate layer thickness keeps on increasing and consequently the heat transfer coefficient of condensing steam decreases. Among the top-, the side-, and the bottom-regions of the tube the top-region is the most effective in causing condensation as the drainage of condensate formed here is quite appreciable. Owing to this there exists a thin condensate layer

over it. Hence, any small additional change in the thickness of condensate layer would amount to a steep reduction in heat transfer coefficient . The same is not true with the side-region where the thickness of condensate layer is appreciably more than that at top-region. The thickness of condensate layer at bottom-region is still much higher. In view of the already existing thick layer of the condensate over the side- and the bottom-region, an additional change in its value due to the increase in cooling water flow rate does not reduce the value of heat transfer coefficient as steeply as at the top-region. This fact explains clearly that the increase in cooling water flow rate has a continuously diminishing effect on condensing heat transfer coefficient at the side-, and the bottom-regions of the tube.

5.3.14 EFFECT OF STEAM PRESSURE ON CIRCUMFERENTIAL CONDENSING HEAT TRANSFER COEFFICIENT OF FIRST ROW TUBE

Figures 5.20 and 5.21 have been drawn to show the typical variation of circumferential condensing heat transfer coefficient when steam pressure is changed and the respective cooling water flow rates are 11.6 lpm and 17.1 lpm .

From these plots the following characteristic features are distinctly noted :

1. The condensing heat transfer coefficient decreases from top- to side- to bottom-regions for all the steam pressures investigated. This behaviour is easily explainable in view of the progressively increasing thickness of condensate layer along the circumference of the tube from
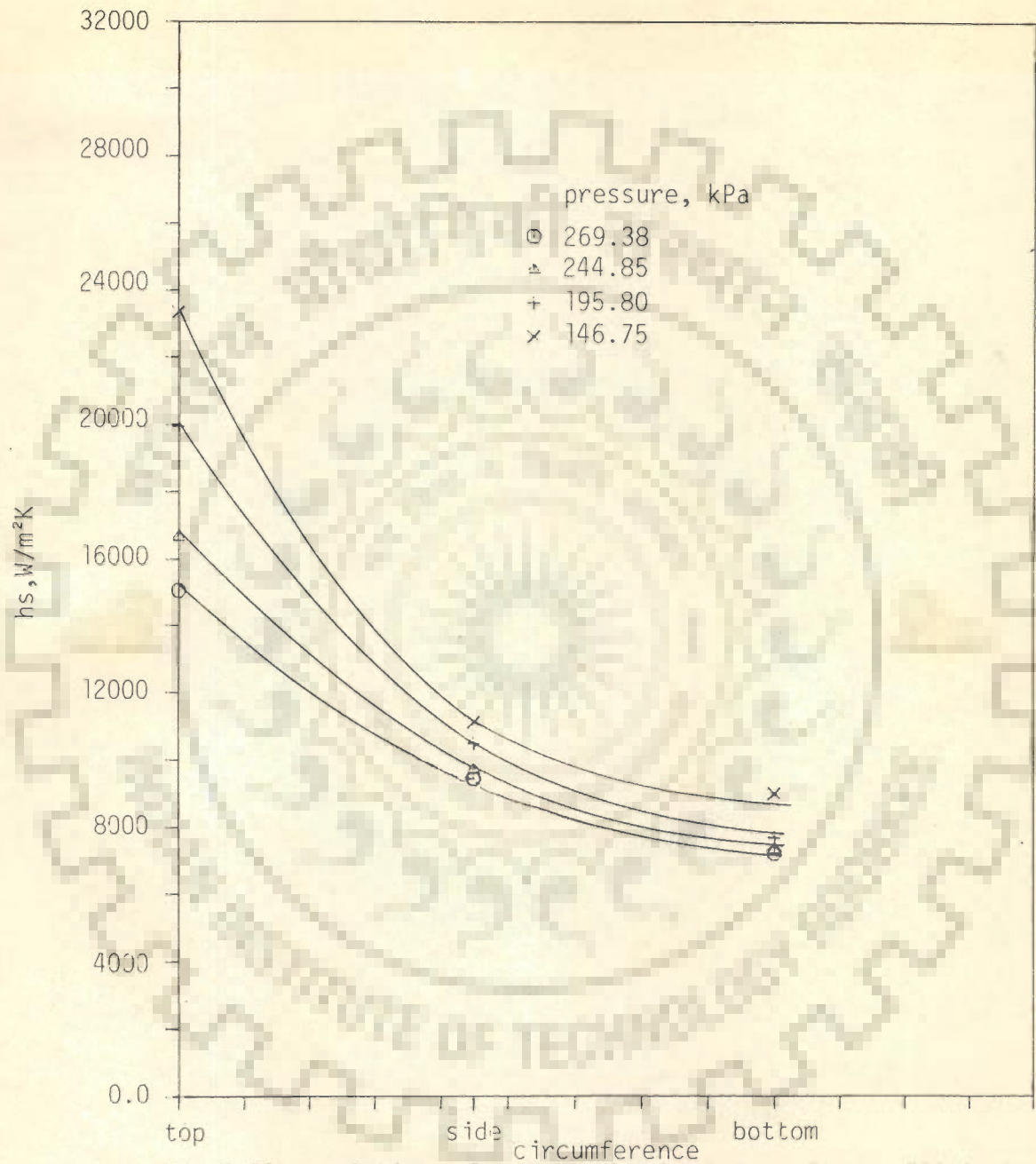
Fig.5.20 variation of condensing heat transfer coefficient
along the circumference of the first row tube for
various steam pressures (W= 11.6 lpm and x =2)
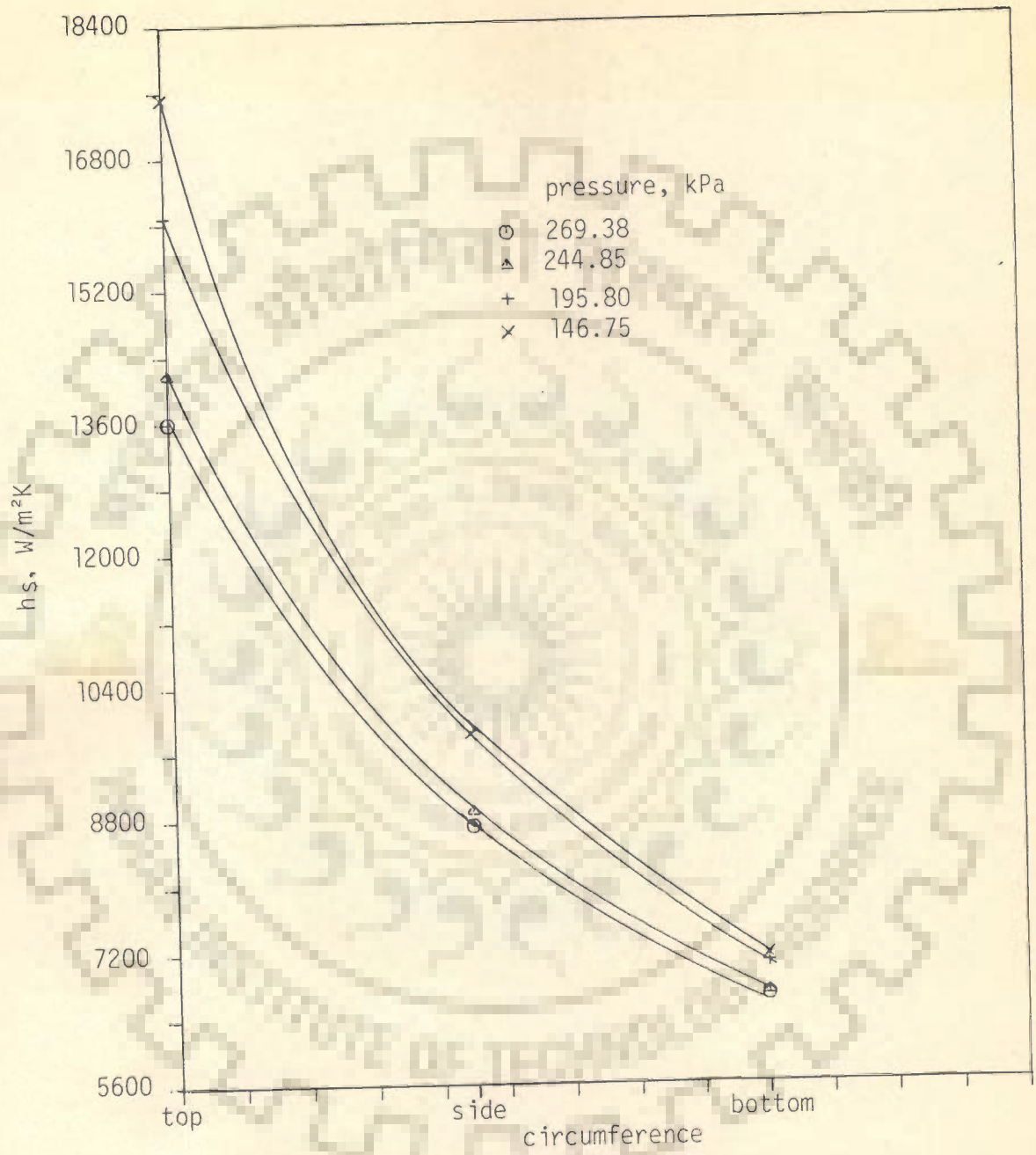
Fig.5.21 variation of condensing heat transfer coefficient along the length of first row tube for various steam pressures (w =17.1 lpm and x=2)

96

the top- to the bottom- region.

2. With the rise in steam pressure , the rate of condensation increases and so also the thickness of condensate layer. As a result , the heat transfer coefficient reduces. This, of course, happens at all the three regions of the tube.

The influence of steam pressure on condensing heat transfer coefficient is more pronounced at the top-region and decreases substantially at the side and the bottom regions. The decreasing influence at the bottom -region is perhaps due to the increased frequency of detatchment of condensate in the form of droplets. This, in turn , develops pulsations in the condensate layer especially lying in the bottom-region. When steam pressure is raised , the condensate layer thickness rises around the tube and thus a reduction in heat transfer coefficient should occur circumferentially. Perhaps due to the substantial pulsations in the condensate layer at the bottom-region, this reduction is annulled somewhat. Of course the extent of annullment decreases as one moves from bottom-to side- to top -regions. Hence the appreciable effect of pressure on top-region is evidently understandable.

5.3.15 EFFECT OF COOLING WATER FLOW RATE ON AVERAGE CIRCUMFERENTIAL CONDENSING HEAT TRANSFER COEFFICIENT ALONG FIRST ROW TUBE LENGTH

The experimental data of circumferential condensing heat transfer coefficient for different segments along the length of tube are averaged , as shown in Appendix B .

Figure 5.22 shows a typical effect of cooling water flow rate on average condensing heat transfer coefficient of the tube. From the plot the following note-worthy observations are made :

1. For a given cooling water flow rate , the average condensing heat transfer coefficient increases from inlet of the tube to its outlet.

This is an expected behaviour and is easily explainable from the fact that cooling water side heat transfer coefficient decreases from inlet to outlet of the tube, whereas the cooling water temperature increases. Both these factors combined together reduce condensation rate continuously from inlet to outlet of the tube. Consequently, the condensate layer thickness keeps on decreasing along the tube length. Thus the values of the condensing heat transfer coefficient increase along the tube length.

2. Decrease in the values of condensing heat transfer coefficient with the increase in cooling water flow rate is obvious. When water flow rate is raised, the condensation rate over the tube length increases resulting in a higher condensate layer thickness. This evidently decreases the value of heat transfer coefficient.

5.3.16 EFFECT OF STEAM PRESSURE ON AVERAGE CIRCUMFERENTIAL CONDENSING HEAT TRANSFER COEFFICIENT ALONG FIRST ROW TUBE LENGTH

Figure 5.23 is a typical plot showing the effect of steam pressure on average heat transfer coefficient. It is noted that

98
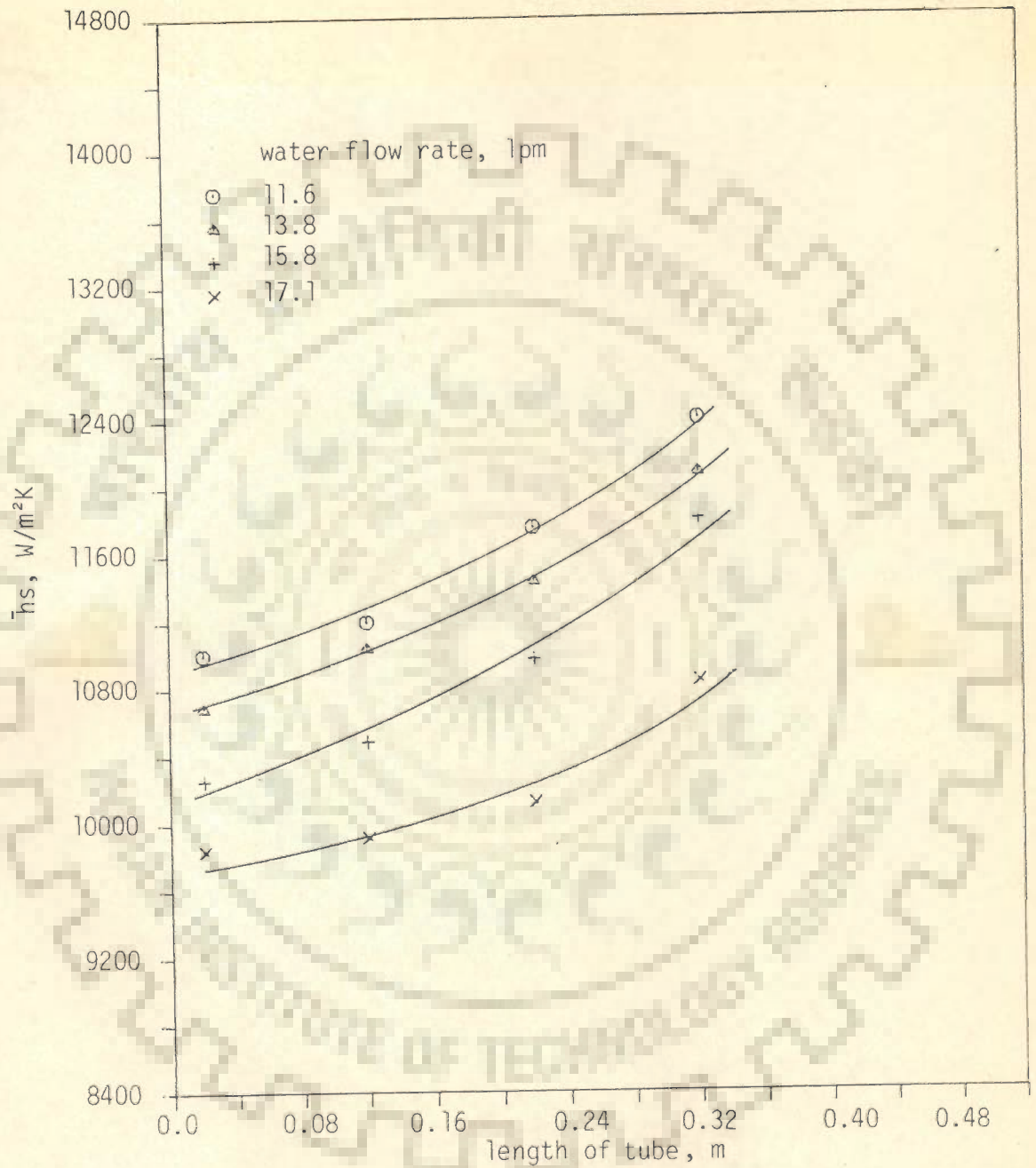
Fig.5.22 effect of cooling water flow rate on average conde-
nsing heat transfer coefficient along the length
of first row tube (Ps = 244.85 kPa)
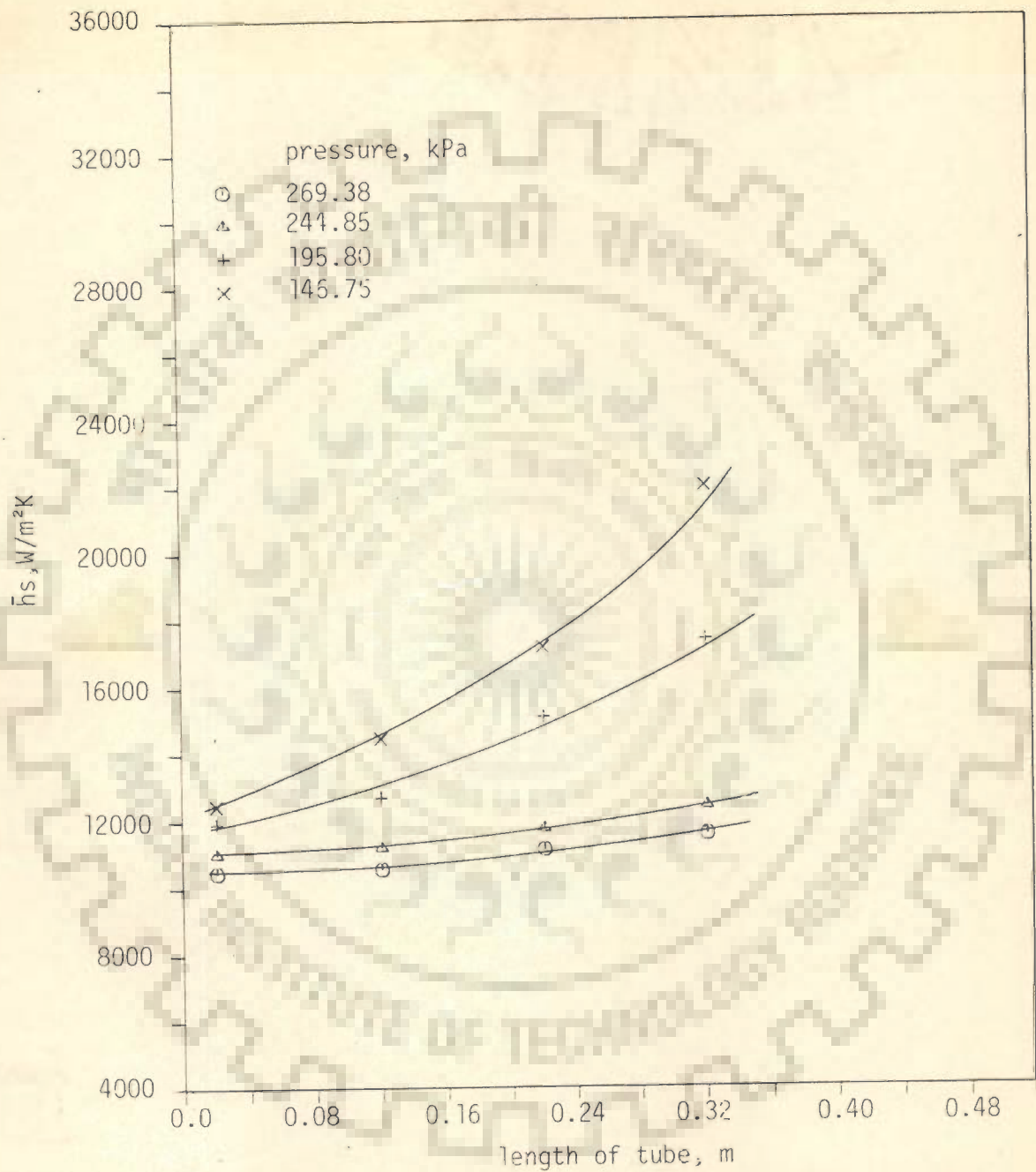
Fig.5.23 effect of steam pressure on average condensing heat transfer coefficient along the length of first row tube (w=11.6 lpm)

100

for all cross sections along the length of the tube, the average condensing heat transfer coefficient decreases with increase in steam pressure. This fact is understandable in view of greater thickness of condensate layer at higher steam pressures.

5.3.17 VARIATION OF WEIGHTED CONDENSING HEAT TRANSFER COEFFICIENT WITH STEAM PRESSURE AND COOLING WATER FLOW RATE

From Figures 5.22 and 5.23 it is noted that the average condensing heat transfer coefficient changes along the length of tube. This information in this form is not convenient for the design calculations. In fact, a design engineer prefers to know the weighted heat transfer coefficient which is a single value for the entire length of a particular tube for a given cooling water flow rate and steam pressure. The weighted values are calculated based on tube length, the procedure followed for its calculation is given in Appendix B.

Figure 5.24 represents the values of weighted heat transfer coefficient as a function of steam pressure with cooling water flow rate as a parameter. It is noted that weighted heat transfer coefficient decreases with increase in steam pressure for a given flow rate. Further it is also noted that for a given steam pressure the values of weighted heat transfer coefficient decrease with the increase in cooling water flow rate. This is obviously an expected observation.

5.3.18 A TYPICAL VARIATION OF OVERALL HEAT TRANSFER COEFFICIENT FOR CONDENSATION OF STEAM ON FIRST ROW TUBE

In Sections 5.3.12 and 5.3.15 the parametric effects on cooling water heat transfer coefficient and average condensing
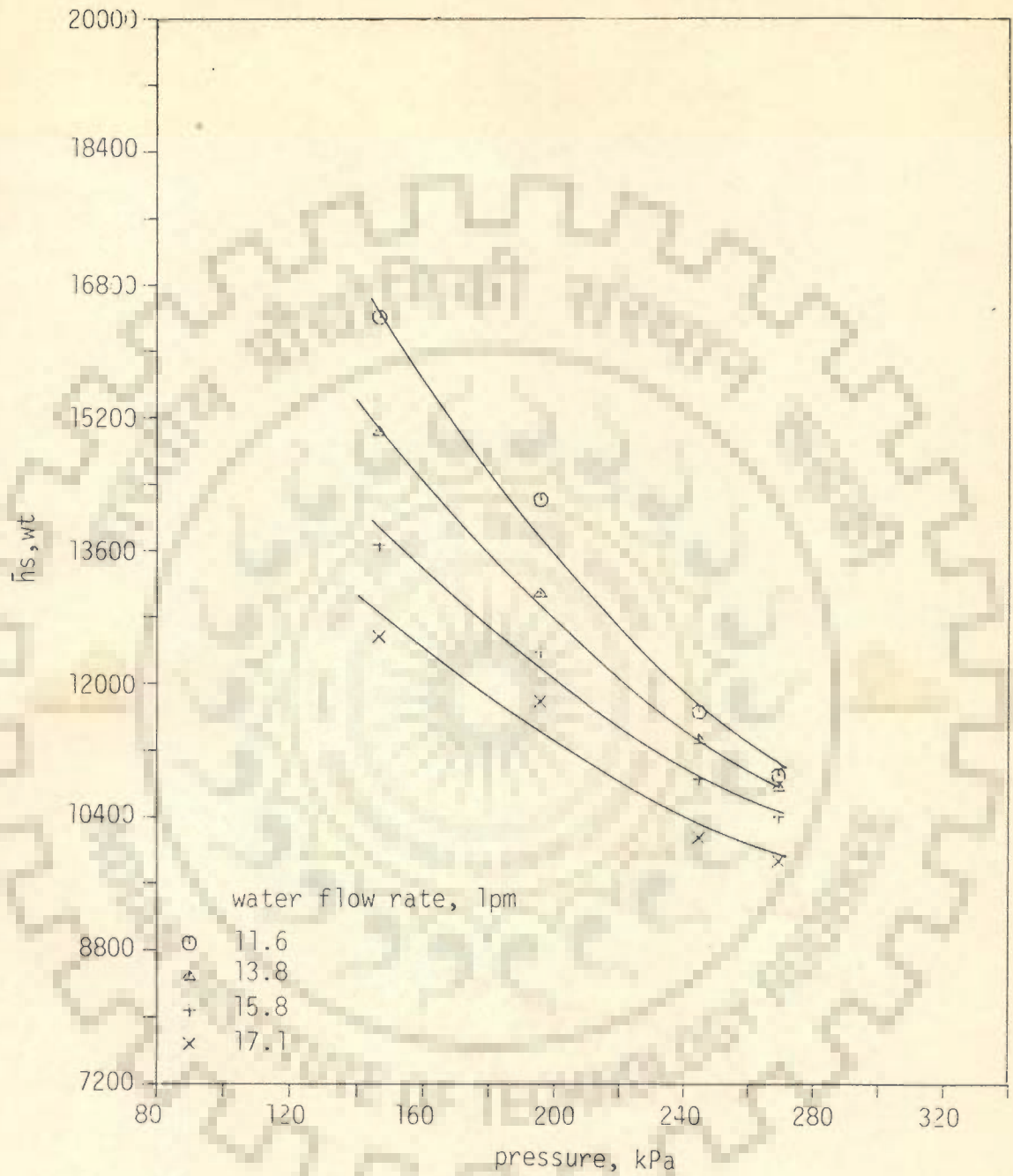
Fig.5.24 effect of steam pressure on weighted condensing
heat transfer coefficient of first row tube for
various cooling water flow rates.

102

steam side heat transfer coefficient along the tube length have been discussed. Now it is important to understand the respective contributions of water-side, and steam-side heat transfer coefficient, and the tube wall conductance to the overall heat transfer coefficient of a condenser having short tubes.

Figure 5.25 provides the variation of average condensing heat transfer coefficient, tube wall conductance, water side heat transfer coefficient and overall heat transfer coefficient along the length of tube. It is noted that the average condensing heat transfer coefficient increases whereas the water-side heat transfer coefficient decreases and the conductance due to tube wall remains constant. As regards the overall heat transfer coefficient, it fairly remains' constant.

5.3.19 COMPARISON BETWEEN EXPERIMENTAL WEIGHTED CONDENSING HEAT TRANSFER COEFFICIENT OF FIRST ROW TUBE AND PREDICTED VALUES FROM AVAILABLE CORRELATIONS

A literature review reveals that many investigators have studied the condensation of vapours including steam on horizontal tubes. Based on their experimental/ theoretical studies they have recommended correlations of condensing heat transfer coefficient for the horizontal tube as a function of wall temperature , physico-thermal properties of condensate, saturation temperature of vapour and diameter of the tube.

In this section attempt has been made to compare the experimental values of weighted heat transfer coefficient of top row tube with those predicted from various correlations. These correlations are due to Mikheyev(23), Henderson and
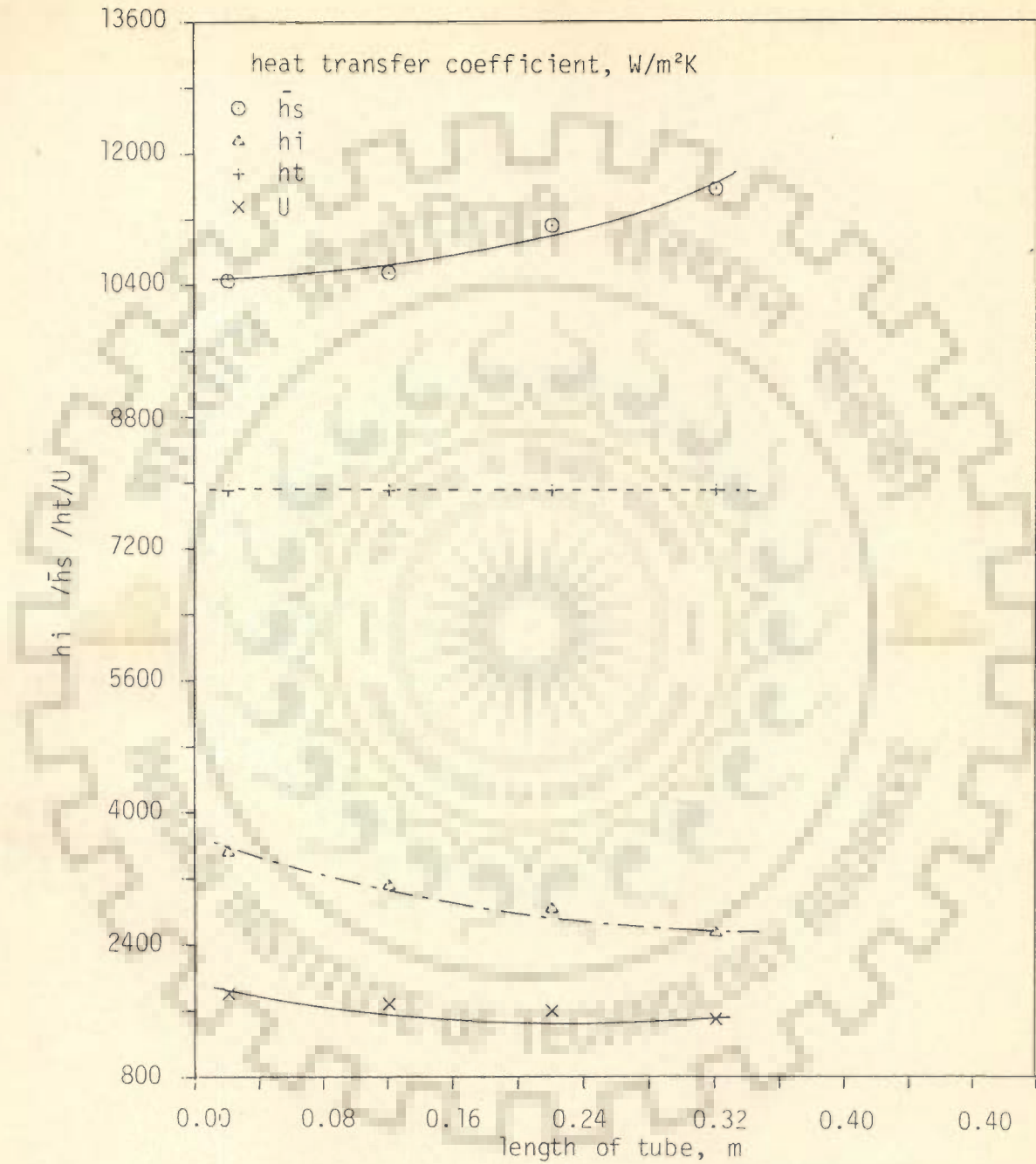
Fig.5.25 variation of individual and overall heat transfer
coefficient along the length of the first row
tube (Ps = 269.38 kPa and W= 11.6 lpm)

104

Marchello(11), Nusselt(1), Othmer and Berman(13), Peck and Reddie(14), Bromely(17), Rohsenow(18), Chen(34), and White(19).

The above mentioned correlations have been extensively described in Literature Review of Chapter 2 . The important points regarding these correlations, which merit emphasis, are as follows :

Correlation due to Mikheyev(23) is based on large number of experimental data for condensation of steam on tube including some data for Ethyl alcohol, Acetone, Benzene, Ammonia and air .

The Henderson and Marchello(11) correlation represents one of the recent studies and is an attempt to modify Nusselt correlation by incorporating the effect of condensate falling in the form of drops from the bottom of tube. They, in absence of any rigorous analysis, opted to include Ohnesorge Number in their correlation.

Correlations recommended by Nusselt(1),Bromley(17) , Rohsenow(18) and Chen(34) are based on their respective theoretical models considering one or other assumptions.

The correlation due to Othmer and Berman(13) is purely empirical in nature and is based on experimental data for the condensation of vapours of 18 alcohols, esters and ketones. The experimental data for steam are not included.

Correlation due to Peck and Reddie(14) is based on mass of experimental data related to condensation of many organic vapours and comparatively limited data of steam condensation.

White's correlation(19) is based on the experimental

data for the condensation of R-12 on horizontal tube only.

Figures 5.26 through 5.34 have been drawn between $\overline{h}_{wt,exptl}/\overline{h}_{wt,predt}$ and steam pressure for different cooling water flow rates in order to compare the experimental values of present investigation with those predicted from earlier correlations . The ratio $\overline{h}_{wt,exptl}/\overline{h}_{wt,predt}$ is represented by R and steam pressure by P in above plots for the sake of convenience . The predicted values of heat transfer coefficient , $\overline{h}_{wt,predt}$ for the calculation of R in Figures 5.26 through 5.34 are calculated using the respective correlation of Mikheyev (23), Henderson and Marchello (11), Nusselt (1), Othmer and Berman (13), Peck and Reddie (14), Bromley (17), Rohsenow (18), Chen (34) and White (19), respectively.

A scrutiny of these plots reveals the following note-worthy observations :

1. The values of R in Figure 5.26 for all the steam pressures and cooling water flow rates are scattered around the horizontal line , representing a value equal to unity , within +10% and -18 %. This indicates that deviation between $\overline{h}_{wt,exptl}$ and $\overline{h}_{wt,predt}$ from correlations due to Mikheyev is within +10% to -18%. This seems to be a reasonable agreement between Mikheyev's correlation and the present experimental data . This agreement is perhaps due to the fact that Mikheyev's correlation is based on experimental data largely for steam condensation.

106
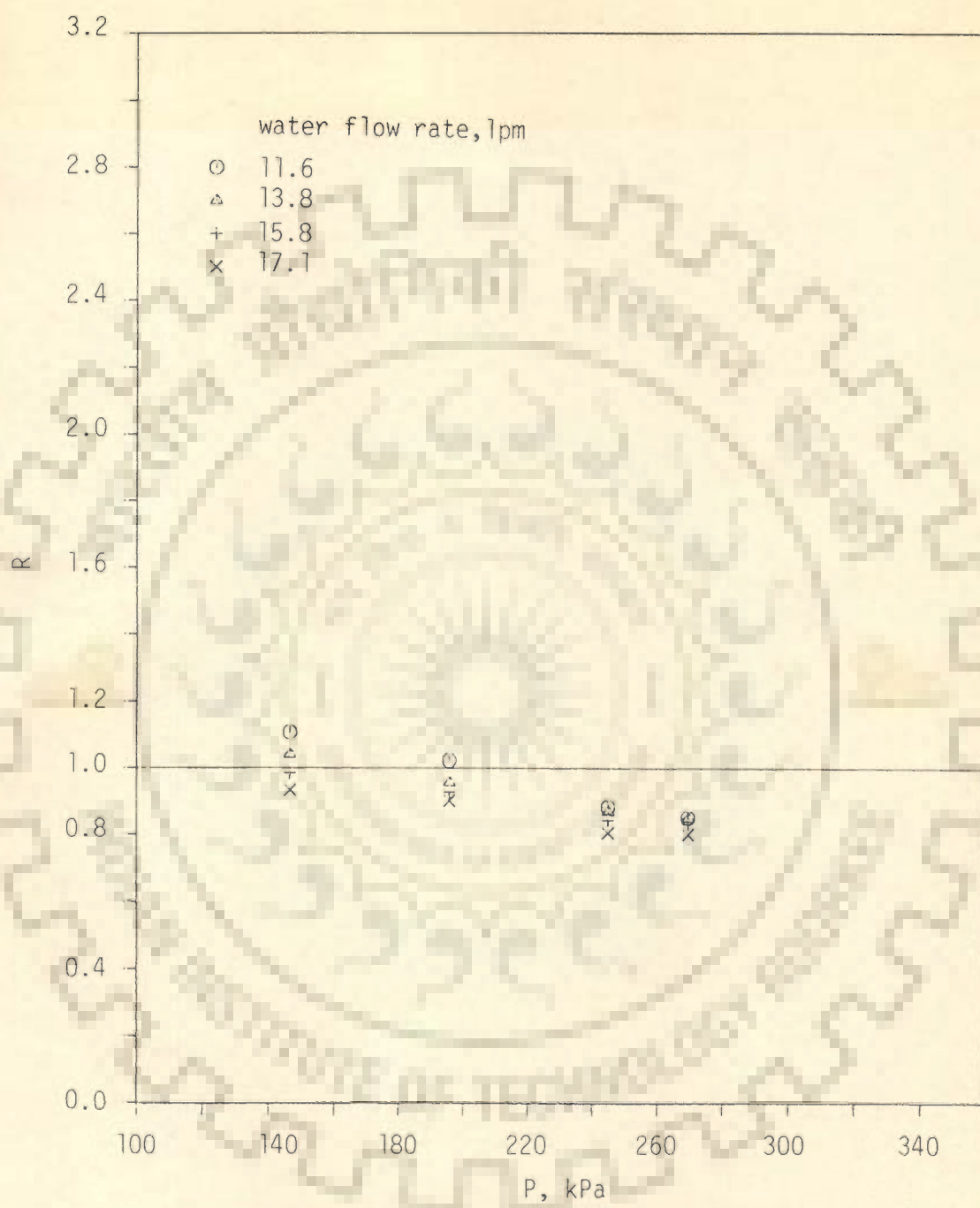
Fig.5.26 comparison between experimental weighted condensing heat transfer coefficient and predicted values from Mikheyev' correlation, Eq.(2.27) for first row tube.
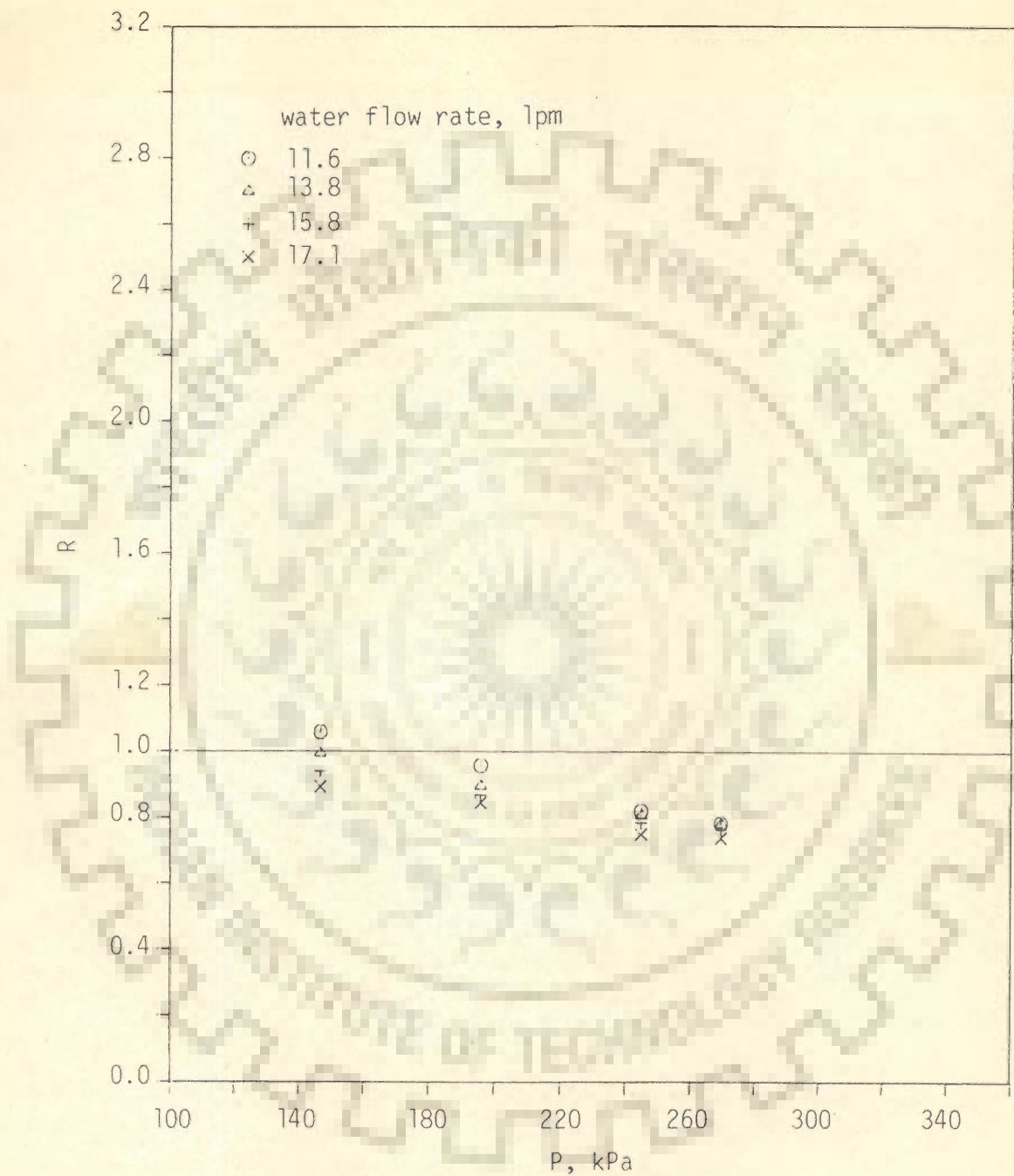
Fig.5.27 comparison between experimental weighted condensing heat transfer coefficient and predicted values from Henderson and Marchello' correlation, Eq.(2.26) for first row tube.
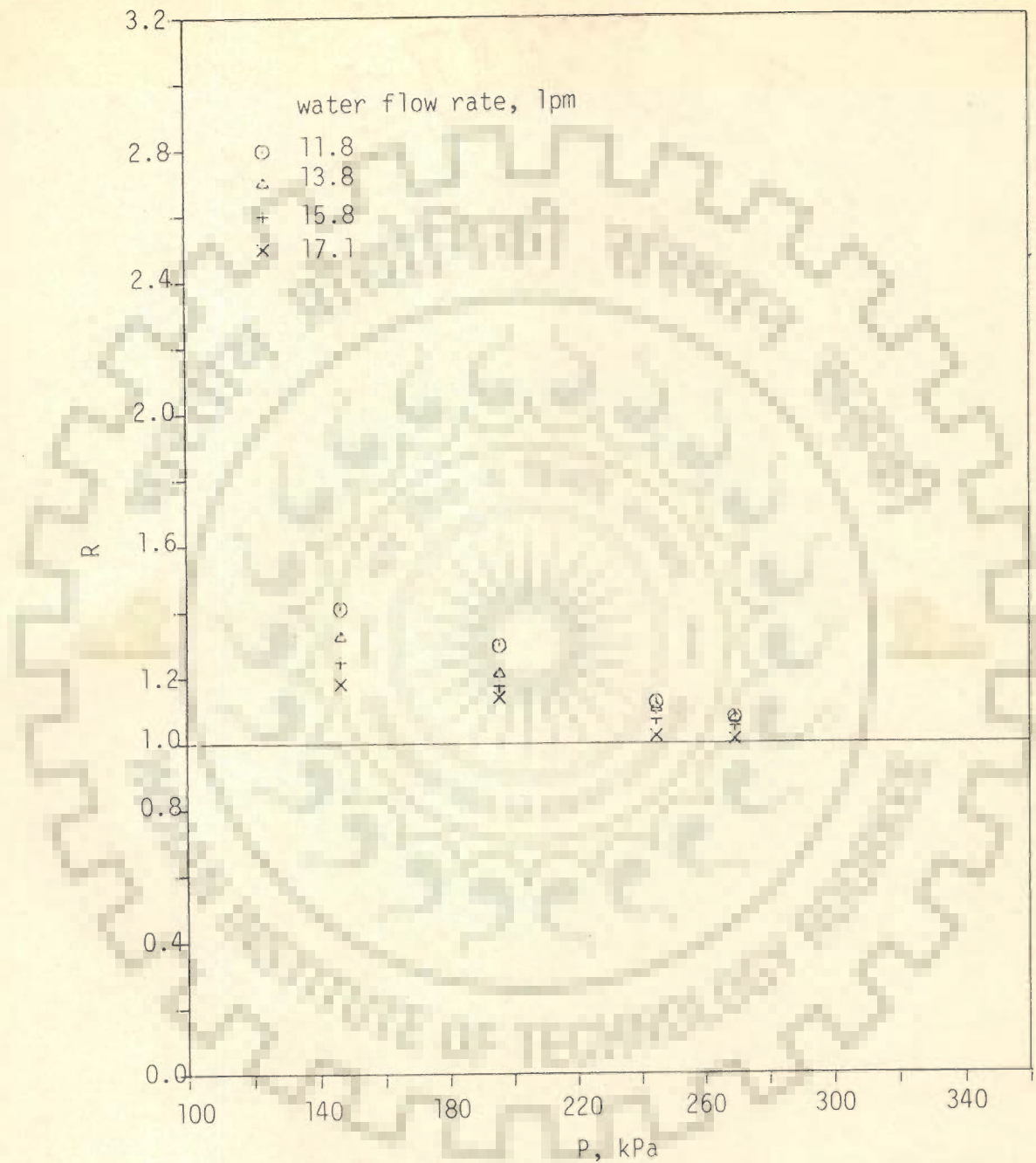
Fig.5.28 comparison between experimental weighted condensing heat transfer coefficient and predicted values from Nusselt' correlation, Eq.(2.3) for first row tube.
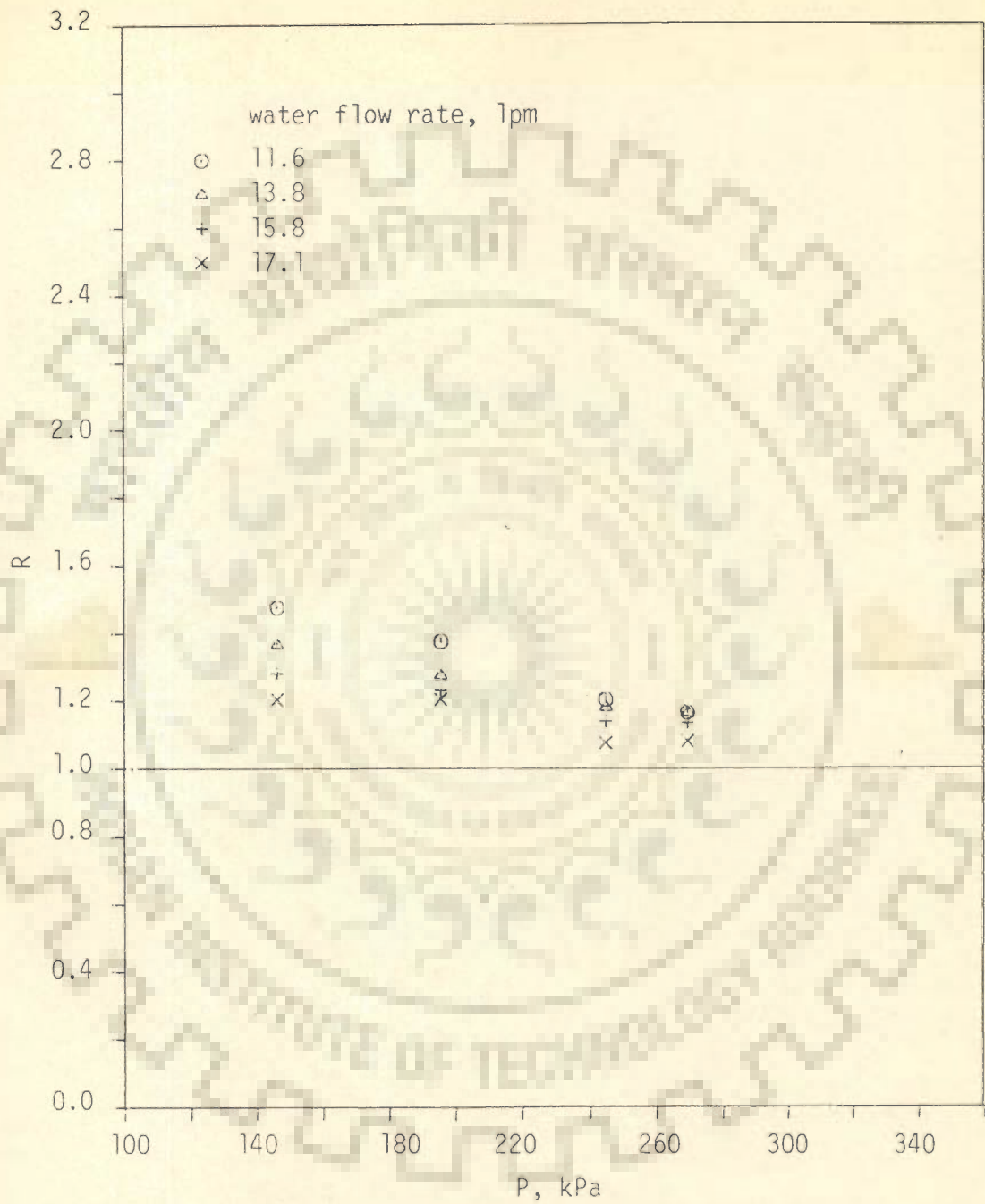
Fig.5.29 comparison between experimental weighted condensing heat transfer coefficient and predicted values from Othmer and Berman' correlation, Eq.(2.7) for first row tube.

110
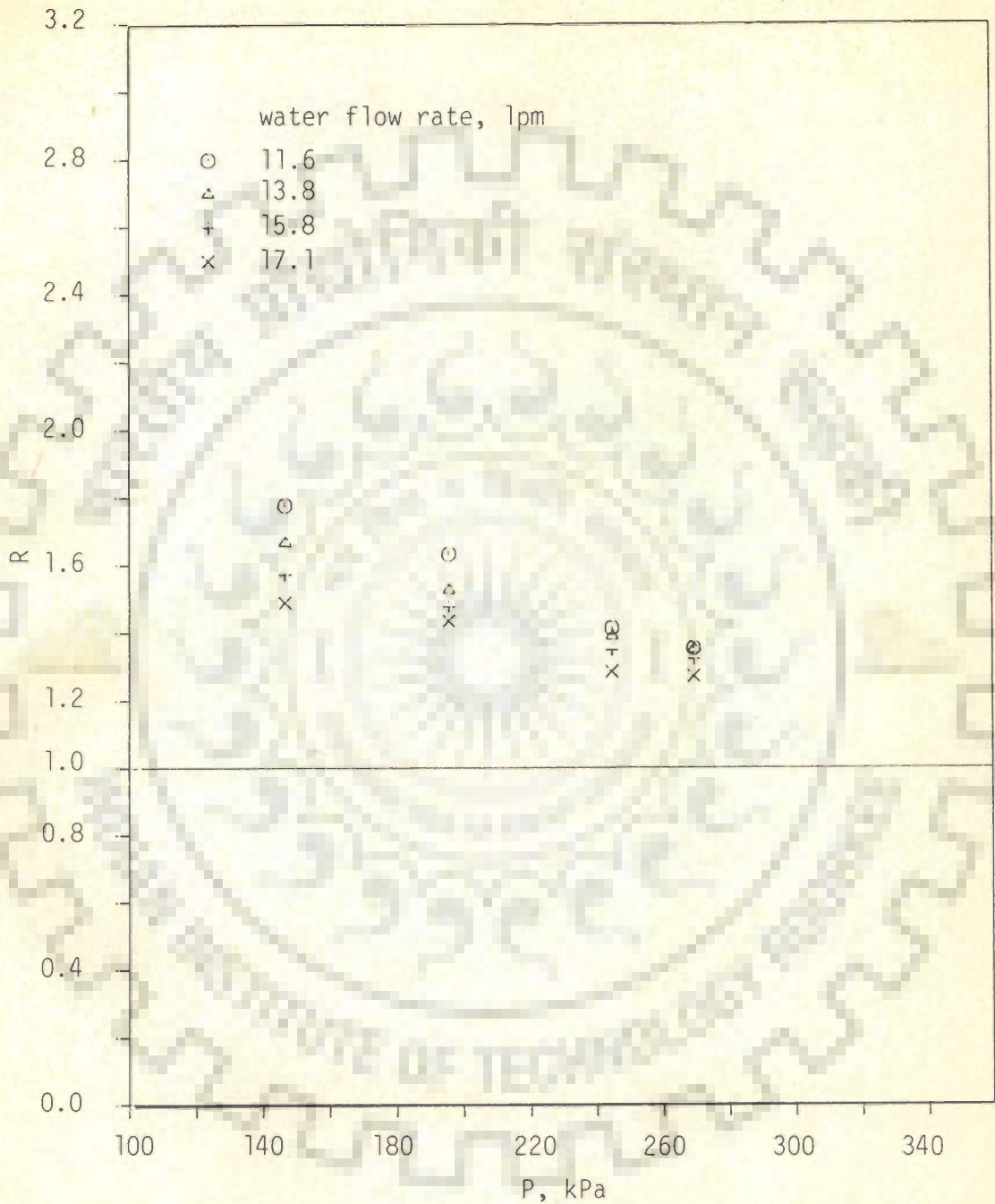
Fig.5.30 comparison between experimental weighted condensing heat transfer coefficient and predicted values from Peck and Reddie' correlation, Eq.(2.8) for first row tube.

111
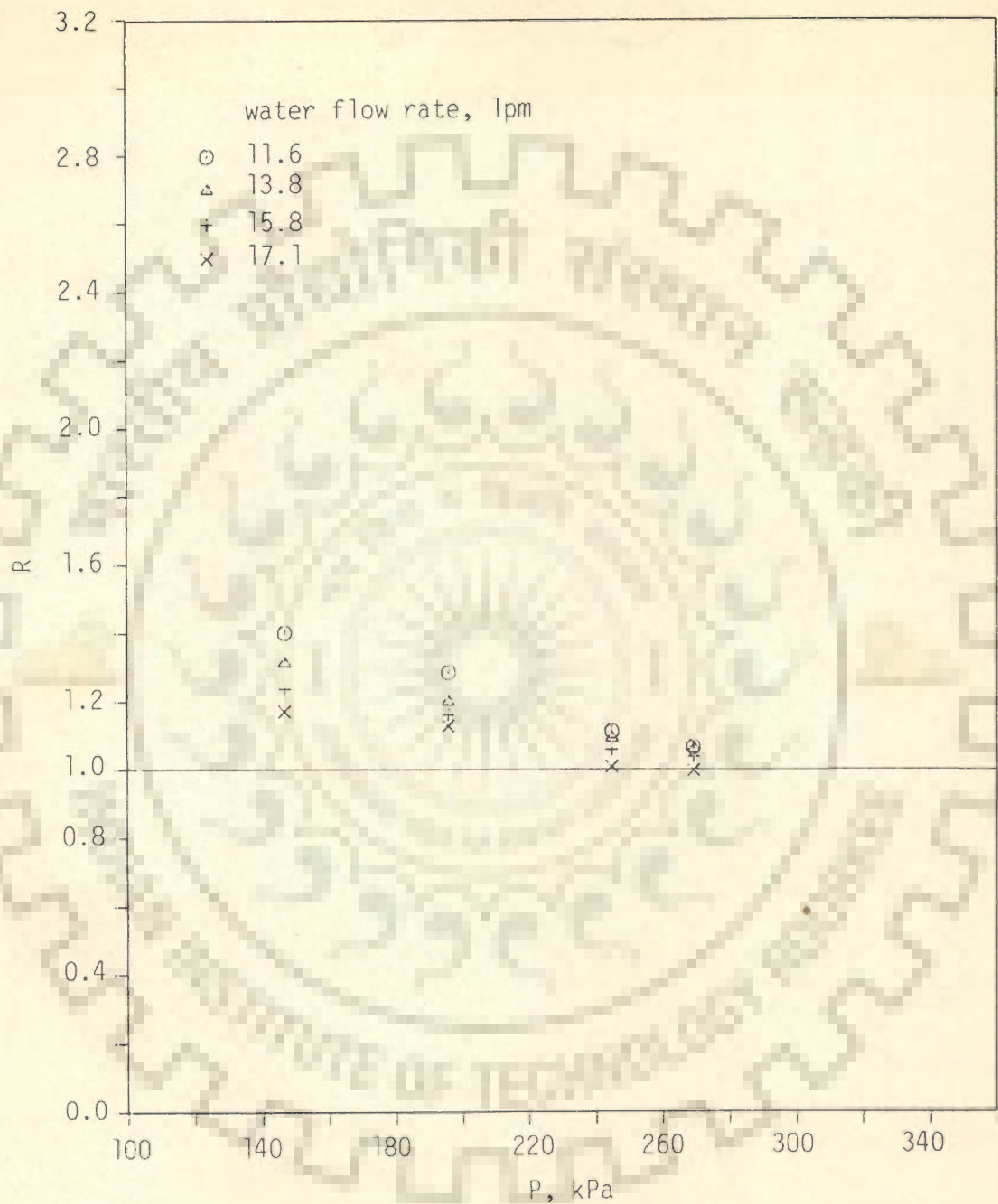
Fig.5.31 comparison between experimental weighted condensing heat transfer coefficient and predicted values from Bromley' correlation, Eq.(2.18) for first row tube.

112
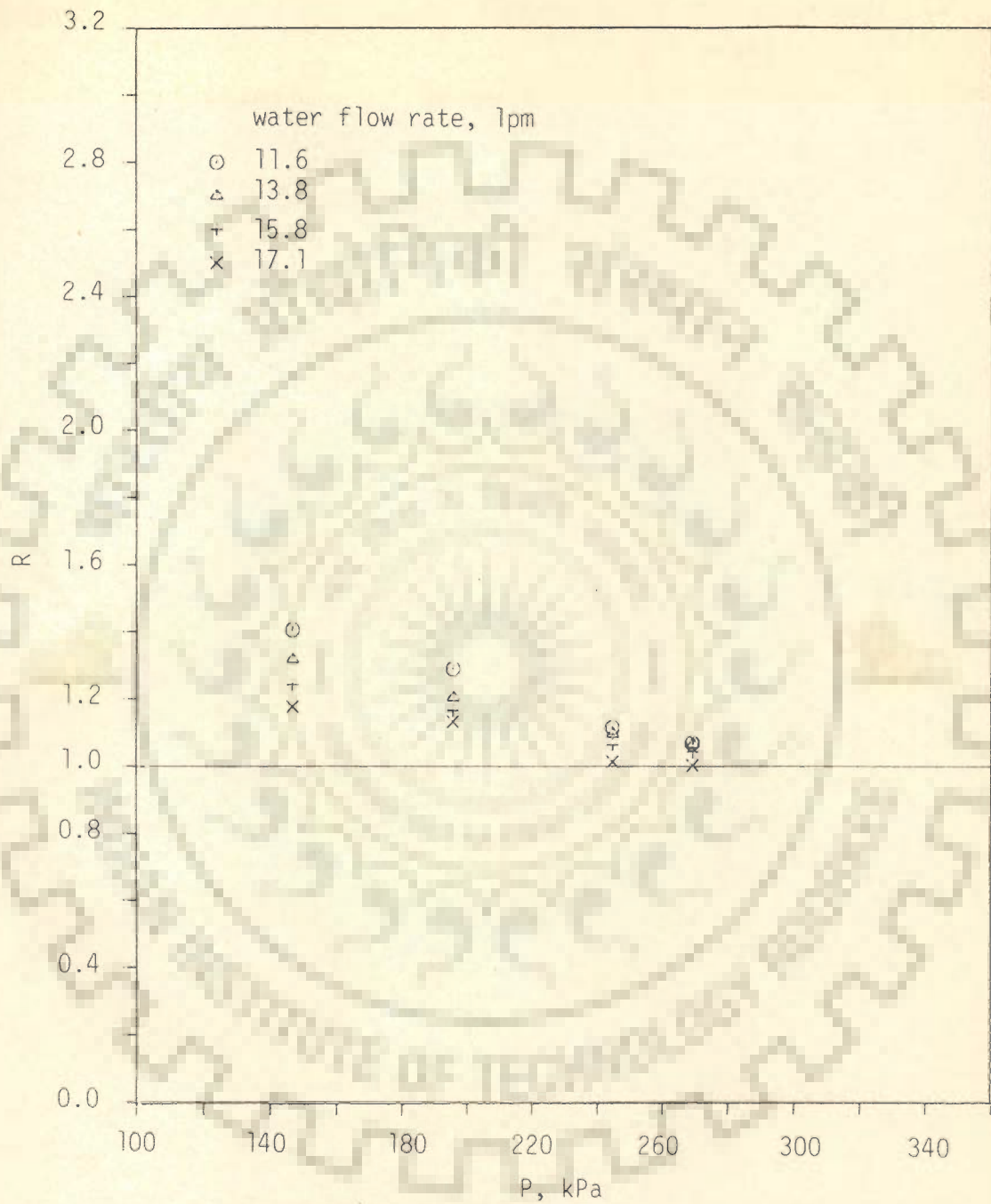
Fig.5.32 comparison between experimental weighted condensing heat transfer coefficient and predicted values from Rohsenow' correlation, Eq.(2.20) for first row tube.
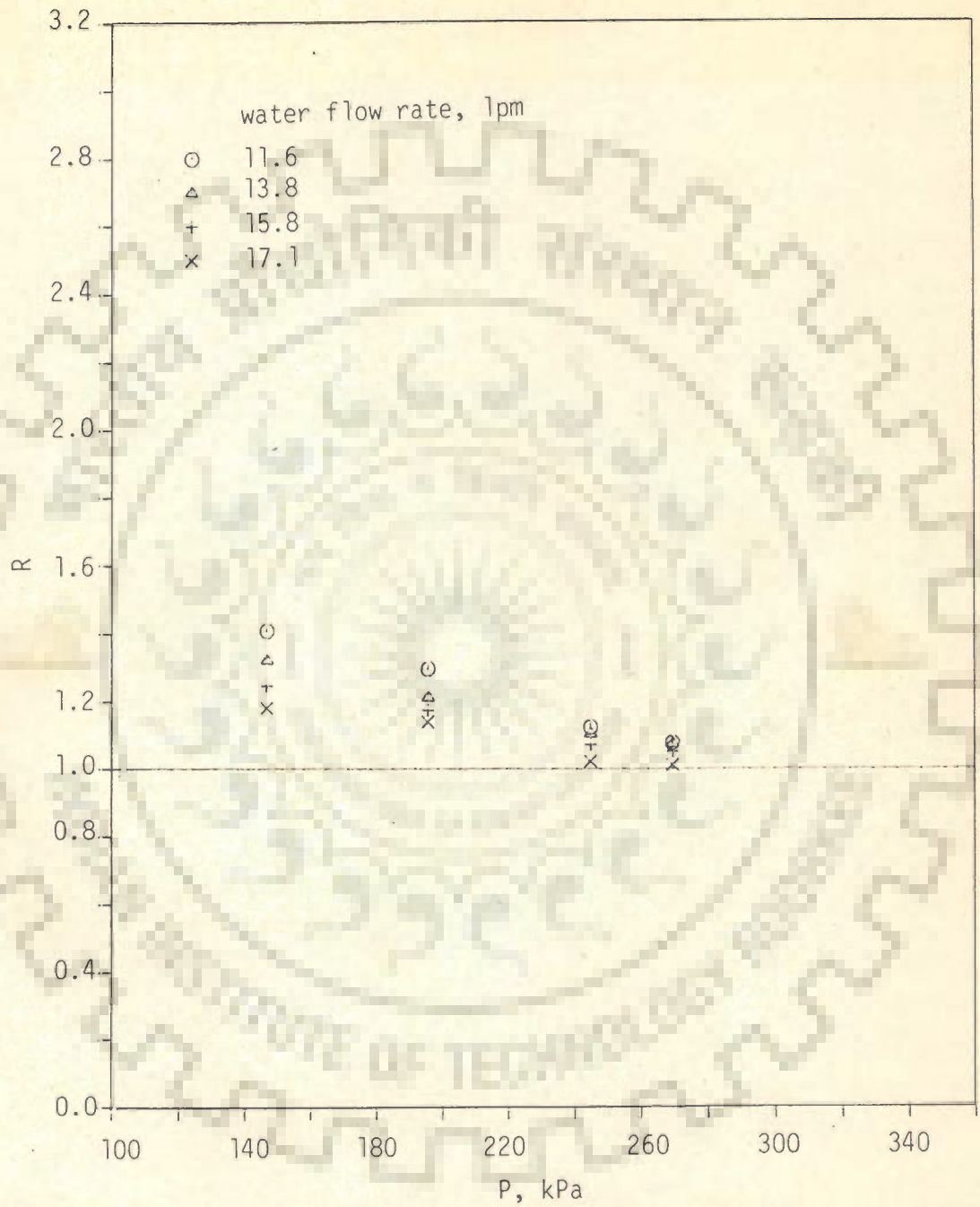
Fig.5.33   comparison between experimental weighted condensing
           heat   transfer   coefficient   and   predicted   values
           from Chen' correlation, Eq.(2.25) for first row
           tube.

114
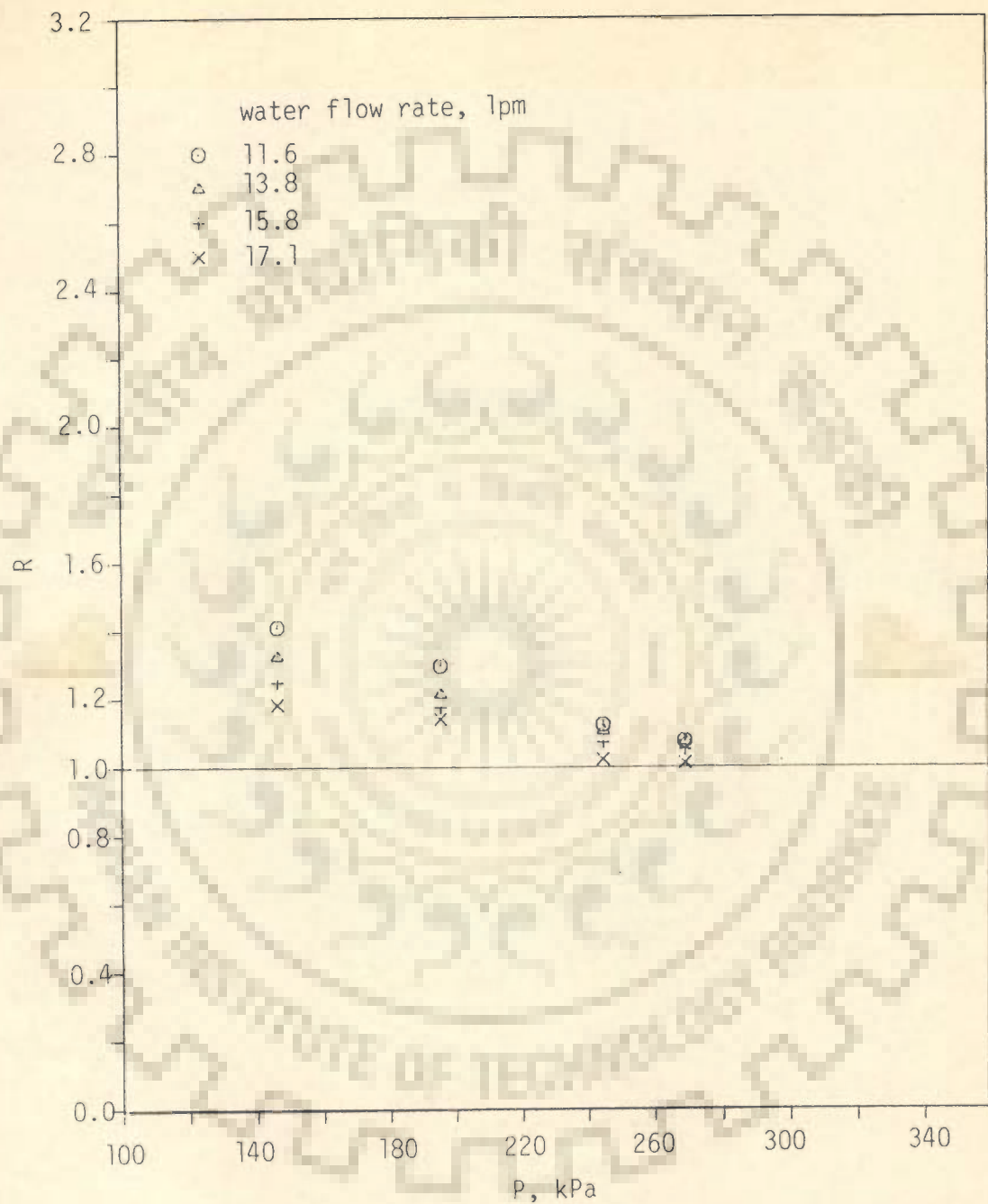
Fig.5.34 comparison between experimental weighted condensing
heat transfer coefficient and predicted values
from White' correlation, Eq.(2.21) for first row
tube

115

2. Figure 5.27 , based on the values of $\bar{h}_{wt,predt}$ from correlation of Henderson and Marchello(11) shows a deviation within +6% to -26%. This also represents an acceptable agreement.

This seems to be owing to the fact that this correlation is a modification of Nusselt's correlation accounting for the effect of falling of condensate in the form of drops.

3. For all steam pressures and cooling water flow rates , the values of R in Figures 5.28 through 5.34 are always greater than unity suggesting that correlations of Nusselt(1), Othmer and Berman (13), Peck and Reddie (14), Bromley (17), Rohsenow (18), Chen (34) and White (19) always underpredict the values of $\bar{h}_{wt,predt}$.

The underpredicted values of $\bar{h}_{wt,predt}$ from correlation due to Nusselt(1) vary from 2% to 42% as pressure decreases from 269.38 kPa to 146.75 kPa whereas for the same pressure range the underpredicted values are 8% to 48% , 26% to 78%, 0% to 40% , 0% to 40% , 2% to 40% and 2% to 40% for the respective correlations due to Othmer and Berman(13) , Peck and Reddie(14), Bromley(17), Rohsenow(18), Chen(34) and White(19).

The underpredicted values from the above correlations are evidently understandable as these correlations are either theoretical in nature or

116

empirical based on experimental data of either organic vapours only or limited data points of steam condensation on horizontal tubes.

4. Finally , it can be concluded that correlation due to Mikheyev (23) correlates the present experimental data the best, followed by that due to Henderson and Marchello(11). The remaining correlations always underpredict.

It is important to mention that from Figure 5.26 it is found that the value of R at a steam pressure of 146.75 kPa is greater than unity. As pressure increases the value of R decreases, becomes unity and then further on it attains value smaller than unity. The possible reason for this behaviour perhaps is that the present experiments are for short tubes where cooling water heat transfer coefficient hi decreases from its inlet to outlet continuously from a large value. Indeed it never attains the asymptotic value as is the case with long tubes. The lowest value of hi in short tube always remains greater than the asymptotic value as seen in Figure 5.17. For short tubes due to higher value of hi the condensation rate is higher than that for long tubes. This results in making the condensate layer thicker in case of short tube for a given set of cooling water flow rate and steam pressure. In other words, experimental values of weighted condensing heat transfer coefficient for short tubes are likely to be smaller than those for long tubes. This explains the value of R smaller than unity at steam pressures greater than 195.8 kPa. At pressures below

195.8 kPa, it seems logical that the values of R should be greater than unity. This may be perhaps due to the fact that at lower pressures, in the range from 146.75 kPa to 195.8 kPa, the condensation rate gets reduced due to small value of steam pressure. As the value of R changes from values greater than unity to those less than unity when steam pressure increases from 146.7 kPa to 269.38 kPa, one can expect value of R equal to unity at some intermediate steam pressure between these pressure values. In the present investigation this occurs at 195.8 kPa.

A similar behaviour is exhibited in all the remaining plots of Figures 5.28 through 5.34, and the value of R is always greater than unity at lower steam pressure. With increase in steam pressure the difference by which R is greater than unity keeps on diminishing. This observation is in accordance with the arguments already attributed to explain the variation in values of R with steam pressure, P in Figure 5.26.

5.4 CONDENSATION OF QUIESCENT STEAM ON THE TUBE BUNDLE

Keeping in view the physics of condensation over a tube bundle of a multitubular condenser it may be mentioned that it is characterized by simultaneous condensation of vapours on all the tubes of the bundle. As a result, the condensate layer thickness on a tube keeps on increasing upto a certain value, beyond which the tube cannot bear it any more and the condensate begins to drop off till it attains some specified minimum thickness. Now due to further condensation the condensate layer thickness again reaches a value when condensate dropping off repeats. Thus a periodic fluctuation of condensate layer thickness between

maximum and minimum values sets in. This phenomenon takes place on all the tubes of the bundle. It is important to mention that the thickness of condensate layer on second row-tube is always greater than that on first row-tube for a given set of operating and geometric parameters. Similarly, for all downrows of tubes of the bundle respective values of the condensate layer thickness vary in increasing order. This is so due to the downward flow of the condensate from tubes. In other words ,the thermal resistance due to the condensate layer around tubes increases in the downward direction of the tube bundle.

Circumferential and longitudinal variation of condensate layer thickness on tubes lying in different rows should implicitly possess the same characteristic behaviour as demonstrated by first row-tube that the thickness of the condensate layer at top-region is less than that at side-region and still less than that at bottom-region at a given cross-section of the tube. Further, the values of the thickness of condensate layer at various cross-sections keep on decreasing continuously along the tube for a given value of steam pressure and cooling water flow rate.

It is important to mention that the present experimental setup does not have the facility to measure the thickness of condensate layer either longitudinally or circumferentially . But it has the provision of thermocouples embedded in the wall of the tubes. Thus the respective readings of the thermocouples can be considered as measure of condensate layer thickness at various positions on the tubes, since the

latter is a measure of the thermal resistance. As a matter of fact , for given steam pressure and cooling water flow rate the wall temperature of a tube at any position is dictated by the magnitude of thermal resistance due to steam condensate .

Therefore, the values of the circumferential wall temperature of the tubes of the bundle employed in the present investigation should be examined.

5.4.1 CIRCUMFERENTIAL WALL TEMPERATURE OF TUBES IN DIFFERENT ROWS

Figures 5.35 and 5.36 have been drawn to represent the typical variation of circumferential wall temperature of top-, side-, and bottom-regions at different distances from leading edges of first, second, third and fourth row tubes for steam pressures of 269.3 kPa and 146.7 kPa, respectively. The data related to all the tubes are for similar conditions of steam pressure , cooling water flow rate and distance along tube-length. These plots help in identifying the effect of condensate falling down from first row tube on the second , from second row tube on the third , and from third row tube on the fourth row tube.

The following characteristic features emerge out of these plots :

1. For a given cooling water flow rate, steam pressure and a distance along the tubes from their leading edges, the temperature at the top-region is consistently greater than that at the side-region and still greater than that at the bottom-region for all the four tubes of the bundle.

120

FIG.5.35 VARIATION OF TOP-, SIDE-, AND BOTTOM-REGION TEMPERATURE OF FIRST, SECOND, THIRD AND FOURTH ROW TUBES ALONG THEIR LENGTH (PS=269.3 KPA)

121

SYMBOLS	POSITION OF A TUBE	TUBE NO. FROM TOP	
☉	TOP	T-1	FIRST
△	SIDE	T-2	SECOND
+	BOTTOM	T-3	THIRD
		T-4	FOURTH
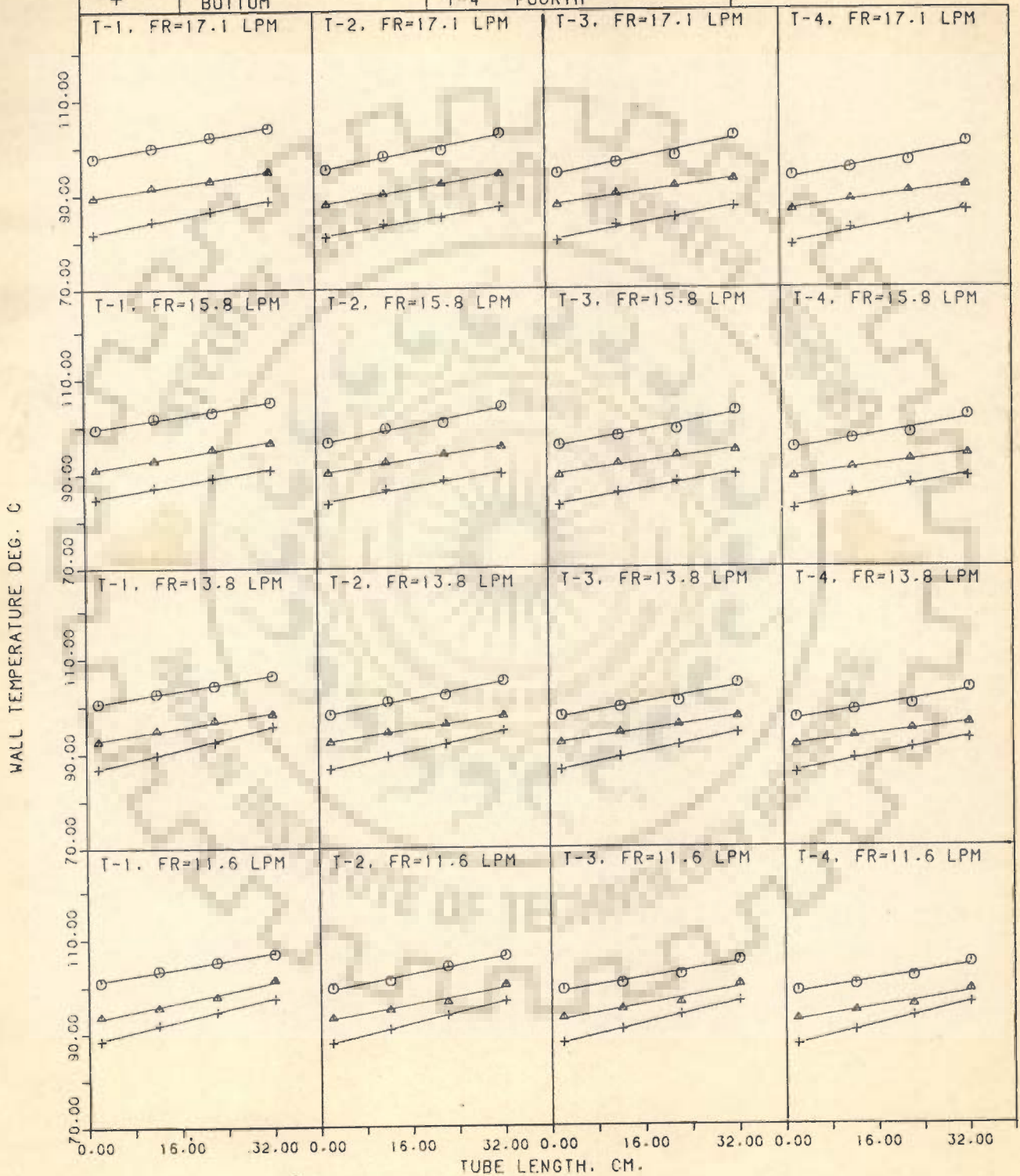
FIG.5.36 VARIATION OF TOP-,SIDE-,AND BOTTOM-REGION TEMPERATURE OF FIRST, SECOND,THIRD AND FOURTH ROW TUBES ALONG THEIR LENGTH(PS=146.7 KPA)

122

2. For a given cooling water flow rate, steam pressure and distance for all the tubes from their leading edges the respective temperatures of the top-, side-, and bottom-regions of first row tube are always higher than the corresponding values for the second row tube. They are still higher than those for third row- and still further higher than those of fourth row- tubes. In other words, for similar operating and geometric parameters, it can be concluded that the temperature for a given region and cross section is the highest for first row tube followed by the second, third and fourth row tubes in decreasing order.

The above behaviour of tubes lying in different rows is expected one in view of the progressively increased thickness of condensate layer on tubes from first row down to fourth row. As a matter of fact ,the condensate dropping off first row tube joins the condensate layer already existing on second row tube. This results in increasing its condensate layer thickness. Likewise, the condensate layer thickness of third row tube still increases and still further for fourth row tube . As a result, the thermal resistances for them for steam condensation assume values in increasing order from first row tube to fourth row tube. Owing to this, at any given region on tubes the wall temperature decreases continuously from first row tube to fourth row tube. This , as a matter of fact , is in accordance to the physics of condensation of steam on tube bundle as stated in Section 5.4.

5.4.2 AVERAGE CIRCUMFERENTIAL WALL TEMPERATURE ALONG THE LENGTH OF TUBES IN DIFFERENT ROWS

As stated in Section 5.4.1, there exists a temperature variation along the circumference of first, second, third and fourth row-tubes for a given set of steam pressure, cooling water flow rate and distance on tube-length. However, for the sake of convenience , it is considered desirable to show the effect of cooling water flow rate and steam pressure on the average values of circumferential wall temperature along the length of tube lying in first-, second-, third-, and fourth- rows.

Figure 5.37 represents average values of circumferential wall temperature versus tube length with steam pressure as para- meter. Figure 5.38 is also a similar plot with cooling water flow rate as parameter. From these plots it is clearly seen that the characteristic features shown by first row- tube are also exhibited by second, third, and fourth row tubes.

The following points are noted from these plots :

1. For all the tubes the average wall temperature increases along the tube length for all values of cooling water flow rate and steam pressure.

2. At fixed steam pressure and distance from the leading edge , the average wall temperature of tube decreases with increase in cooling water flow rate. This is an expected behaviour. With the rise in cooling water flow rate, the water side heat transfer coefficient increases , which in turn enhances the rate of steam condensation. Conse

SYMBOLS	STEAM PRESSURE.KPA	TUBE NO. FROM TOP	
⊙	269.3	T-1	FIRST
△	244.8	T-2	SECOND
+	195.8	T-3	THIRD
×	146.7	T-4	FOURTH
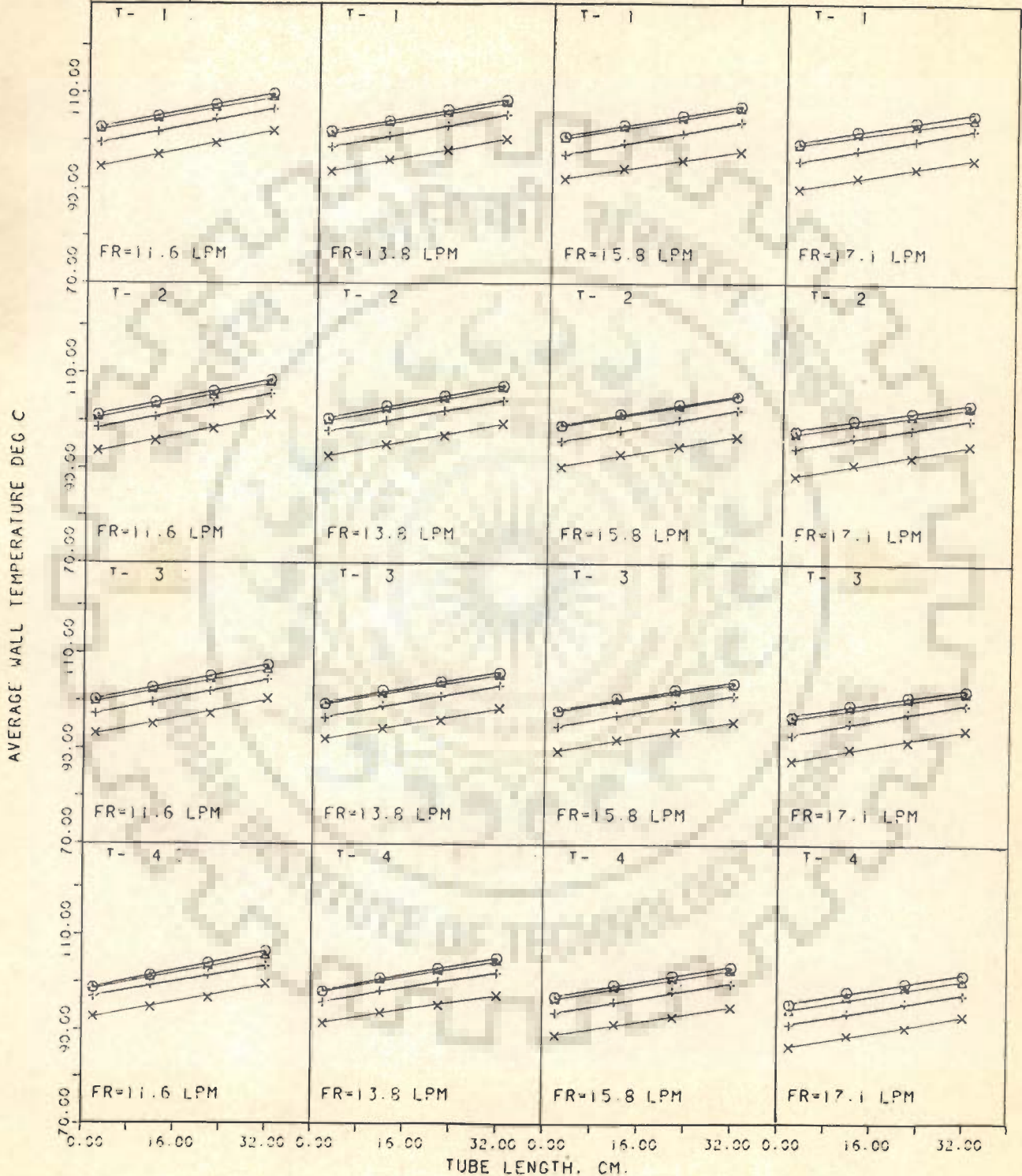
FIG.5.37 VARIATION OF AVERAGE WALL TEMPERATURE OF FIRST.SECOND.THIRD AND FOURTH ROW TUBES ALONG THEIR LENGTHS AS A FUNCTION OF PRESSURE

125

SYMBOLS	WATER FLOW RATE.LPM	TUBE NO. FROM TOP	
⊙	11.6	T-1	FIRST
△	13.8	T-2	SECOND
+	15.6	T-3	THIRD
×	17.1	T-4	FOURTH
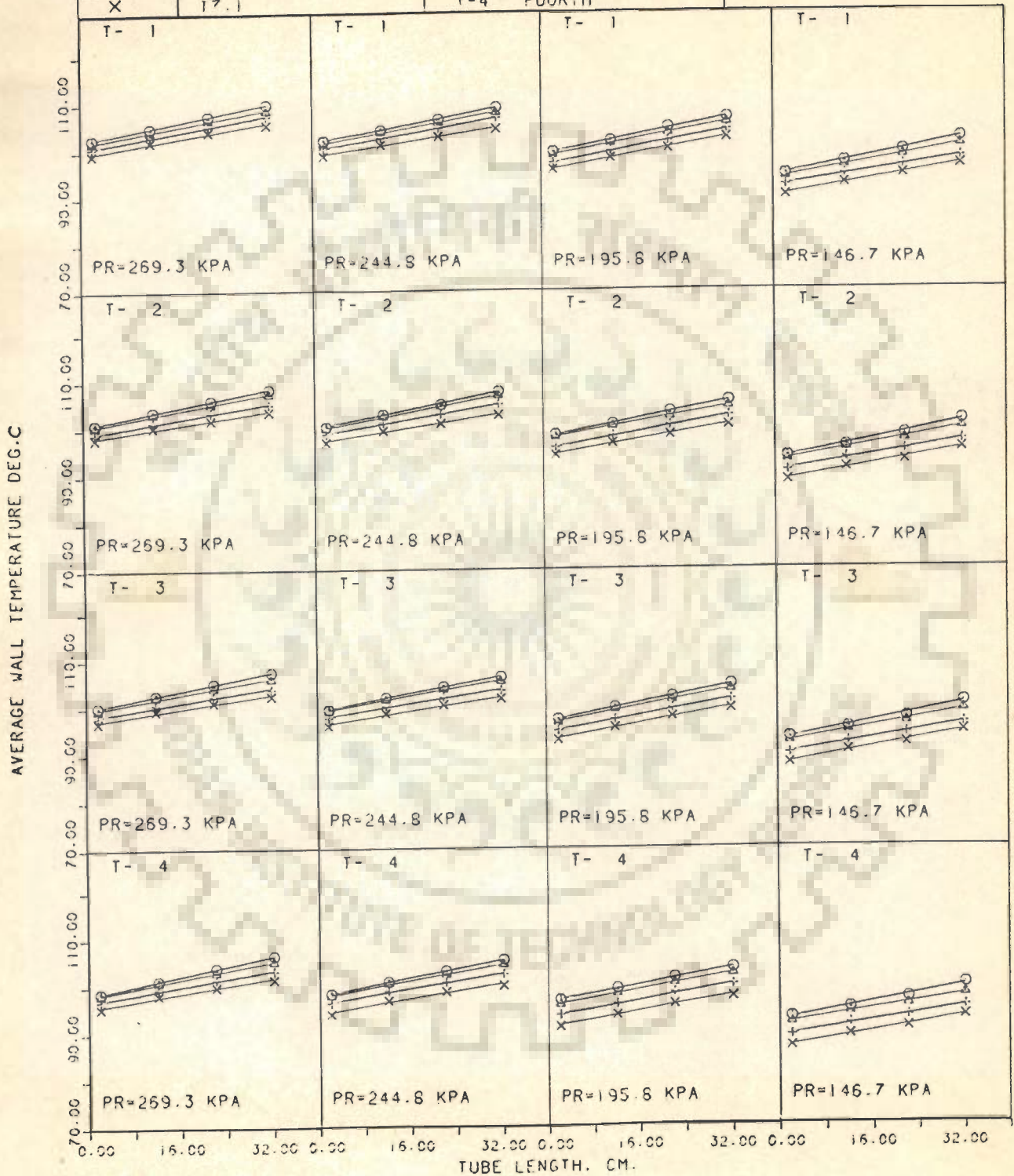
FIG.5.38 VARIATION OF AVERAGE WALL TEMPERATURE OF FIRST,SECOND,THIRD AND FOURTH ROW TUBES ALONG THEIR LENGTH AS A FUNCTION OF COOLING WATER FLOW RATE

126

quently , the condensate layer thickness becomes greater giving rise to greater thermal resistance. Due to this the wall temperature assumes lower values.

3. For a given set of cooling water flow rate, steam pressure and distance from leading edge of tube, the value of average wall temperature decreases progressively from first row tube down to fourth row tube.

The above behaviour is evidently justified due to continuous increase in the value of the condensate layer thickness from the first row tube to fourth row tube.

5.4.3 AVERAGE CIRCUMFERENTIAL WALL TEMPERATURE DISTRIBUTION OF TUBES OF THE BUNDLE : GENERALIZED CORRELATIONS

It is worthwhile to obtain generalized correlation to determine the average wall temperature as a function of cooling water flow rate , inlet temperature of cooling water , steam pressure and distance from the leading edge of the tube for various rows.

Employing nonlinear optimization regression technique the following equations have been obtained :

First row-tube :

$$\bar{t}_w = 61.626 - 0.7286*w + 1.303*ti + 0.07164*P + 21.7857*L$$
$$...(5.4)$$

Second row-tube :

$$\bar{t}_w = 60.560 - 0.8153*w + 1.3756*ti + 0.06805*P + 21.727*L$$
$$...(5.6)$$

127

Third row-tube :

$$\bar{t}_w = 60.945 - 0.8171*w + 1.3348*ti + 0.06668*P + 20.105*L$$
...(5.7)

Fourth row tube :

$$\bar{t}_w = 61.274 - 0.9072*w + 1.3561*ti + 0.06364*P + 21.3613*L$$
...(5.8)

The values of average wall temperature predicted by Eqs.5.6,5.7, and 5.8 are plotted against the experimentally-determined values in Figures 5.39, 5.40, and 5.41, respectively. It is observed from these plots that the two values match excellently within a maximum deviation of ± 2 % only.

Equation 5.4 for the first row tube has been written above for the sake of totality of information . In fact, this equation and Figure 5.15 arising out from it have been already discussed in Section 5.3.10 .

5.4.4 LOCAL CONDENSING HEAT TRANSFER COEFFICIENT FOR TUBES OF THE BUNDLE

As stated in Section 5.4, the value of condensate layer thickness changes circumferentially as well as longitudinally for all the tubes of the bundle in different rows. This suggests that heat transfer coefficient during condensation should also change circumferentially and longitudinally in a likewise fashion. It is worthrepresenting the experimental data in a suitable manner so as to reinforce the above conceptualization of Section 5.4.

Figure 5.42 represents typical values of top-region condensing heat transfer coefficient for tubes of all the rows
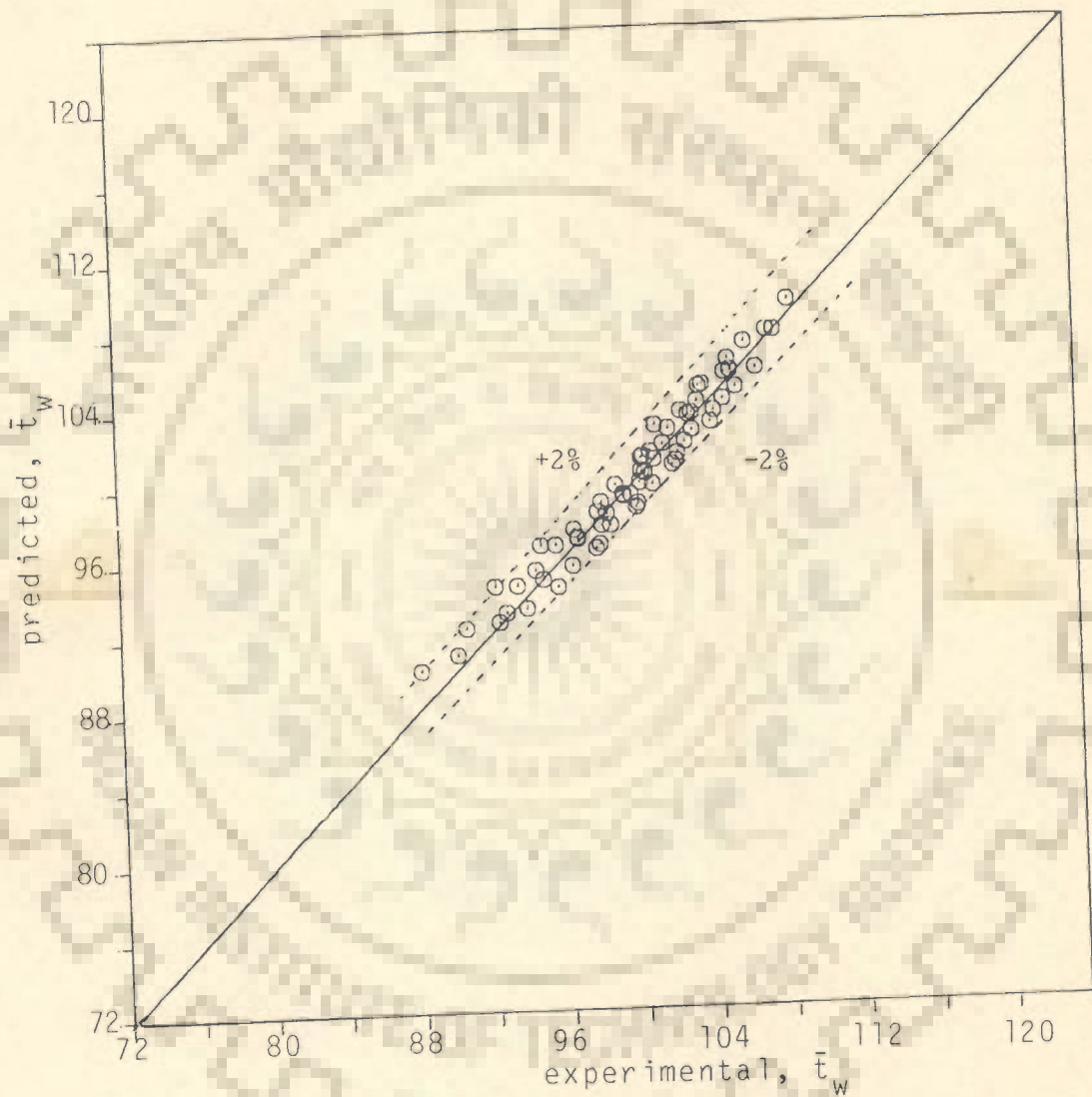
Fig.5.39 comparison between experimental and predicted
average wall temperature($\bar{t}_w$) of second row
tube from present model, Eq.(5.6)
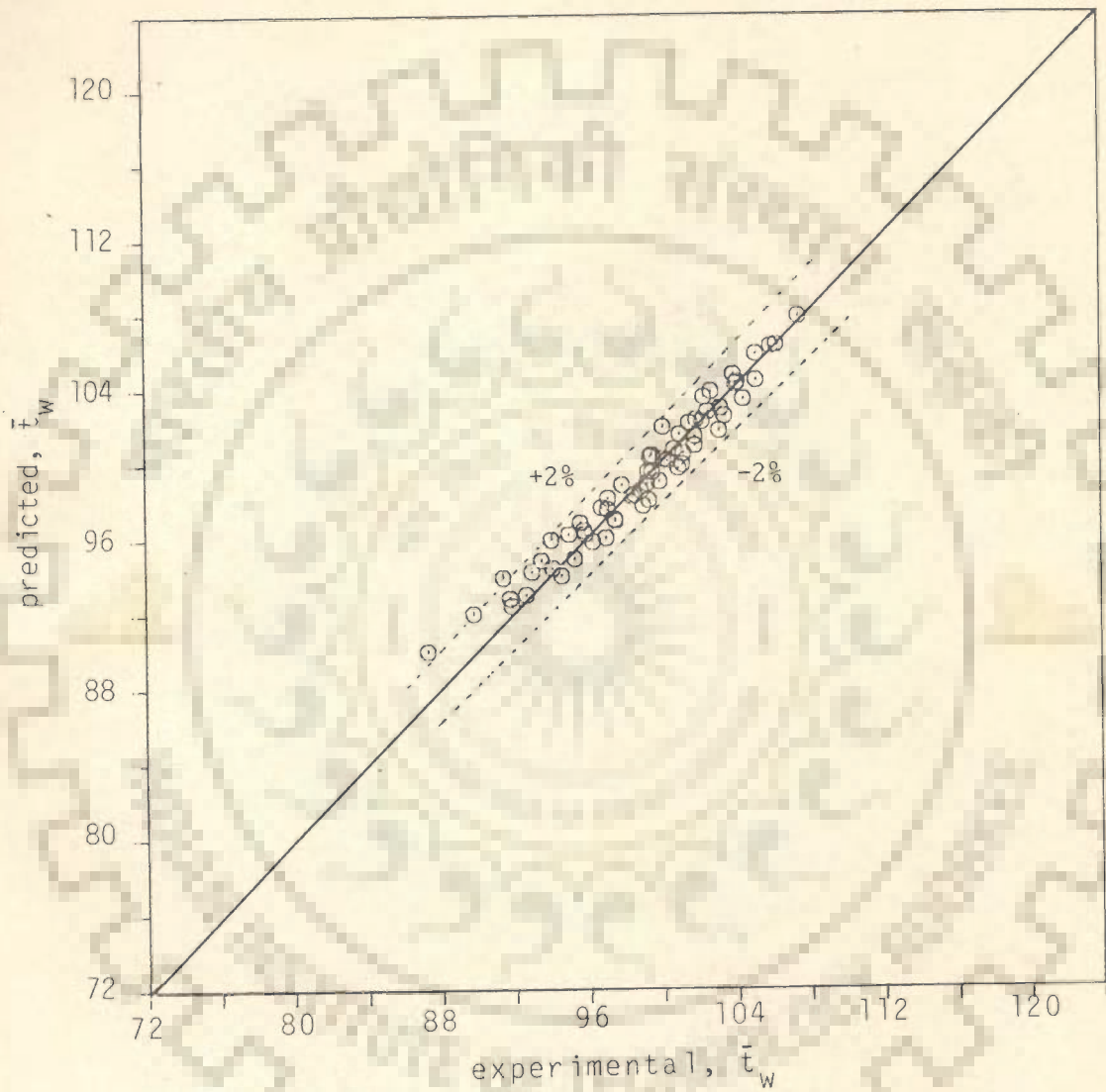
Fig.5.40 comparison between experimental and predicted
average wall temperature ($\bar{t}_w$) of third
row tube from present model, Eq.(5.7)
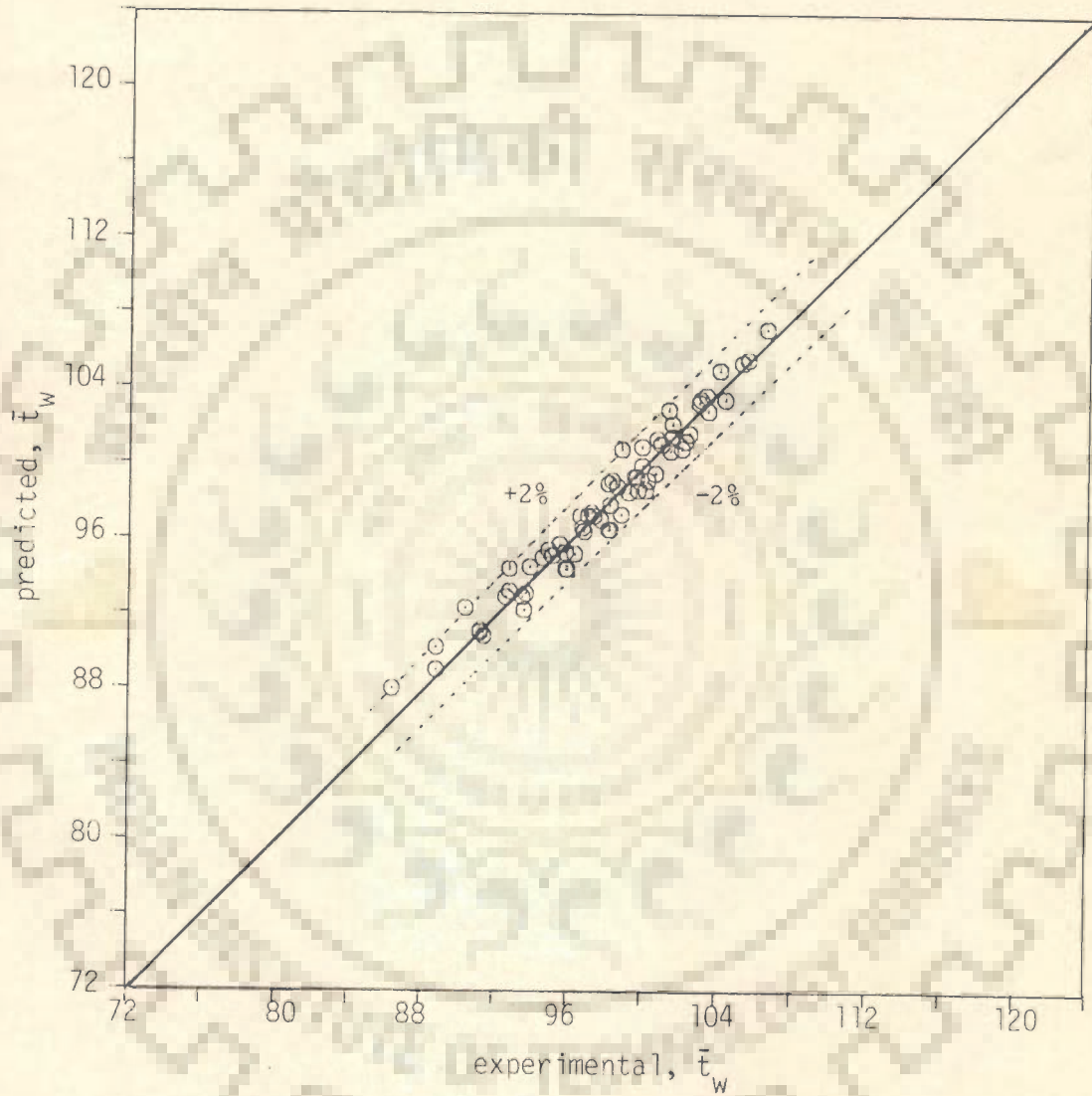
Fig.5.41 comparison between experimental and predicted average
wall temperature($\bar{t}_w$) of fourth row tube from present
model, Eq. (5.8)
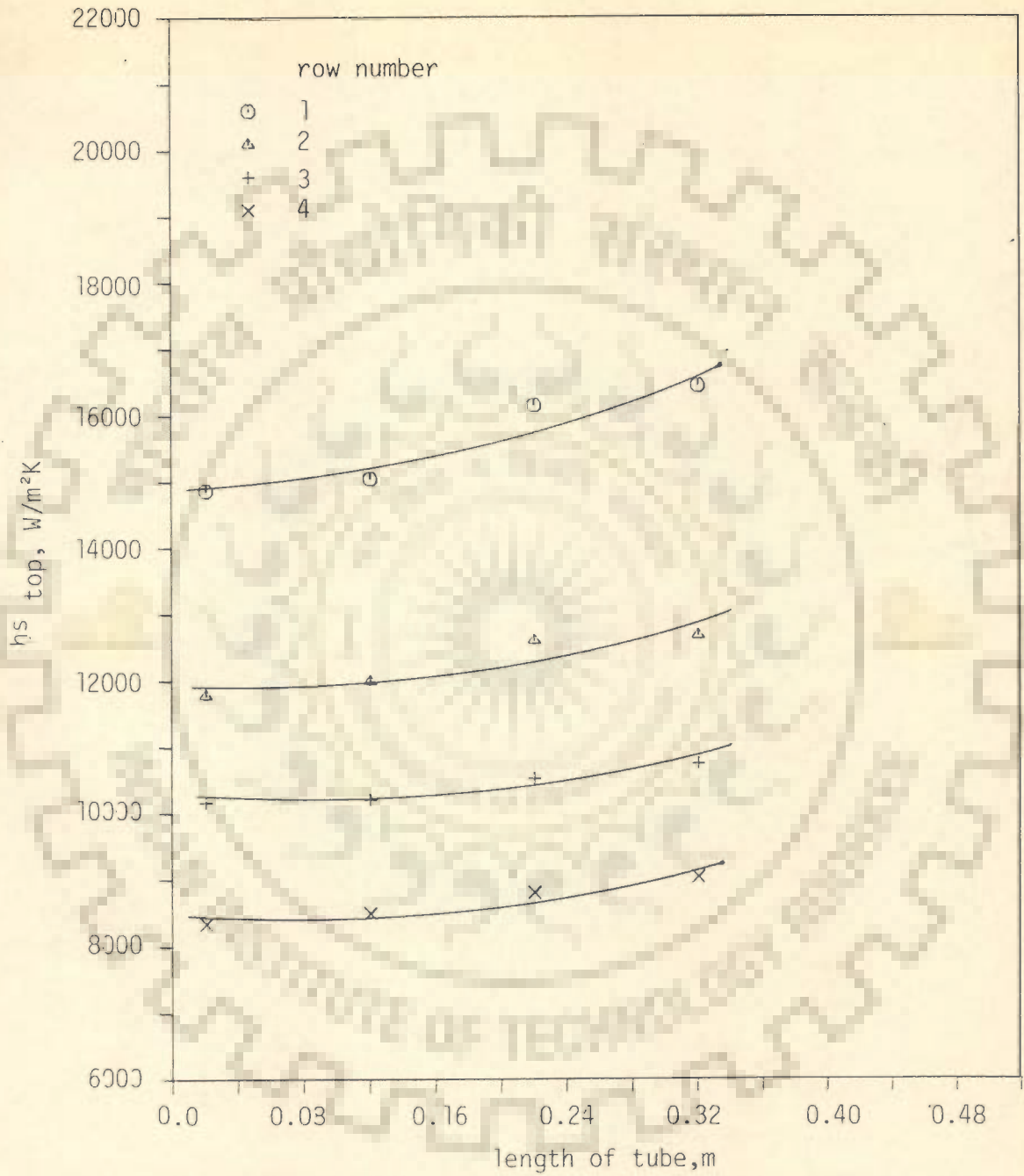
Fig.5.42 variation of condensing heat transfer coefficient
at top-region along the length of tubes in different
rows (Ps= 269.38 kPa, w= 11.6 lpm)

of the bundle as ordinate and the tube length as abscissa, for a steam pressure of 269.38 kPa and cooling water flow rate of 11.6 lpm. From this plot, the following note-worthy observations are made :

1. For the entire lengths of the tubes, the top-region wall temperatures for the first row tube are always the highest followed by those for the second-, third-, and fourth-row tubes in decreasing order.

This behaviour is attributed to the fact that the thickness of condensate layer at the top-region of the first row-tube is the lowest and hence the thermal resistance at the top-region is also the lowest, followed by thermal resistances of corresponding-region of second, third, and fourth row tube in increasing order. Accordingly the value of heat transfer coefficient of first row-tube at its top-region along the length is the highest followed by the values at the corresponding region of second-, third- and fourth-row tubes in decreasing order.

Figure 5.43 is a typical plot between side-region condensing heat transfer coefficient and length of tubes lying in first-, second-, third-, and fourth-row for steam pressure of 269.38 kPa and cooling water flow rate of 11.6 lpm. From this plot, it is amply clear that the values of side-region heat transfer coefficient of first row-tube are always the highest followed by those for second, third, and fourth row-tubes in decreasing order. This behaviour follows from the continuously increasing thickness of condensate layer from first to fourth

Fig.5.43 variation of condensing heat transfer coefficient at side-region along the length of tubes in different rows (Ps= 269.38 kPa, w=11.6 lpm)

134

row-tube.

Figure 5.44 provides the distribution of bottom-region condensing heat transfer coefficient over the entire length of the tubes in different rows of the bundle for a steam pressure of 269.38 kPa and cooling water flow rate of 11.6 lpm. This plot also exhibits the expected similar trend as in Figures 5.42 and 5.43.

A re-examination of Figures 5.42, 5.43 and 5.44 also reveals the fact that the heat transfer coefficient increases along the length of tubes. This is easily understandable in view of the fact that along the tube length the heat transfer coefficient of cooling water decreases continuously whereas its temperature increases. These two factors combined together reduce the condensation rate progressively along the tube. Consequently the condensate layer thickness or thermal resistance decreases longitudinally. Due to this the condensing heat transfer coefficient along the tube increases.

5.4.5 AVERAGE CIRCUMFERENTIAL CONDENSING HEAT TRANSFER COEFFICIENT ALONG TUBES OF THE BUNDLE

The average values of condensing heat transfer coefficient for the tubes in different rows are shown in Figures 5.45 and 5.46 for different steam pressures but a fixed cooling water flow rate of 11.6 lpm. It is found that the experimental data for all the tubes exhibit a similar trend showing a gradual increase in the value of average heat transfer coefficient along the tube. It is also seen that the average heat transfer coefficients of first, second, third, and fourth row-tubes are in the

135

Fig.5.44 variation of condensing heat transfer coefficient at bottom-region along the length of tubes in different rows (Ps=269.38 kPa, w =11.6 lpm)

Fig.5.45 variation of average condensing heat transfer coefficient along the length of tubes in different rows (Ps= 269.38 kPa, w=11.6 lpm)
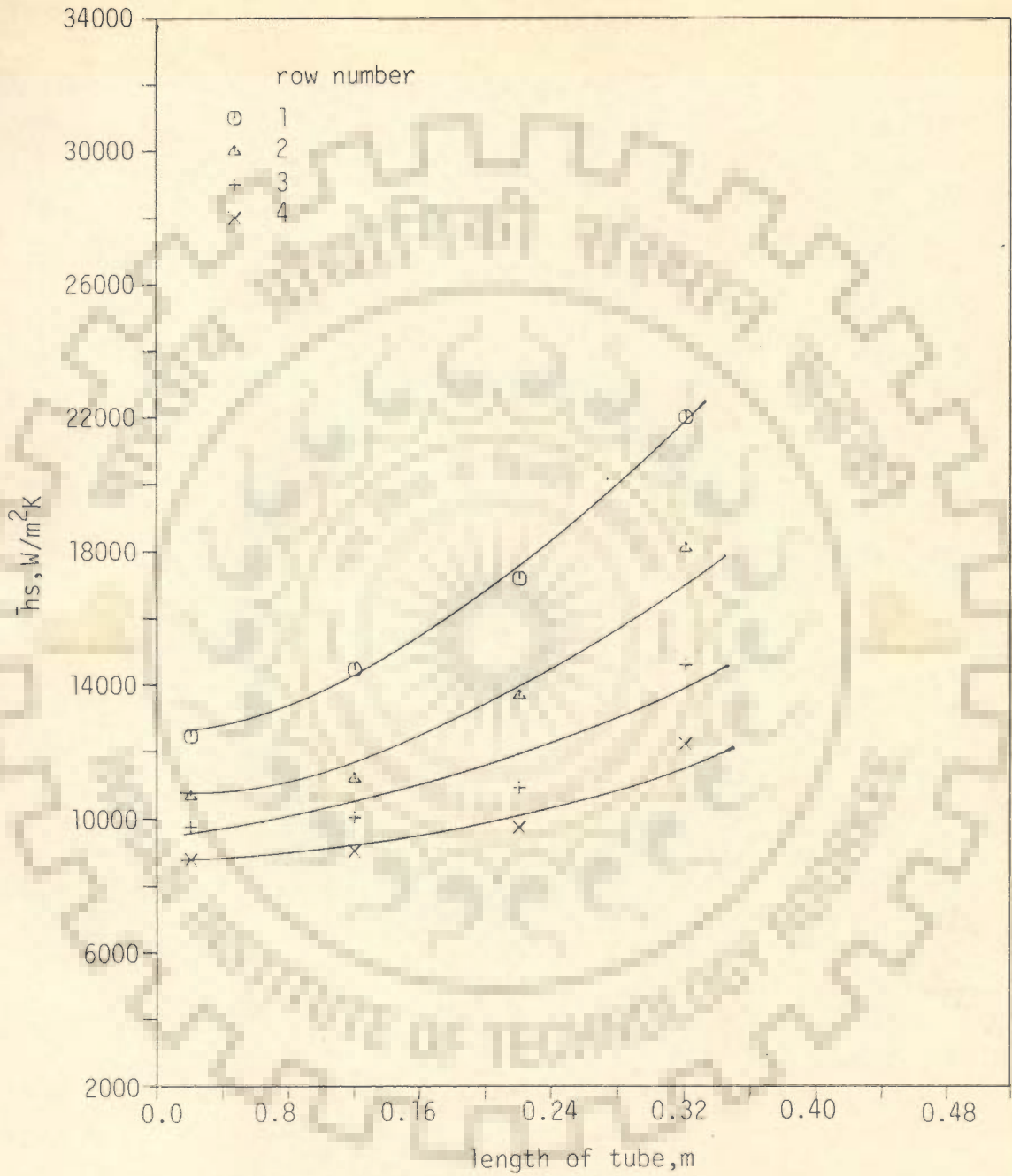
Fig.5.46 variation of average condensing heat transfer coefficient along the length of tubes in different rows (Ps=146.75 kPa, w =11.6 lpm)

138

decreasing order.

5.4.6 GENERALIZED CORRELATION OF HEAT TRANSFER COEFFICIENT FOR THE TUBE BUNDLE

In order to obtain a generalized correlation, it is thought adequate and desirable that the values of average heat transfer coefficient of Section 5.4.5 should be expressed as weighted values, $\bar{h}_{wt}$. This, indeed, is more meaningful and convenient from the point of view of design of such condensers.

Appendix B details the method of calculating the values of $\bar{h}_{wt}$ for a given test run. After obtaining the values of h_{wt} for tubes of the bundle for various steam pressures and cooling water flow rates a plot is drawn between $\bar{h}_{n,wt}/\bar{h}_{1,wt}$ and the row number n, as shown in Figure 5.47. The quantity $\bar{h}_{n,wt}/\bar{h}_{1,wt}$ represents a ratio between weighted value of heat transfer coefficient of nth row-tube and weighted average value of heat transfer coefficient of first row-tube for a set of given operating parameters.

All the data points of present investigation tabulated in Appendix A are found to be correlated by the following equation within $\pm$ 10 % for the range of steam pressure from 146.7 kPa to 269.38 kPa and cooling water flow rate from 11.6 lpm to 17.1 lpm, respectively :

$$\frac{\bar{h}_{n,wt}}{\bar{h}_{1,wt}} = n^{0.83} - (n-1)^{0.83} \qquad \ldots(5.10)$$

Refering to Section 5.3.19 it can be recalled that the experimental data of present investigation for the first row tube are best correlated by Mikheyev's correlation within +10% to
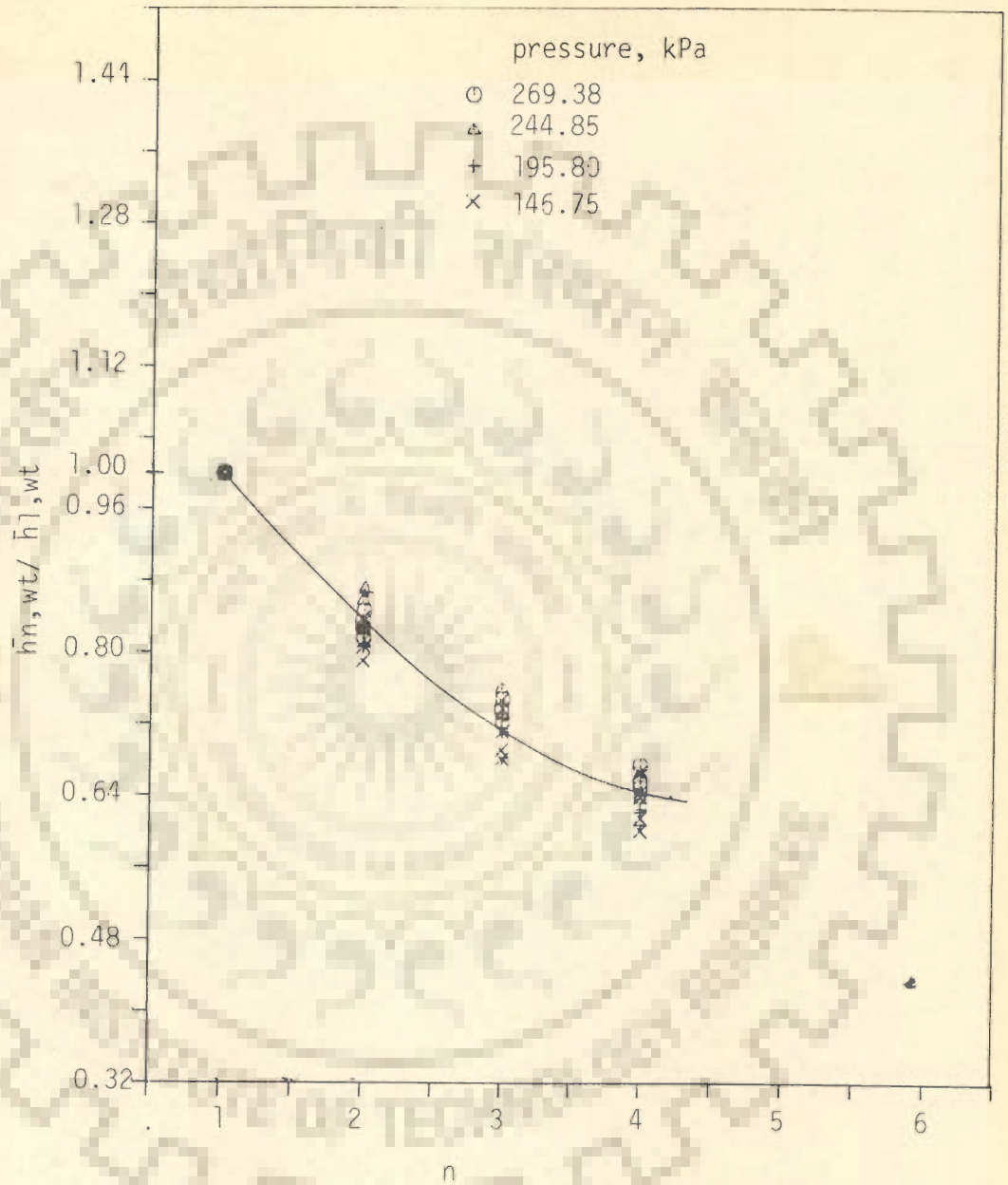
Fig.5.47 a plot between $(\bar{h}_n,wt)/(\bar{h}_1,wt)$ and row number, n
for different steam pressures and cooling water
flow rates

-18%. Thus the value of $\bar{h}_{1,wt}$ required for Eq.5.10 can be calculated from Mikheyevs correlation Eq.2.27 for the prediction of the values of $\bar{h}_{n,wt}$ for the tubes in rows other than the first row.

5.4.7 COMPARISON BETWEEN PRESENT CORRELATION (EQ.5.10) AND EARLIER CORRELATIONS

An examination of Section 2.2 reveals that the correlations relevant to present investigation ,i.e., condensation of pure quiescent vapours on horizontal tube bundle arrayed in vertical rows, are due to Jakob(24), Kern(26),Grant and Osment(28), Short and Brown(29),Withers and Young(32) and Young et al(33). They have recommended their correlations for computing $\bar{h}_{n,wt}/\bar{h}_{1,wt}$ for condensation of vapours on tube bundles employed in their studies. These have been described in Chapter 2. However , their salient features are given below :

Jakob(24), using Nusselt's model and assuming the condensate falling as continuous sheet directly on to the top of the tube below and taking $(t_s - t_w)$ the same for all the tubes,has recommended his correlation as follows :

$$\frac{\bar{h}_{n,wt}}{\bar{h}_{N1,wt}} = n^{3/4} - (n-1)^{3/4} \qquad (2.28)$$

Kern(26), assuming that condensate falls down as discrete droplets causing ripples in condensate film, obtained the following correlation :

$$\frac{\bar{h}_{n,wt}}{\bar{h}_{1,wt}} = n^{0.833} - (n-1)^{0.833}$$

$$...(2.30)$$

141

Grant and Osment(28) have also succeeded in correlating their experimental data by the following Equation :

$$\frac{\bar{h}_n}{h_{N1}} = (\Gamma n/\Upsilon n)^{-0.223} \qquad \ldots (2.31)$$

Short and Brown(29), based on their experimental data for the condensation of Freon-11 on a bundle of horizontal tubes arrayed in vertical rows, have recommended a correlation as follows :

$$\frac{\bar{h}_n}{h_{N1}} = (\Gamma n/\Upsilon n)^{-0.25} \qquad \ldots (2.32)$$

Wither and Young(32) have recommended following equation for the calculation of weighted condensing heat transfer coefficient for horizontal tubes in a vertical row :

$$\bar{h}_n = 0.725 \ C_n \ n^{-1/4} \ (NC)^{1/4} \qquad \ldots (2.34)$$

where NC is $(k^3 \varrho^2 g \lambda) / (\mu d_o \Delta t)$ and for 25 mm tube $C_n = 1.07 \ n^{0.170}$.

Young et al(33) have recommended Equations 2.37 through 2.41 to calculate the condensing heat transfer coefficient. These equations can be expressed in the following form :

$$\bar{h}_n = K_1 \ (NC)^{1/4}$$

where the respective values of the constant K_1 are 0.655, 0.576, 0.551, 0.498 and 0.464 for row number 1,2,3,4,5.

Figure 5.48 provides a comparison among the predicted values from above correlations and the present correlation, Eq.5.10. It may be mentioned that the values of $\bar{h}_n/\bar{h}_{N1}$ from correlations of Grant and Osment(28) and Short and Brown(29) for the purposes of comparison are obtained using the present
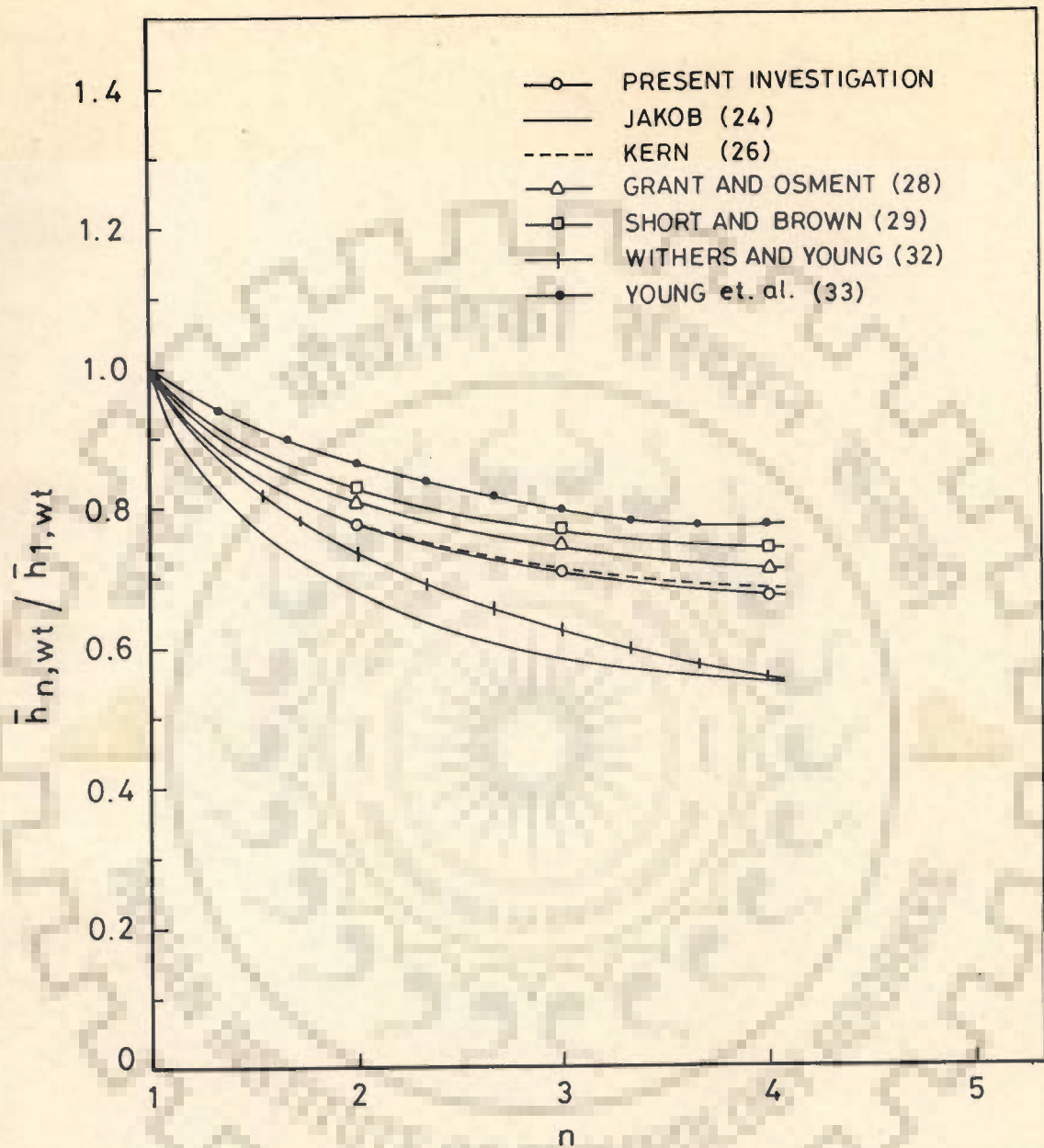
Fig.5.48. A plot of $\bar{h}_{n,wt}/\bar{h}_{1,wt}$ and row number, n from present investigation Eq. 5.10 and earlier investigations

experimental data.

From this plot the following important conclusions are drawn :

1. The predictions from Kern, Eqn. 2.30 and the present correlation, Eq.5.10 agree excellently with a negligible deviation.

It is important to mention that Eq.5.10 of present investigation and Eq.2.30 due to Kern(26) are of same form having the respective values of exponent of n as 0.83 and 0.833. Due to this an excellent agreement between present investigation and that of Kern(26) is easily understandable.

2. The values due to Grant and Osment(28), and Short and Brown(29) are always greater than those of present investigation. However, the deviation is within a maximum of +5.0% .

It is important to mention that Butterworth(30) has also observed that the correlations due to Grant and Osment , Kern, and Short and Brown are in close agreement amongst themselves. This is further supported by the present investigation.

3. The maximum deviation between the predicted values from the correlations due to Withers and Young (32),Young et al(33) and the present experimental results are -16.8 % and 18.28 respectively.

4. Correlation due to Jakob(24) underpredicts the values with a maximum deviation of -18.3%.

It may be emphasized that the predictions from Jakob's correlations are the most conservative. The observation that Jakob's correlation is a conservative one is in conformity with the findings reported by Marto(36) who undertook a comprehensive comparison amongst various available correlations.

CONCLUSIONS

The main conclusions drawn from the present investigation are as follows:

A. For the First Row Tube

1. In the present investigation it is distinctly and evidently established that the wall temperature of the first row tube changes not only circumferentially but also longitudinally. It is also found that the value of the average circumferential wall temperature continuously increases along the entire length of tube. This is so due to the continuously decreasing values of cooling water-side heat transfer coefficient. In this respect the average circumferential wall temperature distribution of short tube is unlike that of long tube (L/d > 50) having high flow rate of cooling water. Based on the present experimental data the simplified generalized correlation for average circumferential wall temperature of first row tube has been obtained in terms of cooling water flow rate , its inlet temperature , steam pressure , and distance from the leading edge of the tube as follows :

tw=61.626- 0.7286*w+1.3030*ti+0.07164*P+21.7857*L

2. In view of the nonisothermal surface attained in the case of short tubes it is important to know the value of weighted wall temperature for the calculation of condensing heat transfer coefficient from an available correlation. The present investigation has succeeded in recommending the following empirical functional relationship for the weighted wall temperature for the short tube in the following form, based on the present experimental data :

$$twt = 57.489 - 0.07183*w + 1.6306*ti + 0.07096*P$$

The experimentally-determined weighted wall temperatures of the first row tube of the bundle show a good agreement with the model of Bromley within a maximum deviation of +35 % .

3. The experimental data for the condensation of quiescent steam on first row tube of the bundle are correlated best by the Mikheyev correlation within a maximum deviation of -18.0 % to 10 %, followed by the correlation due to Henderson and Marchello within a maximum deviation of -26 % to 6% . The maximum deviations between the experimental data of the present investigation and those predicted by Nusselt ,Othmer and Berman, Peck and Reddie ,Bromley ,Rohsenow, and White are 40% , 48%, 78%, 40%, 40% , and 40% respectively.

B. For the Tube Bundle

1. Like the first row tube, the wall temperatures of second- ,third-, and fourth-row tubes also change both circumferentially and longitudinally. The value of the average circumferential wall temperature for the short tube in each row also continuously increases along the entire length of the tubes. The proposed equations relating average circumferential wall temperatures of short tube in different rows to other parameters are as follows:

(i) Second Row Tube

tw=60.560 -0.8153*w+1.3756*ti+0.0680*P+21.727*L

(ii) Third Row Tube

tw=60.945 -0.8171*w+1.3348*ti+0.0666*P+20.105*L

(iii) Fourth row tube

tw=61.274 -0.9072*w+1.3561*ti+0.0636*P+21.3613*L

2. For the determination of weighted condensing heat transfer coefficient for short tubes in second-, third-, and fourth- rows , based on the present experimental data, the following empirical correlation is recommended within a maximum deviation of $\pm$10%.

$$\frac{h_{n,wt}}{h_{1,wt}} = n^{0.83} - (n-1)^{0.83}$$

It is further recommended that $h_{1,wt}$ can be calculated from Mikheyev's correlation. The predicted values from the correlation deviate from experi-

148

mental values of h_1,wt within a maximum range of -18% to 10% only. Now with the values of h_1,wt from Mikheyev's correlation , a design engineer can calculate hwt for the tubes lying in second- third-, and fourth -rows using above correlation.

3. It is also found that the predictions from Kern's correlation and the experimental values of weighted condensing heat transfer coefficient of the present investigation agree excellently within a negligible deviation. The values due to Grant & Osment ,and Short & Brown are always greater than those of present investigation within a maximum deviation of 5%. This, of course,is in conformity with the observations of Butterworth. Further it is to underline that the predicted values from the correlation due to Withers and Young differ from the present experimental values within -16.8 % . The maximum deviation between the predictions from the correlation of Young et al and experimental value is within 18.3% . Correlation due to Jakob underpredicts the values with a maximum deviation of -18.3% .

It may be emphasized that the predictions from the correlations due to Jakob , and Withers and Young are the most conservative. The observation that Jakob's correlation is a conservative one is in conformity with the findings reported by Marto.
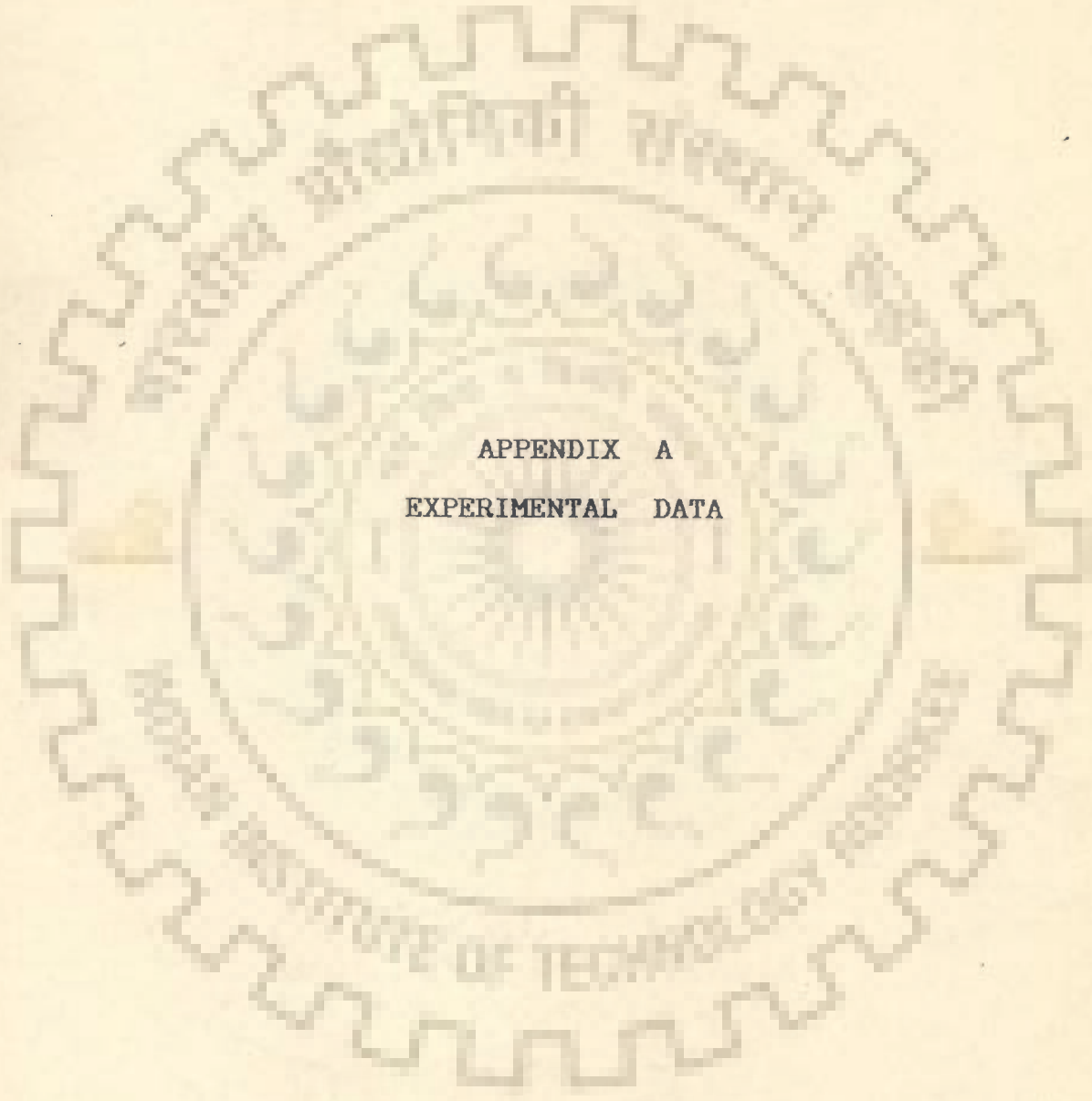
RECOMMENDATIONS FOR FUTURE STUDIES

For the furtherance of knowledge in the area of condensation of vapours including steam on the bundle of horizontal short tube condensers the following recommendations are made :

1. In view of the wide applications of condensers in process industries employing condensation of vapours of organic liquids, it shall be of practical importance if the investigation be also carried out for the condensation of organic vapours in order to provide circumferential and longitudinal temperature distribution of tubes in different rows of the bundle for the design of short tube condensers. Such data shall also help in obtaining a more generalized correlation for the average circumferential wall temperature of the condenser tubes.

2. It shall be of yet another practical importance and immediate application if the experimental data for the circumferential and longitudinal temperature distributions of the short tube condenser, during condensation of vapours, are also obtained for the bundles having their tubes on a triangular/square pitch as practiced in industrial condensers.

3. Experiments should be conducted to collect data for the condensation of steam and other organic vapours on bundles of tubes of different diameters. This shall provide the effect of tube diameter on condensing heat transfer coefficients.

APPENDIX   A
EXPERIMENTAL   DATA

TABLE-A.1   CORRECTED WALL TEMPERATURES OF CONDENSER TUBES

row no.	thermocouple position	cross-section, x				cooling water exit temp.,°C
		1	2	3	4	
first	top	112.50	114.02	116.00	117.14	
	side	102.46	104.56	107.34	110.30	32.82
	bottom	93.38	96.70	99.12	102.16	
second	top	109.58	111.36	113.34	114.54	
	side	101.38	104.00	106.36	109.14	32.18
	bottom	92.56	96.14	98.70	101.72	
third	top	107.85	109.54	111.34	112.94	
	side	100.74	103.20	106.00	107.96	31.65
	bottom	92.12	95.56	98.16	101.55	
fourth	top	104.90	107.12	109.14	110.98	
	side	99.68	102.02	105.00	107.34	31.14
	bottom	91.72	94.83	97.92	101.30	

```
average steam bulk temperature    = 129.82  °C          run no.  1
condensate temperature            = 129.69  °C
cooling water inlet temperature   =  23.90  °C
condensate flow rate              =   0.80 lpm
cooling water flow rate           =  11.6  lpm      heat loss ≈ 5%
```

TABLE-A.2   CORRECTED WALL TEMPERATURES OF CONDENSER TUBES

row no.	thermocouple position	cross-section, x				cooling water exit temp.,°C
		1	2	3	4	
first	top	111.90	113.42	115.40	116.50	
	side	101.34	103.78	106.36	108.38	31.80
	bottom	92.56	95.40	97.92	100.48	
second	top	109.34	111.02	112.43	113.84	
	side	100.60	103.45	105.86	107.68	31.09
	bottom	91.58	95.08	97.48	100.33	
third	top	107.28	109.42	10.644	111.68	
	side	100.00	102.72	104.74	106.32	30.63
	bottom	91.12	94.68	97.00	100.04	
fourth	top	104.54	106.70	108.54	110.04	
	side	99.27	101.78	103.62	105.68	30.27
	bottom	90.55	94.18	96.66	99.75	

```
average steam bulk temperature    = 129.83  °C          run no.  2
condensate temperature            = 129.74  °C
cooling water inlet temperature   =  24.09  °C
condensate flow rate              =   0.82 lpm
cooling water flow rate           =  13.8  lpm      heat loss ≈ 6%
```

TABLE-A.3   CORRECTED WALL TEMPERATURES OF CONDENSER TUBES

row no.	thermocouple position	cross-section, x				cooling water exit temp.,°C
		1	2	3	4	
first	top	110.92	112.74	114.66	115.62	
	side	100.40	103.18	105.00	106.96	30.85
	bottom	91.14	94.14	96.45	99.30	
second	top	107.95	109.55	110.88	112.06	
	side	99.05	101.85	103.72	105.16	30.24
	bottom	90.10	93.35	96.02	98.26	
third	top	105.85	108.10	109.38	110.03	
	side	98.55	101.25	102.98	104.50	29.83
	bottom	89.54	92.92	95.34	97.34	
fourth	top	103.74	105.58	107.36	109.02	
	side	98.25	100.70	102.51	104.34	29.46
	bottom	89.08	92.34	94.66	96.65	

average steam bulk temperature   = 129.85 °C   run no.   3
condensate temperature   = 129.69 °C
cooling water inlet temperature   = 24.02 °C
condensate flow rate   =   0.7   lpm
cooling water flow rate   = 15.8   lpm   heat loss ≈ 2%

TABLE-A.4   CORRECTED WALL TEMPERATURES OF CONDENSER TUBES

row no.	thermocouple position	cross-section, x				cooling water exit temp.,°C
		1	2	3	4	
first	top	109.95	111.74	113.22	114.30	
	side	98.66	101.60	103.33	105.15	30.24
	bottom	89.54	92.85	95.55	97.05	
second	top	107.23	108.85	110.16	111.05	
	side	98.06	100.50	101.86	103.82	29.68
	bottom	88.75	91.76	93.80	95.96	
third	top	105.02	107.28	108.66	109.26	
	side	97.43	99.54	101.02	102.36	29.31
	bottom	88.24	91.27	93.61	95.65	
fourth	top	102.34	104.45	105.96	107.35	
	side	96.17	99.03	100.31	101.91	29.11
	bottom	88.03	91.06	93.34	95.28	

average steam bulk temperature   = 129.87 °C   run no.   4
condensate temperature   = 129.75 °C
cooling water inlet temperature   = 23.90 °C
condensate flow rate   =   0.87 lpm
cooling water flow rate   = 17.1   lpm   heat loss ≈ 9%

TABLE-A.5   CORRECTED WALL TEMPERATURES OF CONDENSER TUBES

row no.	thermocouple position	cross-section, x				cooling water exit temp.,°C
		1	2	3	4	
first	top	111.80	113.23	114.84	116.00	32.23
	side	101.48	103.65	106.13	109.10	
	bottom	92.91	96.11	98.52	101.55	
second	top	108.77	110.56	111.68	113.79	31.65
	side	100.36	102.25	104.90	106.35	
	bottom	92.15	95.35	97.80	101.15	
third	top	106.86	108.86	110.26	111.80	31.21
	side	100.09	102.25	104.90	106.35	
	bottom	91.75	94.81	97.52	100.83	
fourth	top	104.46	106.48	108.05	109.88	30.73
	side	99.25	101.56	103.86	105.81	
	bottom	91.15	94.03	97.22	100.81	

average steam bulk temperature   = 126.59 °C   run no. 5
condensate temperature   = 126.38 °C
cooling water inlet temperature = 23.92 °C
condensate flow rate   =   0.75 lpm
cooling water flow rate   = 11.6   lpm   heat loss ≈ 6%

TABLE-A.6   CORRECTED WALL TEMPERATURES OF CONDENSER TUBES

row no.	thermocouple position	cross-section, x				cooling water exit temp.,°C
		1	2	3	4	
first	top	110.96	112.95	114.18	112.95	30.92
	side	100.50	102.75	105.16	107.16	
	bottom	92.16	95.14	97.47	100.25	
second	top	107.95	109.81	111.08	112.95	30.36
	side	99.95	102.51	105.16	107.31	
	bottom	91.53	94.75	97.06	99.76	
third	top	106.31	107.86	109.52	110.58	29.98
	side	99.61	102.00	104.31	105.37	
	bottom	91.15	94.15	96.66	99.55	
fourth	top	103.71	105.75	107.14	108.88	29.56
	side	98.98	101.39	102.90	104.62	
	bottom	90.55	93.55	96.48	99.35	

average steam bulk temperature   = 126.61 °C   run no. 6
condensate temperature   = 126.46 °C
cooling water inlet temperature = 23.80 °C
condensate flow rate   =   0.80 lpm
cooling water flow rate   = 13.8   lpm   heat loss ≈ 8%

TABLE-A.7   CORRECTED WALL TEMPERATURES OF CONDENSER TUBES

row no.	thermocouple position	cross-section, x				cooling water exit temp., °C
		1	2	3	4	
first	top	109.86	111.66	113.51	114.75	30.12
	side	99.75	102.35	103.85	105.90	
	bottom	91.05	93.88	96.06	99.02	
second	top	107.25	109.18	110.32	112.16	29.63
	side	98.65	100.96	102.75	104.86	
	bottom	90.21	92.98	95.36	97.75	
third	top	105.38	107.25	108.79	109.65	29.29
	side	98.08	100.36	102.15	103.41	
	bottom	89.48	92.52	94.81	96.90	
fourth	top	102.74	104.66	106.11	107.45	28.97
	side	97.16	99.48	101.36	103.10	
	bottom	88.92	92.15	94.31	96.66	

average steam bulk temperature   = 126.62 °C   run no. 7
condensate temperature   = 126.43 °C
cooling water inlet temperature   = 23.80 °C
condensate flow rate   =   0.75 lpm
cooling water flow rate   = 15.7   lpm   heat loss ≈ 3%

TABLE-A.8   CORRECTED WALL TEMPERATURES OF CONDENSER TUBES

row no.	thermocouple position	cross-section, x				cooling water exit temp., °C
		1	2	3	4	
	top	108.76	110.36	111.51	113.40	30.12
	side	98.55	100.71	102.25	103.32	
	bottom	88.76	92.15	94.56	96.06	
second	top	106.38	108.35	109.40	11.184	29.75
	side	97.06	99.46	100.68	102.00	
	bottom	91.58	95.08	97.48	100.33	
third	top	104.36	106.32	107.76	108.39	29.41
	side	96.56	98.91	100.38	101.75	
	bottom	86.98	90.25	92.52	94.55	
fourth	top	100.65	102.99	104.45	105.55	29.16
	side	94.75	97.58	99.30	100.64	
	bottom	86.35	89.55	92.16	93.56	

average steam bulk temperature   = 126.57 °C   run no. 8
condensate temperature   = 126.47 °C
cooling water inlet temperature   = 24.19 °C
condensate flow rate   =   0.80 lpm
cooling water flow rate   = 17.1   lpm   heat loss ≈ 6%

TABLE-A.9   CORRECTED WALL TEMPERATURES OF CONDENSER TUBES

row no.	thermocouple position	cross-section, x				cooling water exit temp.,°C
		1	2	3	4	
first	top	107.86	109.83	112.37	114.09	
	side	99.11	101.00	103.90	106.10	31.50
	bottom	91.40	94.18	96.95	99.36	
second	top	106.00	108.18	110.36	112.80	
	side	98.50	100.35	102.75	104.86	31.00
	bottom	90.94	93.33	96.55	99.09	
third	top	103.75	106.38	107.82	110.65	
	side	97.35	99.55	101.65	103.76	30.58
	bottom	90.55	92.96	96.15	98.99	
fourth	top	103.19	105.50	107.56	108.52	
	side	96.98	99.58	100.76	102.76	30.17
	bottom	90.35	92.68	95.96	98.86	

average steam bulk temperature   = 119.60 °C   run no.   9
condensate temperature   = 119.33 °C
cooling water inlet temperature   = 24.19 °C
condensate flow rate   =   0.65 lpm
cooling water flow rate   = 11.6   lpm   heat loss ≈ 5%

TABLE-A.10   CORRECTED WALL TEMPERATURES OF CONDENSER TUBES

row no.	thermocouple position	cross-section, x				cooling water exit temp.,°C
		1	2	3	4	
first	top	106.76	109.18	110.73	113.09	
	side	98.55	100.56	103.06	104.56	30.41
	bottom	90.52	93.29	95.56	98.38	
second	top	105.56	107.42	108.96	111.31	
	side	98.19	99.95	102.16	103.32	29.93
	bottom	89.81	92.85	95.05	98.05	
third	top	103.00	105.89	107.36	109.76	
	side	97.13	99.15	101.10	102.36	29.61
	bottom	89.15	92.14	94.55	97.55	
fourth	top	101.78	104.38	105.76	107.38	
	side	96.54	98.32	100.31	101.35	29.26
	bottom	88.95	91.71	94.38	97.35	

average steam bulk temperature   = 119.62 °C   run no. 10
condensate temperature   = 119.47 °C
cooling water inlet temperature   = 24.19 °C
condensate flow rate   =   0.63 lpm
cooling water flow rate   = 13.8   lpm   heat loss ≈ 2%

TABLE-A.11   CORRECTED WALL TEMPERATURES OF CONDENSER TUBES

row no.	thermocouple position	cross-section, x				cooling water exit temp.,°C
		1	2	3	4	
first	top	105.75	107.55	109.68	112.36	
	side	96.75	99.35	101.02	103.02	29.61
	bottom	88.50	91.51	93.78	96.38	
second	top	103.42	105.18	107.45	109.31	
	side	96.13	98.64	100.19	101.75	29.16
	bottom	87.75	90.45	93.07	95.80	
third	top	101.55	103.93	106.18	107.76	
	side	95.54	97.29	99.36	100.74	28.87
	bottom	86.95	90.03	92.52	95.16	
fourth	top	99.76	101.96	104.03	105.86	
	side	94.53	96.40	98.55	99.15	28.62
	bottom	86.55	89.463	91.95	94.25	

average steam bulk temperature = 119.58 °C   run no. 11
condensate temperature   = 119.29 °C
cooling water inlet temperature = 23.92   °C
condensate flow rate   = 0.67 lpm
cooling water flow rate   = 15.8 lpm   heat loss ≈ 4%

TABLE-A.12   CORRECTED WALL TEMPERATURES OF CONDENSER TUBES

row no.	thermocouple position	cross-section, x				cooling water exit temp.,°C
		1	2	3	4	
first	top	104.78	106.35	108.36	110.62	
	side	95.50	98.06	99.35	101.70	29.43
	bottom	86.51	89.39	91.95	94.52	
second	top	102.16	104.00	104.89	106.58	
	side	94.58	97.16	98.75	100.30	29.02
	bottom	85.56	88.51	91.12	94.06	
third	top	100.15	102.51	104.46	105.80	
	side	93.56	95.75	97.85	99.06	28.74
	bottom	84.65	87.92	90.51	93.16	
fourth	top	97.82	100.03	101.33	103.52	
	side	92.15	94.39	96.53	96.96	28.57
	bottom	83.62	86.52	89.47	91.18	

average steam bulk temperature = 119.62 °C   run no. 12
condensate temperature   = 119.36 °C
cooling water inlet temperature = 23.92   °C
condensate flow rate   = 0.74 lpm
cooling water flow rate   = 17.1 lpm   heat loss ≈ 8%

TABLE-A.13 CORRECTED WALL TEMPERATURES OF CONDENSER TUBES

row no.	thermocouple position	cross-section, x				cooling water exit temp., °C
		1	2	3	4	
first	top	101.05	103.50	105.34	106.92	
	side	93.68	95.55	97.86	101.35	30.22
	bottom	88.52	91.95	94.65	97.45	
second	top	99.61	101.12	104.12	106.35	
	side	93.25	95.02	96.64	100.16	29.73
	bottom	87.88	90.84	93.72	96.82	
third	top	99.01	100.25	102.06	105.08	
	side	92.88	94.66	96.06	99.90	29.38
	bottom	87.54	90.35	93.41	96.35	
fourth	top	98.50	99.78	101.48	104.36	
	side	92.38	94.06	95.42	98.61	28.99
	bottom	87.01	89.93	93.00	95.90	

average steam bulk temperature   = 110.71 °C   run no. 13
condensate temperature   = 110.56 °C
cooling water inlet temperature   = 23.92 °C
condensate flow rate   =   0.53 lpm
cooling water flow rate   = 11.6   lpm   heat loss ≈ 3

TABLE-A.14 CORRECTED WALL TEMPERATURES OF CONDENSER TUBES

row no.	thermocouple position	cross-section, x				cooling water exit temp., °C
		1	2	3	4	
first	top	100.66	102.75	104.38	106.46	
	side	92.76	95.04	97.08	98.37	29.26
	bottom	87.01	89.96	92.58	95.86	
second	top	98.34	100.98	102.38	105.34	
	side	92.53	94.58	96.25	97.92	28.77
	bottom	86.83	89.51	92.06	94.88	
third	top	97.80	99.55	100.69	104.44	
	side	92.00	94.08	95.66	97.32	28.52
	bottom	86.22	88.97	91.44	93.93	
fourth	top	97.12	98.68	99.89	103.28	
	side	91.42	93.25	94.68	97.86	28.33
	bottom	85.53	88.61	90.81	92.71	

average steam bulk temperature   = 110.69 °C   run no. 14
condensate temperature   = 110.44 °C
cooling water inlet temperature   = 23.87 °C
condensate flow rate   =   0.57 lpm
cooling water flow rate   = 13.8   lpm   heat loss ≈ 8%

TABLE-A.15 CORRECTED WALL TEMPERATURES OF CONDENSER TUBES

row no.	thermocouple position	cross-section, x				cooling water exit temp., °C
		1	2	3	4	
first	top	99.56	101.88	103.04	105.28	
	side	91.11	93.09	95.35	96.71	28.82
	bottom	84.87	87.38	89.38	91.02	
second	top	96.75	99.69	100.86	104.22	
	side	90.32	92.56	94.24	95.72	28.47
	bottom	83.84	86.82	88.75	90.12	
third	top	96.02	97.88	99.21	103.07	
	side	89.42	91.88	93.56	94.56	28.28
	bottom	83.11	85.86	88.15	89.57	
fourth	top	95.27	97.03	98.18	101.91	
	side	89.02	90.96	92.56	93.75	28.06
	bottom	82.22	85.48	87.58	88.98	

average steam bulk temperature   = 110.70 °C   run no.. 15
condensate temperature   = 110.56 °C
cooling water inlet temperature = 23.81 °C
condensate flow rate   =   0.59 lpm
cooling water flow rate   = 15.7   lpm   heat loss ≈ 4%

TABLE-A.16 CORRECTED WALL TEMPERATURES OF CONDENSER TUBES

row no.	thermocouple position	cross-section, x				cooling water exit temp., °C
		1	2	3	4	
first	top	97.86	100.08	102.37	104.18	
	side	89.55	91.78	93.12	94.98	28.84
	bottom	81.85	84.62	86.78	88.86	
second	top	95.46	98.26	109.40	11.184	
	side	88.15	90.34	92.36	94.36	28.62
	bottom	81.21	83.93	85.26	87.53	
third	top	94.44	96.58	98.01	102.18	
	side	87.57	89.88	91.48	92.86	28.42
	bottom	80.06	83.35	84.88	87.15	
fourth	top	93.68	95.27	96.66	100.68	
	side	86.45	88.65	90.32	91.45	28.25
	bottom	79.08	82.50	84.28	86.25	

average steam bulk temperature   = 110.73 °C   run no. 16
condensate temperature   = 110.47 °C
cooling water inlet temperature = 24.03 °C
condensate flow rate   =   0.65 lpm
cooling water flow rate   = 17.1   lpm   heat loss ≈ 7%

SAMPLE CALCULATION

The calculations shown in this Appendix has been performed with the help of DEC-2050 main frame computer at computer centre , University of Rorrkee, Roorkee . The necessary computer programme in Fortran-IV language is given in Appendix C.

B.0 DIMENSIONS OF THE CONDENSING TUBE

outside diameter, do = 0.0288 m

inside diameter ,di = 0.0250 m

length , L   = 0.341 m

B.1 HEAT TRANSFER AREA OF THE CONDENSING TUBE

outside surface area , Ao = π do.L
= 0.0308529 sq.m

inside surface area ,Ai = π di.L
= 0.026768 sq.m

B.2 COOLING WATER TEMPERATURE PROFILE ALONG THE LENGTH OF THE CONDENSER TUBE

In the present investigation , temperature profile of the cooling water along the length of the condenser tube has not been measured for reasons explained in Section 5.1 .Therefore, an iterative procedure, detailed below , was employed to develop it.

The length of the condenser tube is considered to be devided in four segments, designated by symbol s(=I,II,III and IV). The method of division of the length into various isothermal segments is depicted clearly in Fig 3.4 (a).

Following step-wise procedure is used to calculate temperature of cooling water ,to,s , at the end of a given segment :

step-1   A value of $t_{o,s}$ is considered based on the assumption that the temperature of cooling water rises linearly along the length of the tube.

step-2   Heat pickedup by cooling water in a given segment ,Q_s is calculated by the following equation :

$$Q_s = mc(t_{o,s} - t_i) \qquad \qquad \ldots (B.1)$$

step-3   Using experimentally determined valu of $t_{wo,s}$ the valu of $t_{wi,s}$ is calculated by the following equation :

$$t_{wi,s} = t_{wo,s} + Q_s/(2\pi.k_w*L_s) \ln(d_o/d_i) \ldots (B.2)$$

step-4   The value of $h_{ia,s}$, an value of average water side heat transfer coefficient from leading edge to the segment in question, is determined from following equation :

$$h_{ia,s} = 0.021 \, Re^{0.8} \, Pr^{0.43} (Pr/Pr_w)^{0.25} \epsilon_s \, k/d_i$$
$$\ldots (B.3)$$

The value of Re, Pr and k in Eq. (B.3) , are determined corresponding to the mean temperature ,$t_b(=(t_i+t_{o,s})/2)$. Wrereas Pr_w is calculated at tempreature , $t_{wi,s}$.

step-5   Heat transfer coefficient based on inside surface area,$U_{i,s}$ is calculated by the following equation:

$$1/U_{i,s} = 1/h_{i,s} + d_i/(2 \, k_w) \ln(d_o/d_i) \qquad \ldots (B.4)$$

step-6   Substitution of $U_{i,s}$ and mc in the following equation provides new value of temperature,$t'_{o,s}$:

$$t'_{o,s} = \frac{(t_i(mc-U_{i,s}*A_{i,s}/2) + U_{i,s}*A_{i,s}*t_{wo,s})}{(mc + U_{i,s}*A_{i,s}/2)}$$
$$\ldots (B.5)$$

step-7   Deviation between $t_{o,s}$ and $t'_{o,s}$ ($= |t_{o,s}-t'_{o,s}|$) is

calculated

step-8 If the deviation $| t_{o,s} - t'_{o,s}| > 0.01$, Step 1 to 7 are repeated using $t'_{o,s}$ as the new value of $t_{o,s}$ till deviation becomes < 0.01 .

step-9 Calculation for the next segment is carried out as given below :

(i) Value of $hi(hi_{a,s})$ for the region comprising of the segment in question and that preceding one is calculated using Step 1 to 4.

(ii) Heat transfer coefficient , $hi_{,s}$, for the segment in question is obtained by the following equation :

$$hi_{,s} = \frac{hi_{a,s+1} \cdot L_{c,s+1} - hi_{a,s} \cdot L_{c,s}}{L_{c,s+1} - L_{c,s}} \quad \ldots (B.6)$$

(iii) Step 5 to 8 are reperated to gety the desire convergence.

step-10 Step 9 is repeated for other segments

To demonstrate the above procedure of calculation , Run No. 13 of Table A-13, as reproduced below , is selected.

Atmospheric pressure(at Roorkee, India) = 735 mm of Hg.

Flow rate of cooling water = 11.6 lpm

Steam pressure = 146.75 kPa

Steam temperature = 110.71 °C

Inlet temperature of cooling water = 23.92 °C

Outlet temperature of cooling water = 30.22 °C

wall temperature at the top-,side-,and bottom-positions of top-row tube in various segments are as

follows :

<div align="center">

Wall temperature(s) ,°C

segment No.	top	side	bottom
I	101.05	93.68	88.52
II	103.50	95.55	91.95
III	105.34	97.86	94.65
IV	106.92	101.35	97.45

</div>

step-1 :. Temperature of cooling water at the end of segment-I is:

$$t_{o,I} = t_i + L_{c,s}(t_o - t_i)/L$$

$$= 23.92 + 0.071(30.22-23.92)/0.341$$

$$= 25.23 \ ° \ C$$

step-2: Heat picked by cooling water in segment -I is :

$$Q_I = mc(t_{o,I} - t_i)$$

Values of specific heat ,Cp and density , ρ are determined corresponding to the mean temperature of $t_{o,I}$ and t_i.

mean temperature = t_I = ½(25.23 +23.92) =24.57°C

Density and specific heat of water at 24.58 °C are 994.98 kg/m³ and 4.1829 kJ/kg °C.

Substituting the above values in Eq. B.1

$$Q_I = 11.6 * 994.98*4.1829*(25.23-23.92)/60$$

$$= 1054.04 \ W$$

step-3: Average temperature of cooling water side wall is determined from Eq. B-2. The average temperature of wall in a given segment is calculate by:

$$t_{wo,s} = 1/3(t_{wo,top} + t_{wo,side} + t_{wo,bottom}) \quad ...(B.7)$$

$$t_{wo,I} = 1/3(101.05 + 93.68 +88.52) = 94.42 \ °C$$

Similarly $t_{wo,II} = 97.00$ °C , $t_{wo,III} = 99.28$ °C and

$t_{wo,IV} = 101.90$ °C

Substiotuting the above values in Eq. B.2 :

$t_{wo,I} = 94.42 - 1054.04 \ln(0.0288/0.0250)/(2\pi 16.432*0.071)$

$= 74.07$ °C

The value of thermal conductivity of the material of tube has been taken from Perry et. al(63).

step-4 : Physical properties of cooling water at mean temperature of 24.58 are :

$\rho = 994.98$ kg/m³ $\mu = 906.2116 \ 10^{-6}$ Ns/M²

$\lambda = 2442.83$ kJ/kg $k = 0.60859$ W/m°C

$Cp = 4.1829$ kJ/kg°C

velocity of water $= 11.6*4*10^{-3}/(\pi*0.025^2*60)$

$= 0.3938$ m/s

$Re = 0.0250*0.3938*994.98*10^6/906.2116 = 10,809.1$

$Pr = 4.1829*10^3*906.2116*10^{-6}/0.60859 = 6.2284$

The value of Prw is calculated at the temperature $t_{wi,I}(=74.07°C)$. At this temperature the required physical properties of cooling water are :

$Cp = 4.1898$ kJ/kg°C $\mu = 385.72*10^{-6}$ Ns/m²

$k = 0.67012$ W/m°C

$Prw = 4.1898*10^3*385.72*10^{-6}/0.67012 = 2.4116$

Substituting the values of Re,Pr,Prw,k,di and ϵ_I in Eq. B.3 the value of $h_{ia,s}$ is :

$h_{ia,s} = 0.021(10809)^{0.8}(6.2284)^{0.43}(6.2284/2.4116)^{0.25}*$

$*1.4286*0.60859/0.0250$

$$= 3417.48 \ W/m^2 °C$$

The value of ϵ_I has been taken from Table 2.1.

step-5: Heat transfer coefficient based on inside surface area $U_{i,I}$ is obtained from Eq. B.4.

$$1/U_{i,I} \quad = \quad 1/3417.48 + 0.025/(2*16.435)\ln(0.0288/0.0250)$$

$$U_{i,I} \quad = 2498.2 \ W/m^2 °C$$

step-6: Temperature $t'_{o,I}$ is calculated by the Eq. B.5 where $mc = 11.6*994.945*4.1782/60 = 803.70 \ kJ/°C$

and $U_{i,I}*A_{i,I} = 2498.2*\pi*0.025*0.071 = 13.931 \ W/°C$

Substituting the value of mc and $U_{i,I} * A_{i,I}$ in Eq. B.5 the value of $t'_{o,I}$ comes out to be :

$$t'_{o,I} = \frac{23.92(803.7-13.931/2)+ 13.931*94.42}{(803.7 + 13.931/2)}$$

$$= 25.125 \ °C$$

step-7: Deviation in the assumed and calculated value of $t_{o,I}$:

deviation $= | \ 25.23-25.114| \ = 0.115 \ > 0.01 \ °C$

step-8: Calculations are made from step-1 to step-7 using the next trial value of $t_{o,I}$ as 25.114 °C. The results are as follows:

$t_{wi,I} = 75.334 \ °C$; $Q_I = 971.56 \ W$; $h_{ia,I} = 3450.4 \ W/m^2 °C$

$U_{i,I} = 2504.46 \ W/m^2 °C$; $t'_{o,I} = 25.130 \ °C$;

$h_{i,I} = 3450.4 \ W/m^2 °C$

Deviation $= |25.114-25.130| = 0.005 < 0.01$

step-9: Calculation for $h_{ia,II}$ in the region comprising both the segments I and II are made in a similar manner as for segment I. The details are as follows :

(i) Mean temperature of wall of the segment I + II is :

B-6

$$two, {\scriptstyle I+II} = \frac{two, {\scriptstyle I}*L_1 + two, {\scriptstyle II} L_2}{L_1 + L_2}$$

$$= (94.42*0.071 + 97.0*0.10)/0.171 = 95.928 \text{ °C}$$

Heat picked, Q_{I+II} up by cooling water in segment I and II is calculated based on physical properties of cooling water at $t_{o,I+II}$ [= $(t_i + t_{o,I+II})/2$]

$t_{o,I+II} = 23.92 + (30.22 - 23.92)*0.171/0.341 = 27.077 \text{ °C}$

Physical properties of cooling water at this temperature are:

$\rho = 994.48$; $Cp = 4.18141$; $\mu = 891.57$; $k = 0.60984$

$Q_{I+II} = 11.6*994.48*4.1814*(27.079 - 23.92)/60$

$= 2540.5 \text{ W}$

Mean temperature of wall , $t_{wi,I+II}$, in both segments(I+II) can be calculated by Eq. B.2 as:

$$t_{wi,I+II} = 95.928 - \frac{2540.5*\ln(0.0288/0.025)}{2*\pi*16.435*0.071}$$

$$= 75.57 \text{ °C}$$

The value of $h_{ia,II}$ is calculate using Eq. A.3

$h_{ia,II} = 3192.1 \text{ W/m}^2 \text{ °C}$

(ii)   Value of water side heat transfer coefficient $h_{ia,II}$ for segment II is given by Eq. B.6

$h_{i,II} = (3192.1*0.171 - 3450.4*0.071)/(0.171 - 0.071)$

$= 3008.7 \text{ W/m}^2 \text{ °C}$

(iii)   Steps 5 to 7 are repeated to get $U_{i,II}$ and $t'_{o,II}$ and the deviation. These are :

$U_{i,II} = 2263.29 \text{ W/m}^2 \text{ °C}$; $t_{o,II} = 26.702 \text{ °C}$

Deviation = $|26.702 - 27.077| = 0.375 > 0.01$

Calculations are repeated from step 2 to 9 using $t_{o,II}$ as 26.702 °C. Results of all the iterations made for segment 2 are given in Table-B.2.

Table B.2 Results of iterations for segment II

Parameter(s)	Iteration(s)		
	1	2	3
$t_{o,II}$	27.077	26.702	26.720
$t_{wo,I+II}$	95.93	95.93	95.93
Q_{I+II}	2540	2238	2253
$t_{wi,I+II}$	75.57	77.67	77.55
$h_{ia,II}$	3192	3219	3217
$h_{i,II}$	3009	3055	3052
$U_{i,II}$	2263	2289	2288
$t'_{o,II}$	26.702	26.720	26.719
Deviation	0.375	0.018	0.001

step-10: Calculation for segments 3 and 4 are made in the same manner as for segment 2. The final values of variables for different segments are given in Table B.3.

Table B.3 Values of different variables for various segments

Parameter(s)	segment(s)			
	1	2	3	4
$t_{o,s}$	25.111	26.675	28.145	29.108
Q_s	971.5	1277.3	1201.0	786.7
$Q_{c,s}$	971.5	2248.8	3349.8	4236.5
$h_{i,s}$	3450	3052	2772	2482

$$\Sigma Q_s = 4236.5W$$

* based on indivedual length of a segment since length of various segment on condensing tube are different (0.071,0.1,0.1,and 0.07 m), heat picked up by cooling water Qs do not show any particuler trend. However, based on the normalised length of L/d ,they represent a decreasing trend in conformity to the variation of t_o,s .

B.3. HEAT PICKED UP BY COOLING WATER IN TOP ROW TUBE

Average temperature of cooling water = $\frac{1}{2}(t_i +t_o)$

$$= \frac{(23.92+30.22)}{2}$$

$$= 27.07°C$$

Density and heat capacity of water correspondong to 26.97°C are 994.399 kg/m³ and 4.1782 kJ/kg°C respectively.

Heat picked up by cooling water = $Vpc(t_o -t_i)$

$$=11.6*994.399*4.1782(30.22-23.92)/60$$

$$= 5060.5 \text{ W}$$

B.4 HEAT PICKED-UP BY COOLING WATER IN VARIOUS SEGMENTS OF TOP ROW TUBE

The calculated value of heat picked -up by cooling water is 824(=5060.5-4236.5) W less than that observed experimentally. Therfore, the balance of 824 W is distributed amongst the segments based on the calculated value of Qs by them. The final values of Qs¹ are :

Q'_I = 971.5 + 971.5*824/4236.5 = 1160.45 W

Q'_{II} = 1277.3 + 1277.3*824/4236.5 = 1525.73 W

Q'_{III} = 1201.0 + 1201.0*824/4236.5 = 1434.59 W

Q'_{IV} = 786.7 + 786.7*824/4236.5 = 939.71 W

$\Sigma Q's$ = 5060.5 W

B.5 ESTIMATION OF CONDENSING HEAT TRANSFER COEFFICIENT, h_o

Value of condensing heat transfer coefficient at a given circumferential positon of a given segment, $h_{os,position}$ is calculated by :

$$h_{os,position} = \frac{Q'_s}{\pi d_o L_s (t_v - t_{ws,position})}$$

Where subscript, position represents the top-, the side-, and the bottom- region on the condenser tube.

$h_{oI,top} = 1160.45/(\pi * 0.0288 * 0.071(110.71-101.05))$

$= 18700.3$ W/m²°C

$h_{oI,side} = 1160.45/(\pi * 0.0288 * 0.071(110.71-93.68))$

$= 10607$ W/m²°C

$h_{oI,bottom} = 1160.45/(\pi * 0.0288 * 0.071(110.71-88.52))$

$= 8140.86$ W/m²°C

Values of condensing heat transfer coefficients for other segments at the top-, the side-, and the bottom-regions of the tube are calculated in the same manner and tabulated below :

Table B.4 Heat Transfer Coefficient In Various Segments

position	Heat Transfer Coefficient, W/m²°C			
	Segment			
	I	II	III	IV
top	18700	23328	29421	39023
side	10607	11098	12301	15813
bottom	8141	8969	9843	11164

The average value of condensing heat transfer coefficient for a given segment is given by :

$h_{o,s} = 1/3[h_{os,top} + h_{os,side} + h_{os,bottom}]$

$\bar{h}_{o,I} = 1/3[18700 + 10607 + 8141] = 12482.6 \quad W/m^2 \, ^\circ C$

Similarly :

$\bar{h}_{o,II} = 1/3[23328.1 + 11098.6 + 8969.4] = 14465.3 \quad W/m^2 \, ^\circ C$

$\bar{h}_{o,III} = 1/3[29421.0 + 12301.5 + 9843.5] = 17188.7 \quad W/m^2 \, ^\circ C$

$\bar{h}_{o,IV} = 1/3[39023.6 + 15813.4 + 11164.1] = 22000.4 \quad W/m^2 \, ^\circ C$

Weighted value of heat transfer coefficient for the whole tube is calculated as :

$$\bar{h}_{wt} = \frac{h_{o,I}*L_I + h_{o,II}*L_{II} + h_{o,III}*L_{III} + h_{o,IV}*L_{IV}}{(L_I + L_{II} + L_{III} + L_{IV})}$$

$$= \frac{(12482.6*0.071 + 14465.3*0.1 + 17188.7*0.1 + 22000.4*0.07)}{0.07 + 0.1 + 0.1 + 0.07}$$

$$= 13697.9 \quad W/m^2 \, ^\circ C$$

B.6 WEIGHTED HEAT TRANSFER COEFFICIENT PREDICTED BY EARLIER INVESTIGATORS

Weighted condensing heat transfer coefficient for the first row tube at pressure 146.75 kPa and cooling water flow rate of 11.6 lpm has been calculated by using models of Nusselt (Eq.2.2), Mikheyev (Eq.2.27), Othmer and Berman(Eq.2.7), Peck and Raddie (Eq.2.10), Bromeley(Eq.2.18), Rohsenow(Eq.2.20), Chen(Eq. 2.25), Henderson(Eq.2.26), and White (Eq.2.21) for comparison with experimentally obtained value.

Weighted wall temperature, t_{wt}

$$t_{wt} = \frac{t_{wo,I}*L_I + t_{wo,II}*L_{II} + t_{wo,III}*L_{III} + t_{wo,IV}*L_{IV}}{L_I + L_{II} + L_{III} + L_{IV}}$$

$$=(94.42*0.071+97.*0.1+99.28*0.1+101.90*0.07)/0.341$$

$$= 98.14 \ °C$$

Physical properties of water at 98.14 °C are :

μ = 287.78E-06 Ns/m² ; p = 959.22 kg/m³

= 2261.7 kJ/kg   Cp = 4.2183 kJ/kg°C   k = 0.68243 W/m°C

Prw = (Cpμ/k) = 1.778

Film temperatute = (98.14 + 110.71)/2 = 104.43 °C

μ = 270.98E-06 Ns/m²   ; p = 956.14 kg/m³

= 2245.0 kJ/kg   k = 0.68348 W/m°C Cp =4.22561 kJ/kg°C

v =0.69155 kg/m³ ; σ = 57.9898E-03 N/m

Pr =(270.98E-06*4.22561E 03)/0.68348 = 1.675

$$h_{Nusselt} = 0.725 \ \frac{(0.68348^3*956.14^2*9.81*2245.0)}{270.98E-06*0.0288*(110.71-98.14)}$$

$$= 11591.3 \ W/m^2°C$$

h_{othmer} = 11111.3 W/m²°C

$h_{Bromley}$ = 11692.2 W/m²°C

h_{Peck} = 11213   W/m²°C

$h_{Rohsenow}$ = 11685.9 W/m²°C

h_{Chen} = 11647 W/m²°C

$h_{Henderson}$ = 15503 W/m²°C

h_{White} = 11639.3 W/m²°C

Physical properties of water at saturation temperature 110.71°C :

μ = 257.44E-06 Ns/m² ; p = 950.09 kg/m³

= 2228.07 kJ/kg ; k = 0.68520 W/m°C ; Cp =4.23419 kJ/kg°C

$h_{Mikheyev}$ = 14818.8 W/m²°C

B.7 CALCULATION OF AVERAGE AND WEIGHTED CONDENSING HEAT TRANSFER COEFFICIENT FOR THE BUNDLE OF TUBES

The average and weighted condensing heat transfer coefficient for second -, third-, and fourth -row tubes has been calculated as per procedure shown for first row-tube given in Section B.5. The calculated value are given in Table B.5.

Table B.5 Average condensing heat transfer coefficient for tube bundle

	Segment(s)			
	I	II	III	IV
First-row tube	12482	14465	17188	22000
Second-row tube	10666	11186	13673	18099
Third-row tube	9755	10040	10923	14599
Fourth-row tube	8788	9046	9747	12228

The weighted condensing heat transfer coefficient for the bundle of tubes are given below:

	Weighted condensing heat transfer coefficients
First-row tube	: 16398 W/m² °C
Second-row tube	: 13226 W/m² °C
Third -row tube	: 11176 W/m² °C
Fourth-row tube	: 9887 W/m² °C

B.8 CALCULATION OF $\bar{h}_{n,wt}/\bar{h}_{1,wt}$ VALUES :

$$\bar{h}_{1,wt}/\bar{h}_{1,wt} = 1.0 \; ; \; \bar{h}_{2,wt}/\bar{h}_{1,wt} = 0.806$$

$$\bar{h}_{3,wt}/\bar{h}_{1,wt} = 0.681 \; : \; \bar{h}_{4,wt}/\bar{h}_{1,wt} = 0.603$$

B.9 CALCULATION OF $h_{n,wt}/h_{1,wt}$ DUE TO GRANT AND OSMENT(28) AND SHORT AND BROWN(29)

Heat picked-up by :

First-row tube : 5060.5 W

Second-row tube : 4667.9 W

Third -row tube : 4391.4 W

Fourth-row tube : 4075.4 W

$h_{1,wt}/h_{1,wt} = 1.0$; $h_{2,wt}/h_{1,wt} = [(5060.5+4667.9)/4667.9]^{-0.233}$

$$= 0.8427$$

$h_{3,wt}/h_{1,wt} = [(5060.5+4667.9+4391.4+4075.4)/4391.4]^{-0.233}$

$$= 0.7617$$

Similarly $h_{4,wt}/h_{1,wt} = 0.7056$

In the same way the values of $h_{n,wt}/h_{1,wt}$ have been calculated for Short and Brown' model.

```
C  LANGUAGE  :  FORTRAN         COMPUTER  :  DEC-2050
C  THIS PROGRAM PERFORMS FOLLOWING JOBS :
C  (A) CONVERTS THERMOCOUPLE E.M.F. TO TEMPERATURE
C          CORRECTS IT CONSIDERING OFFSET VALUES, AND TABULATES
C  (B) IT DOES COMPLETE ANALYSIS TAKING RAW DATA AVAILABLE FROM
C      THE Z-80 MICROPROCESSOR UPTO FINAL RESULT
C
C  SUBROUTINES  :
C  --------------------------------
C
C
C  1. CONV  : CONVERTS E.M.F. TO TEMPERATURE
C  2. CORR  : CORRECTS TEMPERATURES AND CALCULATES ACTUAL
C             FLOW RATE OF COOLING WATER FROM CALIBRATION
C             DATA OF ROTAMETERS
C  3. TABLE : TABULATES THE PRIMARY DATA (RAW DATA) FOR
C             EACH RUN
C  4. LAGINT: USE FOR LAGRANGIAN INTERPOLATION FOR PHYSICO-
C     LAG     THERMAL PROPERTIES AND , DETERMINATION OF SIGMA
C  5. PROP  : RETURNS PHYSICAL PROPERTY OF LIQUID AT
C             DEMAND TEMPERATURES TO MAIN PROGRAMME
C  6. COMP  : DOES PRIMARY ANALYSIS OF DATA
C  7. ACT   : DOES COMPLETE ANALYSIS OF DATA ,
C             PRIDICTS COOLING WATER TEMPERATURE PROFILE,
C             HEAT TRANSFER COEFFICIENT, COMPARES IT
C             WITH AVAILABLE CORRELATIONS AND GENERATES
C             DATA FILES FOR PLOTTING
C  8. EXER  : DOES ERROR ANALYSIS FOR EACH RUN
C  9. AVG   : CALCULATES AVERGAE TEMPERATURES FOR TUBE BUNDLE
C  10.TABL6 : TABULATES INTERMEDIATE CALCULATIONS OF EACH RUN
C  *********************************************************
C  DIMENSION EMF(70),TE(70),EC(15),AM(15),CI(15),RN1(5),EL1(5,5)
```

```
  1,F(5),RE1(12),BKO(12),CORR(70),NTT(8),PPT(8,33),PPL(8,33)
  2,PACT(4,30),PSCR(4,30),NSC(4),DEL(4),X(33),Y(33),V(5),Q(5)
  1,CF(5),CFT(4,4),SP(4,50)
    OPEN(UNIT=1,DEVICE='DSK',DIALOG)
    READ(1,10),(EC(I),AM(I),CI(I),I=1,11)
C     EC(I) EMF VALUES FOR WHICH TEMPERATURE EMF LINEAR RELATIONS
C     ARE GIVEN
C     AM(I) ,CI(I) ARE THE SLOPE AND INTERCEPT OF THE STRAIGHT LINE
C     EQUATION TE(I)=EMF(I)*AM(I)+CI(I)
C     FRC   FLOWRATE OF CONDENSATE
C     F(I)  FLOWRATES OF COOLANT THROUGH ROTAMETER
C     PR    VAPOUR PRESSURE IN KG/SQ.CMM
    N=56
    READ(1,*),(RE1(I),I=1,12),(BKO(I),I=1,12),N1
    READ(1,*)(RN1(I),I=1,5)
    READ(1,*)((EL1(I,J),J=1,5),I=1,5)
    DO 20 KP=1,7
    READ(1,*),NT
    READ(1,*),(PPL(KP,JJ),JJ=1,NT),(PPT(KP,JJ),JJ=1,NT)
    NTT(KP)=NT
20  CONTINUE
    READ(1,*),(CORR(JJ),JJ=1,56)
    DO 33 IL=1,4
33  READ(1,*),(CFT(IL,IT),IT=1,4)
    DO 30 KT=1,4
    READ(1,*),NS
    READ(1,*),(PACT(KT,JJ),JJ=1,NS),(PSCR(KT,JJ),JJ=1,NS)
    NSC(KT)=NS
30  CONTINUE
    DO 51 KK=1,4
51  READ(1,*),(SP(KK,K1),K1=1,48)
```

C-2

```
      DO 32 KTT=1,1
      DO 31 IRP=1,4
      DO 52 K2=1,48
52    SP1(K2)=SP(IRP,K2)
      READ(1,*),(F(I),I=1,4),FRC,PS
      READ(1,*),(EMF(I),I=1,N)
60    CONTINUE
      CALL CONV(N,EMF,EC,AM,CI,TE)
70    CONTINUE
      DO 40 KL=1,4
40    DEL(KL)=TE(49+KL-1)-TE(54)
      CALL CORRT(TE,F,CORR,PACT,PSCR,NSC,N,CF,SP1)
      DO 34 IKL=1,4
34    CF(IKL)=CFT(IRP,IKL)
      TS=TE(55)
      DO 50 KT=1,4
50    DEL(KT)=TE(49+KT-1)-TE(54)
      PRINT 42
42    FORMAT(///10X,'TABLE-2:CORRECTED TEMPERATURE DISTRIBUTION')
      CALL TABLE(TE,DEL)
10    FORMAT(6F10.6)
      CALL COMP(TE,CF,FRC,TS,PS,RN1,EL1,RE1,BKO,PPL,PPT,NTT)
31    CONTINUE
32    CONTINUE
      STOP
      END
      SUBROUTINE CONV(N,EMF,EC,AM,CI,TE)
      DIMENSION EMF(70),TE(70),EC(15),AM(15),CI(15)
      DO 30 I=1,N
      DO 40 J=1,11
      EEMF=EMF(I)
```

C-3

```
       EEC=EC(J)
       IF(EEMF)50,50,60
60  IF(EEMF-EEC)70,70,40
40  CONTINUE
50  TE(I)=0.000
       IF(EEMF.EQ.5.646)TE(55)=129.85
       GO TO 30
70  TE(I)=EMF(I)*AM(J)+CI(J)
30  CONTINUE
       RETURN;END
       SUBROUTINE TABLE(TE,DEL)
       DIMENSION TE(70),DEL(4)
       IA=1;IB=2;IC=3;ID=4
       PRINT 10
       PRINT 20
       PRINT 30
       PRINT 10
       PRINT 40,(TE(J),J=24,33,3)
       PRINT 50,IA,(TE(J),J=25,34,3),TE(48),TE(49),DEL(1)
       PRINT 60,(TE(J),J=26,35,3)
       PRINT 10
       PRINT 40,(TE(J),J=36,45,3)
       PRINT 50,IB,(TE(J),J=37,46,3),TE(46),TE(50),DEL(2)
       PRINT 60,(TE(J),J=38,44,3),TE(1)
       PRINT 10
       PRINT 40,(TE(J),J=2,11,3)
       PRINT 50,IC,(TE(J),J=3,12,3),TE(12),TE(51),DEL(3)
       PRINT 60,(TE(J),J=4,13,3)
       PRINT 10
       PRINT 40,(TE(J),J=14,23,3)
       PRINT 50,ID,(TE(J),J=15,21,3),TE(47),TE(47),TE(52),DEL(4)
```

C-4

```
      PRINT 60,(TE(J),J=16,22,3),TE(48)
      PRINT 10
      PRINT 80,TE(55),TE(55),TE(53),TE(54)
      WRITE(10,*),(TE(J),J=24,33,3)
      WRITE(10,*),(TE(J),J=25,34,3)
      WRITE(10,*),(TE(J),J=26,35,3)
      WRITE(10,*),(TE(J),J=36,45,3)
      WRITE(10,*),(TE(J),J=37,46,3)
      WRITE(10,*),(TE(J),J=38,44,3),TE(1)
      WRITE(10,*),(TE(J),J=2,11,3)
      WRITE(10,*),(TE(J),J=3,12,3)
      WRITE(10,*),(TE(J),J=4,13,3)
      WRITE(10,*),(TE(J),J=14,23,3)
      WRITE(10,*),(TE(J),J=15,21,3),TE(47)
      WRITE(10,*),(TE(J),J=16,22,3),TE(48)
   80 FORMAT(T11,'VAPOUR TEMPERATURE DEG. C=',2(2X,F6.2)/T11
     1,'CONDENSATE TEMPERATURE DEG. C=',F6.2/T11,'COOLANT
     2 TEMPERATURE DEG. C=',F6.2)
   10 FORMAT(10X,80('-'))
   20 FORMAT(10X,16X,'POSITION FROM LEFT',16X,'MECHANICAL',2X,'COOL
     1ANT',4X,'TEMP'//)
   30 FORMAT(10X,17X,'1',7X,'2',7X,'3',7X,'4',13X,'HAND',4X,'OUT',
     1 18X,'RISE'/)
   40 FORMAT(18X,'TOP ',2X,4(F6.2,2X)/)
   50 FORMAT(10X,'TUBE ',I1,2X,'SIDE',2X,4(F6.2,2X),8X,F6.2,3X,F6.2,
     1 13X,F6.2/)
   60 FORMAT(18X,'BOTM',2X,4(F6.2,2X))
      RETURN;END
      SUBROUTINE LAGINT(X,Y,N,XINT,YOUT)
C     THIS SUBROUTINE PERFORMS LAGRANGIAN INTERPOLATION WITHIN
C     A SET OF (X,Y) PAIRS TO GIVE THE Y VALUE CORRESPONDING
```

C-5

```
C    TO XINT.THE DEGREE OF THE INTERPOLATING POLYNOMIAL IS
C    ONE LESS THAN THE NUMBER OF POINTS SUPPLIED
C    PARAMETERS ARE -
C       X        ARRAY OF VALUES OF THE INDEPENDENT VARIABLE
C       Y        ARRAY OF FUNCTION VALUES CORRESPONDING TO X
C       N        NUMBER OF POINTS
C       XINT     THE X-VALUE FOR WHICH ESTIMATE OF Y IS DESIRED
C       YOUT     THE Y-VALUE RETURNED TO CALLER
     DIMENSION X(33),Y(33)
     YOUT=0.0
     DO 20 I=1,N
     TERM=Y(I)
     DO 10 J=1,N
     IF(I.EQ.J) GO TO 10
     TERM=TERM*(XINT-X(J))/(X(I)-X(J))
10   CONTINUE
     YOUT=YOUT+TERM
20   CONTINUE
     RETURN
     END
     SUBROUTINE PROP(XINT,YOT,PPL,PPT,NTT)
     DIMENSION X(33),Y(33),YOT(8),PPL(8,33),PPT(8,33),NTT(8)
C       XINT     THE X-VALUE FOR WHICH ESTIMATE OF Y IS DESIRED
C       YOT(1)   VISCOSITY NS/M**2 X   10**6
C       YOT(2)   LIQUID DENSITY KG/M**3
C       YOT(3)   LATENT HEAT KJ/KG.
C       YOT(4)   SURFACE TENSION N/M X 10**3
C       YOT(5)   THERMAL CONDUCTIVITY W/M.K
C       YOT(6)   SPECIFIC HEAT KJ/KG.K
C       YOT(7)   VAPOUR DENSITY KG/M**3
C       YOT(8)   VAPOR PRESSURE KN/M**2
```

```
      DO 10 I=1,7
      NL=NTT(I)
      DO 20 KL=1,NL
      Y(KL)=PPL(I,KL)
      X(KL)=PPT(I,KL)
20    CONTINUE
      CALL LAGINT(X,Y,NL,XINT,YO)
      YOT(I)=YO
10    CONTINUE
C     PRINT *,(YOT(I),I=1,7)
      RETURN
      END
      SUBROUTINE CORRT(TEMP,F,CORR,PACT,PSCR,NSC,N1,CF,SP1)
      DIMENSION TEMP(70),CTEMP(70),CORR(70),F(5),CF(5),ACTU(30)
     1,PACT(4,30),PSCR(4,30),NSC(4),SCR(30)
C     TEMP    TEMPERATURE READ BY THERMOCOUPLE
C     CTEMP   CORRECTED TEMPERATURE
C     CORR    OFF SET VALUES FOR EACH THERMOCOUPLE
C     F,SCR   FLOW RATE READ BY ROTAMETERS
C     CF,ACTU CORRECTED FLOWRATES
      DO 10 I=1,56
      RP1=0.0
      IF(I.LE.48)RP1=1.5
      CTEMP(I)=TEMP(I)+CORR(I)
10    CONTINUE
      DO 30 J=1,N1
30    TEMP(J)=CTEMP(J)
      RETURN
      END
      SUBROUTINE COMP(TE,F,FRC,TS,PS,RN1,EL1,RE1,BKO,PPL,PPT,NTT)
C     FRC     CONDENSATE FLOW RATE LPM
```

C-7

```
C    TS          VAPOUR TEMPERATURE DEG. C
C    PS          VAPOUR PRESSURE  KN/SQ.M
C    Q(I)        HEAT PICKED UP BY COOLANT
C    HTC(I)      HEAT TRANSFER COEFFICIENT W/SQ.M.K
C    D1          INSIDE DIAMETER OF TUBE
C    DO          OUTSIDE DIAMETER OF TUBE
C    V           VELOCITY OF COOLANT  M/S
C    TWI         INSIDE WALL TEMPERATURE DEG. C
C    TWO         OUTSIDE WALL TEMPERATURE DEG. C
C    RN          REYNOLDS NUMBER
C    PRN         PRANDTL  NUMBER
C    TCO,TCI     COOLANT OUTLET  INLET TEMP.
C    TQ          TOTAL HEAT GIVEN BY CONDENSATE
     DIMENSION TE(70),F(5),Q(5),HTCI(5),HTCO(5),PRN(5),
    1RN(5),TAV(5),TWI(5),TWO(5),A(5),HF(5),DEV(5),TCO(5),UO(5)
    2,RN1(5),RE1(12),BKO(12),EL1(5,5),YOT(8),PPL(8,33),PPT(8,33)
    3,NTT(8),V(5),PEEXP(5),HTTN(3,4,4),HTTM(3,4,4),HTC(3,4,4),
    1DEV1(3,4,4),DEV2(3,4,4),HTA(5,5),T12(5,5),TAO(5,5)
    1,TAV1(5,5),Q12(5,5),AFT(5),AL1(5),BP(200),AK2(5,5)
     D1=0.025;DO=0.02887
     TCI=TE(54);TCON=TE(53)
     DO 113 IKL=1,4
     AFT(IKL)=F(IKL)
113  CONTINUE
     DO 10 I=1,4
     III=I+48
     PLQ=(TE(54)+TE(III))/2.
     TAV(I)=PLQ
     TCO(I)=TE(I+48)
     CALL PROP(PLQ,YOT,PPL,PPT,NTT)
     TKLO=23900;PRINT*,TKLO,(YOT(KLP),KLP=1,7),PLQ
```

C-8

```
      Q(I)=F(I)*YOT(2)*YOT(6)*(TE(I+48)-TE(54))/60.!Q   WATTS
      PRN(I)=(YOT(6)*YOT(1)*1.E-03)/YOT(5) !CF USED
      V(I)=F(I)*0.004/(3.14*(D1**2)*60.) ! V IN M/S
      RN(I)=(D1*V(I)*YOT(2))/(YOT(1)*1.E-06)
      RN4=RN(I)/1000.
      CALL ACT(TE,RN1,EL1,RN,TS,TCI,F,PPL,PPT,NTT,HTTN,HTTM,
     1DEV2,DEV1,HTC,HTCI,HTA,Q12,T12,TAO,TAV1,AL1,Q,AK2)
106   CONTINUE
C     PRINT*,(F(IP),IP=1,4)
      TSA=112.0
      CALL TABLE6(PS,TS,TSA,FRC,TCON,PHL,TCI,AFT,RN,TCO,AL1,TAO,T12,HTA
     1,TAV1,Q12,Q)
107   CONTINUE
      RETURN;END
      SUBROUTINE TABLE3(TE,PS,FRC,F,HTC,HTTN,DEV2,
     1HTTM,DEV1,PEEXP,PHL,Q,RN,HTCI,TCO,TS)
      DIMENSION F(5),HTC(3,4,4),HTTN(3,4,4),DEV2(3,4,4),HTTM(3,4,4)
     1,HTCI(5),TCO(5),PEEXP(5),TE(70),Q(5),RN(5),DEV1(3,4,4)
C     THIS SUBROUTINE GIVES OPERATING PARAMETER ALONG WITH
C     COMPARISON BETWEEN EXPERIMENTAL AND THEORITICAL VALUES
C     IT ALSO TABULATES EXPERIMENTAL DATA ALONG WITH DEDUCED
C     VALUES
C         TCI    INLET TEMP  OF COOLANT
C         TCO(I) OUTLET TEMP. OF COOLANT TUBEWISE
C         HTC    EXP. HEAT TRANSFER COEFFICIENT
C         HTTN     THEO.        ,,           ,,      DUE TO NUSSELT
C         HTTM     THEO.        ,,           ,,      DUE TO MIKHEYEV
C         DEV2,DEV1    % DEVIATION FROM EXPERIMENTAL VALUE
C         PEEXP        % DEVIATION FROM ERROR ANALYSIS
C         PHL          % HEAT LOSS
      TCI=TE(54);TCON=TE(55)
```

C-9

```
      DO 11 JJ=1,4
11    TCO(JJ)=TE(JJ+48)
      PRINT 10
      PRINT 20
      PRINT 30
      PRINT 40,PS,TS
      PRINT 50,TCI,(TCO(I),I=1,4)
      PRINT 60,(F(I),I=1,4)
      PRINT 70,TCON,FRC,PHL
      DO 180 J=1,4
      PRINT 160,J,TCI,TCO(J),F(J),Q(J),RN(J),HTCI(J),
     1((HTC(KJ,I,J),I=1,4),KJ=1,1)
180         CONTINUE
      PRINT 10
      PRINT 80
      PRINT 90
      PRINT 80
      DO 100 I=1,4
      IF(I.GT.1)GO TO 65
      GO TO 100
65    PRINT
110,I,((HTC(KJ,J,I),HTTN(KJ,J,I),DEV2(KJ,J,I),J=1,4),KJ=1,1)
100         CONTINUE
      PRINT 80
      PRINT 120
10 FORMAT(///T11,'TABLE-3  COMPARISON BETWEEN EXPERIMENTAL RNSULTS
     1 AND/T20, THEORITICAL PRNDICTIONS DUE TO NUSSELT AND MIKHEYEV')
20 FORMAT(T11,'OPERATING PARAMETERS :'///)
30 FORMAT(T11,'VAPOUR :  STEAM'//)
40 FORMAT(T11,'PRNSSURN(KG./SQ.CM)=',F5.2,T40,'SATURATION TEMP
     1(DEG. C)=',F6.2//)
```

C-10

```
50    FORMAT(T11,'COOLANT : INLET TEMP.(DEG. C)=',F6.2/T21,'OUT
     1LET TEMP.(S) DEG. C :'/T21,'TUBE(1)=',F5.1/T21,'TUBE(2)=',
     1F5.2/T21,'TUBE(3)=',F5.2/T21,'TUBE(4)=',F5.2//)
60    FORMAT(T11,'COOLANT FLOW RATE(S) IN L.P.M:'//T21,'TUBE1(TOP)
     1=',F8.2/T21,'TUBE 2=',F8.2/T21,'TUBE 3=',F8.2/
     1T21,'TUBE 4(BOTTOM)=',F8.2//)
70    FORMAT(T11,'CONDENSATE :  TEMPERATURN(DEG.C)=',F6.2,/T21,'FLOW
     1 RATE(L.P.M)=',F8.3/T21,'%HEAT LOSS=',F6.2//)
80    FORMAT(T11,60('-'))
90    FORMAT(T11,'TUBE NO.',T18,'!',T22,'H(EXP)',T32,'!',T36,'H(NUST
     1.)',T46,'!',T50,'% DEV',T58,'!',T62,'H(MIKV)',T72,'!',T76,
     1'% DEV',T84,'% EORRO '/T18,'!',T22,'W/SQ.M.K',T32,'!',T36,
     1'W/SQ.M.K',T46,'!',T62,'W/SQ.M.K',T84,'IN EXP.')
110           FORMAT(T14,I2,T24,F7.2,T38,F7.2,T52,F5.2,T64,F7.2,T78,F5.2,
     1T86,F5.2)
120           FORMAT(///T11,'* N.B - CALCULATIONS ARN BASED UPON THE
     1CALCULATED
     1 WALL TEMPERATURN VALUES '/T11,'NOT THE MEASUED WALL TEMPERA
     1TUE VALUES'////)
160           FORMAT(T11,I2,7(2X,F10.3))
      RETURN
      END
      SUBROUTINE ACT(TE,RN1,EL1,RN,TS,TI,F,PPL,PPT,NTT,HTTN,HTTM
     1,DEV2,DEV1,HTC,HTCI,HTA,Q12,T12,TAO,TAV1,AL1,Q5,AK2)
      DIMENSION AL1(5),AL2(5),RN(5),RN1(5),EL1(5,5),TO(5),F(5),EQ(5,5)
     1,TE(70),AK2(5,5),HTC(3,4,4),HTTN(3,4,4),DEV1(3,4,4),DEV2
     1(3,4,4),YOT(8),TAV1(5,5),EHO(3,4,4),PERR(3,4,4),HTTM(3,4,4)
     2,PPL(8,33), PPT(8,33),NTT(8),HTCI(5),TAO(5,5),Q12(5,5)
     3,T12(5,5),HTA(5,5),SUM1(4,4),SUM3(4),Q5(5),AK5(5,5),HTC5(3,4,4)
     1,OT1(5),OT2(5),RRM(3,4,4),RRN(3,4,4),HTAI1(5),AK6(4,4),AK3(4,4)
     1,AK7(4,4),AK8(4,4),BETA(5),TSUM1(5)
```

C-11

```
C   CALCULATION FOR OUTSIDE CONDENSING HEAT TRANSFER COEFFICIENT
C   BASED ON MEASURED WALL TEMPERATURE
    DO=0.02887;D1=0.025
    AO=3.14*DO*.341;A1=3.14*D1*.341
    PP1=TE(24);PP2=TE(25);PP3=TE(26);PP4=TE(47)
    CALL AVG(TE,TAV1)
    TE(24)=PP1;TE(25)=PP2;TE(26)=PP3;TE(47)=PP4
    DO 30 I=1,4
30  TO(I)=TE(48+I)
    AL1(1)=0.071;AL1(2)=0.171;AL1(3)=0.271;AL1(4)=0.341
    AL2(1)=0.071;AL2(2)=0.1;AL2(3)=0.1;AL2(4)=0.07
    DO 31 IT=1,4
    TAI=TI
    POD=AO/(A1*HTCI(IT))+ALOG(DO/D1)*AO/(2*3.14*0.341*16.435)
    UOD=1./POD
    DO 32 IO=1,4
    ADO=AL2(IO)*3.14*(DO*D1)**0.5
    TD=TI+(TO(IT)-TI)/0.341*AL1(IO)
    DO 33 IKN=1,30
    TD1=(TAI+TD)/2.
    CALL PROP(TD1,YOT,PPL,PPT,NTT)
    PDS=F(IT)*YOT(2)*YOT(6)/(60.*UOD*ADO)
    TAO(IT,IO)=(TAV1(IT,IO)+TAI*(PDS-0.5))/(PDS+0.5)
    T1=TAO(IT,IO)
    IF(ABS(TD-T1).LT.0.01)GO TO 34
    TD=T1
    IF(IKN.EQ.30)PRINT 35
33  CONTINUE
34  TAI=T1
32  CONTINUE
31  CONTINUE
```

C-12

```
35   FORMAT(5X,'CONVERSION NOT COMPLETE')
     DO 110 L=1,4
     V1=F(L)*0.004/(3.14*(D1**2)*60.) ! V IN M/S
     TAI=TI
     TSUM=0.0
     DO 393 ILP=1,4
     TSUM=TAV1(L,ILP)*AL2(ILP)*10.+TSUM
393  CONTINUE
     TQ1=(TAI+TO(L))/2.;TQ2=TS-TQ1;TQ3=TS-TSUM/3.41
     TSUM1(L)=TQ3/TQ2
     DO 100 M=1,4
     SUM=0.0
     GO TO 449
     T1=TAI+(TO(L)-TAI)/.341*AL1(M)
     DO 89 JJ=1,30
     TA1=(TAI+T1)/2.
     CALL PROP(TA1,YOT,PPL,PPT,NTT)
     Q13=(T1-TI)*F(L)*YOT(6)*YOT(2)/60.
     Q11=F(L)*YOT(6)*(T1-TAI)*YOT(2)/60 !Q11 IN WATTS
     RN4=((D1*V1*YOT(2))/(YOT(1)*1.E-06))/1000.
     JP=M
     CALL LAG(RN1,EL1,5,JP,RN4,ELO)
     TW1=SUM-Q13*ALOG(DO/D1)/(2*3.14*16.435*AL1(M))
     AK1=0.021*(D1*V1*YOT(2)/(YOT(1)*1.E-06))**0.8*(YOT(6)*YOT(1)
     1*1.E-03/YOT(5))**0.68*YOT(5)/D1*ELO
     AMC=F(L)*YOT(2)*YOT(6)/60.
     CALL PROP(TW1,YOT,PPL,PPT,NTT)
     AK=16.435
     HTAI=AK1*(YOT(6)*YOT(1)*1.E-03/YOT(5))**-0.25
     P=AO/(A1*HTAI)+ALOG(DO/D1)*AO/(2.*3.14*.341*16.435)
     U=1./P
```

C-13

```fortran
      UA=U*3.14*D1*AL1(M)
      T11=(TAI*(AMC-UA/2.)+UA*TAV1(L,M))/(AMC+UA/2.)
      TOT=ABS(T11-T1)
      T1=T11
39    CONTINUE
449   CONTINUE
      DO 14 IQ=1,M
14    SUM=SUM+TAV1(L,IQ)*AL2(IQ)*10.
      SUM=SUM/(AL1(M)*10)
      IF(M.EQ.1)TI3=TI
      T1=TAI+(TO(L)-TAI)/.341*AL1(M)
      DO 80 JJ=1,30
      TA1=(TAI+T1)/2.
      CALL PROP(TA1,YOT,PPL,PPT,NTT)
      Q11=F(L)*YOT(6)*(T1-TAI)*YOT(2)/60 !Q11 IN WATTS
      TY1=(T1+TI3)/2.
      CALL PROP(TY1,YOT,PPL,PPT,NTT)
      Q13=(T1-TI3)*F(L)*YOT(6)*YOT(2)/60.
      RN4=((D1*V1*YOT(2))/(YOT(1)*1.E-06))/1000.
      JP=M
      CALL LAG(RN1,EL1,5,JP,RN4,ELO)
      TW1=SUM-Q11*ALOG(DO/D1)/(2*3.14*16.435*AL1(M))
      AK1=0.021*(D1*V1*YOT(2)/(YOT(1)*1.E-06))**0.8*(YOT(6)*YOT(1)
     1*1.E-03/YOT(5))**0.68*YOT(5)/D1*ELO
      AMC=F(L)*YOT(2)*YOT(6)/60.
      CALL PROP(TW1,YOT,PPL,PPT,NTT)
      TLK1=60400;PRINT*,TLK1,(YOT(KPL),KPL=1,7)
      AK=16.435
      HTAI=1.00*AK1*(YOT(6)*YOT(1)*1.E-03/YOT(5))**-0.25
      HTAI1(M)=HTAI
      IF(M.EQ.1)HTAT2=HTAI1(1)
```

C-14

```fortran
      IF(M.EQ.1)GO TO 445
      HTAT2=(HTAI1(M)*AL1(M)-HTAI1(M-1)*AL1(M-1))/(AL1(M)-AL1(M-1))
445   CONTINUE
      P=1/HTAT2+ALOG(DO/D1)*(3.14*0.025)/(2*3.14*16.435)
      U=1./P
      UA=U*3.14*D1*AL2(M)
      IF(M.EQ.1)T11=(TAI*(AMC-UA/2.)+UA*TAV1(L,M))/(AMC+UA/2.)
      T11=(TI3*(AMC-UA/2.)+UA*TAV1(L,M))/(AMC+UA/2.)
      TOT=ABS(T11-T1)
      TKL2=61700
      T1=T11
      IF(TOT.LT.0.01)GO TO 90
80    CONTINUE
90    AK5(L,M)=Q13 !FOR HEAT FLUX OUTER DIA
      AK6(L,M)=Q13
      TI3=T1
      Q12(L,M)=Q11
      T12(L,M)=T1
      HTA(L,M)=HTAT2
100   CONTINUE
      PSUM=0.0
      RRT=AK6(L,1)
      DO 540 JJ1=1,4
      AK6(L,JJ1)=AK6(L,JJ1)/RRT
      PSUM=PSUM+AK6(L,JJ1)
540   CONTINUE
      EXTRA=Q5(L)-Q12(L,4)
      EXT1=EXTRA/PSUM
      DO 541 KK1=1,4
      AK2(L,KK1)=(AK6(L,KK1)*EXT1+AK5(L,KK1))
      ADG=(TI+TO(L))/2.
```

C-15

```
      CALL PROP(ADG,YOT,PPL,PPT,NTT)
      AK3(L,KK1)=AK6(L,KK1)*60*EXT1/(F(L)*YOT(6)*YOT(1))
      AK8(L,KK1)=AK6(L,KK1)*EXT1
      AK7(L,KK1)=AK3(L,KK1)
      AK3(L,KK1)=AK3(L,KK1)+T12(L,KK1)
      AK2(L,KK1)=AK2(L,KK1)/(3.14*DO*AL2(KK1))
541   CONTINUE
      PLK=TE(47)
      TAC=(SUM+TS)/2.
      CALL PROP(TAC,YOT,PPL,PPT,NTT)
      Q33=0.0
      PGH=TE(47)
      TTT=(TI+TO(L))/2.
      DELT=(TS-TTT)
      CALL PROP(TS,YOT,PPL,PPT,NTT)
      KLPT=66500
      RX=DO/(HTAI1(4)*D1)+(DO-D1)*DO/(2*16.435*(DO*D1)**0.5)
      BETA(L)=(RX**4*YOT(5)**3*YOT(2)*(YOT(2)-YOT(7))*9.81*YOT(3)/
     1(YOT(1)*1.E-09*1.5*DO*DELT))**0.333
110   CONTINUE
      P=TE(47);Q=TE(48);R=TE(1);P1=TE(24);Q1=TE(25)
      DO 10 I=1,4
      IF(I.EQ.3)K=2;IF(I.EQ.1)K=24;IF(I.EQ.2)K=36;IF(I.EQ.4)K=14
      DO 20 J=1,4
      IF(I.EQ.2.AND.J.EQ.4)TE(47)=R
      IF(I.EQ.4.AND.J.EQ.4)TE(24)=P
      IF(I.EQ.4.AND.J.EQ.4)TE(25)=Q
      IK=K
      DO 51 KJ=1,3
      PKJI=KJ
      IF(I.EQ.4.AND.J.EQ.4.AND.KJ.EQ.2)TE(IK)=PGH
```

C-16

```fortran
      HTC(KJ,J,I)=AK2(I,J)/(TS-TE(IK))
      HTC5(KJ,J,I)=AK5(I,J)/(TS-TE(IK))
C     ERROR ANALYSIS FOR LOCAL HEAT TRANSFE COEFFICIENT
      EQ(I,J)=YOT(2)*YOT(6)/60.*(((T12(I,J)-TAI)*0.1)**2+(F(I)
     1*0.025)**2*(T12(I,J)**2+TAI**2))**0.5
      DEL=(TS-TE(IK))
      EHO(KJ,J,I)=AK2(I,J)/DEL*((EQ(I,J)/Q12(I,J))**2+(0.025/25.)
     1**2+(0.001/AL2(J))**2+(0.025/DEL)**2*(TS**2+TE(IK)**2))**0.5
      PERR(KJ,J,I)=EHO(KJ,J,I)*100./HTC(KJ,J,I)
C     ERORR ANALYSIS END
      TA=(TE(IK)+TS)/2.
      CALL PROP(TA,YOT,PPL,PPT,NTT)
      HTTN(KJ,J,I)=0.728*(YOT(5)**3*YOT(2)**2*9.81*YOT(3)/(YOT(1)*
     11.E-09*DO*(TS-TE(IK))))**0.25
C     CONVERSION FACTOR USED =KJ(1000)/STO WATTS
      DEV2(KJ,J,I)=(HTC(KJ,J,I)-HTTN(KJ,J,I))/HTC(KJ,J,I)*100.
      TEE=TE(IK)
      CALL PROP (TEE,YOT,PPL,PPT,NTT)
      PRW=YOT(6)*YOT(1)*1.E-03/YOT(5)
      CALL PROP(TA,YOT,PPL,PPT,NTT)
      PRN=YOT(6)*YOT(1)*1.E-03/YOT(5)
      HTTM(KJ,J,I)=0.42*(9.81*DO**3*YOT(2)**2*YOT(3)*1.E 03/(YOT(1)
     1*1.E-06*YOT(5)*(TS-TE(IK))))**0.28*(PRN/PRW)**0.25*YOT(5)/DO
      DEV1(KJ,J,I)=(HTC(KJ,J,I)-HTTM(KJ,J,I))/HTC(KJ,J,I)*100.
      RRM(KJ,J,I)=HTC(KJ,J,I)/HTTM(KJ,J,I)
      RRN(KJ,J,I)=HTC(KJ,J,I)/HTTN(KJ,J,I)
   51 IK=IK+1
      K=K+3
   20 CONTINUE
   10 CONTINUE
      TE(47)=P;TE(24)=P1;TE(25)=Q1
```

```
      PRINT 120
      PRINT 130
      PRINT 140
      PRINT 150
      PRINT 200
      DO 190 I=1,4
      PRINT 160,((HTC(KJ,J,I),PERR(KJ,J,I),J=1,4),KJ=1,1)
      PRINT 170,I,((HTC(KJ,J,I),PERR(KJ,J,I),J=1,4),KJ=2,2)
      PRINT 180,((HTC(KJ,J,I),PERR(KJ,J,I),J=1,4),KJ=3,3)
190        CONTINUE
      DO 390 I=1,4
      SUM2=0.0
      DO 391 J=1,4
      SUM=0.0
      DO 392 K=1,3
      SUM=HTC(K,J,I)+SUM
392 CONTINUE
      SUM1(I,J)=SUM/3.
      PN=1.0
      IF(J.EQ.1.OR.J.EQ.4)PN=0.7
      SUM2=PN*SUM1(I,J)+SUM2
391 CONTINUE
      SUM3(I)=SUM2/3.4
390 CONTINUE
      WRITE(8,*),(SUM3(I),I=1,4)
      PRINT 130
120        FORMAT (///T11,'TABLE 4:EXPERIMENTAL HEAT TRANSFER
COEFFICI
   1ENT(S)'/)
130        FORMAT(T11,100('-'))
140        FORMAT(T50,'THERMOCOUPLE POSITION(S)')
```

C-18

```
150        FORMAT(T30,'1',T52,'2',T73,'3',T92,'4')
160        FORMAT(/T18,'TOP',2X,4(F8.2,4X,F5.1,4X))
170        FORMAT(T11,'TUBE-',I1,T18,'SIDE',1X,4(F8.2,4X,F5.1,4X))
180        FORMAT(T18,'BOT',2X,4(F8.2,4X,F5.1,4X)/)
200        FORMAT(T20,4(4X,'EXP',9X,'% DEV'))
   PRINT 210
   PRINT 230
   PRINT 240
   DO 300 I=1,1
   DO 310 II=1,2
   IF(II.EQ.1)PRINT 250
   IF(II.EQ.2)PRINT 251
   PRINT 260
   K11=II+(II-1)
   K22=K11+1
   PRINT 270,((HTC(KJ,J,I),HTTM(KJ,J,I),DEV1(KJ,J,I)
   1,HTTN(KJ,J,I),DEV2(KJ,J,I),J=K11,K22),KJ=1,1)
   PRINT 280,((HTC(KJ,J,I),HTTM(KJ,J,I),DEV1(KJ,J,I)
   1,HTTN(KJ,J,I),DEV2(KJ,J,I),J=K11,K22),KJ=2,2)
   PRINT 290,((HTC(KJ,J,I),HTTM(KJ,J,I),DEV1(KJ,J,I)
   1,HTTN(KJ,J,I),DEV2(KJ,J,I),J=K11,K22),KJ=3,3)
310        CONTINUE
300        CONTINUE
   PRINT 230
   PRINT 320
320        FORMAT(T18,'* HEAT TRANSFER COEFFICIENTS ARE IN W/SQ.M.K')
210 FORMAT(///T11,'TABLE-5:COMPARISON BETWEEN EXPERIMENTAL AND
   1THEORITICAL HEAT TRANSFER COEFFICIENTS'/)
230 FORMAT(T11,100('-'))
240 FORMAT(T72,'THERMOCOUPLE POSITIONS')
250 FORMAT(T42,'1',T92,'2')
```

C-19

```
51 FORMAT(T42,'3',T92,'4')
60 FORMAT(T24,2('EXP',7X,'MIK',6X,'% DEV',5X,'NUS',6X,'% DEV'
  1,5X))
70 FORMAT(T16,'TOP',1X,10(F8.1,2X))
80 FORMAT(T10,'TUBE-1',T16,'SIDE',10(F8.1,2X))
90 FORMAT(T16,'BOTM',10(F8.1,2X))
   PRINT*,(F(IIP),IIP=1,4)
   DO 501 L=1,i
   DO 501 M=1,4
   TL1=TAV1(L,M)
   CALL PROP(TL1,YOT,PPL,PPT,NTT)
   PRW=YOT(6)*YOT(2)*1.E-03/YOT(5)
   TLA=(TS+TL1)/2.
   CALL PROP(TLA,YOT,PPL,PPT,NTT)
   PRN=YOT(6)*YOT(2)*1.E-03/YOT(5)
   ANUS=0.725*(YOT(5)**3*YOT(2)**2*9.81*YOT(3)/(YOT(1)*
  11.E-09*DO*(TS-TL1)))**0.25
   AMEK=0.42*(9.81*DO**3*YOT(2)**2*YOT(3)*1.E 03/(YOT(1)
  1*1.E-06*YOT(5)*(TS-TL1)))**0.28*(PRN/PRW)**0.25*YOT(5)/DO
   OTHM=1.620*(Q5(L)/(.341*YOT(3)*YOT(1)*1.E-03))**-0.5*
  1(YOT(1)**2*(1.E-12)/(YOT(2)**2*YOT(5)**3*9.81))**-0.3333
   PECK=ANUS*(0.0206*(YOT(3)*YOT(1)*1.E-03/(YOT(5)*(TS-TL1)))**.5
  1+0.79)
   SA1=YOT(5)**3*YOT(2)*(YOT(2)-YOT(7))*9.81
   SA2=YOT(3)*(1+0.4*(TS-TL1)*YOT(6)/YOT(3))**2
   SA3=DO*YOT(1)*(1.E-09)*(TS-TL1)
   BROM=0.728*((SA1*SA2)/SA3)**0.25
   ROHS=ANUS*(1+0.68*(TS-TL1)*YOT(6)/YOT(3))**0.25
   C1=YOT(6)*(TS-TL1)/YOT(3)
   C2=YOT(5)*(TS-TL1)/(YOT(1)*YOT(3)*1.E-03)
   CHEN=ANUS*((1+0.68*C1+0.02*C1*C2)/(1+0.95*C2-0.15*C1*C2))**0.25
```

C-20

```fortran
      HEND=ANUS*0.057*(YOT(1)*1.E-06/((YOT(2)*DO*YOT(4)*1.E-03)**.5)
     1)**-0.373
      WHIT=0.728*(YOT(5)**3*YOT(2)**2*9.81*YOT(3)/(YOT(1)*
     11.E-09*DO*(TS-TL1)))**0.25
      WRITE(3,57),AMEK,ANUS,OTHM,PECK,BROM,ROHS,CHEN,HEND,WHIT
7     FORMAT(10(F7.1,2X))
C     CALCULATION OF WEIGHTED AVERAGE HEAT TRANSFER COEFFICIENT
01    CONTINUE
      DO 502 KK=1,1
      SUM=0.0
      DO 503 KL=1,4
03    SUM=SUM+AL2(KL)*TAV1(KK,KL)*10.
      SUM=SUM/3.41
      CALL PROP(SUM,YOT,PPL,PPT,NTT)
      QP1=85100;PRINT*,QP1,(YOT(IKL),IKL=1,7)
      PRW=YOT(6)*YOT(2)*1.E-03/YOT(5)
      TLA=(TS+SUM)/2.
      CALL PROP(TLA,YOT,PPL,PPT,NTT)
      QP2=85400;PRINT*,QP2,(YOT(IKL),IKL=1,7)
      PRN=YOT(6)*YOT(2)*1.E-03/YOT(5)
      ANUS=0.725*(YOT(5)**3*YOT(2)**2*9.81*YOT(3)/(YOT(1)*
     11.E-09*DO*(TS-SUM)))**0.25
      CALL PROP(TS,YOT,PPL,PPT,NTT)
      QP3=85750;PRINT*,QP3,(YOT(IKL),IKL=1,7)
      PRN1=YOT(6)*YOT(2)*1.E-0E/YOT(5)
      AMEK=0.42*(9.81*DO**3*YOT(2)**2*YOT(3)*1.E 03/(YOT(1)
     1*1.E-06*YOT(5)*(TS-SUM)))**0.28*(PRN/PRW)**0.25*YOT(5)/DO
      CALL PROP(TLA,YOT,PPL,PPT,NTT)
      OTHM=1.620*(Q5(KK)/(.341*YOT(3)*YOT(1)*1.E-03))**-0.5*
     1(YOT(1)**2*(1.E-12)/(YOT(2)**2*YOT(5)**3*9.81))**-0.3333
      PECK=ANUS*(0.0206*(YOT(3)*YOT(1)*1.E-03/(YOT(5)*(TS-SUM)))**.5
```

C-21

```fortran
      1+0.79)
      SA1=YOT(5)**3*YOT(2)*(YOT(2)-YOT(7))*9.81
      SA2=YOT(3)*(1+0.4*(TS-SUM)*YOT(6)/YOT(3))**2
      SA3=DO*YOT(1)*(1.E-09)*(TS-SUM)
      BROM=0.728*((SA1*SA2)/SA3)**0.25
      ROHS=ANUS*(1+0.68*(TS-SUM)*YOT(6)/YOT(3))**0.25
      C1=YOT(6)*(TS-SUM)/YOT(3)
      C2=YOT(5)*(TS-SUM)/(YOT(1)*YOT(3)*1.E-03)
      CHEN=ANUS*((1+0.68*C1+0.02*C1*C2)/(1+0.95*C2-0.15*C1*C2))**0.25
      HEND=ANUS*0.057*(YOT(1)*1.E-06/((YOT(2)*DO*YOT(4)*1.E-03)**.5)
     1)**-0.373
      WHIT=0.728*(YOT(5)**3*YOT(2)**2*9.81*YOT(3)/(YOT(1)*
     11.E-09*DO*(TS-SUM)))**0.25
  02           CONTINUE
      RETURN
      END
      SUBROUTINE AVG(TE,TAV1)
      DIMENSION TE(70),TAV1(5,5)
      P=TE(47);Q=TE(48);R=TE(1);P1=TE(24);Q1=TE(25)
      DO 10 I=1,4
      IF(I.EQ.3)K=2;IF(I.EQ.1)K=24;IF(I.EQ.2)K=36;IF(I.EQ.4)K=14
      DO 20 J=1,4
      IF(I.EQ.2.AND.J.EQ.4)TE(47)=R
      IF(I.EQ.4.AND.J.EQ.4)TE(24)=P
      IF(I.EQ.4.AND.J.EQ.4)TE(25)=Q
      TAV1(I,J)=(TE(K)+TE(K+1)+TE(K+2))/3.
      K=K+3
  20 CONTINUE
  10 CONTINUE
      TE(47)=P;TE(24)=P1;TE(25)=Q1
      RETURN;END
```

C-22

```
SUBROUTINE EXER(HTCI,HTCO,UO,TS,TCI,TCO,PEEXP,V,Q,PPL,PPT,NTT)
DIMENSION HTCI(5),UO(5),TCO(5),PEEXP(5),V(5)
1,YOT(8),HTCO(5),Q(5),PPL(8,33),PPT(8,33),NTT(8)
EDO=0.000025;ETS=0.025;EV=0.004747;EL=0.001;DO=0.02887
D1=0.025;AL=0.341;AK=16.435              !GIVE THE VALUE
PRINT*,(HTCO(I),V(I),I=1,4)
PRINT*,(Q(I),I=1,4)
DO 10 I=1,4
AK1=HTCI(I)/(V(I)**0.8*D1**-0.2)
TAV=(TCI+TCO(I))/2.;CALL PROP(TAV,YOT,PPL,PPT,NTT)
EHI=((AK1*0.8*V(I)**-0.2*D1**-0.2*EV)**2+(AK1*V(I)**0.8*-0.2*
1D1**-1.2*EDO)**2)**0.5
DELT=TCO(I)-TCI
EQ=(YOT(2)**2*YOT(6)**2*((EV*DELT)**2+2.*(V(I)*ETS)**2))**0.5
AO=3.14*0.02887*0.341;DET=TS-(TCI+TCO(I))/2.
EUO=(1./(AO*DET)**2*(EQ**2+(Q(I)/DO*EDO)**2+(Q(I)/AL*EL)**2)
1+1.5*(Q(I)/(3.14*DET**2)*ETS)**2)**0.5
EHO=HTCO(I)**2*((EUO/UO(I)**2)**2+(DO*EHI/(HTCI(I)**2*D1))**2
1+((1./(HTCI(I)+D1)+1./(2.*AK)*ALOG(DO/D1)+1./(2.*AK))*EDO)
1**2+((DO/(HTCI(I)*D1**2)+DO/(2.*AK*D1))*EDO)**2.)**0.5
PEEXP(I)=EHO/HTCO(I)*100.
10  CONTINUE
RETURN;END
SUBROUTINE LAG(X,YY,N,N1,XINT,YOUT)
C   THIS SUBROUTINE PERFORMS LAGRANGIAN INTERPOLATION WITHIN
C   A SET OF (X,Y) PAIRS TO GIVE THE Y VALUE CORRESPONDING
C   TO XINT.THE DEGREE OF THE INTERPOLATING POLYNOMIAL IS
C   ONE LESS THAN THE NUMBER OF POINTS SUPPLIED
C   PARAMETERS ARE -
C       X       ARRAY OF VALUES OF THE INDEPENDENT VARIABLE
C       Y       ARRAY OF FUNCTION VALUES CORRESPONDING TO X
```

C-23

```
      N       NUMBER OF POINTS
      XINT  THE X-VALUE FOR WHICH ESTIMATE OF Y IS DESIRED
      YOUT  THE Y-VALUE RETURNED TO CALLER
      DIMENSION X(5),Y(20),YY(5,5)
      DO 30 J=1,N
   30 Y(J)=YY(N1,J)
      YOUT=0.0
      DO 20 I=1,N
      TERM=Y(I)
      DO 10 J=1,N
      IF(I.EQ.J) GO TO 10
      TERM=TERM*(XINT-X(J))/(X(I)-X(J))
   10 CONTINUE
      YOUT=YOUT+TERM
   20 CONTINUE
      RETURN
      END
   13 FORMAT(10X,'PRESSURE OF VAPOUR PHASE(KG./SQ.CM.)=',F5.2,10X
     1,'SATURATION TEMP.(DEG.C)=',F5.1)
   14 FORMAT(10X,'MEASURED TEMPERATURE(DEG.C)=',F5.1)
   15 FORMAT(10X,'COOLANT INLET TEMPERATURE(DEG.C)=',F5.1)
   16 FORMAT(///10X,'COOLANT FLOWRATE(S) L.P.M.',10X,'RE. NO.',10X
     1,'OUTLET TEMP(S) (DEG.C)')
  C28 FORMAT(/10X,'HEAT FLUX DISTRIBUTION ALONG THE LENGTH'/
  C   1/10X,4(F8.1,3X))
   17 FORMAT(/10X,'TUBE-',I2,T31,F5.2,T47,F7.1,T74,F6.2)
   18 FORMAT(/10X,'DISTANCE OF GRID POINTS FROM LEFT HAND IN METER'
     1/2X,5(5X,F5.3,5X))
   19 FORMAT(//10X,'DISTRIBUTION OF TEMP. ALONG THE EXPOSED LENGTH
     1 OF TUBE'/10X,'CONSIDERING INSIDE HEAT TRANSFER COEFFICI
     1ENT TO BE CONSTANT'/)
```

C-24

```
0    FORMAT(5(5X,F7.2,3X))
1    FORMAT(//10X,'DISTRIBUTION OF TEMP. ALONG THE EXPOSED LENGTH
    1 OF THE TUBE'/10X,'CONSIDERING VARIABLE HEAT TRANSFER CO
    1EFFICIENT'/)
3    FORMAT(/10X,'DISTRIBUTION OF INSIDE HEAT TRANSFER COEFFICIENT
    1S(WATT/SQ.M.DEG.C)'/)
4    FORMAT(/10X,'DISTRIBUTION OF AVERAGE OUTER WALL TEMP.(S)'/)
5    FORMAT(//10X,'DISTRIBUTION OF HEAT PICKED UP ALONG THE LENGHT
    1 OF TUBE (WATT)',10X,'ACTUAL HEAT PICKED UP(WATT)'/)
6    FORMAT(10X,'CONDENSATE FLOW RATE(L.P.M)=',F5.3/10X,'CONDENSA
    1TE TEMP.(DEG.C)=',F5.1/10X,'PERCENTAGE HEAT LOSS=',F5.1)
7    FORMAT(5(5X,F7.4,5X),10X,F7.1)
9    FORMAT(1H1)
     RETURN;END
```

SOFTWARE FOR INTERFACING OF Z-80/UP WITH DMM

The progamme given below was used for interfacing Z-80 uP with Keithley 192 model programmable DMM with IEEE-488 interface.

Addr	Code	Label	Op	Operand	Comment
1800	C3001A		JP	START	
1803	14	PASETUP:	DB	14	;Int.Low bit mode
1804	CF		DB	CF	
	FF		DB	FF	
	97		DB	97	
	FF		DB	FF	
1808	16	PBSETUP:	DB	16	
	CF		DB	CF	
	A7		DB	A7	
	97		DB	97	
	FF		DB	FF	
180D	35	CTCO:	DB	0011 0101B	2b Timer
	21		DB	21H	time constt.
	18		DB	18	int. low
1810	D7	CTCI:		1101 0011B	Counter reset
	DE		DB	DEH	
	1A		DB	1A	INT. LOW
1813	00	COUNT:	DB	00H	No of reading in buffer block
1814	00 00		DW		PA int. service addr.
1816	00 00		DW		PB -do-
1818	00 00		DW		CTCO int. addr.
181A	20 18		DW	1820	CTC1 int. addr.
181C	00 00		DW		CTC2 int. addr.
181E	00 00		DW		CTC3 int. addr.
1820	18 16	ISRI:	JR	SPACE	
1822	00				
1823	00 00	STBUF:	DW	00 00	
1825	00 00		DW	00 00	Current data string
1827	00 00		DW	00 00	
1829	00 00	SUM:	DW	00 00	Temp.sum started here
182B	00 00		DW	00 00	
182D	00 00		DW	00 00	(6 kbytes)
182F	00 00	COUNT:	DW	00 00	No of readings in current channel(BCD)
1831	00 20	MOHANTY	DW	20 20	Points to high byte of running buffer entry (IY+16)
1833	00	SCANS:	DB	00	
1834	00 01	TEMP:	DW	00 01	
1836	01 00	FILE:	DW	00 00	FILE NO.

```
1838      0D          SPACE:    DEC   C
1839      FB                    EF
183A      ED 4D                 RETI
183C      25          KEY:      DB    00       (IY+25)
183D      FF
183E      82
183F      FF
1840                  ST1:
                      CTCO      EOU   40H
                      PIO       EOU   80H
1840      0E 82                 LD    C,(PIO+2)  PA Setting up
1842      21 03 18              LD    HL,PASETUP
1845      06 05                 LD    B,05
1847      ED B3                 OTIR
1849      0E 83                 LD    C,(PIO+3)  PB setting
184B      06 05                 LD    B,05H
184D      ED B3                 OTIR
184F      0E 40                 LD    C,CTCO       CTCO Setting up
1851      06 03                 LD    B,03H
1853      ED B3                 OTIR
1855      0E 41                 LD    C, CTCO+1
1857      06 03                 LD    B,03H
1859      ED B3                 OTIR
185B      ED 5E                 IM    2
185D      21 23 18              LD    HL,STBOF
1860      CD 2B 19              CALL  BEEP
1863      3E 10                 LD    A,00 01 00 00 initialize PB
1865      D3 81                 OUT   (PIO+1),A
1867      3E 18                 LD    A,18H    int. high.
1869      ED 47                 LD    I,A          addr
186B      FD 21 23 18           LD    IY,STBUF
186F      00 00                 DW    00 00 H
1871      DB 81       NOTRIG:   IN    A,(PIO+1)
1873      CB 7F                 BIT   7,A
1875      20 FA                 JR    NZ,NOTRIG
1877      DB 81                 IN    A,(PIO+1)  Read int. time and
1879      CB 47                 BIT   0,A        Put in C
187B      20 04                 JR    NZ,$1
187D      0E 14                 LD    C,14H      i.e. 20 secs.
187F      18 0A                 JR    OUT
1881      CB 4F       $1 :      BIT   1,A
1883      20 04                 JR    NZ,$2
1885      0E 0A                 LD    C,0AH      i.e. 10 secs.
1887      18 02                 JR    OUT
1889      0E 05       $2:       LD    C,05H      i.e.  5 secs.
188B      3E FF       OUT       LD    A,1111 1111B   PUT LED
188D      D3 02                 OUT   (02),A     OH
188F      CD 3E 19    WAIT:     CALL  RDBYTE
1892      FE 0D                 CP    SO       Is it SO
1894      20 F9                 JR    NZ,WAIT  NO! DO AGAIN
1896      3E D1                 LD    A,D3       YES! START COUNTER
1898      D3 41                 OUT   (CTCO+1),A  JP JAS
189A      FB                    EI
189B      21 25 18    STRING:   LD    HL,1825H
189E      06 12                 LD    B,12H
```

```
18A0    08                          EX      AF,AF'
18A1    37                          SCF
18A2    08                          EX      AF,AF'
18A3    CD 3E 19    MORE:           CALL    RDBYTE
18A6    D6 30                       SUB     30H
18A8    FA C1 18                    JP      M,NOUT
18AB    FE 09                       CP      09H
18AD    F2 C1 18                    JP      P,NOUT
18B0    08                          EX      AF,AF'
18B1    3F                          CCF
18B2    38 06                       JR      C,ROT
18B4    08                          EX      AF,AF'
18B5    B6                          OR      (HL)
18B6    77                          LD      (HL),A
18B7    23                          INC     HL
18B8    18 06                       JR      HO
18BA    08          ROT:            EX      AF,AF'
18BB    07                          RLCA
        07                          RLCA
        07                          RLCA
        07                          RLCA
18BF    77                          LD      (HL),A
18C0    00          HO:             DB      OO
18C1    10 EO       NOUT:           DJNZ    MORE
18C3    21 30 18                    LD      HL
18C6    11 35 18                    LD      DE
18C9    06 02                       LD      B,02H
18CB    DD 21 2E 18                 LD      IX
18CF    CD 1D 19                    CALL    MADDI
18D2    21 2E 18                    LD      HL,182E
18D5    11 28 18                    LD      DE,1828
18D8    06 06                       LD      B,06H
18DA    DD 21 2E 18                 LD      IX,182E
18DE    CD 18 19                    CALL    MADD
18E1    70 C3 60 19                 JP      THERE
18E4    FF
18E5    FF
18E6    FF
18E7    FF
18E8    FC
18E9    FD
18EA    34
18EB    10
18EC    FD 7E 10                    LD      A,(IY+16)
18EF    FE 38                       CP      38
18F1    28 06                       JR      Z,DONE
18F3    CD 2B 19                    CALL    BEEP
18F6    C3 71 18                    JP      NOTRIG
18F9    CD 83 19    DONE:           CALL    TAPE
18FC    FD 36 0E 00                 LD      (IY+1E),00   HIGH  RUNNING
                                                         BUFFER
1900    FD 36 0F 20                 LD      (IY+1F),20   LOW RUNNING BUFF.
1904    C3 71 18                    JP      NOTRIG
1907    00
1908    D5          TRANS:          PUSH    DE
```

```
1909    C5                      PUSH    BC
190A    21 29 18                LD      HL,SUM
190D    ED 5B 31 18             LD      DE,(MOHANTY)
1911    01 08 00                LD      BC,0008H
1914    ED B0                   LDIR
1916    ED 53 01 18             LD      (MOHANTY),DE
191A    C1                      POP     BC
191B    D1                      POP     DE
191C    C9                      RET
191D    AF          MADD:       XOR     A
191E    1A          MADD1:      LD      A,(DE)
191F    8E                      ADC     A,(HL)
1920    27                      DAA
1921    DD 77 00                LD      (IX),A
1924    1B                      DEC     DE
1925    2B                      DEC     HL
1926    DD 2B                   DEC     IX
1928    10 F4                   DJNZ    MADDI
192A    C9                      RET
192B    F5                      PUSH    AF
192C    C5                      PUSH    BC
192D    D5                      PUSH    DE
192E    E5                      PUSH    HL
192F    21                      LD      HL,0200
1930    00
1931    02
1932    CD                      CALL    3E05
1933    E2
1934    05
1935    3E                      LD      A,40
1936    40
1937    D3                      OUT     (02),A
1938    02
1939    E1                      POP     HL
193A    D1                      POP     DE
193B    C1                      POP     BC
193C    F1                      POP     AF
193D    C9                      RET
193E    DB          L1:         IN      4,(81)
193F    81
1940    CB                      BIT     5,A
1941    6F
1942    20                      JRNZ    ,L1
1943    FA
1944    CB                      RES     4.A
1945    A7
1946    D3                      OUT     (81),A
1947    81
1948    DB                      IN      A,(80)
1949    80
194A    57                      LD      D,A
194B    3E                      LD      A,08
194C    08
194D    D3                      OUT     (81),A
194E    A1
```

```
194F    DB          L2:     IN      A,(81)
1950    81
1951    CB                  BIT     5,A
1952    6F
1953    28                  JRZ     ,L2
1954    FA
1955    CB                  RES     3,A
1956    9F
1957    D3                  OUT     (81),A
1958    81
1959    CB                  SET     4,A
195A    E7
195B    D3                  OUT     (81),A
195C    81
195D    74                  LD      A,D
195E    2F                  CPL
195F    C9                  RET
1960    21 25 18    THERE:  LD      HL,1825
1963    3E 00               LD      A,00H
1965    77                  LD      (HL),A
1966    23                  INC     HL
1967    77                  LD      (HL),A
1968    23                  INC     HL
1969    77                  LD      (HL),A
196A    23                  INC     HL
196B    77                  LD      (HL),A
196C    79                  LD      A,C
19CD    E6 FF               AND     FFH
196F    C2 9B 18            JR      NZ,STRING
1972    CD 08 19            CALL    TRANS
1975    06 08               LD      B,08H       11 BYTES
1977    3E 00               LD      A,00H
1979    21 29 18            LD      HL,1829
197C    77          B1:     LD      (HL),A
197D    23                  INC     HL
197E    10 FC               DJNZ    B1
1980    C3 E9 18            JP      HERE
1983    CD 23 1A    TAPE:   CALL    DELAY
1986    CD 2D 05            CALL    SUMI
1989    32 B5 1F            LD      (STEPBF+6),A
198C    21 A0 0F            LD      HL,4000
198F    CD DE 05            CALL    TONEIK
1992    21 AF 1F            LD      HL,STEPBF
1995    01 07 00            LD      BC,7
1998    CD A7 05            CALL    TAPEOUT
199B    21 A0 0F            LD      HL,4000
199E    CD E2 05            CALL    TONE2K
19A1    CD 3A 05            CALL    GETPTR
19A4    CD A7 05            CALL    TAPEOUT
19A7    21 A0 0F            LD      HL,4000
19AA    CD E2 05            CALL    TONE2K    MAKE SCANE 0
19AD    3E 00               LD      A,00H     Inc.FILE NO.
19AF    32 33 18            LD      (1833),AH
19B2    21 37 18            LD      HL,1837
19B5    11 35 18            LD      DE,1835
```

```
19B8        06 02           LD      B,02
19BA        DD 21 37 18     LD      IX,1837
19BE        CD 1D 19        CALL    MADD
19C1        C9              RET
19C2        FF              RST7
19C3        FF              RST7
19C4        FF              RST7
19C5        FC              CALL  M,FFFF
19C6        FF
19C7        FF
19C8        FF              RST  7
19C9        FF              RST  7
19CA        FE              CP  FF
19CB        FF
19CC        FF              RST  7
19CD        FF              RST  7
19CE        D3              OUT         (FF),A
19CF        FF
19D0        FF              RST  7
19D1        FF              RST  7
19D2        FF              RST  7
19D3        FF              RST  7
19D4        FF              RST  7
19D5        F7              RST  6
19D6        FF              RST  7
19D7        7E              LD          A,(HL)
19D8        FF              RST  7
19D9        BD              CPL
19DA        15              DEC D
19BB        FF              RST  7
19DC        AD              XORL
19DD        FF              RST  7
19DE        28              JR   Z
19DF        FF
19E0        50
19E1        FF
19E2        FF
19E3        DF
19E4        FF
19E5        D3
19E6        FF
19E7        7F
19E8        FF
19E9        9F
19EA        6C
19EB        FF
19EC        E0
19ED        FF
19EE        34
19EF        FF
19F0        C3
19F1        FF
19F2        FF
19F3        FF
19F4        FF
```

```
19F5      FF
19F6      FF
19F7      FF
19F8      FF
19F9      EF
19FA      F9
19FB      FF
19FC      E3
19FD      FF
19FE      FF
19FF      FF
1A00      21 B1 1F    START:   LD      HL,1FB1 TAKING 56 REAGS.
1A03      36 00                LD      (HL),00H 2000-21C0 IS
1A05      23                   INC     HL          one buffer
1A06      36 20                LD      (HL),20H
1A08      23                   INC     HL
1A09      36 C0                LD      (HL),C0
1A0B      23                   INC     HL
1A0C      36 21                LD      (HL),21
1A0E      C3 40 18             JP      ST1
1A11      3E 50       DELAY:   LD      A,0101 0000
1A13      D3 81                OUT     (PBDATA),A
1A15      0E 0A                LD      C,05H
1A17      3E D1                LD      A, DIH
1A19      D3 41                OUT     (CTCO+1),A
1A1B      FB                   EI
1A1C      79          $1:      LD      A,C
1A1D      E6 FF                AND     FFH
1A1F      28 00                JR      Z,$2
1A21      18 FA                JR      $1
1A23      21 36 18    $2:      LD      HL,1836
1A26      11 B0 1F             LD      DE,1FB0
1A29      7E                   LD      A,(HL)
1A2A      12                   LD      (DE),A
1A2B      1B                   DEC     DE
1A2C      23                   INC     HL
1A2D      7E                   LD      A,(HL)
1A2E      12                   LD      (DE),A
1A2F      F3                   DI
1A30      C9                   RET
```

ERROR ANALYSIS

The measurement of the dimensions of the condenser tube, temperature of wall, steam temperature, cooling water flow rate and its inlet and outlet temperature always has some inaccuracies due to the inherent limitations associated with instruments. Therefore, error is involved in the prediction of condensing heat transfer coefficient. In order to find out the extent of error in the present experimentation, error associated with the predicted parameter was calculated for several experimental runs. This Appendix presents a typical sample calculation of error analysis for Run No. 13 of Table A-13 of Appendix A.

Error in a parameter is calculated by the following Equation :

$$E_x = \left[\sum_{i=1}^{n} \frac{\delta x}{\delta y_i} E_{y_i} \right]^{1/2}$$

where E represents error, x parameter which is a function of N parameters (i=1,....n) and y_i is the ith variable.

E.1 ERROR IN THE SURFACE AREA OF CONDENSER TUBE, E_A :

Since $A = \pi d_o l$

hence $E_A = [(\pi l E_{D_o})^2 + (\pi d_o E_l)^2]^{1/2}$

where E_{D_o} and E_l denote the error associated with diameter and length respectively.

$$d_o = 0.0288 \text{ m} \quad ; \quad E_{D_o} = 0.0001 \text{ m}$$

$$L = 0.341 \text{ m} \quad ; \quad E_L = 0.001 \text{ m}$$

$$A = \pi*0.0288*0.341 = 0.03085 \text{ m}^2$$

$$E_A = [(\pi*0.341*0.0001)^2 + (\pi*0.0288*0.001)^2]^{1/2}]$$

$$= 1.402E-04 \text{ m}$$

E.2 ERROR IN THE MEASUREMENT OF HEAT PICKED-UP

$$Q = w\rho C_p(t_o-t_i)/60 \quad W$$

$$E_Q = \frac{1}{60}[(\rho C_p(t_o-t_i)E_w)^2+(wC_p\rho E_{t_o})^2+(-wC_p\rho E_{t_i})^2]^{1/2}$$

$$E_w = 0.1 \text{ lpm} \quad ; \quad E_{t_o} = 0.025°C \quad ; \quad E_{t_i} = 0.025°C$$

$$t_o = 30.22°C \quad ; \quad t_i = 23.92°C \quad ; \quad t_o-t_i = 6.3°C$$

$$Q = 11.6*993.33*4.1829(30.22-23.92)/60$$

$$= 5060.5 \text{ W}$$

$$E_Q=\frac{1}{60}[(4.1829*993.3*6.3*0.1)^2+(11.6*4.1829*993.3*0.025)^2$$

$$+(-11.6*4.1829*0.025)^2]^{1/2}$$

$$= 52.057 \text{ W}$$

E.3 ERROR IN PREDICTING CIRCUMFERENTIAL CONDENSING HEAT TRANSFER COEFFICIENT

It is assumed that the temperature profile of the cooling water is almost linear, which is true within the range of experimental errors (Ref. Fig. 5.9). This is assumed with an aim to reduce the complexity of calculation without sacrificing accuracy to a large extent.

$$Q_I = \frac{Q}{L}*L_I = \frac{5060.5*0.071}{0.341} = 1053.7 \text{ W}$$

$$E_{Q_I} = [(E_Q.L_I/L)^2+(Q.E_{L_I}/L)^2+(-Q.L_I.E_L/L^2)^2]^{1/2}$$

$$E_{QI} = [(52.057*0.071/0.341)^2 + (5060.5*0.001/0.341)^2$$

$$+ (-5060.5*0.071*0.001/(0.342)^2)^2]^{1/2}$$

$$= [114.19461 + 220.256 + 18.941]^{1/2} = 18.547 \text{ W}$$

like-wise :

$$E_{QII} = 21.7313 \text{ W} \; ; \; E_{QIII} = 21.7313 \text{ W} \; ; \; E_{QIV} = 18.597 \text{ W}$$

$$E_{(ts-two)} = [(E_{ts})^2 + (-E_{two})^2]^{1/2}$$

$$= [(0.025)^2 + (0.025)^2]^{1/2} = 0.0355°C$$

$$A_I = \pi*0.071*0.0288 = 6.4239 \times 10^{-3} \text{ m}^2$$

$$E_{AI} = [(\pi*0.071*0.0001)^2 + (\pi*0.0288*0.001)^2]^{1/2}$$

$$= 0.00009 \text{ m}^2$$

$$h_{o,I,side} = 9643.24 \text{ W/m}^2°C \; ; \; h_{o,I,bottom} = 7399.8 \text{ W/m}^2°C$$

$$h_{o,I,top} = \frac{Q_I}{A_I(ts-two,top)} \; ; \quad t_1 = two,top$$

$$= 1053.7/0.00642(110.71-101.05) = 16990.44$$

$$E_{ho,I,top} = \left[\left(\frac{E_{QI}}{A_I(ts-t_1)} \right)^2 + \left(-\frac{Q_I}{(ts-t_1)} . E_{AI} \right)^2 + \right.$$

$$\left. \left(\frac{-Q_I}{A_I(ts-t_1)^2} . E_{(ts-t_1)} \right)^2 \right]^{1/2}$$

$$= \left[\left(\frac{18.547}{0.00642(110.71-101.05)} \right)^2 + \left(\frac{1053.7*0.00009}{(0.00642)^2(110.71-101.05)} \right)^2 \right.$$

$$\left. + \left(-\frac{1053.7*0.0288}{0.00642*(110.71-101.05)} \right)^2 \right]^{1/2} = 347.24 \text{ W/m}^2°C$$

Error in $h_{o,I,top} = 347.24*100/16990 = 2.04\%$

like-wise error in $h_{o,I,side}$ and $h_{o,I,bottom}$ were calculated

Error in $h_{o,I,side}$ = $(E_{h_{o,I,side}}/h_{o,I,side})*100$

$$= 205.47/9643.29 = 2.1\%$$

Error in $h_{o,I,bottom}$ = $159.57/7399.8 = 2.1\%$

E.4 ERROR IN AVERAGE CIRCUMFERENTIAL HEAT TRANSFER COEFFICIENT

$$E_{h_{o,I}} = 1/3[(E_{h_{o,I,top}})^2+(E_{h_{o,I,side}})^2+(E_{h_{o,I,bottom}})^2]^{1/2}$$

$$= 144.63 \text{ W/m}^2 \text{°C}$$

$$h_{o,I} = 11344.3 \text{ W/m}^2 \text{°C}$$

Error in $h_{o,I}$ = $(144.63/11344.3)*100 = 1.27\%$

In the same manner error in $h_{o,II}$, $h_{o,III}$, and $h_{o,IV}$ have been calculated :

$E_{h_{o,II}}$=148.65 W/m^2°C ; $h_{o,II}$=14116 W/m^2°c ; error in $h_{o,II}$=1.05 %

$E_{h_{o,III}}$=195.69 W/m^2°C ; $h_{o,III}$=17842W/m^2°c ; error in $h_{o,III}$=1.09%

$E_{h_{o,IV}}$=303.208 W/m^2°C; $h_{o,IV}$=24406W/m^2°C ; error in $h_{o,IV}$=1.24%

E.5 ERROR IN WEIGHTED HEAT TRANSFER COEFFICIENT

h_{wt} = $(h_{o,I}*L_I +h_{o,II}*L_{II} +h_{o,III}*L_{III} +h_{o,IV}*L_{IV})/L$

$$E_{h_{wt}} = \left[\left(-\frac{h_{wt}}{L} . E_L \right)^2 + \sum_{i=I}^{IV} \frac{L_i}{L} . E_{h_{o,i}} + \sum_{i=I}^{IV} \frac{h_{o,i}}{L} . E_{L_i} \right]^{1/2}$$

$$= 141.856 \text{ W/m}^2 \text{°C}$$

Error in h_{wt} = $141.856/16815.4$

$$= 0.8 \%$$

REFERENCES

1. Nusselt,W.,Die Oberflacher-Kondensation des-wasserdampfes, VDIZ ., Vol.6o,pp.541-546 and 569-575,1916 (in ref. 56)

2. McAdams,W.H.,Heat Transmission,McGraw Hill Book Company Inc.

3. Pierce,B.O.,"A Short Table of Integrals",Boston,Mass.,Ginn and Co.,1929 (in ref. 17)

4. Parr,S.W.,Engineer,113,559 ,1921 (in ref. 17)

5. Othmer,D.F.,Ind. Eng. Chem.,21,576 ,1929

6. Backer,E.M., and Muller, A.C., Trans.,Am.Inst.Chem.Engrs.,33, 531-558 (1937)

7. Wallace,J.L.,and Davison,A.W.,Ind.Eng.Chem.,30,948-953,1938

8. Kirkbride,C.G.,Trans.Am.Inst.Chem.Engrs.,30, 170-186 1933-34

9. Baker,E.M.,and U.Tsao, Trans. Am.Inst.Chem.Engrs.,36,517-539, 783,1940

10. Fujii.T. , Uehara, H. and Kurata,C.,'Laminar Filmwise Condensation Of Flowing Vapour On A Horizontal Cylinder',Int. J. Heat and Mass Transfer,Vol.15,pp.235-246,1972

11. Henderson,C.L.,and Marchello,J.M.,"Role of Surface Tension and Tube Diameter in Film Condensation on Horizontal Tubes",AIChE Journal Vol.13,No.3,pp. 613-614,1967

12. Chen,M.M.,'An Analytical Study Of Laminar Film Condensation : Part-1-Flat Plates',J. of Heat Transfer,pp.48-54,Feb. 1961

13. Othmer, D.F.,and Berman,S.,"Condensation of Vapours",Ind.Eng. Chem.,Vol.35,No.10,pp.1068-1077,Oct.1943

14. Peck,R.E.and Reddie,W.A,"Heat Transfer Coefficients for-Vapours Condensing on Horizontal Tubes",Ind.Eng.Chem.

,Vol.43, no.12 ,pp.2926-2931,Dec. 1951

15. Bromley,L.A.,'Steam Condensing On a Horizontal Tube' ,unpub-
    lished M.S. Thesis ,Illinois Institute of Technology,1943
    (in ref. 17)

16. Taso,U.,'Heat Transfer Coefficient Of Condensation Of Vapour
    Of Nonmiscible Liquids On Horizontal Pipes',Ph.D. Thesis,The
    university of Michigan ,1939 (in ref. 14)

17. Bromley, L.A., Brodkey, R.S. and Fishman,N.,"Heat Transfer in
    Condensation-Effect of Temperature Variation Around a Hori-
    zontal Condenser Tube", Ind.Eng.Chem. ,Vol.44, No.12, pp.2962
    -2966,Dec. 1952

18. Rohsenow,W.M.,"Heat Transfer and Temperature Distribution in
    Laminar Film Condensation",Trans.ASME,pp.1645-1648,Nov. 1956

19. White,R.E.,"Condensation of Refrigerant Vapours Apparatus and
    Film Coefficient for Freon-12",J.Soc.Refg.Engg.,pp.375-379
    1948

20. Drew,T.B.,Nagie,W.M. and Smith,W.Q.,Trans. Am. Inst.Chem.
    Engrs.-Vol.31,pp.605-621 ,1935

21. Minkowycz,W.J. and Sparrow,E.M.,"Condensation Heat Transfer
    in Presence of Non-condensables,Interfacial Resistance,
    Superheating,Variable Poperties and Diffusion" ,Int. J. Heat
    Mass Transfer, Vol.9, pp.1125-1144 (1966)

22. Poots,G. and Miles,R.G.,"Effect of Variable Physical Proper-
    ties on Laminar Film Condensation of Saturated Steam on a
    Vertical Flat Plate",Int.J.Heat and Mass Transfer ,Vol.10,
    pp.1677-92 ,1967

23. Fundamentals of Heat Transfer,Mikheyev,M.,Mir Publishers,-
    Moscow,1977

24. Jakob,M.,Heat Transfer, Vol. 1,pp.667-673,Wiley,New York,1949

25. Berman,L.D.,'Heat Transfer With Steam Condensation On a Bundle Of Horizontal Tubes',Thermal Engg.,Vol.28,pp.218-224,1981

26. Kern,D.Q.,'Mathematical Development Of Loading in Horizontal Condensers',AIChE J.,Vol.4,pp.157-160,1958

27. Grant,I.D.R.,'In Notes For Condensation and Condenser Course',Birniehell Institute,NEL ,1972 (in ref. 36)

28. Grant,I.D.R. and Osment,b.d.j.,'The Effect Of Condensate Drainage On Condenser Performance ',NEL Rept 350, East Kilbride ,Scotland,April 1968 (in ref. 36)

29. Short,B.E. and Brown,H.E.,'Proc. I Mech E, Gen. Disc.,Heat Transfer, pp.27-31 1951 (in ref. 36)

30. Butterworth,d.,'Developments In The Design Of Shell And Tube Condensers', ASME paper 77-WA/HT-24,Atlanta,Ga.,Dec. 1977 (in ref. 36)

31. Nobbs,D.W.,'The Effect Of Downward Vapour Velocity Inundation On The Condensation Rates On Horizontal Tubes And Tube Banks',Ph.d. Thesis ,univ. of Bristol,Bristol,England,Apr. 1975 (in ref. 36)

32. Withers,J.G. And Young,E.H.,'Steam Condensation On Vertical Rows Of Horizontal Corrugated and Plain Tubes',Ind. Eng. Chem. Process Des. Develop.,Vol.10,No,1,,1971

33. Young,F.L. and Wholenberg,W.J.,'Condensation of Saturated Freon-12 Vapour On a Bank Of Horizontal Tubes', Trans. ASME 64(8),PP.789-794 1942

34. Chen,M.M.,'An Analytical Study Of Laminar Film Condensation-

,Part-2-Single and Multiple Horizontal Tubes',J.Heat Transfer, Vol.83,pp.55-60 ,1961

35. Eissenburg, D. and Bogue, D., 'Test Of An Enhanced Horizontal Tube Condenser Under Conditions Of Horizontal Steam Flow',Heat Transfer,Vol.1,pp.1-11,Paris 1970

36. Marto,P.J.,'Heat Transfer And Two Phase Flow During Shell Side Condensation'.Heat Transfer Engineering Vol.5, No.1-2,1984

37. Owen, R.G.,and Lee ,W.C.,'Some Recent Developement in Condensation Theory',Chemical Eng. Res. Des. Vol. 61,Nov. 1983

38. Watson ,R.G.H.,Brunt,J.J. and Birt,D.C.P.,'Dropwise Condensation Of Steam ', International Developments In Heat Transfer ,pt.2,pp.296-301,ASME,New York 1961

39. Young, E.H. and Briggs,D.E.,'The Condensing Of Low Pressure Steam On Vertical Rows Of Horizontal Copper and Titanium Tubes',AIChE J.,Vol.12,pp.31-35,1966

40. Fuks,S.N.,'Heat Transfer With Condensation Of Steam Flowing In a Horizontal Tube Bundle',Teploenergetika,Vol.4,pp.35-39,1957

41. Isachenko,V.P. and Glushkov,A.F.,'Heat Transfer With Steam Condensing On a Horizontal Tube And With a Flow Of Condensate Above', Teploenergetika,Vol.16,pp.79-81,1969

42. Eissenberg, D.M.,'An Investigation Of The Variables Affecting Steam Condensation On The Outside Of A Horizontal Tube Bundle ,Ph.D. Thesis ,Univ. of Tennessee, Knoxville, Dec. 1972

43. Fujii,T.,'Vapour Shear And Condensate Inundation: A Overview' ,Power Condenser Heat Transfer Technology,eds.P.J.Marto and R.H.Nunn,pp.193-233,Hemisphere,New York,1981

44. Al-Arabi,M.,'Turbulent Heat Transfer in The Entrance Region of a Tube',Heat Transfer Engineering,Vol.3,Nos 3-4,pp.76-82,Jan-June 1982

45. Boelter,L.M.K.,Young,G. and Iversion ,H.W.,'An Investigation Of Aircraft Heaters-Distribution Of Heat Transfer Rate In Entrance Section Of a Circular Tube' ,NACA Tech. Note No. 1451,1948 (in ref. 44)

46. Kays.W. and Perkins,H.,Hand book of heat transfer ,ed. Rohsenow,W. and Hartnett,J.,sEC. 7,McGraw Hill BOOK Co.,New York,1973 (in ref. 44)

47. Hausen, H.,Z. Ver. deut. Ingr., Beih. Verfahrenstech., No. 4, pp. 91-98,1943

48. Eckert,E.R.G. and Jr.Drake,R.M.,Heat and Mass Transfer,McGraw -Hill Book Co.,Inc.,New York,1959

49. Hartnett,J.P. and Minn,M.,'Experimental Determination of The Thermal Entrance Length For The Flow Of Water And Of Oil In Circular Pipes', Transactions of ASME ,pp.1211-1220 Nov. 1955

50. Deissler,R.G.,'Analysis Of Turbulent Heat Transfer And Flow In The Entrance Region Of a Smooth Passages 'NACA TN 3016 Oct. 1953

51. Latzko,H.,'Der Warmeubergang An Einen Turbulentten Flussig-keits Oder Gasstrom',Zeitschrift fur ang ewandte Mathematik und Mechanik,Vol.1 1921

52. Allen,R.W. and Eckert,E.R.G.,'Friction And Heat Transfer Mea-surement To Turbulent Flow of Water(Pr=7 and 8) at a Uniform Wall Flux',J. of Heat Transfer,pp.301-310,Aug. 1964

53. Faber,M.,'Measuring Industrial Signals Takes In Plant Know-How',Electronic Design,April 29,pp.157-164,1982

54. Sylvan,J.,'Isolation And Conditioning Clean Up Industrial Signals',Electronic Design, April 29, pp.169-178,1982

55. Jr.Faber,M.L.,'Proper Measurement Techniques Reduce Thermo-couple Errors',E.D.N.,June 9,pp.115-119,1982

56. Collier,J.G.,'Convective Boiling and Condensation',McGraw Hill Book Co.,Inc.,New York,1972

57. Bisesi, C.H., unpublished M.S. thesis ,Illinois Institute of Technology , Chicago ,III, 1942 (in ref. 17)

58. Brodkey , R.S., unpublished M.S. thesis , University of California, Berkley , Calif. ,1950

59. Lee, W.C. and Rose, J.W.,'Film condensation on a horizontal Tube-Effect of Vapour Velocity", Heat Transfer, 1982, Vol.5, pp.101-106,Munich,1982

60. Sugawara,S.,Michiyoshi,I.,and Miramiyama,T.,The Condensation of Vapour Flowing Normal to Horizontal Pipe,Proc.6th Jan. Natl.Congr.Appl. Mech.,111-4,pp.385-388,1956

61. Rohsenow,W.M.,Webber,J.H. and Ling,A.T.,"Effect of Vapour Velocity on Laminar and Turbulent Film Condensation", Trans. ASME, pp.1637-1643, Nov. 1956

62. Shekriladze,I.G. and Gomelari,V.I.,"Theoratical Study of Laminar Film Condensation of Flowing Vapour"Int.J.Heat Mass Transfer,Vol.9,pp. 581-591,1966

63. Perry, R.H. and Chilton, C.H., ' Chemical engineer's Handbook', 5th Ed., Mc Graw Hill, New York